5-2015

Artifical neural network models for the analysis of permeable pavement performance.

Ata Radfar
University of Louisville

ARTIFICIAL NEURAL NETWORK MODELS FOR THE ANALYSIS OF PERMEABLE PAVEMENT PERFORMANCE

by

Ata Radfar

B.Sc., Iran University of science and Technology (IUST), 2007
M.Sc., Ferdowsi University of Mashhad, 2011

A Dissertation
Submitted to the Faculty of the
J.B. Speed School of Engineering of the University of Louisville
in Partial Fulfillment of the Requirements
for the Degree of

Doctor of Philosophy in Civil Engineering

Department of Civil and Environmental Engineering
University of Louisville
Louisville, Kentucky

May 2015

ARTIFICIAL NEURAL NETWORK MODELS FOR THE ANALYSIS OF PERMEABLE PAVEMENT PERFORMANCE

By

Ata Radfar

B.S., Iran University of Science and Technology, 2007

M.S., Ferdowsi University of Mashhad, 2011

A Dissertation Approved on

April 10, 2015

by the following Dissertation Committee:

_____

Dissertation Director: Dr. Thomas D. Rockaway

_____

Dr. J.P. Mohsen

_____

Dr. Zhihui Sun

_____

Dr. W. Mark McGinley

_____

Dr. William E. Biles

DEDICATION

I dedicate my dissertation work to my family and friends. A special feeling of gratitude to my loving wife, whose words of encouragement and push for tenacity ring in my ears. Jessica has never left my side and is very special. I also dedicate this work to my sweet mother. Her support, encouragement, and constant love have sustained me throughout my life. I am also very grateful to my brother, Ali, and my sister, Elahe, who have always loved me and taught me to work hard. I will always appreciate all they have done.

ACKNOWLEDGMENTS

First and foremost I wish to thank my PhD advisor and committee chairman, Dr. Thomas Rockaway, for his exquisite attention to detail, his demand for excellence, and most of all patience throughout the entire process. His excitement and willingness to provide feedback made the completion of this research an enjoyable experience. I am very appreciative for the opportunities he provided for me to be a member of the Center for Infrastructure Research (CIR) and actively involved in the construction phase of the projects to get on site experience that led to this research. It was his support that gave me the opportunity to submit the papers at prestigious journals and present the research project at the most scientifically recognized conferences across the nation.

I would also like to acknowledge and thank the other committee members, Dr. William E. Biles, Dr. Zhihui Sun, Dr. W. Mark McGinley, and Dr. J. P. Mohsen who were more than generous with their expertise and precious time and agreeing to serve on my committee. Special thanks goes to Dr. J. P. Mohsen for his encouragement during this process and nominating me to receive Speed school of engineering fellowship.

Finally I would like to thank Mr. Josh Rivard, project manager at the CIR, for allowing me to conduct my research and providing any assistance requested. His brilliant mind, specialty, and willingness to help did make this project fun.

ABSTRACT

ARTIFICIAL NEURAL NETWORK MODELS FOR THE ANALYSIS OF PERMEABLE PAVEMENT PERFORMANCE

Ata Radfar

April 10, 2015

This dissertation is a numerical modeling study based on the findings of the two installed Permeable Interlocking Concrete Pavements (PICPs) in Louisville, KY and twenty one laboratory models. A new model derived to more accurately predict the captured surface runoff volume by the PICPs using Artificial Neural Networks (ANNs). The proposed model relates rainfall parameters and site characteristics to the runoff volume captured by the permeable pavements. The database used for developing the prediction models is obtained from the collected data of the monitored permeable pavements. The performance of the ANN-based models are analyzed and the results demonstrate that the model results compare satisfactorily with measured values. A parametric study is completed to determine the sensitivity of a variety of parameters on the captured runoff volume. The results indicate that the developed model is capable of estimating the captured runoff by the permeable pavements for different rain events and site characteristics. The ANN model considers all significant contributing factors and provides a more precise volume prediction than the linear model.

Clogging, which is mainly caused by sediment deposition, is the other important factor that result in performance failure of PICPs. Measuring Volumetric Water Content (VWC) by Time Domain Reflectometers (TDRs) is an automated method to track the speed of clogging. Monitoring peak VWC during rain events has been used as an indication of clogging progression over the PICP. Five ANN models are developed from the recorded VWC in order to compute the peak VWC from the rainfall parameters and maintenance treatment. A comprehensive set of data including various rain events characteristics obtained from the rain gauge and the conducted maintenance on the PICP are used for training and testing the neural network models. The performances of the ANN models are assessed and the results demonstrate satisfactory model accuracy when compared to the measured values. A parametric study was completed and the results indicate that the models are capable of estimating the peak VWC of the permeable pavements for different locations. The models consider all the contribution factors and provide more precise prediction values than the linear model. Peak 5 minute intensity, the previous rainfall depth, and the cumulative rainfall depth from the installation are the most critical parameters with respect to the hydrologic performance of the PICP.

Finally, twenty one model configurations with different combinations of slope, gap size, and joint filling material were built to study clogging progression and permeable pavement performance. In this study, a neural network model was used to predict the clogging progression rate with critical PICP characteristics. The results indicate that the model is accurately predicting the extent of clogging along the length of permeable pavement. Sensitivity analyses are completed and the results suggest surface slope and location as the most influential parameters on the clogging length. Moreover, the prediction

model for infiltration edge progression is presented to estimate the rainfall depth with 99% accuracy on testing datasets. By predicting the precise cumulative rainfall depth based on the infiltration edge distance and the PICP specifications, the hydrologic operation for each configuration and at any rainfall depth is accessible. The results demonstrate that surface slope and gap size present the highest influence on the infiltration edge progression. By better understanding the effects of pavements' specification and site characteristics and selecting the most efficient pavement configuration, improved future design and more effective maintenance operations can be achieved.

TABLE OF CONTENTS

LIST OF FIGURES

LIST OF TABLES

LIST OF EQUATIONS

1. INTRODUCTION

1.1. Background

Rapid growth of urban areas and the associated increase in impervious surfaces has increased the surface water runoff. During extreme rain events large runoff volumes flowing through catch basins and drainage networks may exceed sewer system capacity (Scholz and Grabowiecki 2007). As many communities utilize the same piping network to convey both sanitary and stormwater flow, a system overflow will pollute the surrounding water bodies and degrade the quality of downstream water resources. Also, because of the large unmanaged runoff volume, risk of flooding and channel erosion increases. (Brown and Borst 2013).

There are two general practical solutions to prevent the combined sewer overflows (CSOs), commonly referred to as “gray” and “green” construction practices (Dunn 2010). “Gray” practices are mainly focused on constructing CSO chambers, pipeline, and sewage treatment facilities to more efficiently eliminate, reduce or manage the overflow from the combined sewer systems. “Green” approaches, are mainly focused on installing features which will divert stormwater flow into natural systems before entering the collection systems. This “green” approach, utilizes Low Impact Development (LID) practices which mimic the natural water drainage system and capture rain water at the site. LID techniques are a more recent means of managing surface runoff water and decrease the number of

overflow occurrences and flood risk. LID techniques operate to not only reduce stormwater pollution, but also reduce the potential for erosion (Walsh 2000).

Managing runoff water using LID practices, rather than conveying it to the treatment facility provides many valuable outcomes. First, less wastewater volume is conveyed to the treatment facility and therefore treatment costs, and the need for constructing larger treatment facilities, is reduced. Second, the LID practices can enhance the local water quality as pollutant materials are removed through biological processes. And third, the LID practices capture stormwater to recharge the groundwater or to augment water courses.

1.2. Problem Declaration

Although LID practices present numerous advantages, their effectiveness and design have raised concern. As an example, PICPs, one of the most common LID techniques, need frequent maintenance in order to continue operating properly (Smith 2006). Since surface runoff carries pollutants and debris along its path, permeable pavements are prone to clogging (Scholz and Grabowiecki 2007). However, the maintenance operations necessary to remove the clogged material from the PICP surface and recover surface infiltration rates, are costly and time consuming (Haselbach, Valavala et al. 2006).

The current design approach for PICPs considers the associated drainage area and selected design storm events, as the main factors of hydrologic design (Smith 2006). However, a more complete understanding of hydrologic information, watershed characteristics, and anticipated maintenance requirements are essential for efficient designs. Designing PICPs only based on drainage area and the design storm, systems may not perform adequately due to excessive debris flow. Also, since scheduling maintenance

visits are mainly based on predetermined time intervals, the maintenance operations can be optimized if visits are based on comprehensive watershed information and actual rain event data. Developing PICP designs based on specific information enhances the engineers' ability to predict future performance and ultimately design more efficient systems (Holman-Dodds 2003). Considering all the contributing factors including rain events' variables and site characteristics will lead to an effective and comprehensive design.

1.3. Objective and Scope

Most LID practices are designed based on generalized site characteristics and rainfall parameters and do not take into account specific site information. As a result, many LID practices do not perform properly and excessive maintenance operations are required. A much more robust LID design could be achieved by including more site specific information, unfortunately, there is no guidance on which site specific information to include or how to incorporate it into the analyses. Artificial Neural Network (ANN), however, is a mathematical tool that can effectively manage a large number of variables in order to determine which site variables are effective on system performance and ultimately to reach a more efficient design.

The overall goal of this research is to develop more efficient PICP design guidelines utilizing an ANN model that scrutnize site-specific design variables to predict system performance. This study is based on data obtained from two permeable pavement systems installed in Louisville, KY and one simulated permeable pavement systems constructed in the U.S. Environmental Protection Agency National Laboratory in Edison, New Jersey. The operational, site specific, and collected rainfall data provided the information necessary to develop predictive models for PICP performance; captured runoff, VWC, and

clogging rate. The outline of the completed research with a short description for each of the developed predictive models is briefly presented in the following.

1.3.1. PICP Performance

Gathering information on the operation of PICP is necessary in order to understand their behavior over time. Long-term performance of the PICPs has been investigated with respect to their ability to capture, store, and exfiltrate runoff water. The storage gallery performance of the installed PICPs was assessed over more than a two-year period using both laboratory experimentation and monitoring data from naturally occurring rain events. The results defined the clogging concentration location on the permeable surface, and the maintenance frequency required to retrieve the expected infiltration rates. Water drainage rates from the storage gallery and the hydraulic conductivity of the surrounding soil layers were computed to define a comprehensive view of the hydrologic performance. By better understanding the runoff water movement rate through the storage gallery and the clogging progression on the pavement surface, a more accurate assessment of the PICP operation can be developed.

1.3.2. Captured Runoff Prediction Model

Storage capacity, one of the main hydrologic performance features of the PICPs, was studied in relation to the site characteristics and the rain events properties. ANN was used as a strong tool to develop a model to predict the captured rain water volume by using critical PICPs' parameters. The objective of this research was to develop ANN models to predict the water levels and to determine the runoff volume captured by permeable pavements. The proposed model relates the filter performance with different storm and drainage area characteristics plus permeable pavement properties over time. In order to

verify the applicability of the derived models, they are employed to estimate the water levels of parts of the test results that are not used in the modeling process. A comparative study on the prediction and measured values is also completed for the training and testing datasets. Moreover, sensitivity analysis is completed to determine the efficacy of the contributing factors on the captured runoff by the PICPs. The results obtained from this analysis, can be used to predict the water levels of the storage gallery based on the unique site specifications for each PICP. Determining the maintenance treatments efficiency has been a challenge, however, by conducting a sensitivity analysis the relative importance of maintenance treatments in relation to the storage capacity of the permeable pavements was computed. By determining the relative importance of the studied parameters, the critical parameters were identified and the obtained results used as a tool for design applications. Considering the effective parameters in the LIDs design result in a comprehensive stormwater control plan and better performance is acquired by the controls.

1.3.3. Volumetric Water Content Model

As it is known, the clogging progression deteriorates the permeable pavements performance over time. Sediment accumulation rates are mainly influenced by the storm event parameters and site characteristics. The rain events variables and the last conducted maintenance techniques are scrutinized in the developed ANN models to predict the maximum VWC values during storm events. Several cleaning methods were conducted on the installed PICPs and different rates of effectiveness were observed. Hence, the maintenance treatment was studied as one of the critical factors of site characteristic. In addition to the maintenance treatment, the rain events variables are the second category of input parameters to develop the ANN models. Predicting the peak VWC based on rain

event variables and site characteristic is beneficial to schedule productive maintenance treatment. New prediction models are built using ANN to forecast the peak VWC which is related to the sediment deposition rates. Moreover, a sensitivity analysis is performed to determine the effect of different parameters on surface infiltration rates. The relative importance of the rain events characteristics and the maintenance treatment is quantified to define the most effective variables on the hydrologic performance of PICPs.

1.3.4. Clogging Prediction of PICP Laboratory Model

The effectiveness of permeable pavements and ultimately the captured runoff volume can be correlated to the extent of clogging on the surface. The clogging progression rates vary according to the location, site characteristics, and rain events variables. Site characteristics for each permeable pavement are unique, and observing the same storm events parameters are rare. Therefore, multiple laboratory PICP test specimens were built and exposed to simulated stormwater events so that correlations could be established between the system characteristics and the progression of surface clogging. Twenty one model configurations with different combinations of slope, gap size, and joint filling material were built to study clogging progression and permeable pavement performance. This study utilizes a neural network model to predict the clogging progression rate by considering only the PICP characteristics. The results indicate that the model is capable of accurately predicting the extent of clogging along the length of permeable pavement. Sensitivity analyses are completed to determine the relative importance of the studied parameters on the length of clogging on the permeable surfaces. The results show that slope and location as the most influential parameters on the clogging length. Moreover, the prediction model for infiltration edge progression is able to estimate the rainfall depth with

more than 99% accuracy on testing datasets. By predicting the precise cumulative rainfall depth based on the infiltration edge distance and the PICP specifications, the hydrologic operation for each pavement configuration during any rainfall depth is accessible. The results demonstrate that slope and gap size present the highest influence on the infiltration edge progression. By better understanding the effects of pavement characteristics and choosing the most efficient pavement configuration, systems could be better designed to reduce clogging and more efficient maintenance schedules could be defined.

2. TECHNIQUES SYNOPSIS

2.1. Introduction

The expansive impervious surfaces in urbanized watersheds promote large peak runoff volumes and fast concentration times during rain events. This increased runoff and flow rate carry debris and other pollutants that ultimately degrade the water quality of surrounding water courses. Also, CSOs during heavy rain events lead to an influx of pollution in the water bodies and further water resources degradation are likely to occur. Limiting the number of overflows from Combined Sewer Systems (CSSs) and properly managing surface runoff water enhance the quality of water sources (Legret and Colandini 1999). Urbanization and rainfall pattern alteration are the main reasons of urban hydrology problems and their severe consequences are elaborated in detail. Practical solutions to address the arising issues, and the pros and cons for each method are presented in the following sections.

2.2. Major Causes of Hydrologic Impacts

Forests, grasslands, and other natural terrain have high surface permeability that first capture large volume of rain water and second filter the surface runoff as it slowly releases to surrounding water courses or the ground water system. This natural water cycle, however, is disrupted during urbanization when roads, parking lots, bridges, buildings, and other impervious surfaces are constructed that present much lower surface infiltration rates.

These low permeability surfaces intensify the stormwater runoff, eliminate the groundwater recharge, increase flood risk, and pollute water resources (Ferguson 1998).

Land surface coverage is one of the primary factors that govern the rainfall-runoff process. Urbanization, which is defined as replacement of natural land coverage with nonporous urban landscapes, has been rising during the past several decades and is expected to reach 82.1% in 2030 in the developed countries (Heilig 2012). As a result, stormwater accumulation above the surface and larger runoff volume generation are anticipated (Figure 1).

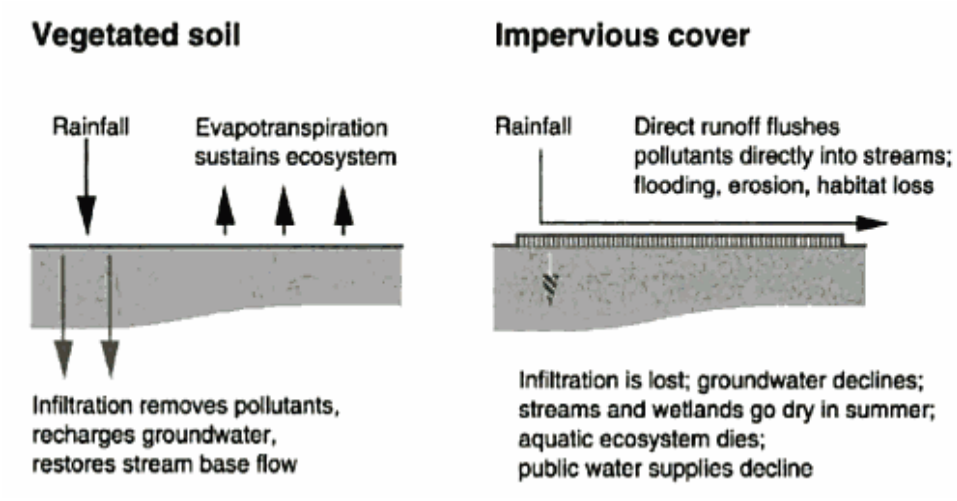

Figure 1. The hydrologic differences between vegetated soil and impervious cover (Ferguson 1998)

The overland flow rate of the stormwater during and after rain events can be shown by a "hydrograph". The typical hydrograph is presented in Figure 2, to compare pervious and impervious areas runoff volume production with each other. It can be concluded from comparing the shape of hydrographs that the impervious areas yield larger peak runoff in a shorter period of time (faster) than the vegetated soil or undeveloped areas. The surface runoff on the impervious surface increases both the flood and CSOs possibilities. Furthermore, the recharge rate to the aquifer decreases for the impervious area in

comparison to the vegetated soil or undeveloped surfaces (White 2002). Hence, surface runoff management can reduce the pollution of water resources and also decrease flood risk.

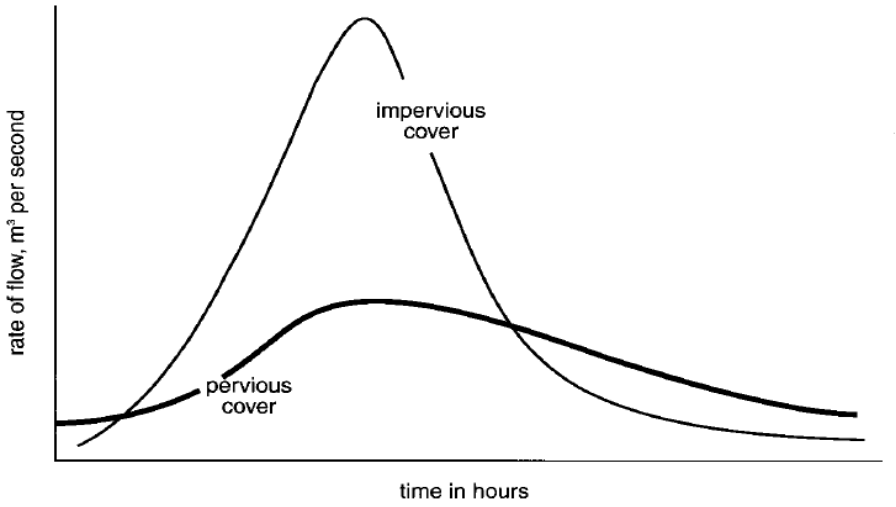

Figure 2. Hydrographs for pervious and impervious surfaces (White 2002)

In addition to the increase in runoff associated with urbanization, the risk of extreme weather and more intense storm events have also been increasing (Meehl, Tebaldi et al. 2009). There have been changes in both duration and intensity of rain events over the past couple of decades as observed in Africa (Ngongondo, Xu et al. 2011), China (Yang, Shao et al. 2010), Korea (Kyoung, Kim et al. 2011), Turkey (Haktanir, Cobaner et al. 2010), the United States (Kelly, Weathers et al. 2009), and Canada (Waters, Watt et al. 2003). Within the Midwest region of the United States specifically, where this study takes place, the increasing frequency of high intensity rain events has been reported by (Villarini, Smith et al. 2011). It is thus important to understand how the frequency and magnitude of rainfall events are changing as they are directly related to hydraulic control of both stormwater sewer systems and agriculture runoff control systems.

2.3. Environmental Degradation Problems

Water quality degradation, CSOs, and high flood risk are the most severe environmental concerns that are directly related to impervious area expansion and increased urban runoff volumes. Pollutants including heavy metals, oil, and hydrocarbons are common materials which are transported by stormwater flow and are likely deposited on the impermeable surfaces over time. The pollutant deposition on the ground surface typically occurs during dry atmospheric conditions, from a variety of industrial or domestic sources including traffic emissions, decomposed litter, de-icing salts, vegetative residues, pet feces, and soil losses (Newman, Coupe et al. 2001). During rain events the pollutants may be carried by stormwater flow and ultimately discharged into water courses without any treatment thus contaminating the receiving waters.

Flood risk is directly affected by unmanaged runoff volume and the impervious surfaces in the watershed area. Increasing runoff volume in urbanized areas result in higher flood risk possibility and natural disasters preparedness is necessary to prevent further consequences. The study on Thames River has demonstrated that between 1974 and 2000, the flood risk has been elevated because of the urbanization that occurred in the upper stream (Nirupama and Simonovic 2007). It has been shown that utilizing pervious surfaces and proper runoff management practices can reduce the flood possibility.

Stream channel erosion and degradation of aquatic habitats are also consequences of uncontrolled stormwater runoff. During a rain event in an urban watershed, the flow volume may change quickly due to the short concentration time. This wide range in flow volume is the main reason of channel erosion and further downstream sediment deposition. It has been publicized that sediment loss because of stream channel erosion in various

locations is increasing (Trimble 1997). Moreover, changes in sedimentation regimes and water quality, the direct result of surrounding watershed land use, adversely affect the freshwater mollusk populations. The habitat loss and water quality were investigated for two watersheds with the same agriculture land coverage in Atlanta, Georgia. Higher water quality and greater species variety has been observed in watersheds with more permeable surfaces (Gillies, Brim Box et al. 2003). Hence, proper stormwater management is required to limit channel erosion and improve quality of water resources.

2.4. Runoff Management Practices

Urbanized communities have been working to manage their high flood and pollution risk through the construction of complex drainage networks. In older cities, sewer systems were often employed to carry domestic sewage, industrial wastewater, and rainwater runoff through the same pipe and discharge the flow off site. The first CSSs, which permitted discharging sewage and rainwater in the same drainage network, were constructed in Europe in the 1840s. During storm events, however, runoff volume may exceed the capacity of the drainage network, and overflow from the CSSs occurred. During these overflow events, large volumes of polluted water entered adjacent water bodies and the increased flow eroded downstream water courses.

In the early 1800s, many communities in the United States relied on a backyard septic system, or worse, did not have a sanitary sewer treatment plan. The rapid urbanization that had occurred in the mid-19th century, prompted the necessity of more efficient sanitary waste water treatment systems. Americans began to investigate European combined systems in the 1870s to figure out the pros and cons of combined sewer systems versus separating the system into two components; stromwater flow and sanitary flow. By

the end of the 19th century, the consensus was to utilize CSSs in the urban areas with higher populations. It was thought that by collecting the waste and stormwater through one drainage network, and ultimately discharging the wastewater into the water bodies, the dilution was sufficient to render it harmless. In the early 20th century, officials realized the environmental and health hazards in untreated wastewater. However, water resource pollution and its consequences were not identified as a significant threat until the middle of the 20th century. It wasn't until the Federal Water Pollution Control Act (FWPCA) was passed in 1965 that CSOs were regulated and water quality standards were enacted.

In 1967, the US Environmental Protection Agency (US EPA) publicized results of a nationwide assessment on environmental issues which highlighted the environmental impact of the CSOs and the necessity to manage the number of overflows. It was found that CSSs were used mostly in the Northeast, the Great Lakes region, and the Ohio River basin, which served about 1,300 municipalities encompassing approximately 36 million people, twice the population served by separated sanitary sewer systems. The study determined that there were about 15,000 overflow locations and approximately 1.2 trillion gallons per year of untreated wastewater and stormwater runoff discharged into water sources. The majority of these CSOs occurred in the communities with population of 25,000 or more. Based on the report it was evident that, it was necessary for communities to reduce the number of CSOs and improve the quality of water resources.

The "end of the pipe" plan, referred as "High Impact" or a "gray" technique, is one possible option for stromwater runoff management. A "gray" technique is mainly focused on collecting surface runoff and removing it quickly from the watershed through drainage networks that maximize the connection between impervious surfaces and catchment

basins. In this approach, constructing additional treatment facilities and larger pipeline systems are necessary to accommodate the large runoff volumes.

A "green" approach, as an environmentally conscious method, is employed to manage runoff water in the watershed by implementing LID techniques (Holman-Dodds 2003). LID practices intercept stormwater flow before it enters the collection system, store runoff water, and gradually release it into the groundwater system. Recharging the groundwater, conserving water resources, and reducing the peak runoff flow by increasing the infiltration and storage capacity of the surfaces are the main benefits of sustainable urban drainage systems. (Dunn 2010). LID practices capture rainwater and manage surface runoff water where it occurs, while traditional approach is mainly based on capturing, conveying, and then treating stormwater off the site.

2.5. LID Techniques

LID installation is an ecologically and economically practical technique for runoff management and water quality improvement. Green practices are capable of protecting water quality and managing runoff water more effectively than traditional stormwater management plans. Preserving natural site condition, reducing the impervious coverage to minimize the generated runoff volume, and managing of stormwater runoff water are the main steps for comprehensive runoff management approach. It has been observed that communities with Green Infrastructure (GI) controls have achieved a more stable situation and healthier environment. The main benefits of installing GI controls and some common LID techniques are described in the following.

Water quality improvement, energy efficiency enhancement, and urban safety improvement are the main benefits of implementing LID practices. LID techniques have

been employed to recreate the flow regime and manage runoff flow at the site. Some LID techniques such as rain barrels, cisterns, and permeable pavement are available to capture, store, and then reuse rainwater for irrigation or other non-potable applications. Through LIDs, rainwater is absorbed by the soil and vegetation instead of entering into the storm and sewer systems. Therefore, by reducing the number of overflows from CSSs and preventing water courses from polluted runoff flow, water quality will be improved.

The term “LID” describes many techniques on a variety of sites that utilize soil, vegetation, and other engineering methods to capture rain water and ultimately enhance the environmental quality. Although LID installation has benefits on urban hydrology such as CSOs volume reduction and improves quality of water resources, the most challenging part is selecting the suitable techniques according to the site characteristics and specific location. Green roof, rain gardens, bioswale, tree boxes, cisterns, rain barrels, infiltration trenches, and permeable pavements are some common LID practices to decrease impervious areas and improve runoff management efficiency (Damodaram, Giacomoni et al. 2010). In the following, permeable pavement, as one of the most common LID technique is presented and a brief description on its operation is presented.

2.5.1. Permeable Interlocking Concrete Pavement

Permeable pavement is a common LID practice that allows rainwater infiltration through the surface into the underlying layers. Permeable pavements have many different forms, including porous concrete, porous asphalt, or interlocking pavers. PICP is constructed by installing paver blocks on the surface and designing a storage gallery underneath it (Smith 2006). Stormwater passes through joints between the paver blocks and flow into a stone reservoir underneath. The porosity of the underlying crushed stone

layers store runoff water that gradually exfiltrates to the surrounding soil layers. Although long-term infiltration performance has been demonstrated and the designated infiltration rates have been measured, the hydrological performance may vary over time due to clogging (Brattebo and Booth 2003). PICP installation and its performances over time are investigated and assessed in more detail in this study.

PICP, as a common form of permeable pavement, is able to capture rainwater through voids and gradually allow surface runoff to seep into the porous medium. It has been shown that recharging the groundwater, reducing stormwater runoff, mitigating the peak flow, and removing the pollutant materials are the main benefits of utilizing PICPs in urban communities. PICPs are capable of removing pollutant materials from the water courses and prevent contaminant materials in surface runoff from further migration into the water resources. The surface roughness of the PICPs provides enough depression storage to keep the pollutants from washing off and getting into the water surface. Infiltration rates of permeable surfaces have resulted in capturing large rainwater volume and exfiltrating stored runoff to the surrounding soil layers. However, debris material that is carried by surface runoff may clog the voids area of the pavements and prevent PICPs of performing properly.

PICPs are constructed with paver blocks, and the drainage is provided through the gaps between the blocks. Because of their specific application and according to their construction materials, PICPs are mainly employed in low-traffic areas like parking lots, sidewalks, alleyways, and parking lane of the streets. However, several airports have started using this type of permeable pavement along the runways edges to capture rainwater. In order to provide enough storage volume, the areas under the permeable

pavements need to be excavated. The excavation depth and the required storage volume are determined by many factors such as groundwater level, rainfall frequency, runoff volume in watershed area, surrounding soil permeability, and downstream drainage considerations (James and Von Langsdorff 2003). Although GI controls such as PICPs present many benefits, there are still a lot of unknown problems concerning their performance, effectiveness and design that need to be discovered. The porous pavements performances are deteriorating because of their tendency to get clogged. In the following section, the main concerns in regard to the PICP functionality are discussed.

A. Performance Failure

It has been observed that the PICPs are prone to clogging and as a result their hydrologic performance degrades over time. Sediment carried by surface runoff water accumulates on the pavement surface or penetrates into the gaps between the blocks which reduces water movement (Al-Rubaei, Stenglein et al. 2012). Fine elements are trapped in the pores of the gravel which reduce the porosity and diminish the infiltration rates (Balades, Legret et al. 1995). Therefore, with less infiltration less stormwater volume is captured through the pavements from the watershed. Thus, scheduling regular and effective maintenances according to the pavements configuration and site characteristics is necessary for proper operation.

The sediment deposition rate varies directly with the infiltration rates of the permeable pavements. It was observed that clogging progresses at a high rate during the first year but the rates are stabilized and lowered afterwards (Balades, Legret et al. 1995). It is shown that the possibility of a permeable pavement to get fully clogged in an actual application is low, which is mainly due to the irregular porous size of the aggregates.

However, it is possible for permeable pavement surface that are located near fine element sources, such as coastal areas, to be entirely covered with sands because of winds or drifts (Haselbach, Valavala et al. 2006).

B. Maintenance Treatment

Maintenance has to be conducted regularly in order to remove the clogging material from the permeable pavement surfaces and restore the designated infiltration rates. Infiltration rate restoration is necessary to keep the pavements performing well and capturing surface runoff water from the watershed. Maintenance operations and their frequency are known to directly affect the efficiency of LID performance. Over time, infiltration rates are reduced as sediments accumulate on the permeable pavement surface and storage volume is reduced as debris penetrates inside the gallery layers. It was observed that the average surface infiltration rates increased after cleaning methods were applied (Brown and Borst 2013).

Different cleaning techniques are available for permeable pavements and the recovery rates of each method are different. Thus, one maintenance technique is not applicable for all types of permeable pavements. It would be prudent to determine the efficacy of the maintenance treatments according to the site characteristics and cleaning method specifications. Therefore, the most effective maintenance treatment can be selected based on the watershed characteristics and permeable pavement attributes. In section 3.2.2, different conducted maintenance treatments and the operation details will be discussed.

Brown and Borst have shown that by determining the threshold for VWC values, the clogging progression rates in relation to the cumulative rainfall depth can be quantified. The VWC threshold to identify the location and the time that surface runoff water is not

infiltrating with a designated rate was equal 0.1 cm^3/ cm^3. Based on the selected threshold and the measured rainfall depth, the sediment deposition progression rates were computed. After PICP construction, the most upgradient TDRs presented the maximum VWC values, and over time the downgradient TDRs show the highest VWC since the upper TDRs are clogged and cannot capture larger rain water volume. The TDRs that record the highest VWC and then due to clogging the measured VWC is then get lowered than 0.1 cm^3/ cm^3 and need cleaning.

ANN as a new nonlinear solutions, develop prediction models to forecast desired variables of the experiments. Neural network models can be used as a useful tool for predicting the main hydrologic performance variables of the PICPs. PICPs' performances are highly dependent on site characteristics and rain events data. Since the clogging progression is influenced by stormevents parameters and site characteristics, therefore proper maintenance can be scheduled accordingly. Moreover, a sensitivity analysis is performed to determine the efficacy of different parameters on the main PICP features. The relative importance of the contributing factors is quantified to define the most effective variables on the hydrologic performance of PICPs.

3. ARTIFICIAL NEURAL NETWORK

Developing prediction models is one of the main ANNs applications to provide the ability of estimating the desired parameters. In contrast to the traditional methods, ANNs are able to learn from data and formulate relationships among different variables with few prior assumptions. Hence, neural network models can develop nonlinear relationships between multiple variables where enough data has been acquired (Zhang, Eddy Patuwo et al. 1998). Neural network models are able to provide accurate formula for real-world problems that can only be understood through empirically obtained data. Experimental observations are employed to train ANN models, and ultimately develop relationships among various parameters.

3.1. Introduction

Artificial Neural Networks, a form of artificial intelligence, simulate the biological structure of the human nervous system. ANNs are capable of learning from experience which was inspired by human brain operation. As a result, ANN models are capable of being employed for completing many tasks in a wide variety of fields (Zhang, Eddy Patuwo et al. 1998). Artificial intelligence techniques are useful tools to solve problems in many disciplines since artificial neurons interconnections are capable of performing massive computations to process data (Basheer and Hajmeer 2000). Remarkable data processing characteristics such as nonlinearity, robustness, ability to learn, and generalization are some factors that make the ANN a robust modeling tool.

Neural network models are strong prediction tools that can establish the nonlinear relationships between variables similar to the statistical models. Statistical models can be developed for the observed conditions; however they are not applicable to the undiscovered problems. ANN models employ the collected data to develop prediction models and compute the relative importance of unknown parameters instead of using the natural relationship between variables. To develop an accurate ANN model, it is important to select the variables that have the highest influence on the model. In this study, the appropriate input variables for the model are chosen based on the prior knowledge and observed results. The common practice is to divide the database into training and test datasets. In this study, approximately one-fourth of the database is dedicated to test data and the rest is analyzed as training data (Shahin, Jaksa et al. 2008).

3.2. Biological Neuron

The neural network operation is inspired by biological neuron structure and operation. The biological neurons are of different types and length, which based on their location in the body, consist of three similar main operational pieces; dendrites, cell body, and axon are the major functional units of a neuron. The simplified graphic presentation of a biological neuron is shown in Figure 3. Signals are received through dendrites from the other neurons, and then get transferred to a nucleus in the cell body to store the information. Signals from the cell body are passed to the dendrites of the other neurons through axon. A large number of dendrites and synapses in a neuron, provide receiving and transferring lots of signals simultaneously (Basheer and Hajmeer 2000). The connection between axons and dendrites in a neuron is represented by the linking between nodes, and the synapses are simulated with the connection weights. In Figure 4, the corresponding neural network

model for a human nervous system with *n* biological neurons, various intensity signals *(x)*, and synaptic strength *(w)* are transferring into a neuron with a threshold equals to *b*.

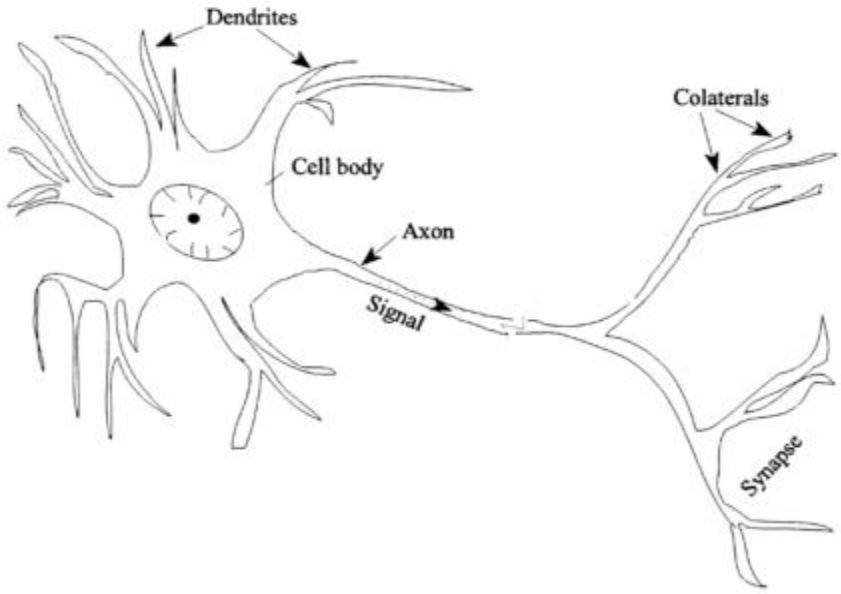

Figure 3. Schematic of biological neuron (Basheer and Hajmeer 2000)

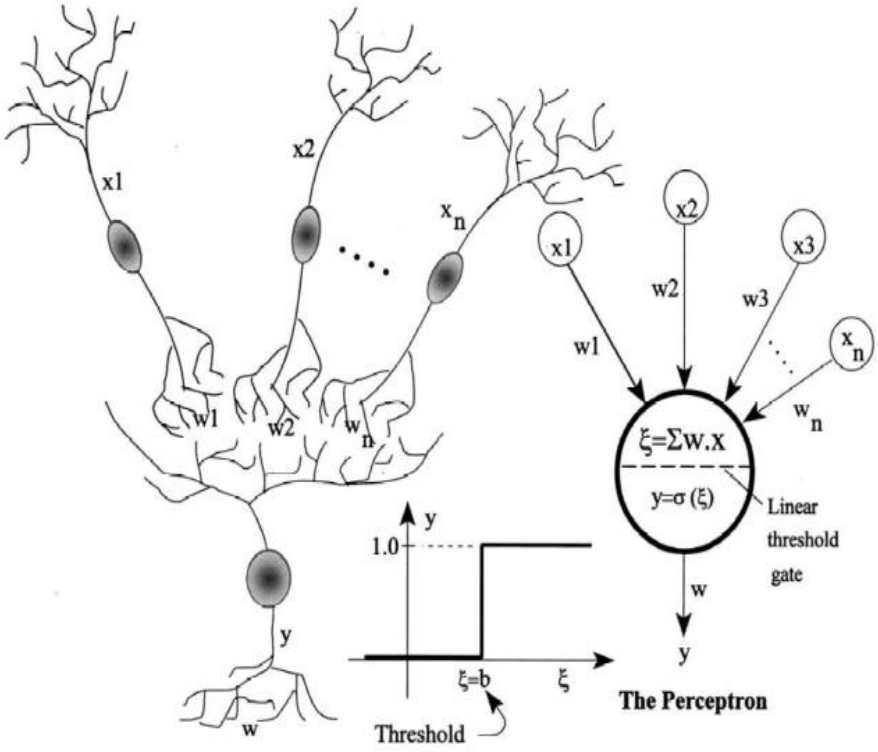

Figure 4. Signal interaction in biological neurons and the equivalent artificial neuron system (Basheer and Hajmeer 2000)

3.3. Artificial Neuron

ANN-based models contain interconnected processing elements or neurons that are organized in an input, output, and one or more intermediate hidden layers (Figure 5). The connection weights are utilized to link the neurons of the two consecutive layers, and they are indicating the relative importance between the two connected neurons. The iteration processes are conducting to discover the relationships between the neurons and the dedicated weights to each connection are updated after process completion. The prepared data are fed to the neural network model through an input layer, and the output layer presents the computed response. The hidden layers assist the computational models to

effectively process the data and ultimately find the intrinsic pattern among the variables (Goh 1995).

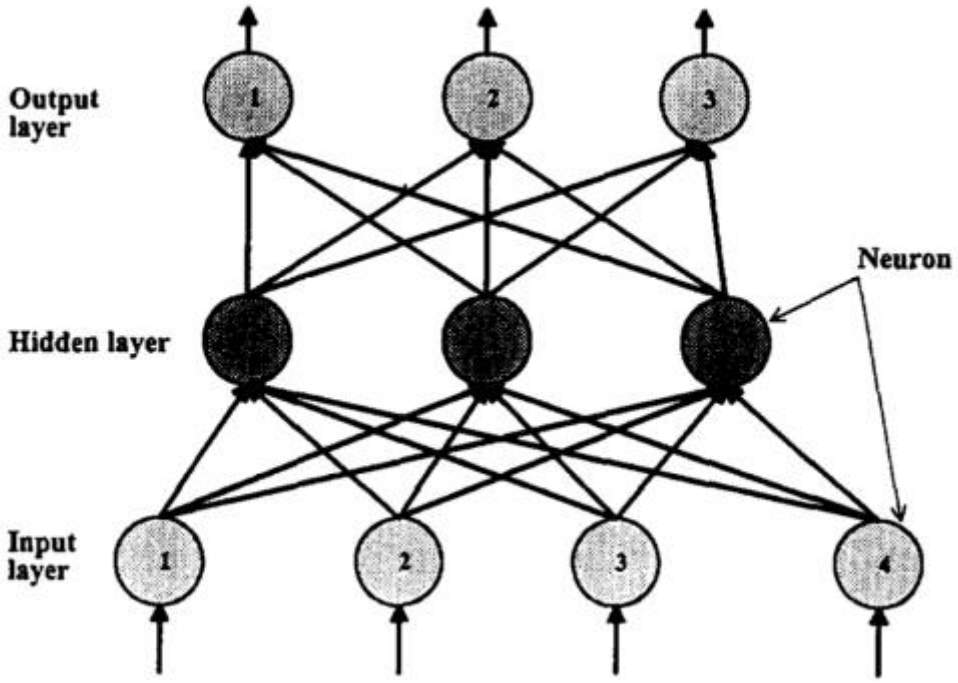

Figure 5. Neural network architecture (Goh 1995)

The computational mechanism provides the neural network's capability of learning, acquiring, and mapping from a set of multiple parameters data to the desired parameters. Training from the observed results and finding the relationships between the measured set of data, is one of the main ANNs specification. In the other words, artificial intelligence models simulating real world problems to explore the associated patterns between input and output data. As stated earlier, ANNs learning ability is inspired from human nervous system in a more simplified version. The learning process requires assessing input parameters with their associated measured output value, and the computational process

adjusts the internal connection strength to reach the least error between the target and ANN outputs (Rafiq, Bugmann et al. 2001).

The neural network model receives the input data, and then the default connection weights are applied to the normalized values. After introducing the obtained values to the activation function, a "net" input (ξ) is produced to the linear threshold gate, and ultimately transmits the signal to the following layer, as the output (y) (Figure 4). In cases where (ξ) is greater than the threshold limit, which is called bias value (b), the neuron is operating, however, if it is lower than the threshold the neuron is not getting activated. The dot product of the input values (x) and their dedicated weights *(w),* provide the "net" input. One is representing as "activation", while 0 is presumed as "deactivation", in the Equation **1**.

$$y = \begin{cases} 1, if & \sum_{i=1}^{n} w_i x_i \geqslant b\ , \\ 0, if & \sum_{i=1}^{n} w_i\ x_i \prec b, \end{cases}$$

Equation 1

The positive connection weights ($w_i \succ 0$) enhance the net signal (ξ) value and demonstrate the existence of relationships between the nodes, whereas negative connection weights prevent the neuron connection's activation which is called the inhibitory link. These connection weights are updated according to the computed difference values between the calculated and the recorded output parameter for each experiment. The iteration process continues in an effect to find the relationships that yields acceptable error (Basheer and Hajmeer 2000).

3.4. Back-propagation Algorithm

Neural network models are capable of being trained using observed experiments and a back propagation (BP) algorithm is the most common method for optimizing connection weights (Pooya Nejad, Jaksa et al. 2009). Feed-forward networks apply the BP algorithm, which are based on first-order gradient descent have been applied to many geotechnical and environmental problems. Some applications of neural network models have led to some accurate relationships being developed such as predicting soil hydraulic conductivity (Schapp and Leij 1998), soil cohesion intercept (Mollahasani, Alavi et al. 2011), rainfall-runoff modelling (Shamseldin 1997) and asphalt concrete permeability (Tarefder, White et al. 2005).

In this study, the back-propagation algorithm is employed to train the ANN model. The back-propagation neural network models with a single hidden layer provides satisfactory prediction results through learning process. The learning phase of ANNs is carried out by feeding the prepared input and the associated output to the model. After multiplying the inputs by their dedicated weights and summing up the products, the nonlinear transfer function, such as sigmoid functions are applied to the results.

3.5. Data Processing

There are two main techniques to develop an ANN model and selecting the appropriate method depends on the available database. ANNs may be developed based on supervised or unsupervised learning method; In these methods the exercised relationship formula employed for error computation. In supervised learning the model can be developed with the set of inputs and corresponding outputs. The error is computed based on the actual and predicted output and the value is used to adjust the connection weights

until the smallest error is acquired. By comparing the real and predicted values the model performance can be measured. However, in unsupervised learning only input is fed to the network and the connection weights are adjusted based on the input to classify the variables into the similar feature classes (Baum and Wilczek 1988).

The neural network models include an input layer, at least one hidden layer, and an output layer. Each layer consists of several nodes which are connected to the processing units of the following layer with connection weights. The schematic diagram of the neural network model is presented in Figure 6. An "epoch" or a cycle is defined as each training process which the weights are updated. At the end of each "epoch", the weights are updated and this iteration process is continued until the computed average sum squared error is minimized and is within the predefined range for the problem (Goh 1995). The connection weights between the neurons are stored for the next phase, and are fed to the other set of data. Hence, the computed weights during training are applied to the testing dataset to compare the ANN predication outputs with the measured values. There is no additional learning processes or updating of the connection weights during the testing phase; however, after assessing the model performance by the selected criteria, the neural network models are able to be employed on real-world problems. The prediction of the desired parameter after providing the inputs to the developed model are reliable and can be used as a design tool.

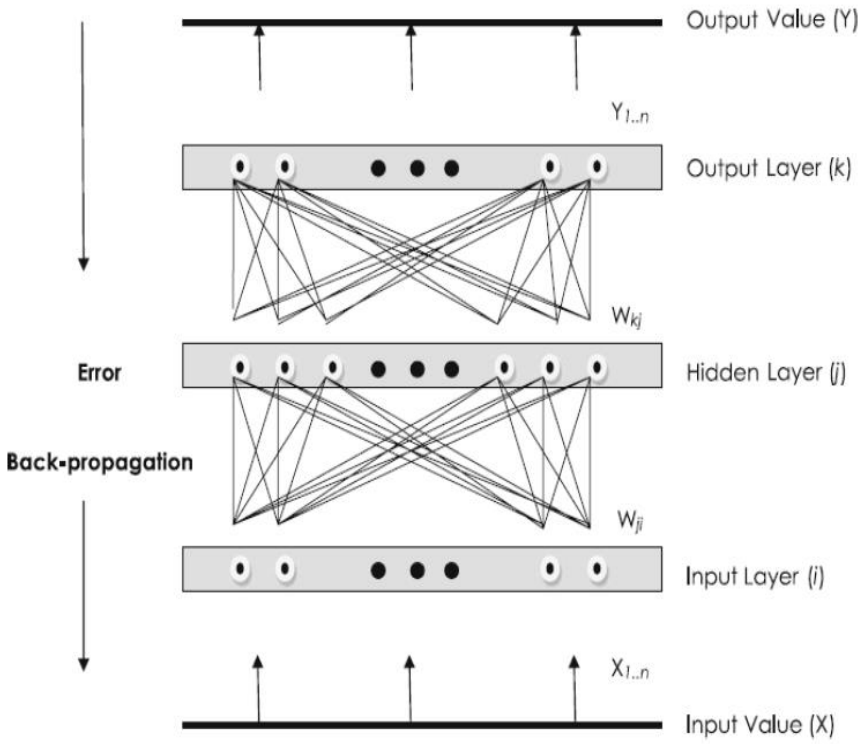

Figure 6. A Schematic diagram of a neural network (Hossein Alavi, Hossein Gandomi et al. 2010)

The input and output values were normalized in this study since the normalization results in faster data processing. The first step to normalize the data is to determine the range of the parameters. Take X_{max} and X_{min} to be the maximum and minimum values, and X_n to be the normalized value of the studied parameter, respectively. The selected normalized range in this study is $L = 0.05$ and $U = 0.95$. The following equations are applied to compute the normalized value for input and output parameter (Equation 2, Equation 3, and Equation 4 (Mollahasani, Alavi et al. 2011).

$$X_n = ax + b$$

Equation 2

$$a = \frac{(U-L)}{(X_{max}-X_{min})}$$

Equation 3

$$b = U - aX_{max}$$

Equation 4

After normalizing the data, an activation function is applied to the sum of the product to obtain the output value. The relationship between the input and the output of a single processing element is given by Equation 5. The connection weights are adjusted through the iteration processes of training datasets to minimize the error. The function to compute the error for test datasets can be expressed as Equation 6; afterwards the model performance is checked with test datasets.

$$h_j = f\left(\sum_{i=1}^{n} x_i w_{ij}\right)$$

Equation 5

Where:

h_j = the output

f() = the activation function

x_i = the activation of ith hidden layer node

w_{ij} = the connection weight between nodes j and I from the previous layer;

$$E = \frac{1}{2}\sum_n \sum_k (t_{k-}^n h_k^n)^2$$

Equation 6

Where:

t_k^n = Predicted output

h_k^n = Real output values

n = Observed events in the database

k = Number of nodes in the output layer.

3.6. Model Performance Evaluation

Changing the architecture of the neural network models such as varying the transfer function or the number of processing elements in the hidden layer result in different prediction accuracies. The inputs to an ANN are normally the predictor variables, while the functional estimating relationships are presented as Equation 5. In the Equation 5, $X_1, X_2, \dots, X_i$ are the independent variables and h_i is a dependent variable. The inputs are typically the observed values, and the outputs are the computed predicted values. In conclusion, the neural network model incorporates the predictor variables and time-based recorded values into ANN model to predict the desired parameter.

The neural network models should be trained prior to predicting the desired parameter. Training process includes determining the connection weights between the neurons of the developed ANN model. It is through computing the connections formulas that a neural network model is capable of solving nonlinear relationships between the input and output parameters. Multi-Layer Perceptron (MLP) models are categorized in a supervised training model since the target response for each observation is available (Zhang, Eddy Patuwo et al. 1998).

The training data are assigned to the input nodes, and consequently the connection weights that yield the highest accuracy are calculated. After accumulating the result in the

hidden layer, the sum is transformed through an activation function to compare with the output value. The training process is employed to obtain the connection weights that minimize the error between the computed and recorded outputs. The following parameters are presented to assess the performance of the neural network models. The model performance needs to be evaluated by observing the criteria parameters. The correlation coefficient (R), Root Mean Squared Error (RMSE) and Mean Absolute Error (MAE) are the parameters that are computed to assess the developed model performance (Equation 7, Equation 8, and Equation 9) (Mollahasani, Alavi et al. 2011).

$$R = \frac{\sum_{i=1}^{n}(h_i-\bar{h}_i)\,(t_i-\bar{t}_i)}{\sqrt{\sum_{i=1}^{n}(h_i-\bar{h}_i)^2}\ \sum_{i=1}^{n}(t_i-\bar{t}_i)^2}$$

Equation 7

$$RMSE = \sqrt{\frac{1}{n}\sum_{i=1}^{n}(h_i - t_i)^2}$$

Equation 8

$$MAE = \frac{1}{n}\sum_{i=1}^{n}|h_i - t_i|$$

Equation 9

Where:

The real and predicted output values for the i^{th} output are

h_i = Real output for the i^{th} event

t_i = Predicted output for the i^{th} event

$\bar{h}_i$ = Average real output values

$\bar{t}_i$ = Average predicted output values

n = Number of studied events

The number of neurons in the hidden layers are governed by consecutive computation. At each iteration process, neurons are added to the hidden layer in order to optimize the model. The neural network models continue processing as long as the computed error on the testing dataset decreases with epochs. After developing the models with the effective input parameters, the architecture of the most accurate prediction models should be found. According to a universal approximation theorem, a single hidden layer is selected for developing the ANN models because single hidden layer provides uniform approximate continuous and nonlinear function (Cybenko 1989). The number of the hidden layers, hidden nodes, learning rate, epochs, and activation function determine the neural network architecture and affect the ANN model performance. More detailed information on the aforementioned parameters and the number of hidden nodes for each ANN model are presented in the results section.

4. PROJECT SETTING

The 1972 Clean Water Act (CWA) has expedited the implementation of LID designs within the United States (United States 2005). CSO policy as defined by the CWA presents a comprehensive national strategy to ensure that municipalities and water quality standards authorities achieve cost effective CSO controls to meet defined environmental objectives (United States 1994). Many communities are now utilizing LID stormwater control systems to reduce runoff volume that enters into the stormwater collection systems and thereby reduce their CSOs. LID practices have shown to be efficient and economically viable options for reducing the amount of pollution entering surface water.

4.1. Project Background

The city of Louisville in the Commonwealth of Kentucky is currently working to mitigate its CSOs in the urbanized area. The Metropolitan Sewer District (MSD) of Jefferson County, the United States EPA, the Kentucky Department for Environmental Protection (KDEP), and the US Department of Justice prepared a consent decree agreement in 2005 to mitigate the effects of these wet weather CSOs. The comprehensive plan, known as the Integrated Overflow Abatement Plan (IOAP), was released for public review in 2008. The IOAP project that was initiated in 2005 is focused on constructing a combination of gray and GI to improve stormwater management within selected watersheds.

The main goals of the IOAP plan within the study area are to eliminate sanitary sewer overflows (SSOs) and reduce CSOs volume during rain events by constructing LID

practices. In partial fulfillment of the IOAP objectives, LID stormwater management controls were constructed in the urbanized neighborhood named “Butchertown”, located in CSO basin 130 of Louisville, a 28-acre portion of the MSD service area. Permeable pavements, tree boxes, and porous asphalts were the selected LID practices to install in the studied watershed area. The characteristics of the stormwater management controls and the site specifications are elaborated in the following sections.

4.1.1. Site characteristics

As the first phase of the project, two PICPs were constructed in the north and south bound parking lane of Adams Street located East of Louisville and less than 1 km south of the Ohio River in December 2011, referred to hereafter as 19G and 19H, respectively (Figure 7). Permeable pavement section 19G is 2.47 m. by 36.6 m. and encompasses a 2900 m^2 drainage area, while PICP 19H is 2.47 m. by 16.8 m. and cover a 1100 m^2 drainage area. The permeable pavement length for 19G is about two times longer than 19H (Table 1).

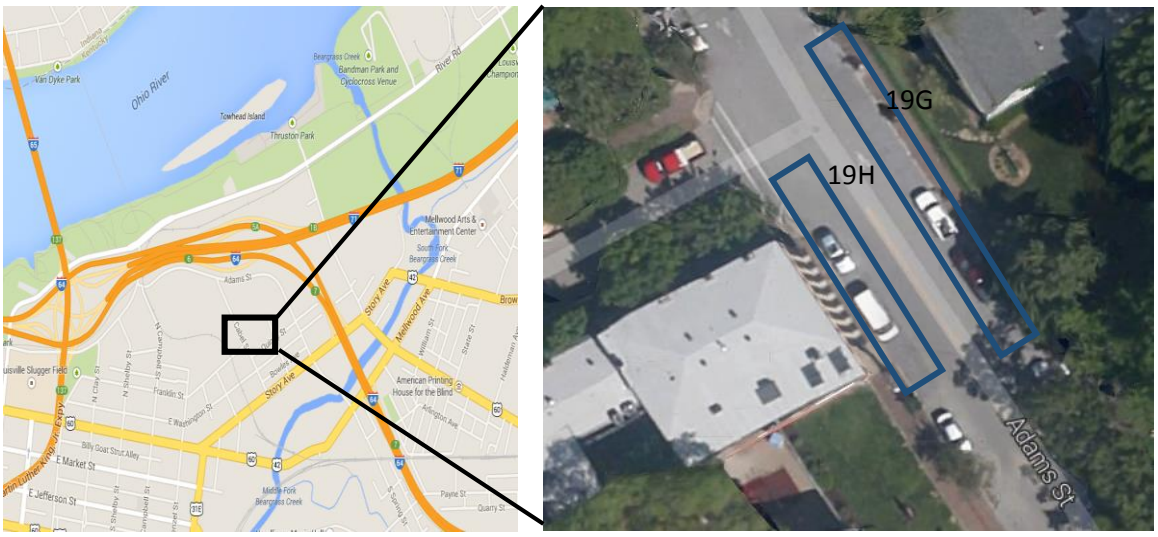

Figure 7. Permeable pavements 19G and 19H location

The PICP surfaces are covered with articulating concrete paver blocks overlying a "T" shaped gravel filled storage gallery (Figure 8). The gallery is approximately 0.6 by 3 m wide and filled with AASHTO No. 3 stone. The top portion of the gallery is filled with compacted AASHTO No. 57 to provide a working base for the PICP system. The gravel storage layer under the top layer and the trench were filled with AASHTO No. 3. Specific design details for 19G and 19H are provided in Table 2.

Table 1. Site Characteristic of Controls 19G and 19H

Site Characteristic	**19G**	**19H**
Design drainage area	2900 m^2	1100 m^2
Impervious area in the drainage area	1770 m^2	650 m^2
Rooftop area	620 m^2	190 m^2
Impervious area draining to the upgradient edge of the permeable pavement strip	881 m^2	398 m^2
Permeable pavement length	36.6 m	16.8 m
Permeable pavement width	2.47 m	2.47 m
Design longitudinal slope along length of paver strip	1.3%	1.9%
Design transverse slope along permeable pavement width at upgradient edge	2.4%	2.3%
Design transverse slope along permeable pavement width at downgradient edge	3.3%	2.3%
Impervious Area: Pavement's Surface Area	18.7:1	15.8:1

Table 2. Permeable pavement Characteristic of Controls 19G and 19H

Control Characteristic	19G	19H
Permeable paver block dimensions	0.298 m square by 0.144 m thick	0.298 m square by 0.144 m thick
Gravel storage layer (top)	0.3 m of AASHTO No. 57	0.3 m of AASHTO No. 57
Gravel storage layer (middle)	0.13 m of AASHTO No. 3	0.15 m of AASHTO No. 3
Gravel storage layer (bottom)	0.6-m-wide by 3.0-m-deep trench filled with AASHTO No. 3	0.6-m-wide by 3.0-m-deep trench filled with AASHTO No. 3

(a)

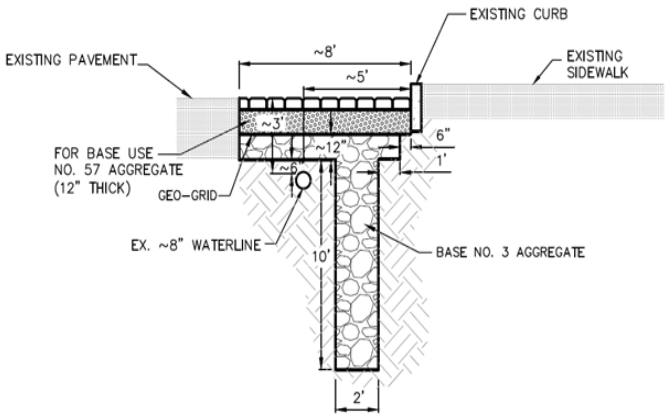

19G STANDARD CROSS-SECTION
(FACING NORTHWEST)

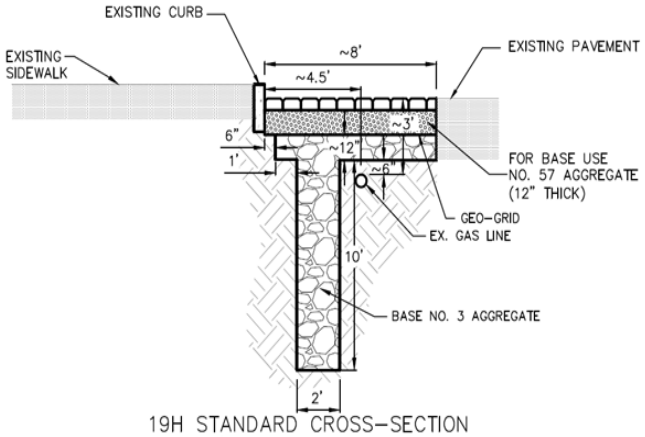

19H STANDARD CROSS-SECTION
(FACING NORTHWEST)

(b)

Figure 8. (a) Permeable pavement cross section schematic of controls 19G and 19H (b) Storage excavation of control 19G

The second phase of the project was completed in March 2013 and included construction of eighteen permeable pavements and six tree boxes. After assessing the results from the initial construction phase, the GI stormwater control designs were modified. The number, location, and length of the permeable pavement strips were altered in addition to drilling a series of shafts instead of conventional trench. In twelve of the eighteen PICP strips, a series of shafts (4 to 14) is used to provide access to deeper soil layers that have higher hydraulic conductivity, and the drainage rate is increased accordingly. Also, tree box design was improved and they are connected in the groups of

two or three to function together. Eleven tree boxes were constructed and linked to each other in the sets of two or three with a 3 ft. deep by 3 ft. wide interconnecting trench.

4.1.2. Instrumentation

A wide variety of LID practices are available and choosing the right type with the right characteristics to meet the desired expectation can be challenging. Modeling the LID techniques' performances and finding a precise assessment of their hydrological function can be influenced by many factors over time. Physical instrumentation was embedded into the control structures to record the main performance variables. The intent was to be able to monitor the exact LID response to a specific rainfall event and compare it with the theoretical design estimates.

In this study, in order to monitor the hydrologic performance of the PICPs and determine an efficient maintenance treatment schedule, an instrumentation plan for the installed PICPs is necessary. Each PICP contained embedded TDRs, pressure transducers and thermistors to measure the main function of characteristics over time. Moreover, a rain gauge is employed to measure the rain events variables that occurred at the site. Temperatures, infiltration rates, exfiltration rates, and stored runoff volume in the storage gallery are the main features that can be cataloged from the installed instruments. By determining such parameters' variation over time and finding their relation with rain events variables, a comprehensive design and maintenance schedule for permeable pavements can be provided.

The TDRs installed within the PICP technique to gather performance data are produced by Campbell Scientific, Inc. The multiparameter smart sensor's model is CS650 that measures electrical conductivity, dielectric permittivity, temperature, and VWC of

soils or other porous media (Figure 9). VWC, which is an indication of the infiltration rates, can be used to monitor the hydrologic performance of the PICPs. By placing the TDRs at 40 cm under the PICP surface a more accurate VWC measurement is achieved through recording dielectric constant of the gravel layers (Campbell Scientific 2011). Equation 10 is employed to compute VWC (θ_v) of AASHTO No. 57 by the dielectric constant (K_a) values.

$$\theta_v = -5.3 \times 10^{-2} + 2.92 \times 10^{-2} K_a - 5.5 \times 10^{-4} K_a^2 + 4.3 \times 10^{-6} K_a^3$$

Equation 10

The plan view of the TDRs at the PICPs (19G and 19H) shown greater numbers of the instruments were installed at the upgradient edge. The concentrated runoff flow from the upside and closer to the curb led to the suggested design to understand the higher clogging rates pattern at the upgradient edge (Figure 10 and Figure 11).

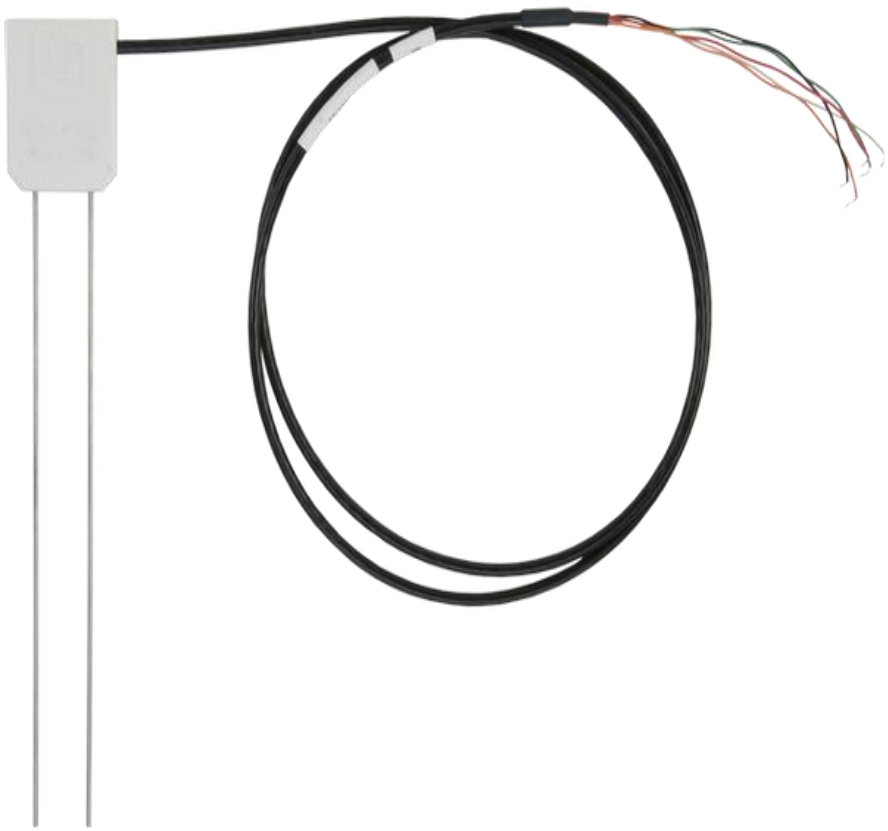

Figure 9. Soil water content reflectometer (CS650)

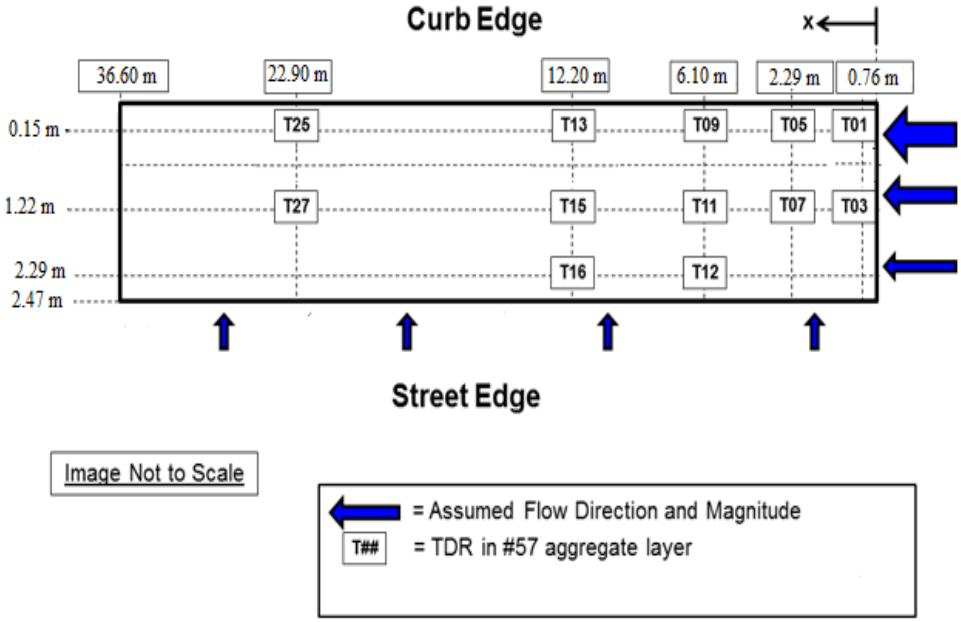

Figure 10. Plan view of TDRs' location at PICP 19G

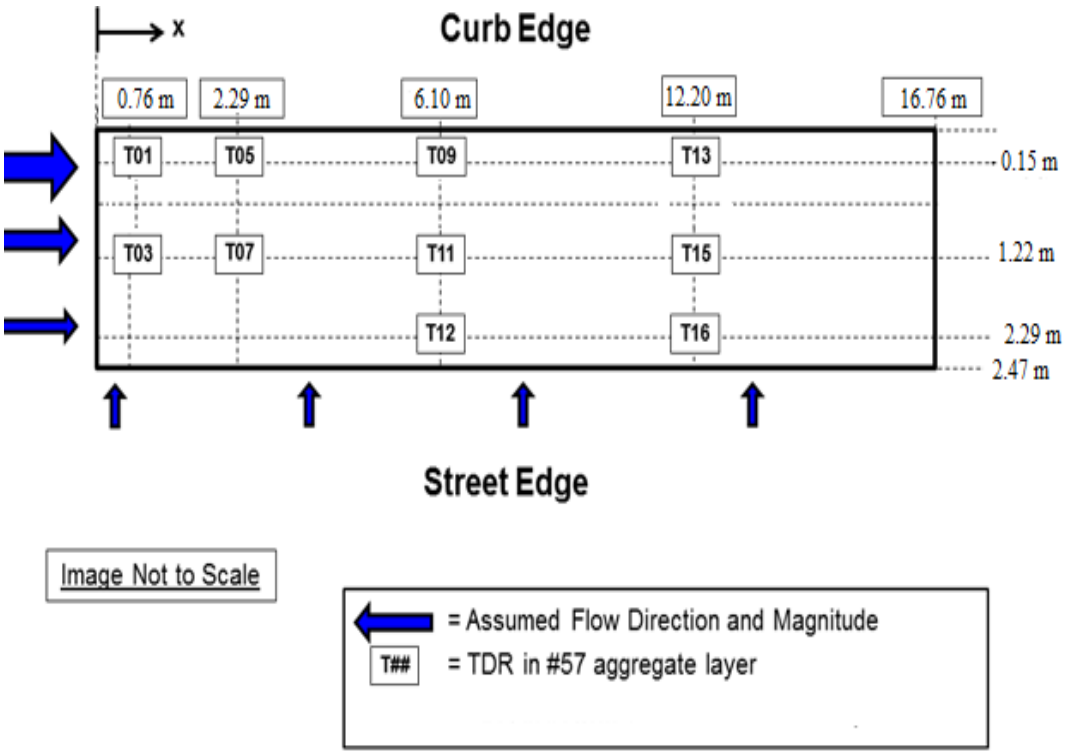

Figure 11. Plan view of TDRs' location at PICP 19H

The pressure transducers incorporated into the galleries are Campbell Scientific Piezometers' model CS405 (Figure 12). The pressure transducers record the water level of the captured runoff by the system at different locations of the PICPs. The piezometers 40L, 41L, and 42L were installed at 0.8, 12.2, and 22.9 m from the upgradient edge, respectively. In PICP 19H, the piezometers (40L, 41L, and 42L) were located at 1.4, 6.1, and 11.9 m from the upper edge, respectively. All the installed piezometers are positioned at 1.22 m from the curb side and 3.8 m under the permeable surface in the gravel layers, and are routed into external data loggers programmed to record data at 1 minute intervals.

Figure 12. Pressure transducer (CS405)

The rain gauge employed in the studied watershed, close to the installed LID practices, to monitor the rain events data continuously. The rain gauge, TR05, which is located less than 0.75 km from the PICP location is monitored and maintained by the MSD of Louisville and Jefferson County. TR05 uses a tipping bucket to record rainfall depths as low as 0.0254 cm. (0.01 in.) in 5 minute intervals. Based on the measured rainfall data, the rainfall depth, peak 5-min and 15-min intensity for each rainfall event are computed. In addition, antecedent dry periods and cumulative rainfall depth prior to each rain event can be calculated from the recorded rainfall data.

4.2. Long Term PICP Performance

The general principle of PICP is to collect, treat, and exfiltrate surface runoff to enrich the groundwater systems, reduce the flood possibility, and improve the quality of water resources (Newman, Coupe et al. 2001). In comparison to traditional drainage systems, stormwater retention and infiltration to the groundwater system is a sustainable and cost effective process, which is suitable for urban areas (Pratt, Newman et al. 1999). Understanding surface runoff water development, water movement rate through PICP

surfaces and filtration layers, storage capacity of the controls, and the hydraulic conductivity of the surrounding soil layers are highly important to define the main contributing factors of PICP performances effectively.

4.2.1. Field and Laboratory Tests

Laboratory tests, including suction infiltrometer tests and the attached solid tests, were carried out on the filled material and the existing soil layers to determine their properties and how they interact with the PICPs operations. Since saturated hydraulic conductivity of the underlying soil layers plays an important role on infiltration, storage and exfiltration performance of the permeable pavement controls, suction infiltrometer tests were conducted to determine the properties of the soil layers. Suction infiltrometer (Mini-Disc) tests were completed at 25%, 50%, and 75% distances of the permeable pavement length from the upgradient edge. The obtained results from the Mini-Disc test is compared to the saturated hydraulic conductivity values which are estimated based on the soil texture and bulk density (Rawls et al. 1998). It can be concluded that mini-disc provides reasonable results that are in the interquartile range values (Table 3).

Table 3. Saturated Hydraulic Conductivity results in Control 19G and 19H

Location	Mini-Disc (mm/hr)	Soil Texture	Bulk Density Classification	Geometric Mean [K_{sat}] (mm/hr)	Interquartile range (IQR) (mm/hr)	n
Storage Gallery of GI control 19G	7.5 5.2 9.5	Loam	High	6.2	2.8 - 16.5	65

Average	**7.4**	**Loam**	**High**	**6.2**	**2.8 - 16.5**	**65**
Storage Gallery of GI control 19H	2.1 0.2 5.4	Clay Loam	High	0.7	0.2 - 3.8	53
Average	**2.6**	**Clay Loam**	**High**	**0.7**	**0.2 - 3.8**	**53**

It is important to conduct the attached solid tests because the gravels for the storage galleries are not perfectly washed and the filled materials contain small particle size sediment that were bound to them. The attached solids in the gravel layers can be washed by runoff water over time clogging the available porous space within the gallery or surrounding materials. In order to conduct the attached solid tests, three sample buckets were obtained from the trucks that carried AASHTO No. 3 for GI control 19G. The total wet weight of unwashed stone, moisture content and sediment of stone fraction for wet and dry basis are computed (Table 4). The wash water for the #3 aggregate was passed through a ½-inch sieve (13 mm), #10 sieve (2 mm) and #200 sieve (75 um). The results for three samples of #3 aggregate (Truck No. 3, 4 and 7) were analyzed and it showed more than the specified 2% of the material by mass that passed through the ½-inch sieve. The maximum attached solid percentage for dry basis is 3.528% which was taken from truck No. 4 (Table 5). Based on the completed tests, Truck No. 7 showed the lowest attached solid percentage in comparison to the other samples (Table 6).

Table 4. Attached solids result for sample ID (KY-25 3AS-130-19D-3)*

Sizes (mm)	Total Recovered Stone and Sediment (Dry Wt.) (gr.)	Sediment/Stone Fraction recovered (dry g/wet kg)	% of the Sample Sediment/Stone Fraction (wet basis)	Sediment/Stone Fraction recovered (dry g/dry kg)	% of the Sample Sediment/Stone Fraction (dry basis)
13	26,574.2	948.0	94.800%	972.10	97.210%
2	23.5141	0.8	0.084%	0.86	**0.086%**
75×10^{-3}	295.2	10.5	1.053%	10.80	**1.080%**
1.5×10^{-3}	443.8764	15.8	1.583%	16.24	**1.624%**
	27,336.8				**2.790%**

**Truck No. 3 with wet weight equals 28.03 kg and moisture Content is 2.5%.*

Table 5. Attached solids result for sample ID (KY-26 3AS-130-19D-4)*

Sizes (mm)	Total Recovered Stone and Sediment (Dry Wt.) (gr.)	Sediment/Stone Fraction recovered (dry g/wet kg)	% of the Sample Sediment/Stone Fraction (wet basis)	Sediment/Stone Fraction recovered (dry g/dry kg)	% of the Sample Sediment/Stone Fraction (dry basis)
13	13,656.5	877.3	87.7278%	964.72	96.472%
2	96.9240	6.2	0.623%	6.85	**0.685%**
75×10^{-3}	117.9093	7.6	0.757%	8.33	**0.833%**
1.5×10^{-3}	284.6279	18.3	1.828%	20.11	**2.011%**
	14,156.0		3.208%		**3.528%**

**Truck No. 4 with wet weight equals 15.57 kg and moisture Content is 9.1%.*

Table 6. Attached solids result for sample ID (KY-28 3AS-130-19D-E)*

Sizes (mm)	Total Recovered Stone and Sediment (Dry Wt.) (gr.)	Sediment/Stone fraction recovered (dry g/wet kg)	% of the Sample Sediment/Stone fraction (wet basis)	Sediment/Stone fraction recovered (dry g/dry kg)*	% of the Sample Sediment/Stone fraction (dry basis)
13	26,050.9	945.0	94.5010%	973.90	97.390%

2	132.6253	4.811	0.481%	4.958	**0.496%**
75×10^{-3}	116.2889	4.218	0.422%	4.347	**0.435%**
1.5×10^{-3}	449.3289	16.300	1.630%	16.798	**1.680%**
	26,749.1		2.533%		**2.610%**

**Truck No. 7 with wet weight equals 27.57 kg and moisture Content is 2.97%.*

One bucket sample with wet weight equal 3.17 kg was obtained from the No. 57 truck for GI control 19G. The wash water for the #57 aggregate will be passed through a #8 sieve (2.4 mm), #10 sieve (2 mm) and #200 sieve (75 um) (Table 7).

Table 7. Attached solids result for sample ID (KY-29 57AS-130-19D-1)*

Sizes (mm)	Total Recovered Stone and Sediment (Dry Wt.) (gr.)	Sediment/Stone fraction recovered (dry g/wet kg)	% of the Sample Sediment/Stone fraction (wet basis)	Sediment/Stone fraction recovered (dry g/dry kg)*	% of the Sample Sediment/Stone fraction (dry basis)
>2.38mm	3,006.0	949.4	94.9433%	978.96	97.896%
2.38	0.9282	0.293	0.029%	0.302	0.030%
2	10.7411	3.393	0.339%	3.498	0.350%
75×10^{-3}	52.9401	16.721	1.672%	17.241	1.724%
	3,070.6		2.041%		2.104%

** Truck No. 1 with wet weight equals 3.17 kg and moisture Content is 3.02%.*

4.2.2. Maintenance Techniques

Deposited sediment on the PICP surface degrades the infiltration rate into the storage gallery and less rain water volume is captured over time. Clogging initiates from the upgradient edge, close to the curbs side and gradually progresses to the downside of the pavement. It has been observed that the clogging progression rates depend on pavement characteristics, precipitation parameters, and drainage area specifications (Pitt and Maestre 2005). Hence, scheduling the most optimum maintenance treatment is highly important in

order to keep PICPs performing properly based on the accumulated sediment amount. The maintenance techniques remove the clogged materials from the pavement surfaces to restore the infiltration capacity and prevent sediment from entering the storage layers through the rainwater drainage path (Balades, Legret et al. 1995). Long term performance of porous pavements depends on the severity of clogging and the maintenance efficiency (Al-Rubaei, Stenglein et al. 2012).

Maintenance treatments were conducted regularly on the installed pavements in order to remove the clogging material from their surfaces and restore the designated infiltration rates (Brown and Borst 2013). Different cleaning techniques were conducted on PICP 19G over the first two years and it is possible to assess the effects of the maintenance treatment on the hydrologic performance of PICPs. In the following, a brief description of each conducted cleaning method on the installed PICPs is elaborated.

A. Street Sweep Truck

The street sweep truck was performed for retrieving the infiltration rates in control 19G after three months of the construction. This initial maintenance was done on March 15, 2012 on control 19G by a truck that covers a width equal to 330 cm. The truck provided vacuuming and mechanical sweeping as the cleaning mechanisms (Figure 13). In order to remove the debris from the surface of the permeable pavements, the sweeper truck passed over the pavement four times.

B. Air Jet Maintenance

Pressurized air jet maintenance was applied to both control 19G and 19H in order to blow the clogging materials. The air jet removes the accumulation materials from the gaps and a street sweeper covers the surface afterwards to collect the discharged debris (Figure

13). Three air jet maintenances were completed consecutively after the first cleaning on the surface with different time periods between them. The first air jet maintenance was employed on May 9, 2012 for the PICPs 19G and 19H, however this cleaning technique was the second completed maintenance for 19G and the first one for 19H. The second and third air jet maintenances were completed on October 5, 2012 and May 15, 2013, respectively.

(a)

(b)

Figure 13. (a) Vacuum maintenance (b) Air jet cleaning method

C. Hydro Excavator Truck

High pressurized water jet was exerted on the permeable pavement surface to remove the accumulated debris from the gaps and the vacuum is used to capture the removed

material. The prototype attachment is connected to the hydro excavator truck to impart the pressure (Figure 14). This cleaning method was executed on the control 19G on September 18, 2013. Hydro excavator truck was the last conducted cleaning method which applies high pressurized water jet to clean the gaps and the attached vacuum collects the removed sediment.

(a)

(b)

Figure 14. Hydro excavator method (a) Prototype attachment (b) Hydro excavator truck

The completed maintenance treatments for controls 19G and 19H during the first two years of their performance are presented in Table 8 and Table 9, respectively. The number of rain events, the total rainfall depth, and the maximum values of the rain event variables that have occurred between maintenances are listed.

Table 8. Maintenance Treatments and rain events characteristics for control 19G

Cleaning Methods	Sweep Truck	Air Jet No. 1	Air Jet No. 2	Air Jet No. 3	Hydro Excavator Truck
Dates	3/15/2012	5/9/2012	10/5/2012	04/15/2013	09/18/2013

Total Rainfall Depth (cm.)	25.73	21.69	40.34	48	51.79
Max Rainfall Depth (cm.)	4.37	4.52	5.92	6.02	7.1
Max Peak 5-min Intensity (mm/hr)	48.77	48.77	115.82	97.54	128.02
Max Peak 15-min Intensity (mm/hr)	29.46	31.50	96.52	48.77	96.52
Number of Rain Events (>0.127cm)	23	12	25	40	35
Rainfall Depth from the installation (cm)	25.73	47.42	87.76	135.76	187.55

Table 9. Maintenance Treatments and rain events characteristics for control 19H

Cleaning Methods	Air Jet Maintenance No. 1	Air Jet Maintenance No. 2	Air Jet Maintenance No. 3
Dates	5/9/2012	10/5/2012	04/15/2013
Total Rainfall Depth (cm.)	47.42	40.34	48
Max Rainfall Depth (cm.)	4.52	5.92	6.02
Max Peak 5-min Intensity (mm/hr)	48.77	115.82	97.54
Max Peak 15-min Intensity (mm/hr)	31.50	96.52	48.77
Number of Rain Events (>0.127cm)	35	25	40

Rainfall Depth from the installation (cm)	47.42	87.76	135.76

4.3. Laboratory Model

Site characteristics for each permeable pavement system are different from each other, and the clogging progression rates vary accordingly. Moreover, the rain events variables are rarely identical, and this fact is another reason that causes different performance in the PICPs. Hence, in order to compare different permeable pavement systems with each other and study the effects of PICPs characteristics on their functionality, previous researchers have constructed a laboratory PICP model. This experimental model with repeatable physical characteristics and a governable flow volume is an effective method to assess the effects of pavements configuration on the clogging patterns. By applying the rain flow on the model that mimics the rain events, the effective PICP characteristics are investigated in this study. Ehsaei A. developed 21 model configurations of slope, gap size, and joint filling material to clogging progression and permeable pavement performance (Ehsaei 2013). This study utilizes a neural network model to predict the clogging progression rate of the different model configurations based on the data collected by Ehsaei.

4.3.1. Model Characteristics

The laboratory model was designed to create different PICP configuration to investigate the effects of pavements characteristics on the hydrologic performance during rain events. Ehsaei's 2013 experimental flume was built to structurally house multiple pavement configurations (Ehsaei 2013) (Figure 15). Interlocking Concrete Paver (ICP) blocks are utilized to cover the flume and provide permeable surface. The flume's inner dimensions for length, width and depth are equal to 228.6 cm (90 inches), 55.88 cm (22

inches), and 60.96 cm (24 inches), respectively. The bottom 35.5 cm. of the flume and the top 5.08 cm filled with AASHTO No. 57 and AASHTO No. 8, respectively to form the storage gallery layers (Table 10).

(a)

(b)

Figure 15. Structure of the flume (a) Surface preparation (b) Edge construction

Table 10. Model Characteritics

Model Characteristics	Parameters	cm
Flow Dimension	Length	229
	Width	56
	Depth	61
Storage Layers	AASHTO No. 8	5.08
	AASHTO No. 57	35.5

It is known that clogging progression and infiltration rates decrement are greatly affected by pavement slope. The results indicated that by increasing the pavement slope from 2% to 10%, less surface permeability was observed (Haselbach, Valavala et al. 2006). Interlocking Concrete Pavement Institute (ICPI) manual suggests the minimum slope of at least 1% for the permeable pavement surface in order to provide sufficient stormwater drainage aptitude (Smith 2006). Although the manual suggests pavement slopes do not exceed 12%, permeable pavement slopes in urban areas are commonly less than 5%. Thus, 1%, 3%, and 5% were the selected slopes in these sets of experiments to investigate the effects of slope.

The gap size between paver blocks is the other pavements characteristic that affect the hydrological performance of PICPs. The joint spaces are prone to clogging by pollutant materials with various particle sizes. Fine elements such as clays, obstruct the voids and therefore prevent rain water from entering the storage gallery layers (Balades, Legret et al. 1995). In order to investigate the gap size efficacy in clogging progression and consequently captured runoff capacity, three different paver block types covered the 1.28

m^2 permeable surface area (Figure 16). The selected blocks are produced with their unique shapes, dimensions, and presenting gap sizes (Table 11). The paver gap sizes utilized in these tests were 6 mm, 9 mm and 12 mm. The flume's paved surface with paver blocks and the storage tank is shown in Figure 17.

(a) **(b)**

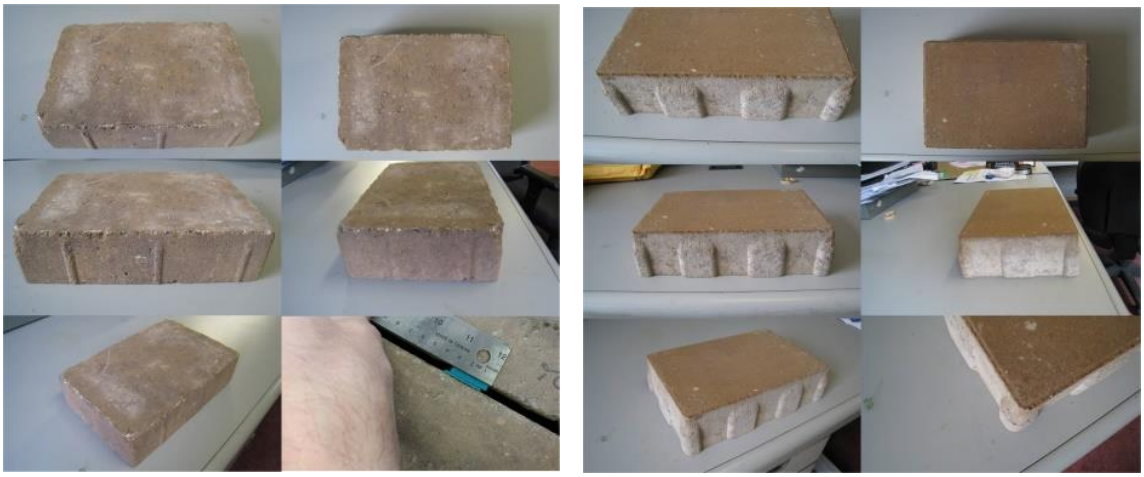

(c)

Figure 16. Paver block types (a) Coventry I ® (b) Eco-Cobble ® (c) Eco-Paver ® (Antunes 2013)

Table 11. Pavers' Characteristics in the Experiment

Gap Size (mm)	Paver Name	Dimensions (mm)
6	Coventry I	L:240, W:159, H:60
9	Eco-Cobble	L:240, W:159, H:60
12	Eco-Paver	L:240, W:157, H:82

(a)

(b)

(c)

Figure 17. Flume's paved surface (a) Conventry I (b) Eco-Cobble (c) Eco-Paver

ICPI manual recommends filling the joints in order to prevent smaller particle penetration and limit clogging to the top 20-25 mm layer of the surface (Smith 2006). Moreover, PICP effectiveness in trapping dissolved heavy metals depends on joint filling material characteristics. Although PICPs with larger gap sizes provide higher infiltration rates, joint filling material is needed to preclude metals from entering groundwater resources (Scholz and Grabowiecki 2007). In order to assess the effect of using joint materials on surface infiltration rates and clogging progression, different experimental models with and without joint materials were developed. Therefore, for each configuration of slopes and gap sizes, two different configurations were investigated. AASHTO No. 8

was used as a filling material between the paver gaps to prevent small debris from entering the storage layers. The experiment number and the detail configuration variables for each test are presented in Table 12.

Table 12. Experiment Variables

Experiment No.	Slope (%)	Paver Gap (mm)	Gap Filling
1	1	6	None
2	1	6	None
3	1	6	None
4	1	6	#8
5	1	9	None
6	1	9	#8
7	1	12	None
8	1	12	#8
9	3	12	#8
10	3	12	None
11	3	9	None
12	3	9	#8
13	3	6	None
14	3	6	#8
15	5	12	None
16	5	12	#8
17	5	9	None
18	5	9	#8
19	5	6	None

20	5	6	#8
21	1	6	#8

4.3.2. Instrumentation Plan

Instrumentation plan is necessary to monitor the hydrologic performance of the flume and determine clogging progression rates during experiments. TDRs installed to measure VWC from the recorded periods to track clogging advancement. The monitoring tools are Campbell Scientific TDRs' model CS616 (Campbell Scientific 2011). Seven TDRs were installed along the flume at 15 cm. under the paver blocks. Table 13 presents the TDRs identification number and the distance from the upgradient edge.

Table 13. TDRs ID and location

TDRs Identification Number	**Location from Upgradient eEdge (cm.)**
TDR01	28.58
TDR02	57.15
TDR03	85.73
TDR04	114.3
TDR05	142.88
TDR06	171.45
TDR07	200.03

5. MATLAB PERFORMANCE CHARACTERIZATION

Appropriately designed interlocking concrete block pavers reduce the amount of pollutants and the number of overflows reaching water bodies. Different forms of LID techniques, including PICPs, have been implemented to control overflows and manage stormwater runoff properly (James and Von Langsdorff 2003). The city of Louisville CSO 130 project is a unique PICP installation because of the location, extensive instrumentation, and continuous monitoring. The PICPs are located in an urbanized community area, where the physical environment can influence their performance and effectiveness. The pavement performance assessment was accomplished analyzing the data thus gaining a complete understanding of pavement performance throughout their clogging and maintenance cycles. The lessons learned from this study can lead to more effective PICP design in the future. Moreover, scheduling efficient cleaning methods based on site characteristics and pavements specifications are conceivable for observing suitable performance of the PICPs.

The results of this study are presented in two main parts; in the first section the overall PICPs performance and the main factors that affecting their operations are investigated. A review of the main hydrologic performance variables including infiltration rates, storage capacity, exfiltration rates, and hydraulic conductivity of surrounding soil layers and their variation over time are presented. After introducing the main variables and the comprehensive assessment on their performance, the second part develops multiple ANN models to estimate the hydrologic variables of the monitored PICPs. Based on the observed

real data, the prediction models are trained to forecast the PICPs operation based on site specifications and pavements characteristics. The accuracy of the models evaluated through comparing the estimated and recorded values with mathematical tools to ensure the models satisfactory result. In addition, by conducting the sensitivity analyses on the contribution factors, the efficacy of the studied parameters are determined. Therefore, the most effective parameters on the PICPs function are computed to improve future design and maintenance operations.

5.1. Overall Performance

The overall performance of a PICP system is influenced by its infiltration rates, storage capacity, exfiltration rates, and hydraulic conductivity of its surrounding soil layers. By better understanding the influence of each of these parameters on the overall system, a more efficient design or operational schedule can be established. Infiltration rates into the storage gallery computed by observing the pressure transducers data. The associated water level increment investigated during and after rain events to measure the infiltration capacity. Captured runoff variation is observed through monitoring the recorded water levels to compare the PICP's operation over time. Also, the exfiltration rates from the gallery layers to the surrounding soil medium calculated by measuring the drawdown rates of water level. Hydraulic conductivity of the soil layers is specified by computing the drainage rates at different levels for each soil layer. The main characteristics of the PICPs and the controlling factors for each of them are elaborated in the following sections to comprehend the PICPs functionality factors.

5.1.1. Gallery Permeability Rates

In the natural environment, both rock and soil materials contain open spaces where water may be stored and through which it can move. Permeability, or hydraulic conductivity, is a measure of the ease of water movement through the open spaces. Since the main application of PICPs is their ability to infiltrate, store, and pass runoff water during rain events, the water movement rates within PICPs have a notable effect on their operation. However, since surface runoff water carries sediment along its path the sediments clog the system through water movement into the system and consequently infiltration rates decrease.

Previous studies have focused on recorded TDR data to quantify surface clogging progression. Brown and Borst have developed the model to remotely determine surface clogging and its progression with cumulative rainfall depth. The proposed model is able to track the clogging length on the PICP surface by monitoring the recorded peak VWC values and schedule the maintenances accordingly (Brown and Borst 2013). However, since the TDRs are installed close to the surface, the results designate only surface infiltration rates. It has been observed that surface clogging is not the only problem that occurs in the practices; small debris is also transported by stormwater and deposited inside the storage gallery ultimately reducing the porosity of the filled material. Therefore, in order to assess overall performance of the entire PICPs other tools are required.

As the void space of the aggregate material decreases, the permeability of the storage gallery diminishes and the time necessary to drain the gallery increase. The available void space within the storage gallery gets reduced due to settlement, debris penetration, biological growth, and sediment accumulation that directly affect the captured runoff.

Infiltration rates at the surface and the permeability of the gallery however is not uniform across the entire length of the PICP practices as sediment accumulation is localized due to surface runoff flow. Therefore, sediment deposition amount and clogging progression rates vary based on site characteristics and rain events' variables.

In this study, the effects of the gallery porosity on the infiltration rates were assessed over a two-year period by observing the water level. The infiltration rates into the storage gallery are computed by monitoring the collected data from naturally occurring rain events and water level variation rates of the installed piezometers. At first, based on the occurred rain events, the associated peak water levels during or until six hours after rain events determined. Then, for all of the occurred rain events in the study period the peak water level equals at least 12 cm and the closest 5 cm water level prior to the peak value are calculated. After obtaining these two values for each rain event and based on the associated time for them, MATLAB codes were written to calculate the infiltration rates.

The gallery permeability's within PICP 19G were calculated and compared for multiple rain events and locations in Figure 18. The maximum gallery permeability measured in piezometer 41L (located 12.2 m from the upgradient edge) is five times greater than the maximum gallery permeability of piezometer 40L (located 0.8 m from the upgradient edge). The significant difference in calculated permeabilities is likely due to the clogging and sediment accumulation along the upgradient edge of the PICP system. The correlation coefficient among the gallery permeabilities are stronger for the initial 200 mm cumulative rainfall depth. However, by increasing the cumulative rainfall depth and rain intensity the gallery permeability calculations display different correlations due to dissimilar clogging patterns. Since the upgradient edge of the PICP practices clogs much faster, the coefficient

of correlation among the permeabilities of the two downgradient piezometers equals 0.89 which demonstrates similar sediments deposition pattern in the downside (Figure 18).

(a)

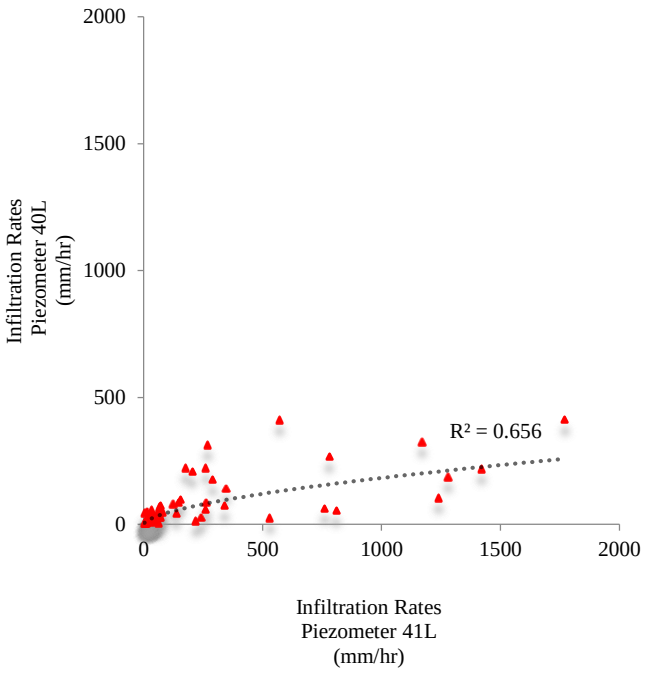

(b)

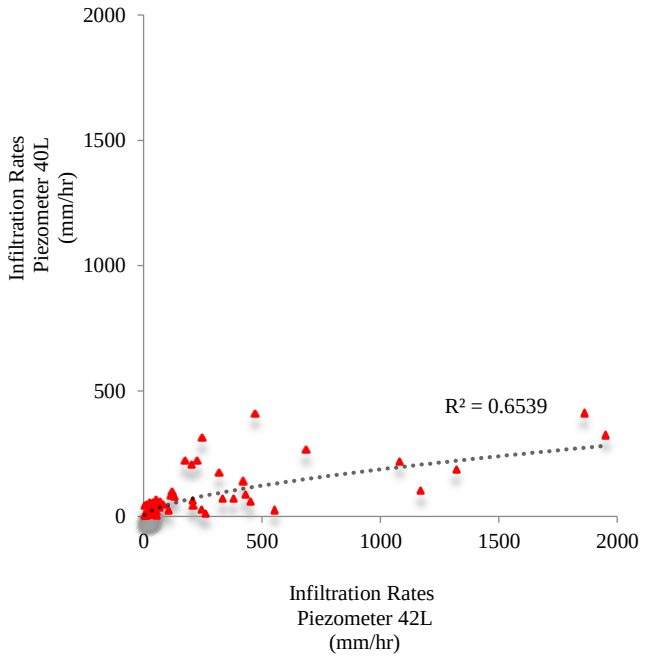

(c)

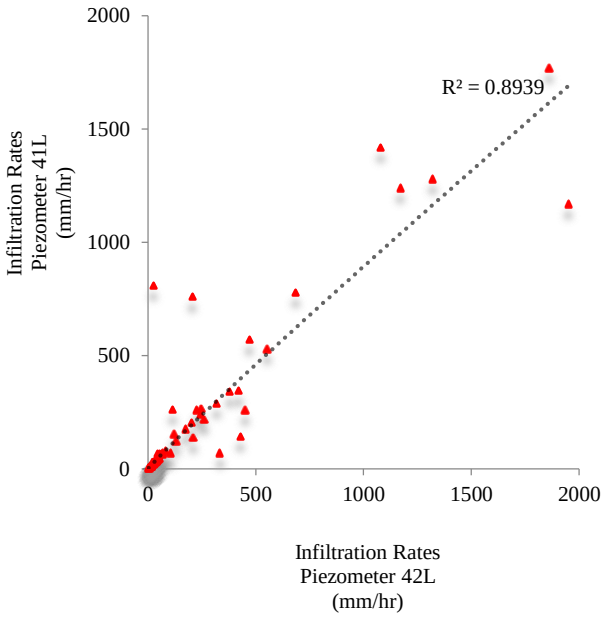

Figure 18. Gallery permeability rates comparison of PICP 19G (a) Piezometer 41L-40L (b) Piezometer 42L-40L (c) Piezometer 42L-41L

The gallery permeability was also calculated at three different locations within PICP 19H (Figure 19). It was observed that the gallery permeability pattern is different than control 19G; the location, the curb condition, and other site characteristics play an important role on the surface runoff flow and should be considered for stormwater management control's design. Because of the curb condition and the alley in the upper side of 19H, the surface runoff flows toward the upper edge of the pavement system and from the sidewalk to the center of the practice (Figure 20).

(a)

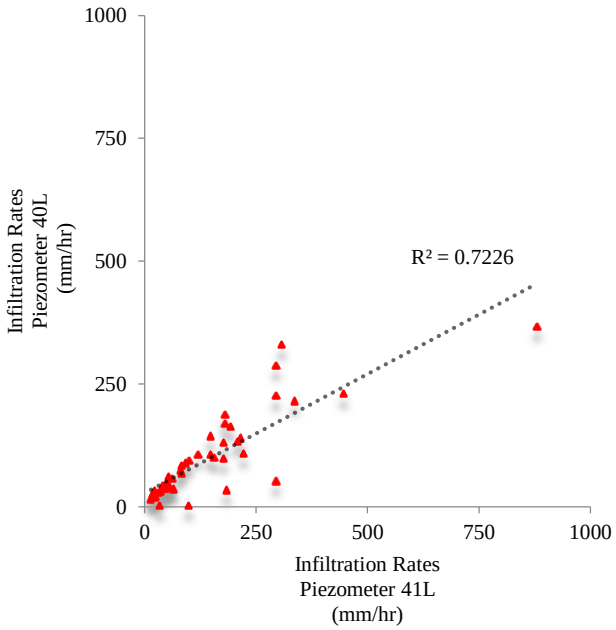

(b)

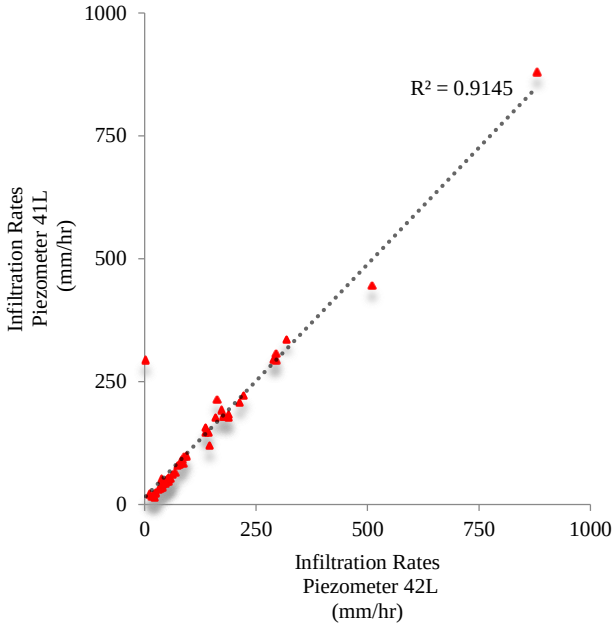

(c)

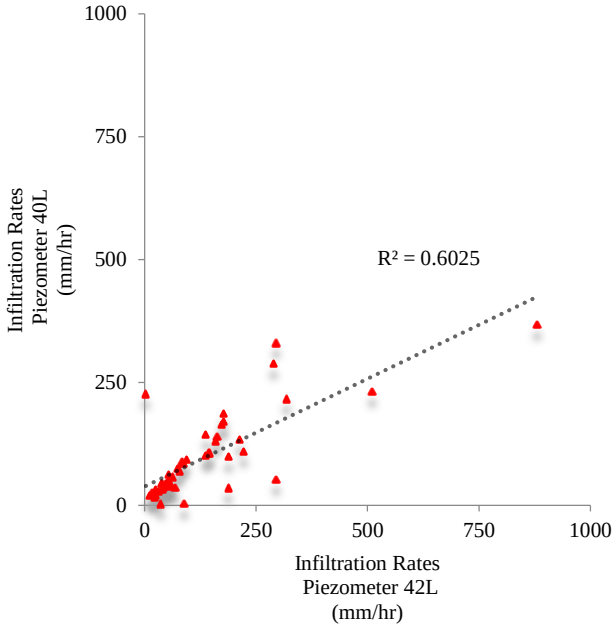

Figure 19. Gallery permeability rates comparison of PICP 19H (a) Piezometer 41L-40L (b) Piezometer 42L-41L (c) Piezometer 42L-40L

(a)

(b)

Figure 20. PICP 19H (a) Upgradient edge (b) Curb Condition

5.1.2. Storage Capacity

During a rain event, the surface runoff is captured by the PICP system and temporarily detained within the storage gallery where it gradually exfiltrates to the surrounding soil layers. The contributing physical factors change the efficiency of the gallery and consequently the gallery storage capacity decreases. The storage capacity of the PICPs varies over time depending on many factors such as the surface properties, available porosity of the filled material, saturation percentage of the base reservoir, and surrounding soil layers characteristics.

Surface property of the PICPs is subjected to vary because of clogging and the site characteristics. Surface clogging which is mainly due to debris accumulation on the PICPs' surface engenders surface infiltration rates decrement. The concentrated flow results in surface clogging with a higher rate in comparison to a dispersed flow. Site characteristics such as road and permeable pavement slopes are the important factors that govern the flow width and the clogging progression. Longitudinal slope along the length, transverse slope along the width at the upgradient and downgradient edge of the PICPs cause runoff flow from the upper side toward the downgradient edge and from the crown of the street to the curb side (Table 1). In addition, smaller particles size of sediment penetrate into the storage gallery and clog the available pour structure (Figure 21). Therefore, reducing the available porosity of the filled material leads to storage capacity reduction of the PICPs.

Saturation percentages of the underlying layers vary according to the preceding rainfall characteristics and specifically Antecedent Dry Period (ADP). Shorter ADP cause the saturation percentage retains high for a longer period and eventually cause lesser storage capacity. Hydraulic conductivity of the surrounding soil layers are highly important factor

on specifying the water drainage rates from the PICPs. Thus, the entered rain water volume in the storage gallery alters and as a result the PICPs are not being able to capture the designated surface runoff water. By observing the recorded water levels in the storage gallery, the PICP's performance in capturing surface runoff water determined.

(a)

(b)

Figure 21. Sediment penetration into the storage gallery (a) Under paver blocks (b) Gravel layers

During rain events, the installed piezometers within the PICPs 19G and 19H measure the water levels. The maximum recorded water levels during or after each rain event calculated and compared for the first two years of their installation (December 2011 until December 2013). There is no need for correcting the recorded water level of the piezometers, since the bottom of the subbase reservoir is level,. Analyses demonstrated discrepancies in the captured runoff water within different sections of each PICP because of different clogging rates. The correlation of coefficient among the water levels reveals the sections with the same hydrologic performance (Figure 22).

(a)

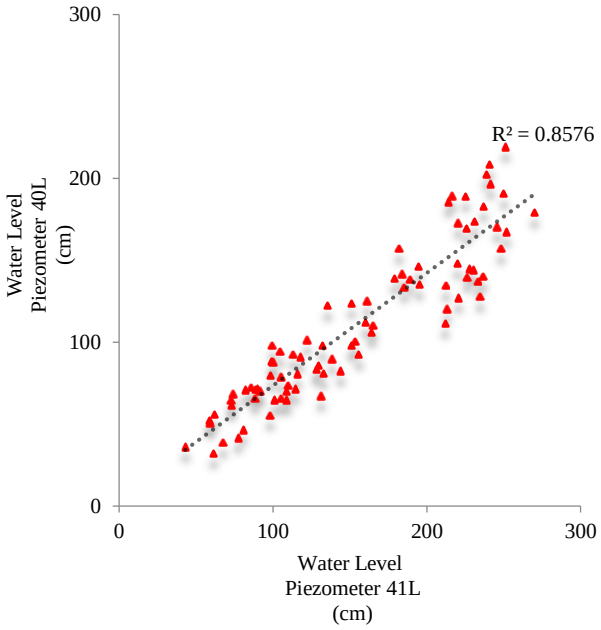
300
200
100
0
0
100
200
300
R² = 0.8576
Water Level Piezometer 40L (cm)
Water Level Piezometer 41L (cm)

(b)

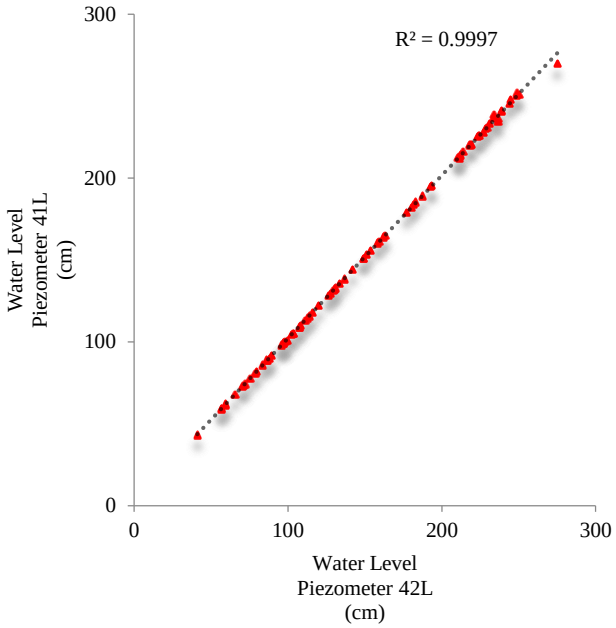

(c)

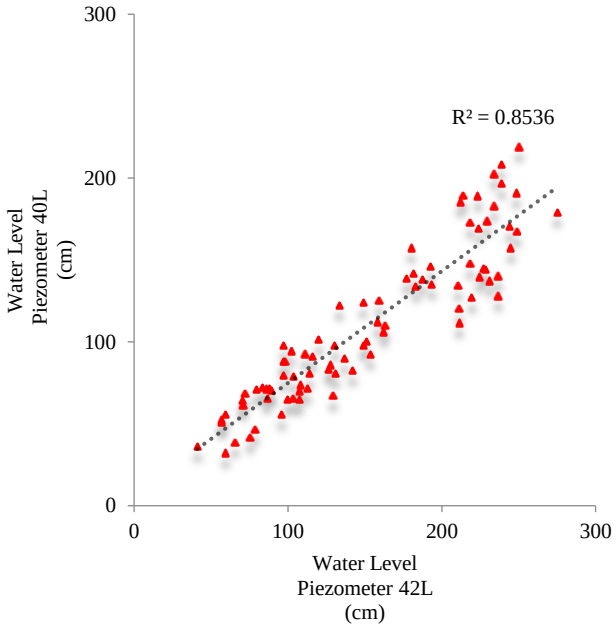

Figure 22. Water level comparison of PICP 19G (a) Piezometer 41L-40L (b) Piezometer 42L-41L (c) Piezometer 42L-40L

The coefficient of correlation between measured peak water levels in 19H is 0.96 and higher for the studied period. The results demonstrate a uniform clogging pattern and similar performance on storage capacity (Figure 23). The height and distance from the curb is an important factor because it controls runoff flow from the sidewalk over the PICP. In PICP 19H, the curb height is not sufficient that cause surface runoff to flow over the sidewalk. It was detected that the surface runoff flow over the sidewalk and in the downside finds its way back to the pavement surface.

By comparing the two capacities, it is observed that the storage capacity loss is proportional to the associated drainage area of the PICPs and the impervious area to the upgradient edge ratio. Since the drainage area for PICP 19G (0.29 ha) is larger than the associated drainage area for PICP 19H (0.10 ha), a greater runoff water volume flows over PICP 19G. Furthermore, the impervious area to the upgradient edge ratio for PICP 19G is 881 m^2, while it is 398 m^2 for 19H (Table 1). Therefore, greater surface runoff volume flow over PICP 19G result in higher sediment deposition rates at the upgradient edge and the perceived storage capacity loss is greater than the loss in PICP 19H.

(a)

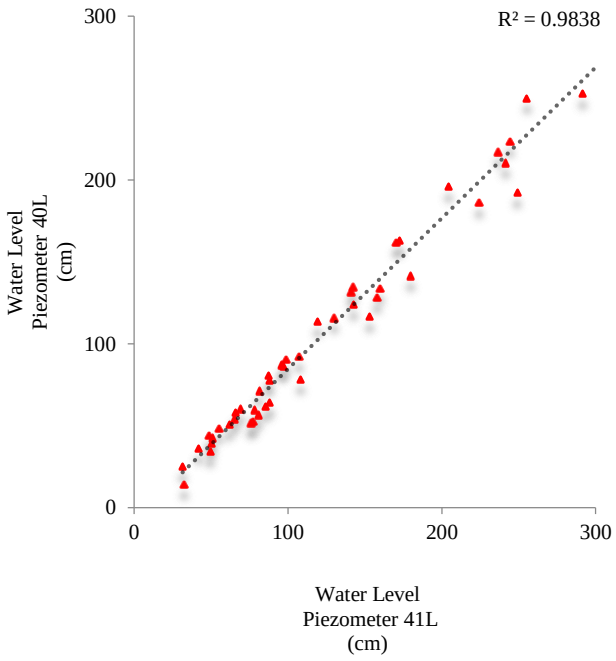
R² = 0.9838
300
200
100
0
0
100
200
300
Water Level Piezometer 40L (cm)
Water Level Piezometer 41L (cm)

(b)

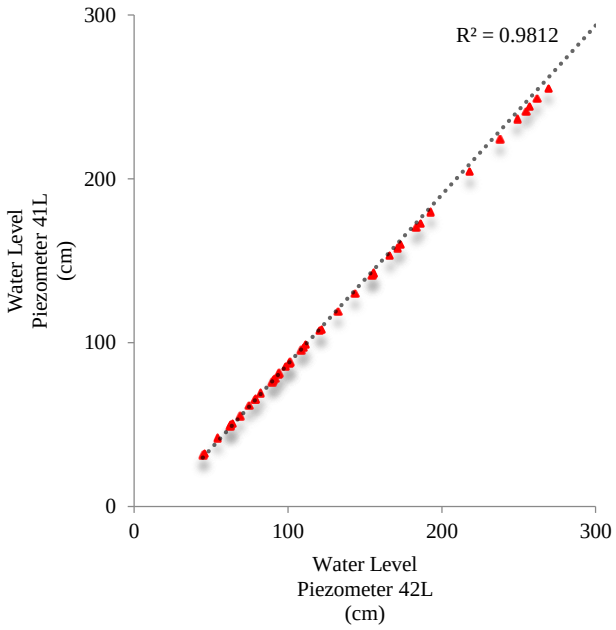
R² = 0.9812
300
200
100
0
0
100
200
300
Water Level Piezometer 41L (cm)
Water Level Piezometer 42L (cm)

(c)

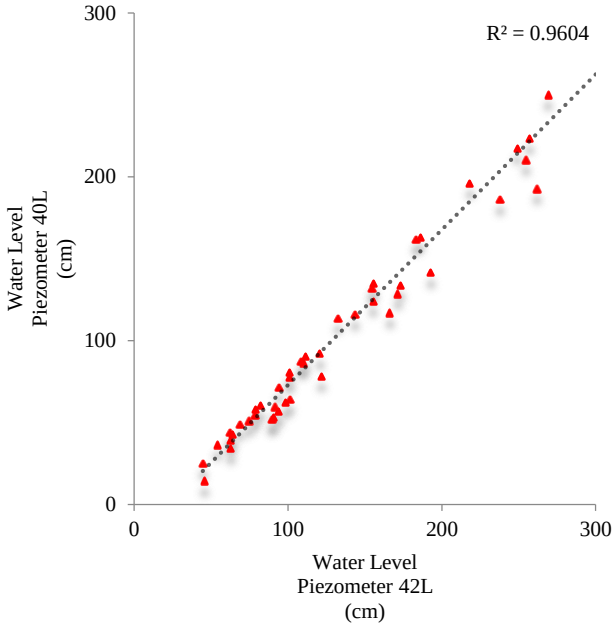

Figure 23. Water level comparison of PICP 19H (a) Piezometer 41L-40L (b) Piezometer 42L-41L (c) Piezometer 42L-40L

5.1.3. Exfiltration Rates

The captured water in the storage gallery gradually exfiltrates from the PICP systems to provide storage capacity for capturing additional surface runoff water. The exfiltration rate is an important hydrologic factor on the PICPs' performance because during long and intense storm events overflow across the surface or through a perforated drainage pipe have been witnessed. At that point, the PICPs are not able to capture rain water and the system would in effect be generating runoff. The exfiltration rates of the PICPs are related to the storage gallery porosity and the surrounding soil layers saturation percentage. Therefore, porous percentage reduction and saturation percentage enlargement in the underlying

layers result in exfiltration rates diminution of the PICPs to the surrounding layers (Figure 24).

(a)

(b)

Figure 24. Block paver settlement (a) Adjacent to street pavement (b) Surcharge load

In this study, the exfiltration rates of the PICPs computed with the same MATLAB codes methodology that was written to compute the gallery permeability rates. The employed formulas modified to compute the water level decrement rates rather than the increment rates in the piezometers. The exfiltration rates at six different sections of the PICPs 19G and 19H calculated and compared with each other (Figure 25 and Figure 26).

The analyses on the exfiltration rates and the detected patterns present similar performance in the two studied practices. The computed exfiltration rates are closer at first, however, by increasing the cumulative rainfall depth beyond 2200 mm the results discrepancies become larger. After certain sediment amount deposition and since it is more likely that the sediment penetrates with a higher rates in the upgradient edge, the exfiltration rates decline faster in the upper side of the practices in comparison to the down side. Although conducting several maintenance methods, the results proved that the maintenances were not able to remove the trapped materials from under the blocks because they only remove debris from the PICP surface. Hence, the maintenances can only restore the surface infiltration rates whereas the exfiltration rates are not able to get restored.

(a)

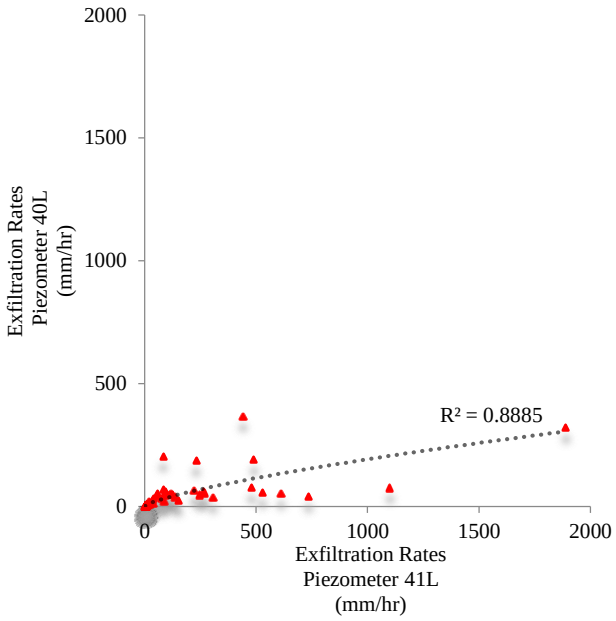
2000
1500
1000
500
0
0
500
1000
1500
2000
Exfiltration Rates Piezometer 40L (mm/hr)
Exfiltration Rates Piezometer 41L (mm/hr)
R² = 0.8885

(b)

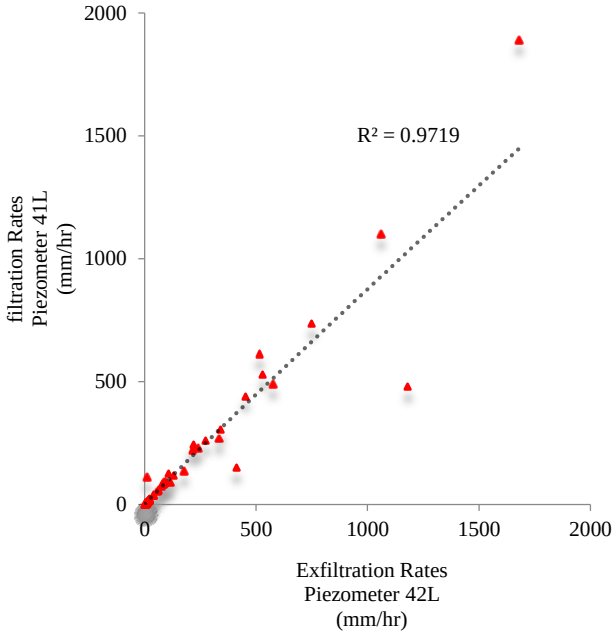

(c)

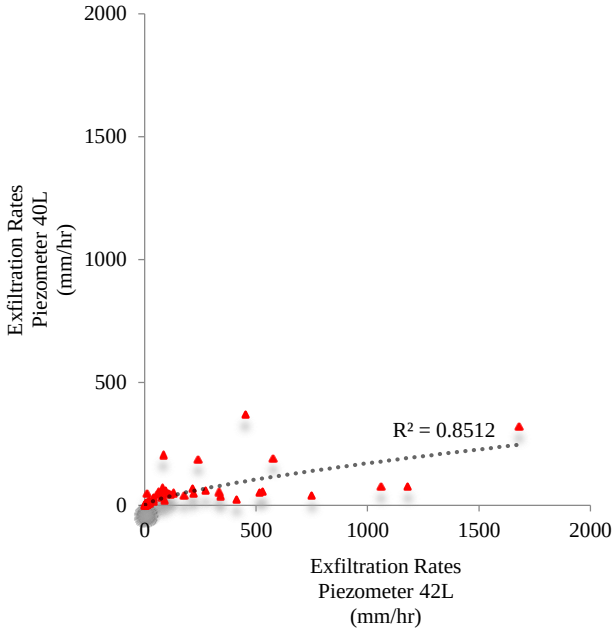

Figure 25. Exfiltration rates comparison of PICP 19G (a) Piezometer 41L-40L (b) Piezometer 42L - 41L (c) Piezometer 42L-40L

(a)

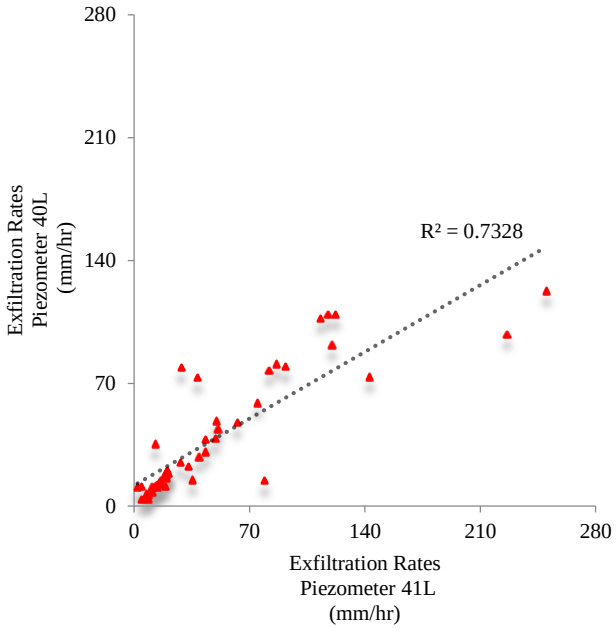
280
210
140
70
0
0
70
140
210
280
R² = 0.7328
Exfiltration Rates
Piezometer 40L
(mm/hr)
Exfiltration Rates
Piezometer 41L
(mm/hr)

(b)

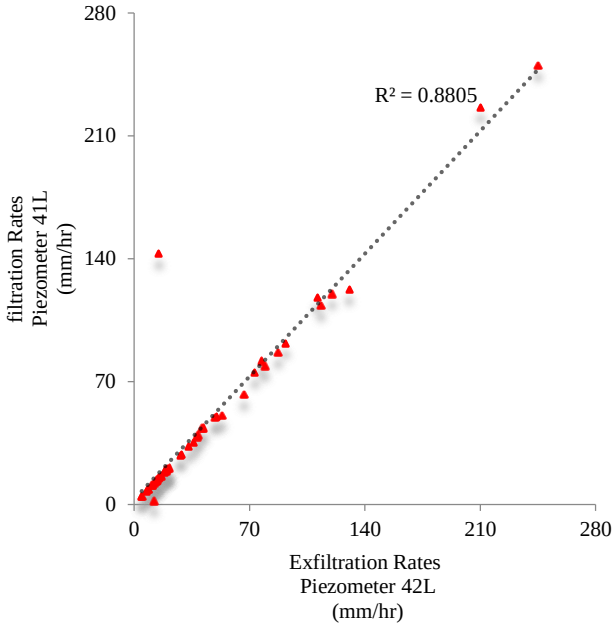

(c)

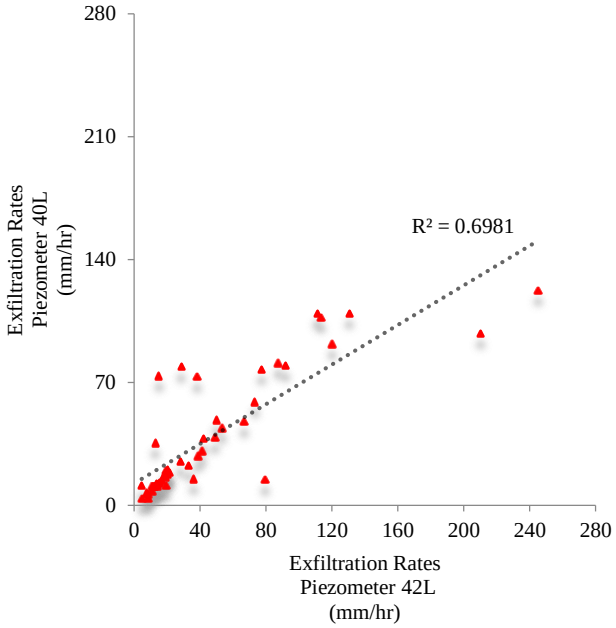

Figure 26. Exfiltration rates Comparison of PICP 19H (a) Piezometer 41L-40L (b) Piezometer 42L-41L (c) Piezometer 42L-40L

5.1.4. Hydraulic Conductivity of Soil Layers

The hydraulic conductivity of the surrounding soil layers highly affects the water drainage rates from the PICPs to the surrounding medium. The hydraulic conductivity of the soil layers vary based on soil characteristics, saturation percentage rate, and the captured water level in the storage gallery. Therefore, it was necessary to collect samples from the underlying soil layers before construction to run tests on soil physical properties and specifically their hydraulic conductivity rates.

The hydraulic conductivity of the surrounding soil layers were computed for the PICPs 19G and 19H. The written MATLAB codes calculate the drainage rates for each soil layer based on the recorded water levels in the piezometers. The analyses on the two monitored PICPs revealed that each soil layer absorb the stored water through their own hydraulic conductivity rates. The measured hydraulic conductivity rates vary vertically because of different soil layers and also horizontally along the PICPs. Various hydraulic conductivity rates demonstrated different water drainage performances within the PICPs. Since at the bottom of the storage gallery retains water longer, higher saturated percentage and lesser hydraulic conductivity rates perceived in the lower soil layers as it can be seen in the Figure 27 and Figure 28. However, by increasing the water level the saturation percentage decreases and the soil layers absorb the water with higher hydraulic conductivity rates. The coefficient of correlation and the relationship between the soil layer levels and the hydraulic conductivities in the PICPs 19G and 19H are shown in Figure 27 and Figure 28.

(a)

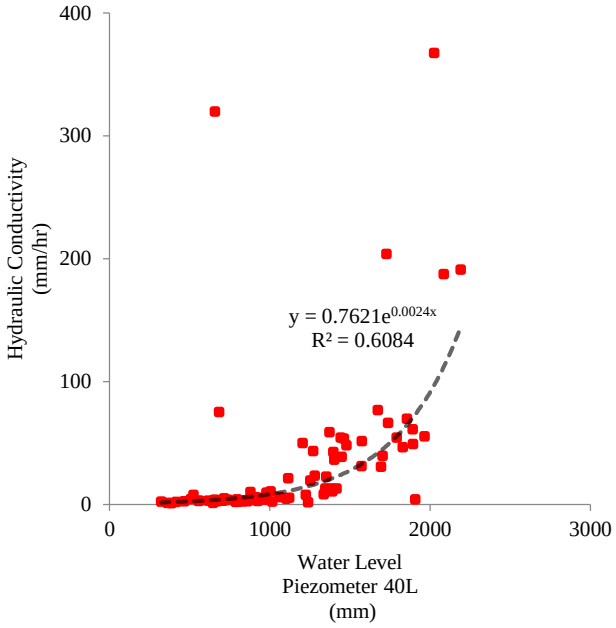
400
300
200
100
0
Hydraulic Conductivity (mm/hr)
y = 0.7621e0.0024x
R² = 0.6084
0
1000
2000
3000
Water Level Piezometer 40L (mm)

(b)

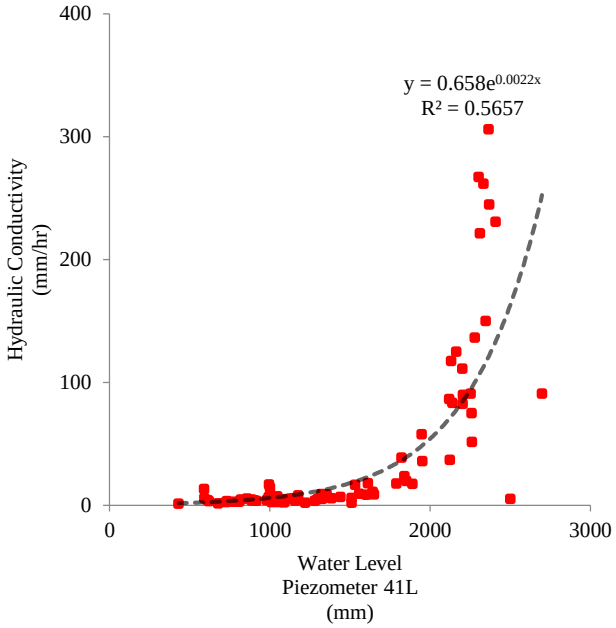
400
300
200
100
0
Hydraulic Conductivity (mm/hr)
y = 0.658e0.0022x
R² = 0.5657
0
1000
2000
3000
Water Level Piezometer 41L (mm)

(c)

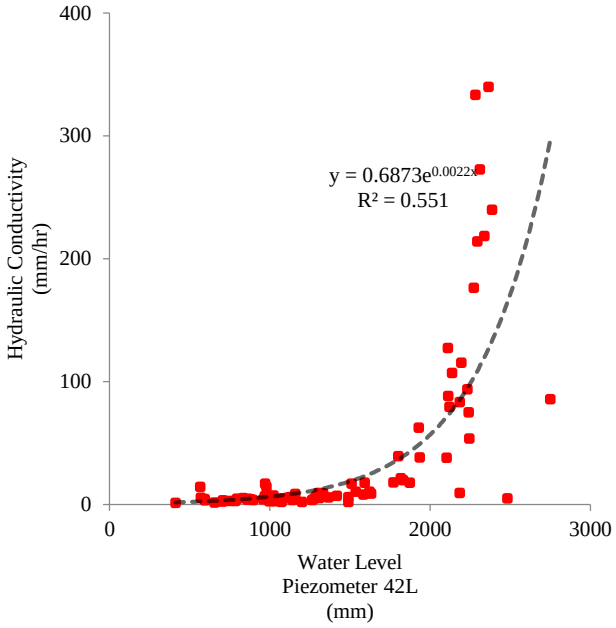

Figure 27. Hydraulic conductivity of soil layers in PICP 19G (a) Piezometer 40L (b) Piezometer 41L (c) Piezometer 42L

(a)

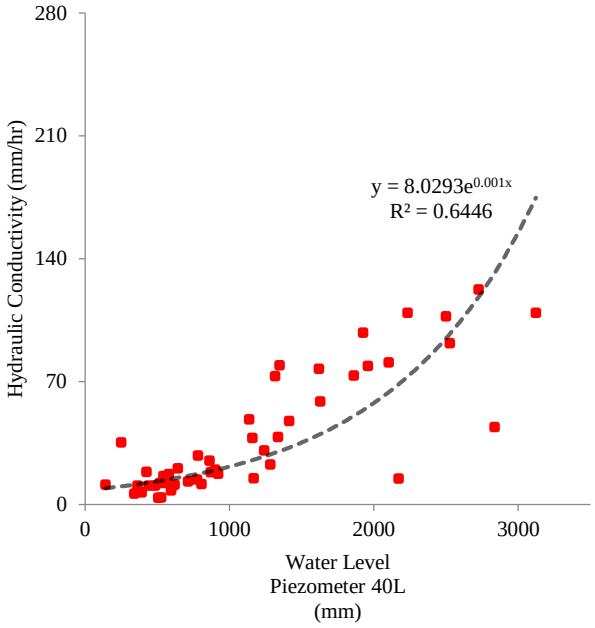
280
210
140
70
0
Hydraulic Conductivity (mm/hr)
y = 8.0293e0.001x
R² = 0.6446
0
1000
2000
3000
Water Level
Piezometer 40L
(mm)

(b)

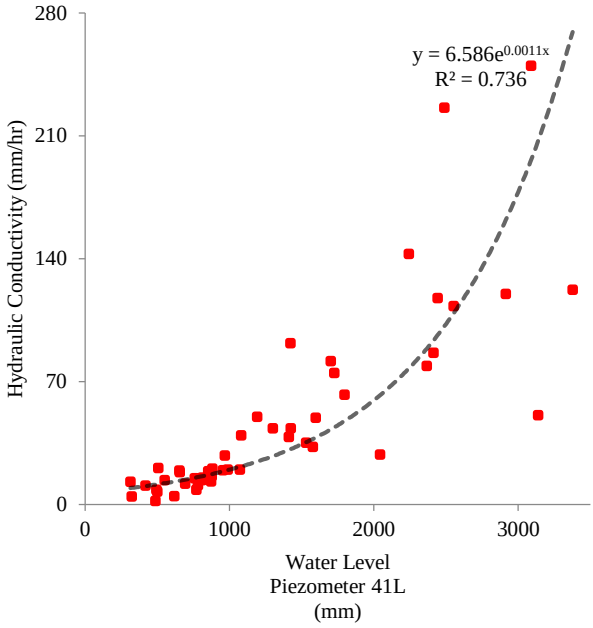

(c)

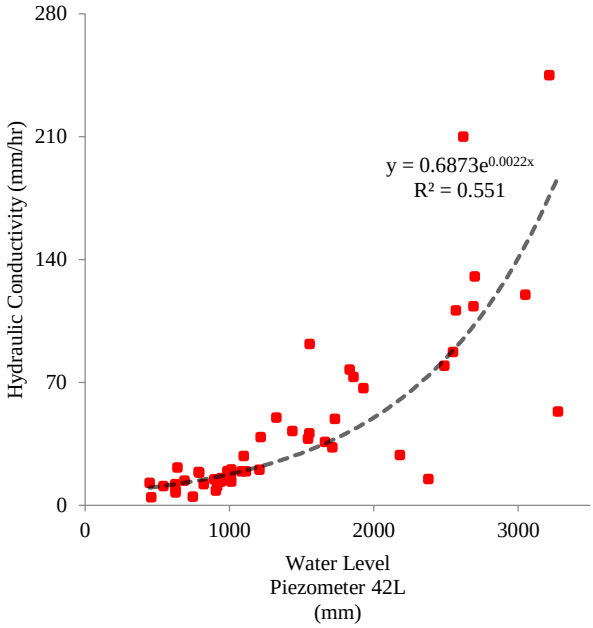

Figure 28. Hydraulic conductivity of soil layers in PICP 19H (a) Piezometer 40L (b) Piezometer 41L (c) Piezometer 42L

6. RESULTS

6.1. Developing Neural Network Models

In this study, new prediction models are built using ANN to forecast the hydrologic characteristics of the PICPs. ANN is utilized as a strong tool to develop the models to predict the main PICPs' performance variables regarding the contributing parameters. Accurate estimation of the main hydrologic characteristics of the PICPs is required to comprehend the permeable pavement's performance. Moreover, a sensitivity analysis is completed to determine the efficacy of the contributing factors on the PICPs' operation. Hence, considering the effective parameters in the PICP design results in a comprehensive stormwater control plan and better PICP performance is achieved through the improved design.

Captured runoff and clogging progression rates, as the main performance features of the PICPs, studied in relation to the site characteristics. The captured runoff models developed through scrutinizing the peak water level in the PICPs elaborated more in detail in section 4.3. The clogging progression rates models, which presented in section 4.4., developed through monitoring the peak VWC of the PICPs. Rain event properties and maintenance treatments are the main factors that are considered in this study to monitor and forecast the PICP performances. The operational information of the monitored PICPs, the recorded rainfall events' data, and the conducted maintenances are the parameters utilized for developing the ANN models; the rainfall events' parameters and the

maintenance methods, as the input variables in the developed models, are studied more in detail in the sections 4.2.1 and 4.2.2.

Twenty one model configurations with different combinations of slope, gap size, and joint filling material were built to study the PICPs' physical characteristics on their performances (section 3.3.). In this study neural network models were developed to predict the clogging and the infiltration edge progression length along several PICPs laboratory tests. Sensitivity analyses were completed to determine the relative importance of the PICPs' specifications on the hydrologic operation for each configuration. Sections 4.5 and 4.6 detail results in regard to the clogging progression and the infiltration edge models, respectively. By better understanding the effects of pavement characteristics and choosing the most efficient PICP configuration, improved PICPs' design and enhanced performances are achievable.

6.1.1. Rainfall Data

The rainfall parameters used for the ANN models were based on two years of rainfall data measured by the rain gauge (TR05) located less than 0.75 km from the installed PICPs. TR05 records rainfall data by utilizing a tipping bucket to measure rainfall depths equal or greater than 0.0254 cm. every 5 minutes. In order to be able to assess the efficacy of rain events on the pavement's function, a compliant definition for rain events is essential. The Environmental Water Resources Institute defines rain events as when the cumulative depth in the rain gauge is equal or greater than 0.127 cm. In addition, the interval between the two measured rainfall data cannot exceed six hours (Environmental Water Resources Institute 2007). The following parameters were derived for each rain event and are utilized as the input parameters in the prediction models.

- Rain event duration (min.): time period from start till end time of rainfall
- Rainfall Depth (cm.): amount measured for each event (> 0.127 cm.)
- Peak 5 min intensity (cm/min): maximum (rainfall depth/5 minutes duration)
- Peak 15 (20) min intensity (cm/min): maximum (rainfall depth/15 (20) minutes duration)
- Peak Duration (min.): period with the maximum peak intensity
- Cumulative rainfall depth before the event from the construction (cm.): rainfall amount measured from the PICP installation prior to event
- Cumulative rainfall depth before the event from the last maintenance (cm.): rainfall amount measured from the last cleaning prior to event
- Antecedent Dry Periods (min.): time period since previous rain event (> 6 hr.)
- Previous Rainfall Depth (cm.): rainfall depth of the last occurred event

Based on the above definition, a total of 153 rain events occurred during the two year study period. The listed rain events characteristics are imported as the input variables to develop ANN models.

6.1.2. Cleaning Methods

As stated in section 3.1.3., maintenance treatments conducted on the two PICPs, 19G and 19H, include a variety of techniques. Street sweep trucks, pressurized air jets, and hydro excavator trucks are the cleaning methods that were completed to remove the debris and accumulated sediment from the joints between the paver blocks and the surface of the PICPs. To be able to assess the impacts of maintenances, specific numbers are assigned for

each cleaning method within the ANN model. The maintenance method during the pavement installation and the first cleaning sets to code 1 and the other cleaning method codes are presented in Table 14. Although three air jet maintenances were conducted on the PICPs, separate codes are assigned to each of them because their efficacies are highly variable.

Table 14. Cleaning Method Codes for ANN model

Maintenance Treatment	Code for PICP 19G	Code for PICP 19H
No Maintenance (New Installation)	1	1
Sweeper Truck	2	_
Air Jet No. 1	3	2
Air Jet No. 2	4	3
Air Jet No. 3	5	4
Hydro Excavator Truck	6	_

6.2. Captured Runoff Model

The ANN models were developed to predict the runoff volume captured by the permeable pavement system. By monitoring the maximum water level within the PICPs, an indication of the storage capacity, the maximum captured water level during or after rain events could be computed. The captured runoff database including the peak water levels, as the output parameter, and the aforementioned input variables (rain events' variables and cleaning method) for the two PICPs 19G and 19H was prepared (Appendix A). Based on the rain events in a two year study, the maximum water levels was found with a written code in MATLAB. The time window that the MATLAB code considers to find

the maximum water levels begins from the start of the rain events till six hours after the end of the events. The peak water level at different locations of the PICPs that determines the storage aptitude is the output variable in the prediction models.

6.2.1. Database Preparation

The comprehensive database was obtained from rain events' characteristics and hydrologic performance of the permeable pavement controls over the two years period from the construction time. The rain events' parameters, the cleaning method codes that are related to each event and the maximum observed water levels in the pressure transducers were used for developing the ANN model. The data from a total of 138 rain events with the relative observed maximum water levels and the cleaning method codes related to each event were analyzed for control 19G (Appendix B). In addition, the dataset for control 19H contained 135 events data parameters in addition to the associated peak recorded water levels in the installed pressure transduces (Appendix C).

It is noteworthy that some of the data were eliminated from the datasets if any parameter values were missed. One hundred and two events of the dataset for control 19G (74%) were randomly chosen for training and the remaining thirty six items (26%) were used for testing the proposed model. Also, in control 19H, the data sets were arbitrarily divided into training and testing subsets. One hundred datasets (74%) were dedicated to train the model while thirty five (26%) events were allocated to test the accuracy of the proposed prediction formula. The parameter values that were allotted for testing the models are presented as bold (Appendix B and Appendix C).

6.2.2. Prediction Model

As stated earlier, developing the prediction models of the main PICPs' performance variables are necessary to improve the operation of the future models. The rain events' parameters and the last conducted cleaning methods on the PICPs are the inputs, and the maximum water level in the piezometers is the output parameters in the prediction models. As a result, the input layer has 10 neurons which each neuron is processing specific parameters while the captured runoff level is the only specified neuron in the output layer. After running the analysis and monitoring the results, the hidden layer characteristics and the desired model architecture that provides the most accurate results (highest correlation coefficient value) was determined.

Based on the developed ANN models, the water levels of the piezometers 40L, 41L and 42L can be predicted for the test dataset (Figure 29, Figure 30, and Figure 31). The predicted and real water levels comparison for piezometer 40L in control 19G demonstrates $R = 1.00$ for the training datasets and $R = 0.79$ for test database (Figure 29). By observing the model performance indices, the hidden layer with 10 neurons is the optimum model for the upgradient pressure transducer.

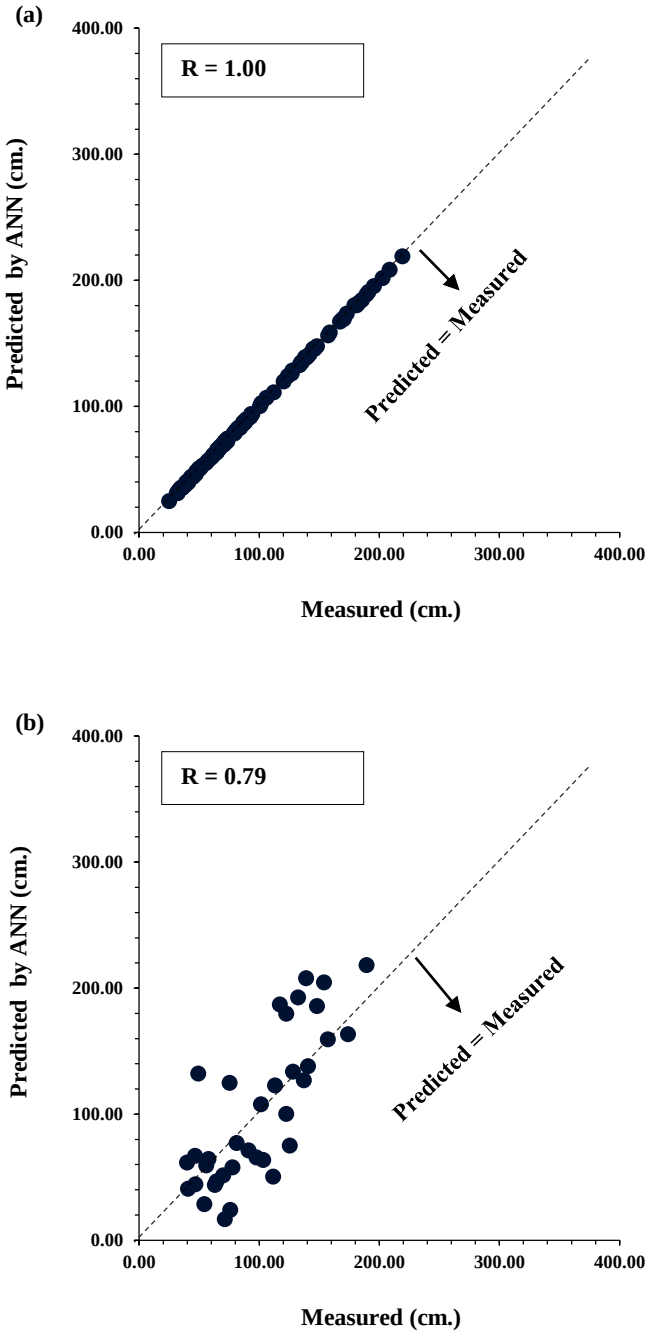

Figure 29. Predicted vs. measured water levels in piezometer 40L of Control 19G (a) Training data; (b) Testing data

The prediction model for water levels in piezometer 41L of control 19G predicts the most accurate results with one hidden layer and 16 neurons. The computed correlation coefficient for training data equals one while for test dataset equaling 0.79 (Figure 30).

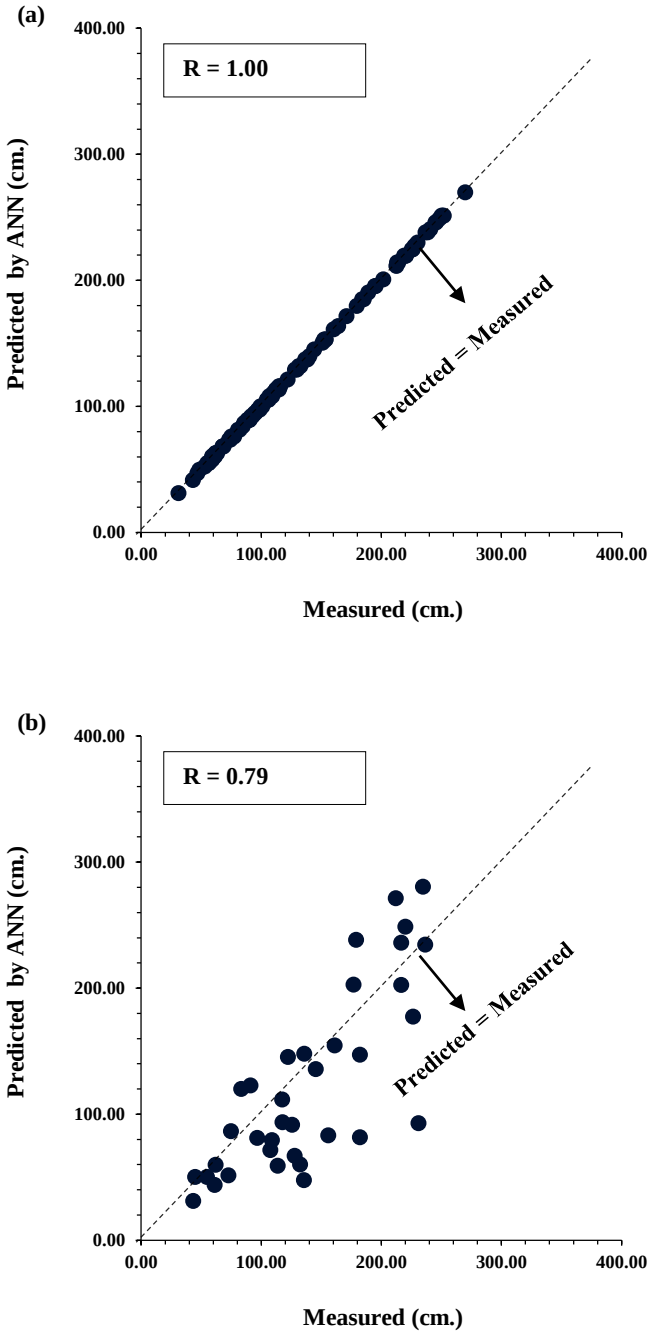

Figure 30. Predicted vs. measured water levels in piezometer 41L of Control 19G (a) Training data; (b) Testing data

The optimum model for the downgradient piezometer in control 19G (42L) has one hidden layer with 10 neurons. Correlation coefficients of 1.00 and 0.79 are obtained for train and test datasets, respectively (Figure 31).

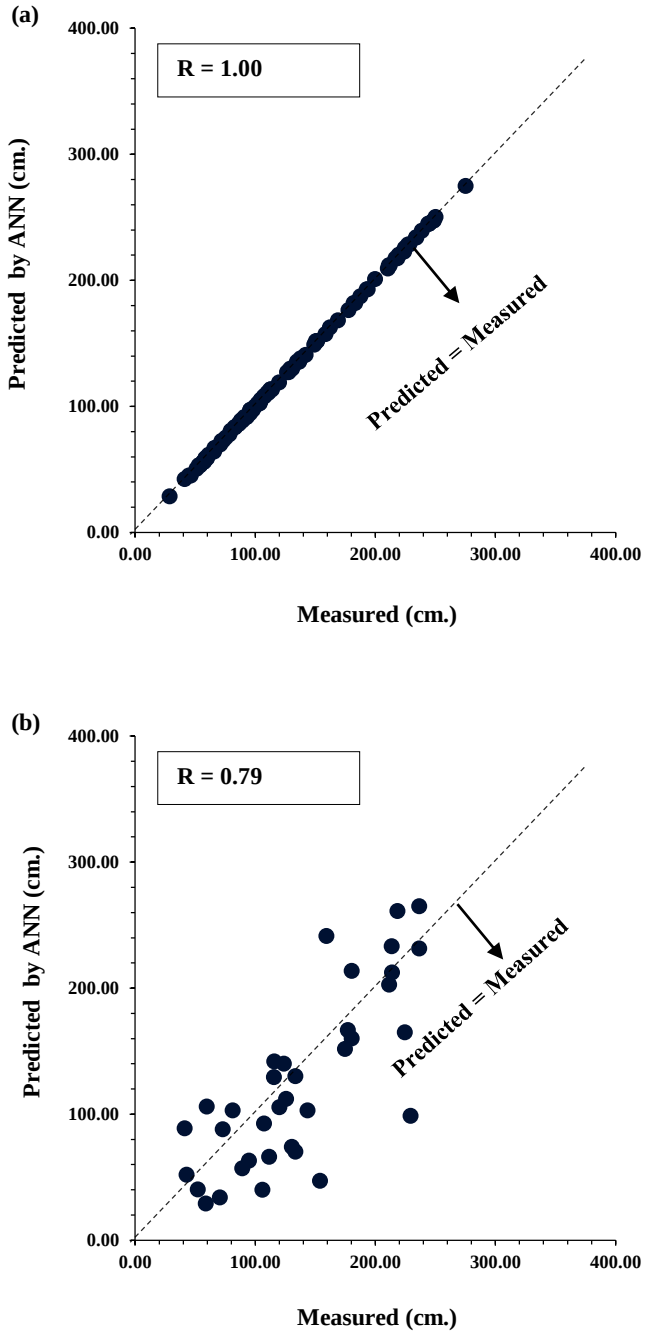

Figure 31. Predicted vs. measured water levels in piezometer 42L of Control 19G (a) Training data; (b) Testing data

The same prediction models were developed for captured runoff volume at three different locations of GI control 19H. The Correlation of coefficient for the upgradient

pressure transducer at 1.4 m from the upper edge equals 1.00 and 0.78 for training and testing subsets, respectively (Figure 32).

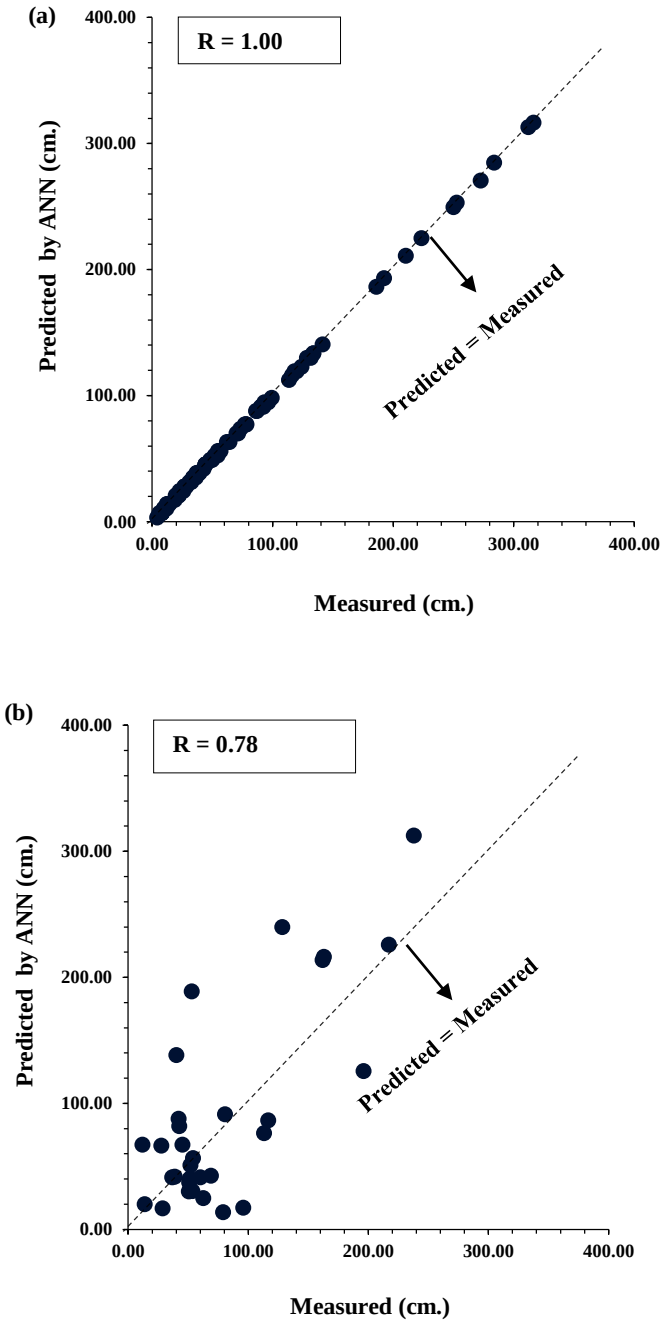

Figure 32. Predicted vs. measured water levels in piezometer 40L of Control 19H (a) Training data; (b) Testing data

The accuracy of the prediction model for the installed piezometer at the center of GI control 19H, which demonstrates the model ability to predict the water levels equaling 0.78 while the correlation coefficient is 1.00 for the training datasets. The prediction results and the model accuracy for training and testing dataset are shown in Figure 33.

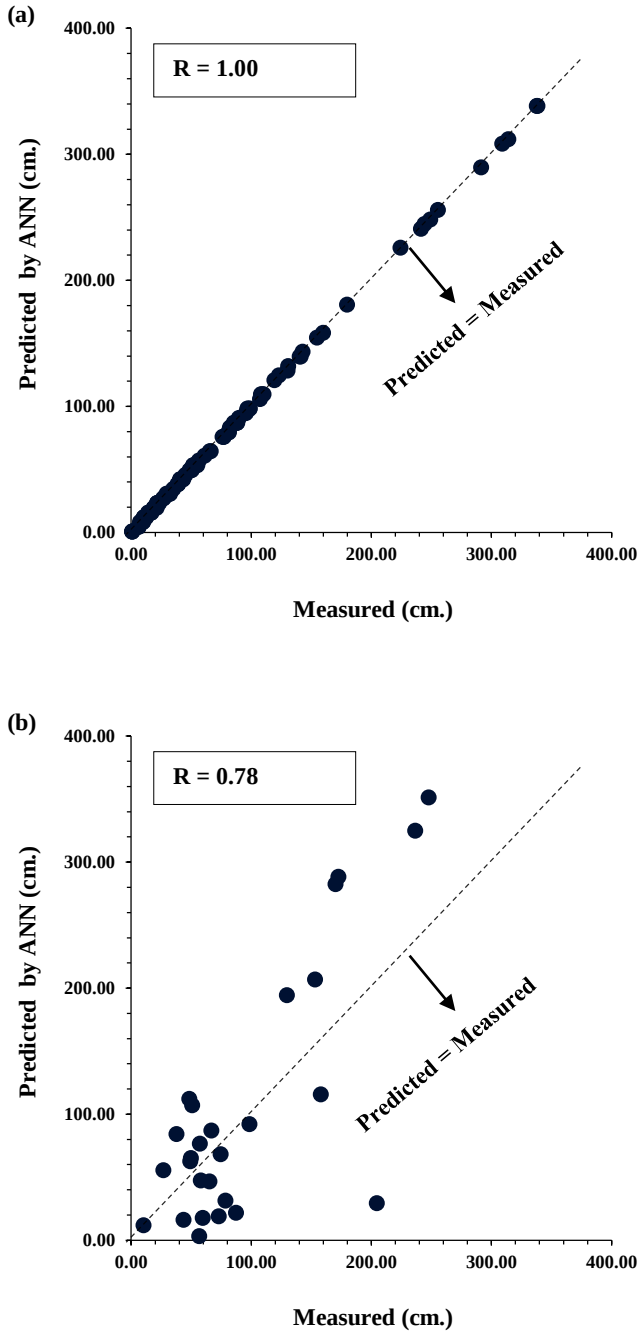

Figure 33. Predicted vs. measured water levels in piezometer 41L of Control 19H (a) Training data; (b) Testing data

The highest correlation coefficient was discovered in the downgradient piezometer of the control 19H that experienced the least clogging concentration. Since the clogging

concentration was more prevalent upgradient within the PICP, the water levels in the upper edge fluctuates more in comparison to the downgradient location. Therefore, the neural network model predicts the water level more accurately at the locations with lower clogging rates. The correlation coefficient of 1.00 and 0.80 were calculated for training and testing subsets of the downside piezometer data, respectively (Figure 34).

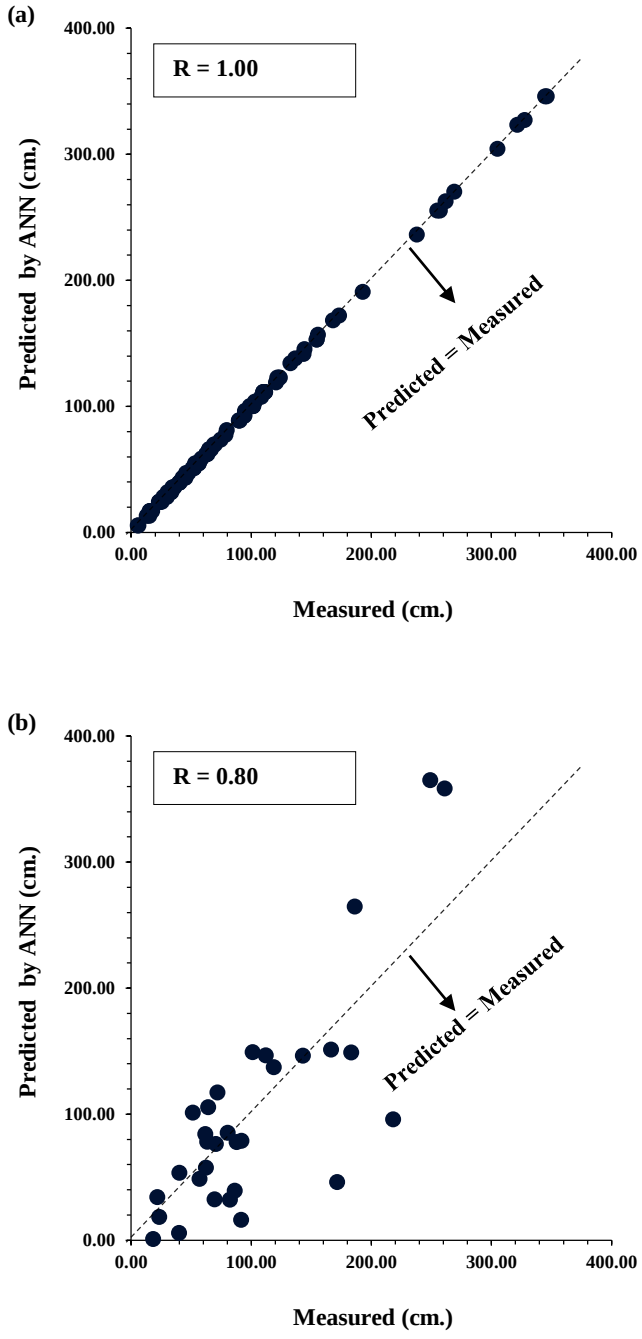

Figure 34. Predicted vs. measured water levels in piezometer 42L of Control 19H (a) Training data; (b) Testing data

6.2.3. Sensitivity Analysis

A sensitivity analysis was completed to determine the relative-importance values of the input parameters in the model. The analysis were completed for three pressure transducers in control 19G and the efficacies of the contributing variables on the captured runoff volume for each piezometer are summarized (Table 15). Since the same variables were used for the models, the average of the relative importance values can be computed to determine the most influential factors on the measured water levels. The analysis revealed that previous rainfall depth, the duration of rain events, ADP, and cumulative rainfall measured from the last conducted maintenance provide the greatest influences on the ability of the PICP to capture surface runoff water. It can be concluded that the stored runoff volume depends mostly on the existing water levels of the storage gallery, saturation percentage of the filled material, and the hydraulic conductivity of the surrounding soil layers. It is observed that all of the aforementioned factors are related to the previous events' properties such as former rainfall depth, ADP, and the cumulative rain depth.

Table 15. Relative importance of the input parameters in piezometers 40L, 41L and 42L of PICP 19G

Input Parameters	Relative Importance (%)			
	Piezometer 40L	Piezometer 41L	Piezometer 42L	Average
Cleaning Method	7.9	9.7	4.4	7.3
Duration	9.9	11.4	11.7	11
Rainfall Depth	10.7	8.4	7.3	8.8

Peak 5 min	7.9	9.1	7.9	8.3
Peak 15 min	12.1	8.9	7.1	9.4
Peak Duration	11.3	7.9	12.0	10.4
Cumulative Rainfall Depth from the installation	9.8	9.3	10.3	9.8
Cumulative Rainfall Depth from the last maintenance	8.5	9.5	13.4	10.5
ADP	8.2	10.4	13.3	10.6
Previous Rainfall Depth	13.8	15.3	12.6	13.9

The same analyses were completed for the ANN models at three different locations of control 19H (Table 16). Cleaning methods, peak 5-min intensity, and rainfall depth are the most influential factors on captured stormwater in control 19H, which is mainly due to the upside site characteristics. The average relative importance of the maintenance, peak 5-min intensity, and rainfall depth are 12%, 12.2%, and 10.9%, respectively. In conclusion, peak 5-min intensity and maintenances are the variables that greatly affect the stored runoff volume by PICP 19H, and therefore considering the aforementioned factors during the design process would result in storing rain water more effectively.

Table 16. Relative importance of the input parameters in piezometers 40L, 41L and 42L of PICP 19H

Input Parameters	Relative Importance (%)			
	Piezometer 40L	Piezometer 41L	Piezometer 42L	Average
Cleaning Method	12.2	12.0	11.8	12
Duration	9.2	9.9	7.8	9
Rainfall Depth	9.4	10.8	12.5	10.9
Peak 5 min	11.7	10.8	14.1	12.2
Peak 15 min	10.6	9.5	11.6	10.6
Peak Duration	12.1	10.9	8.6	10.5
Cumulative Rainfall Depth from the installation	10.0	7.0	10.3	9.1
Cumulative Rainfall Depth from the last maintenance	7.6	9.7	9.9	9.1
ADP	8.4	10.5	8.1	9
Previous Rainfall Depth	8.9	9.0	5.4	7.8

6.3. ANN Model for Volumetric Water Content

ANN models were developed to estimate the peak VWC of the installed TDRs. By monitoring the maximum VWC within the PICPs, an indication of the clogging rates, the maximum VWC during or after rain events could be computed. The peak VWC values of the TDRs obtained with a written code in MATLAB. Based on the occurred rain events in a two year study, the maximum VWC during or after each storm event was found. The time window that the MATLAB code is searching to find the maximum VWC begins from the start of the rain events till six hours after the end of the events. The peak VWC is the output while the rain events' characteristics and maintenance treatment are the input parameters in the prediction models. Based on the developed models, the clogging progression on the PICPs are predicted based on site specifications and cleaning techniques.

6.3.1. Compiled Database

The comprehensive database was prepared from the peak VWC, the complete rain events characteristics and the last maintenance treatment's code. A total of 138 events data and the related maximum VWC were analyzed for developing the neural network model (Appendix D). However, 15 events were eliminated from the datasets because of missing parameters which is mainly due to problems in recording the measurements or in downloading from the data logger. It should be noted that one hundred and two events of the dataset (74%) were randomly chosen for training and the remaining thirty six events (26%) were attributed for testing the proposed model. The testing events are presented as bold in the dataset shown in Appendix D (The same dataset prepared and analyzed for the

PICP 19H and presented in Appendix E).

6.3.2. Prediction Model

The ANN model architecture that yields the most precise results is presented in the following graphs for each developed model. The ANN models were built for those TDRs installed closest to the curb, (0.15m.) since they are subjected to a more concentrated flow. The distances from the upgradient edge for TDR01, TDR05, TDR09, TDR13 and TDR25 are 0.76, 2.29, 6.1, 12.2 and 24.9 m., respectively. The peak VWC dataset drawn from the recorded values by TDRs was used to build the ANN model. The peak VWC measurements were found during or six hours after rain events in a two year study period in order to build ANN model. The results for the developed prediction model, and the comparison of the computed results with real measured values are plotted in the following graphs. Moreover, the relative importances of the input parameters were computed by conducting sensitivity analysis to verify the developed ANN models.

The prediction model was built based on the training dataset to forecast the peak VWC in regard to the rain event parameters and the cleaning methods. The measured and predicted VWC are compared for training and testing datasets and the correlation coefficient is computed for each model. Also, the architecture of the prediction models that give the best result are different as the number of neurons in the hidden layer for each ANN model.

The model architecture that gave the best results for VWC prediction were built with one hidden layer and 13, 10, 17, 16 and 14 neurons for TDR01, TDR05, TDR09, TDR13 and TDR25, respectively. The correlation coefficients for the neural network

models are presented in the following figures (Figure 35, Figure 36, Figure 37, Figure 38, and Figure 39).

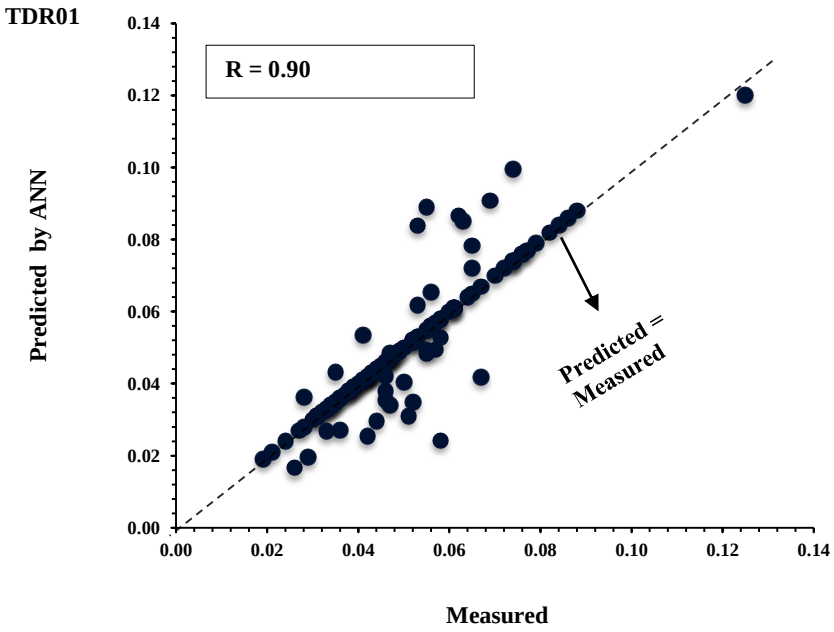

Figure 35. Predicted vs. measured peak VWC in TDR01

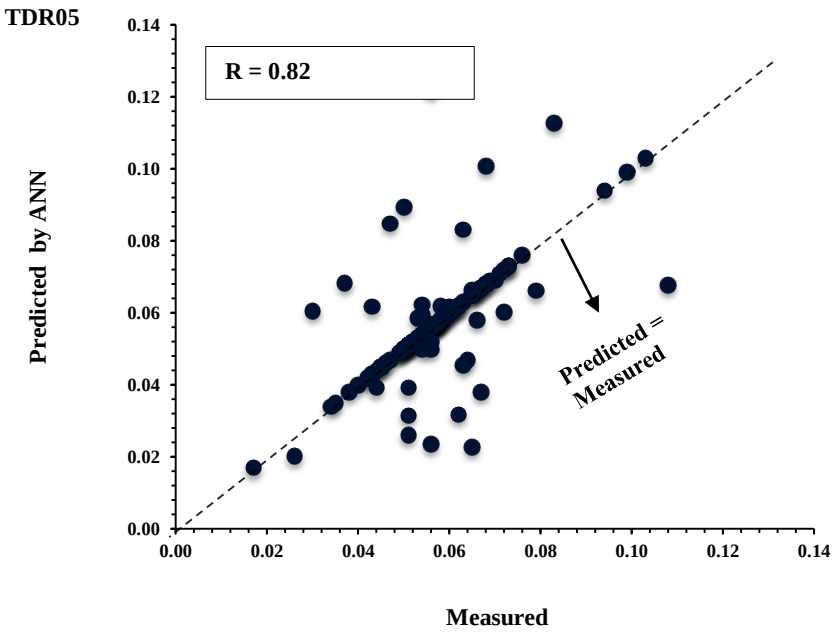

Figure 36. Predicted vs. measured peak VWC in TDR05

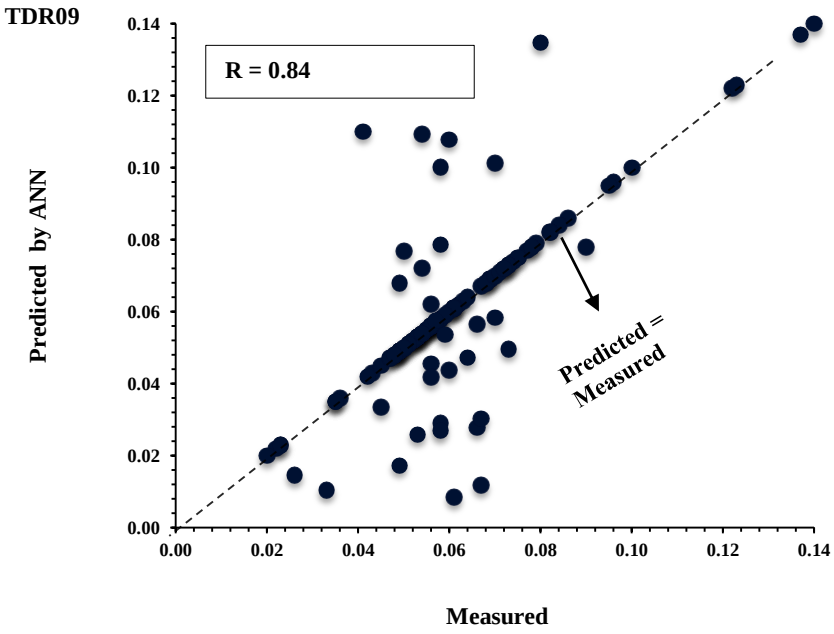

Figure 37. Predicted vs. measured peak VWC in TDR09

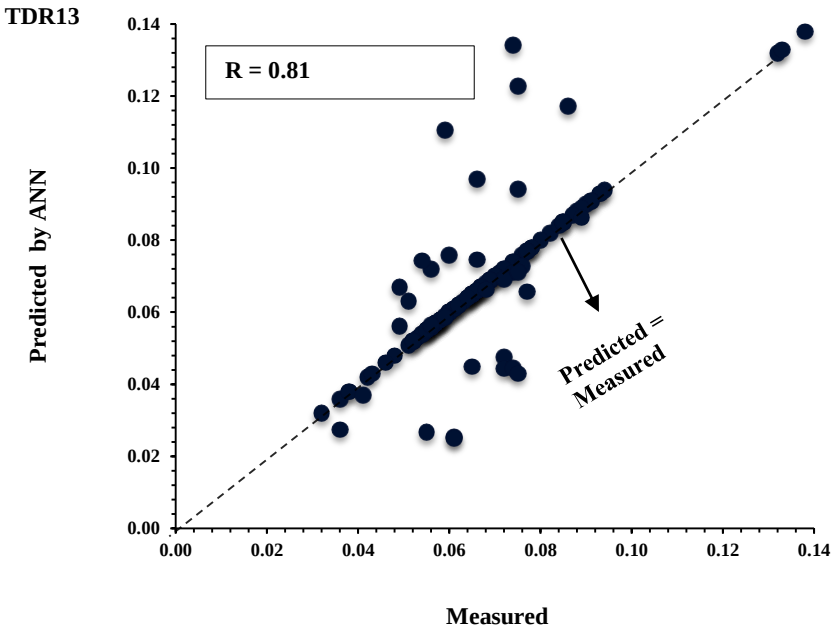

Figure 38. Predicted vs. measured peak VWC in TDR13

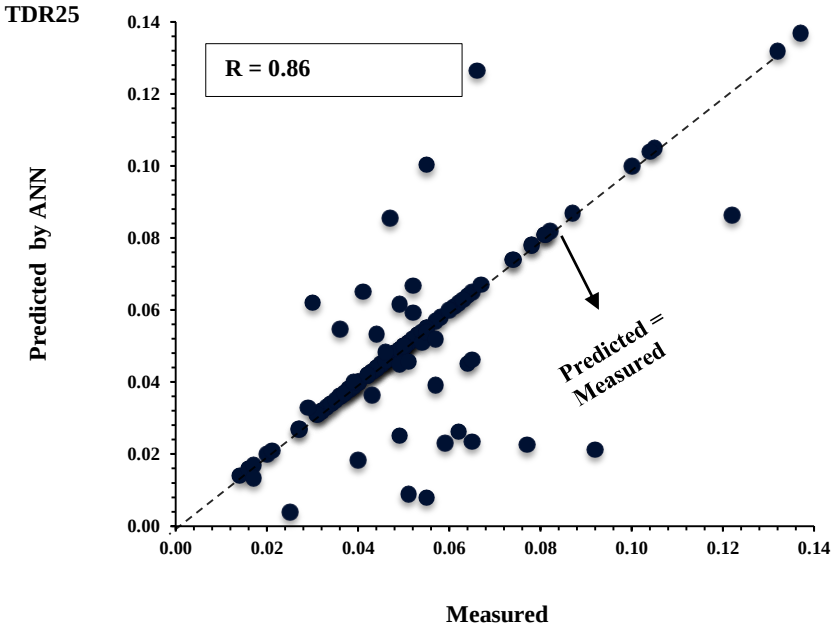

Figure 39. Predicted vs. measured peak VWC in TDR25

The model performance parameters including (R), (RMSE), and (MAE) are computed for all data (Table 17). Based on the performance criteria values for each

prediction model, it can be concluded that all models are able to predict peak VWC to high degree of accuracy. The results show that the neural network model for TDR01, the closest TDR to the upgradient edge, shows the best performance.

Table 17. Performance statistics of models for peak VWC prediction

Model	Correlation Coefficient (R)	Root Mean Squared Error (RMSE)	Mean Absolute Error (MAE)	Number of hidden layer neurons
TDR01	0.90	0.008	0.003	13
TDR05	0.824	0.012	0.005	10
TDR09	0.844	0.021	0.008	17
TDR13	0.807	0.024	0.008	16
TDR25	0.863	0.016	0.006	14

As it was discussed, the dataset was divided into training and testing data and therefore the performance parameters are computed for each dataset separately. The R, RMSE and MAE values of the TDR01 prediction model are, respectively, equal to 1, 0.000003, and 0.000003 for the training data. This model yields R, RMSE and MAE values equal to 0.785, 0.0157, and 0.0129 on the testing data. The dataset that trained the TDR05 model has $R = 1$, $RMSE = 0.000005$, and $MAE = 0.000004$, while the testing dataset presents $R = 0.70$, $RMSE = 0.0240$, and $MAE = 0.0186$, as the criteria parameters. The TDR09 dataset for training has R, RMSE and MAE equaling to 1, 0.000006 and 0.000005, respectively. The testing dataset presents $R = 0.70$, $RMSE = 0.0402$, and $MAE = 0.0321$, as the performance parameters. To develop the prediction model for TDR13 the training dataset has correlation of coefficient equals 1, RMSE and

MAE equals 0.000007, 0.000006, respectively. This model yields $R = 0.67$, $RMSE = 0.0475$, and $MAE = 0.0296$ on the testing data. The neural network model for the closest TDR to the downgradient edge yields $R = 1$, $RMSE = 0.000006$, and $MAE = 0.000005$ for training the ANN model while the testing data for this model presents $R = 0.69$, $RMSE = 0.0304$, and $MAE = 0.0241$.

6.3.3. Sensitivity Analysis

The efficacies of the studied rain event variables and different conducted cleaning methods on the peak VWC values are determined to be the critical parameters in the future designs (Table 18). The average sensitivity of the prediction models to each contributing factor are computed since the same variables were analyzed for all the models. The results of parametric study for VWC indicated that the cleaning method, peak 5-min and 15-min intensity, previous rainfall depth and the cumulative rainfall depth from the installation have the highest influence on VWC values. Peak 5-min intensity has the highest impact on the peak VWC value, since the TDRs are located close to the PICP surface (43 cm below the ground). The result matched the expectation because the rainfall intensity governs the TDRs' peak value. Antecedent Dry Periods (ADP) parameter is the studied variable that present the lowest importance efficacy on the peak VWC.

Table 18. Relative importance of the input parameters in TDRs of PICP 19G

Input Parameters	Relative Importance (%)					
	TDR01	TDR05	TDR09	TDR13	TDR25	Average
Maintenance	10.68	8.40	9.41	11.30	13.04	10.57

Duration	11.08	10.31	9.58	7.60	7.39	9.19
Rainfall Depth	8.11	7.88	7.79	10.88	10.98	9.13
Peak 5 min	10.78	11.88	11.10	9.68	12.08	11.1
Peak 15 min	9.02	11.17	10.72	11.53	10.47	10.58
Peak Duration	11.27	6.67	10.58	10.37	9.33	9.64
Cumulative Rainfall Depth from the installation	10.34	11.28	11.82	10.65	9.35	10.69
Cumulative Rainfall Depth from the last maintenance	8.58	9.60	10.69	9.52	9.25	9.53
ADP	8.48	11.38	6.13	9.81	8.40	8.84
Previous Rainfall Depth	11.66	11.44	12.19	8.66	9.69	10.73

Although it was observed that the clogging is concentrated along the curb, the VWC of the other TDRs were investigated. By analyzing all the twelve installed TDRs, the clogging prediction patterns over the pavement are obtained. In the Appendix H, the prediction vs. the measured peak value for all the installed TDRs are shown separately for training and testing data. In addition, the computed relative importances of the studied

parameters for the developed models with the model architecture characteristics are presented.

6.4. ANN model for Clogging Progression Length

The ANN models were developed to predict the main PICPs' operational variables based on various pavements specifications. By monitoring the maximum VWC of the TDRs along the PICPs, clogging progression length based on the PICPs' specifications can be predicted. Different configurations of the laboratory models with multiple pavements' features and similar site characteristics are set up and 21 experiments with different combination of slope, gap size, and joint filling material are conducted. In addition to developing the prediction models, sensitivity analysis were completed to investigate the efficacy of each variable on the hydrologic performance of PICPs. Pavement slope, gap size between the paver blocks, presence of joint filling material, and the clogging length are the input variables while the cumulative rainfall depth is the output parameter.

6.4.1. Comprehensive Database

The comprehensive dataset are prepared from the conducted experiments on the multiple constructed PICP laboratory models. A total of 118 clogging length data with the relative measured flow volume, which is an indication of cumulative rainfall depth, are prepared and analyzed to develop the clogging length prediction models (Appendix F). It is suggested to dedicate about three fourth of the dataset to train the neural network model and one-fourth of the recorded data to test the model. In this study, 88 recorded data (75%) is randomly chosen to train the prediction model, and 30 experimental results

(25%) are used to test the performance of the ANN-based model (The randomly selected data are presented bold in Appendix F).

6.4.2. Prediction Model

The input parameters that scrutinized in this study are including slope, gap size, filling material characteristic, and location from the upgradient edge, while the output parameter is the cumulative rainfall depth on the permeable pavement. Thus, an input layer has four neurons which each of them represent a variable and one neuron in an output layer is depicted to the rainfall depth. The neural network model architecture with the most accurate results are obtained through five neurons in a hidden layer. The prediction model is developed by training the neural network and then the performance of the proposed model on the test datasets is analyzed. The correlation coefficient of 0.98 and 0.88 are calculated for training and testing datasets, respectively Figure 40. The R, RMSE and MAE values of the prediction model are, respectively, equal to 0.98, 0.003, and 0.0418 for the training data. The proposed model yields R, RMSE and MAE values equal to 0.88, 0.02, and 0.091 on the testing data.

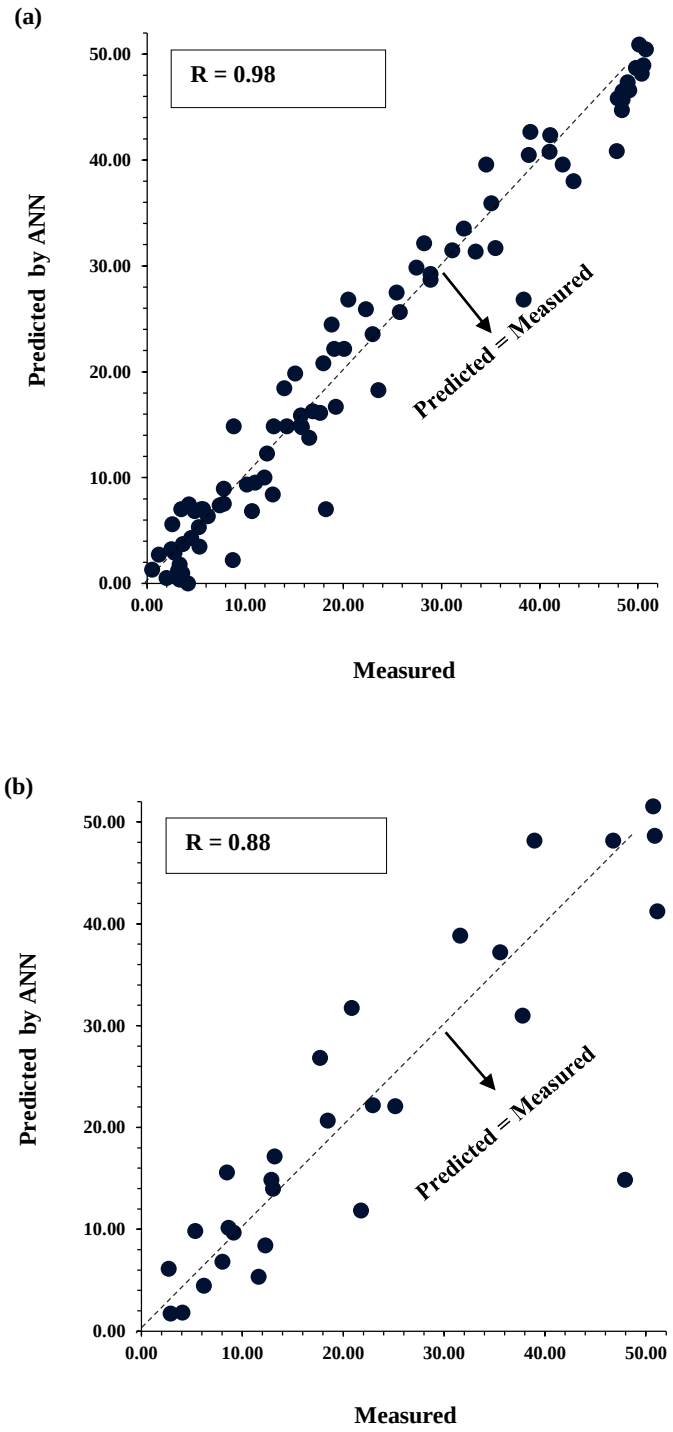

Figure 40. Predicted vs. measured rainfall depth for clogging model (a) Training data; (b) Testing data

6.5. Modeling of Infiltration Edge

The ANN models were developed to predict the infiltration edge length based on various pavements specifications. By monitoring the peak VWC of the installed TDRs along the laboratory PICP models and discovering the maximum recorded value, the infiltration edge distance (from the upgradient edge) determined. Hence, the infiltration edge length based on the PICPs' specifications can be predicted. In addition to developing the prediction models, sensitivity analysis were completed to investigate the efficacy of each variable on the infiltration edge progression of the PICPs. Pavement slope, gap size between the paver blocks, presence of joint filling material, and the infiltration edge are the input variables while the cumulative rainfall depth is the output parameter.

6.5.1. Complied Dataset

The comprehensive database is prepared for developing the infiltration edge prediction model from the conducted experiments on the laboratory models (Appendix G). Slope, gap size, filling material, and infiltration edge length are the studied input variables, while the cumulative rainfall depth is the output parameter. A total of 129 measurement of infiltration edge progression and the relative rainfall depth are completed to develop the neural network model. As previously stated, 96 recorded experiments (74%) are randomly chosen to train the ANN-based model, whereas 33 measurements (26%) are utilized for testing the model performance.

6.5.2. Prediction Model

In order to develop a model to predict the cumulative rainfall depth on the infiltration edge progression, the pavements characteristics and the location from the upgradient are

investigated in the model. Slope, gap size, filling material presence, and the infiltration edge distances from the upgradient are the input parameters, and the cumulative rainfall depth are the predicted parameters. Four neurons in an input and one neuron in an output layers are the neural network model structure.

The accuracy of the prediction model demonstrates the correlation coefficients equaling 0.99 for both the training and testing datasets Figure 41. The infiltration edge dataset for training has R, RMSE and MAE equaling to 0.99, 0.0225 and 0.0225, respectively. The testing dataset presents $R = 0.99$, $RMSE = 0.0013$, and $MAE = 0.0303$, as the performance parameters. The architecture of the model with the best performance are attained with six neurons and a hidden layer.

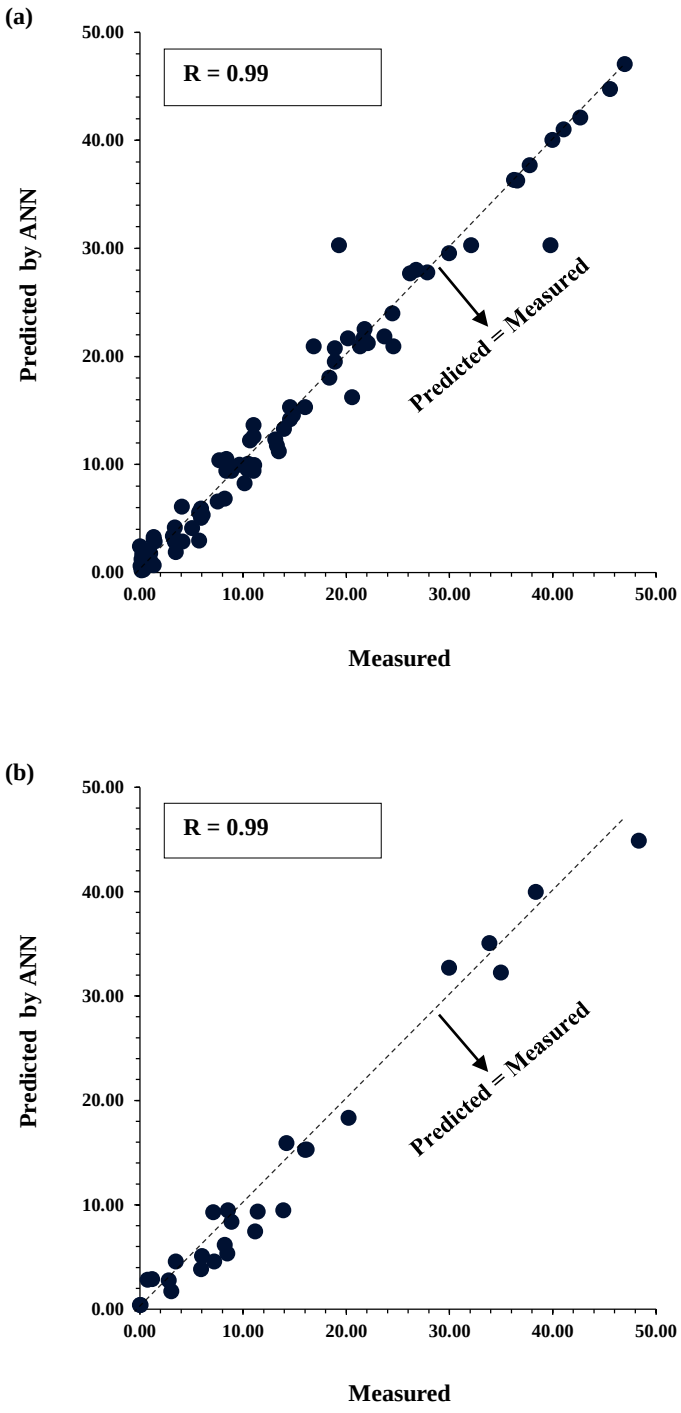

Figure 41. Predicted vs. measured rainfall depth for infiltration edge model (a) Training data; (b) Testing data

6.5.3. Sensitivity Analysis

In addition to the proposed prediction models, sensitivity analyses are conducted to determine the efficacy of each parameter. The relative importance values of the parameters on the clogging length progression according to the cumulative rainfall depth are determined (Table 19). It is concluded that the pavement slope and the distance from the upgradient are the two most effective parameters on the rainfall amount in clogging length progression. Moreover, the same analysis are completed on the infiltration edge of the permeable pavements and the importance of each parameter are presented in Figure 42. It is observed from the results that the slope and gap size of the pavements are presenting the highest influence on rainfall volume and infiltration edge location. The obtained results from the parametric study are in accordance with the experimental results since slope and gap size are the governing factors on surface infiltration rates.

Table 19. Relative importance of the input parameters for the developed models

Relative Importance (%)	Input Parameters			
	Slope	Gap Size	Filling Material	Distance from the Upgradient Edge
Clogging Length	29.3	22.4	22.9	25.4
Infiltration Edge	32.6	28.5	16.8	22.1

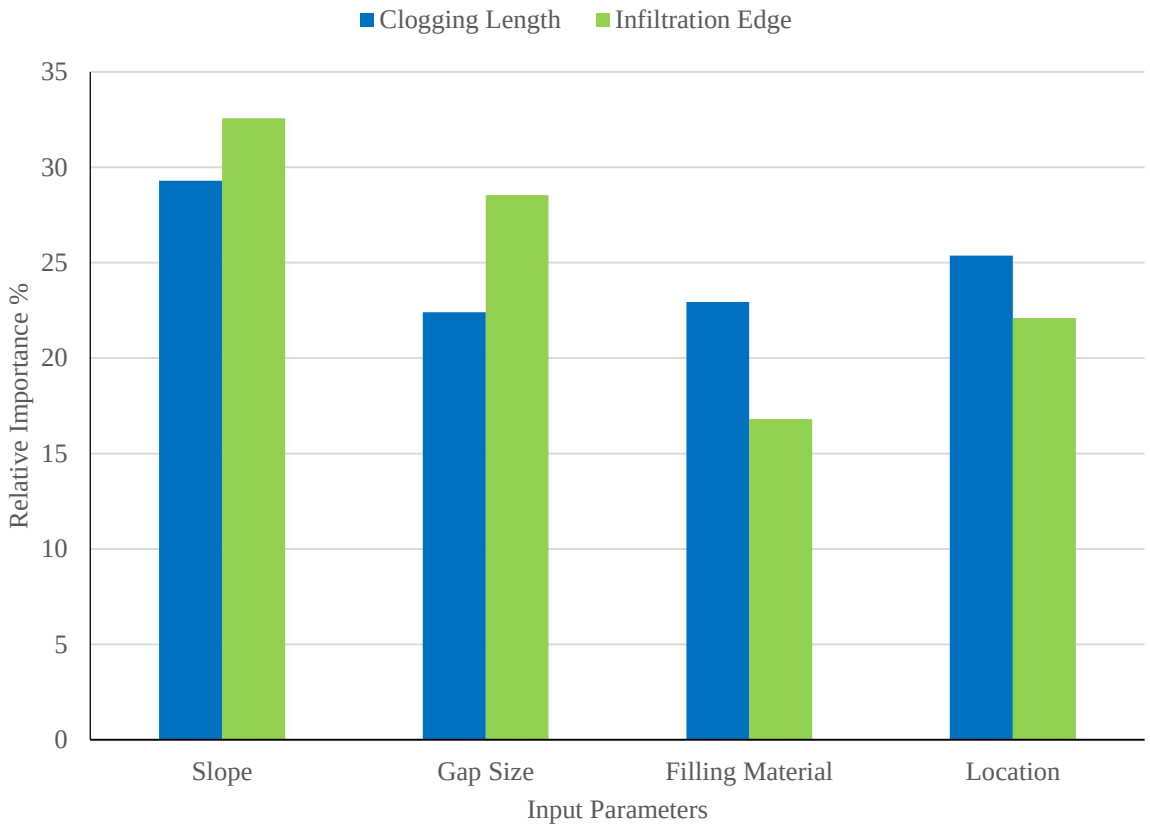

Figure 42. Relative importance of different input parameters for clogging length and infiltration edge models

7. MODELS APPLICATION

The proposed models are the first prediction tools that exploit real-time data sets through constant monitoring of PICPs implementation in urban areas. Accurate estimation of the PICPs hydrologic performance was achieved by gathering rain events' variables and site characteristics variables. Captured runoff and clogging progression models, the two main hydrologic characteristics of the PICPs, were developed through utilizing the measured data in a two-year study period. The ANN models introduce explicit formulations to compute the maximum captured water level and the peak VWC to foresee the PICPs operation and the clogging development. In this chapter, the aim is to apply the established robust tools to predict the captured water level and the clogging progression length in the studied PICPs for a different precipitation data. Therefore, the required maintenances can be anticipated through scrutinizing a new rain events' statistics and exploring the predicted values to keep the PICPs performing well.

7.1. Model Reliability

The predictive capabilities of the models are generally limited to the range of the input data utilized for the model calibration. The distributions of the predictor parameters are not uniform thus the models accuracy vary according to the range of the input data. Although the models were developed through investigating more than 150 rain events in a two-year study period, it is unlikely that user will encounter two identical rain events with the same specifications. Therefore, an assessment on the input and output

parameters used for the model development is required to determine the reliable input ranges to ensure the model yields accurate results.

To evaluate the practicality of using the proposed models for other site characteristics a comprehensive statistical study was completed. The descriptive statistics of the input and output parameters used in the development of ANN models are required to determine the model reliability in other circumstances. By comparing the rainfall data from other time and locations with the statistical indices of the input data, the model reliability can be established. Alavi and Gandomi demonstrated that the ANN models predict more accurately in the ranges with higher densities (Alavi and Gandomi 2011). In order to determine the higher density ranges and visualize the data distribution, obtaining the frequency histograms of the input and output variables are required.

7.1.1. Captured Runoff Model

A complete set of statistical indices values for the input and output parameters of the captured runoff models computed to determine the reliable range for the developed models. The descriptive statistics of the captured runoff database for the PICPs 19G and 19H are given in Table 20 and Table 21. Furthermore, the frequency histograms of the input parameters for the captured runoff models in PICPs 19G and 19H are presented in Appendix I and Appendix J, respectively. The frequency histograms for the output parameters of the developed models are obtained and presented in Figure 43 and Figure 44.

Table 20. Descriptive statistics of the variables used in the captured water model development of PICP 19G

Parameter	Cleaning Method	Duration	Rainfall Depth	Peak 5 min	Peak 15 min	Peak Duration	Cumulative Rainfall Depth from the installation
Mean	3.66	498	1.55	23.19	15.78	14.38	105.29
Standard Error	0.14	46	0.15	2.22	1.53	0.17	5.43
Median	4.00	358	0.83	13.72	9.65	15.00	106.93
Mode	4.00	605	0.25	6.10	3.05	15.00	#N/A
Standard Deviation	1.61	535	1.75	26.05	18.00	1.95	63.78
Sample Variance	2.58	285947	3.08	678.58	323.99	3.81	4068.15
Kurtosis	-0.99	18	7.50	4.64	7.17	2.38	-1.04
Skewness	-0.32	3	2.31	2.13	2.52	-1.12	0.12
Range	5.00	4235	11.23	124.97	94.49	10.00	226.49
Minimum	1.00	10	0.13	3.05	2.03	10.00	1.22
Maximum	6.00	4245	11.35	128.01	96.52	20.00	227.71

Parameter	Cumulative Rainfall Depth from the last maintenance	ADP	Previous Rainfall Depth	Peak Water Level 1	Peak Water Level 2	Peak Water Level 3
Mean	20.22	4305	0.81	95.22	133.72	131.81
Standard Error	1.07	326	0.11	4.01	5.33	5.36

Median	19.77	2993	0.24	81.00	115.30	113.35
Mode	0.00	555	0.03	61.64	112.20	224.40
Standard Deviation	12.51	3828	1.28	47.08	62.66	62.92
Sample Variance	156.53	14652903	1.63	2216.66	3926.60	3958.43
Kurtosis	-0.68	1	6.95	-0.46	-0.99	-0.97
Skewness	0.28	1	2.47	0.71	0.47	0.48
Range	51.23	15880	7.09	194.29	238.80	246.29
Minimum	0.00	365	0.03	24.81	31.10	28.71
Maximum	51.23	16245	7.11	219.10	269.90	275.00

(a)

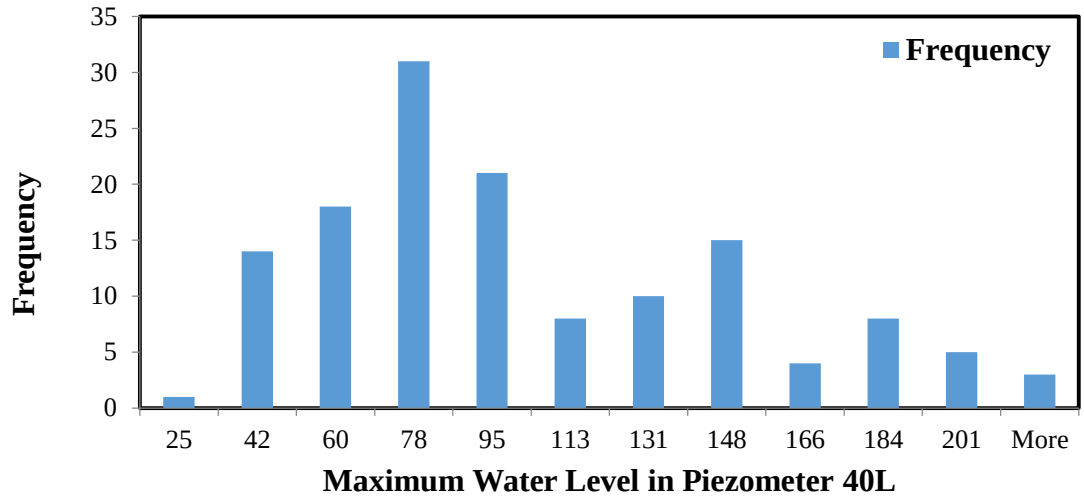
Frequency
35
30
25
20
15
10
5
0
25
42
60
78
95
113
131
148
166
184
201
More
Maximum Water Level in Piezometer 40L

(b)

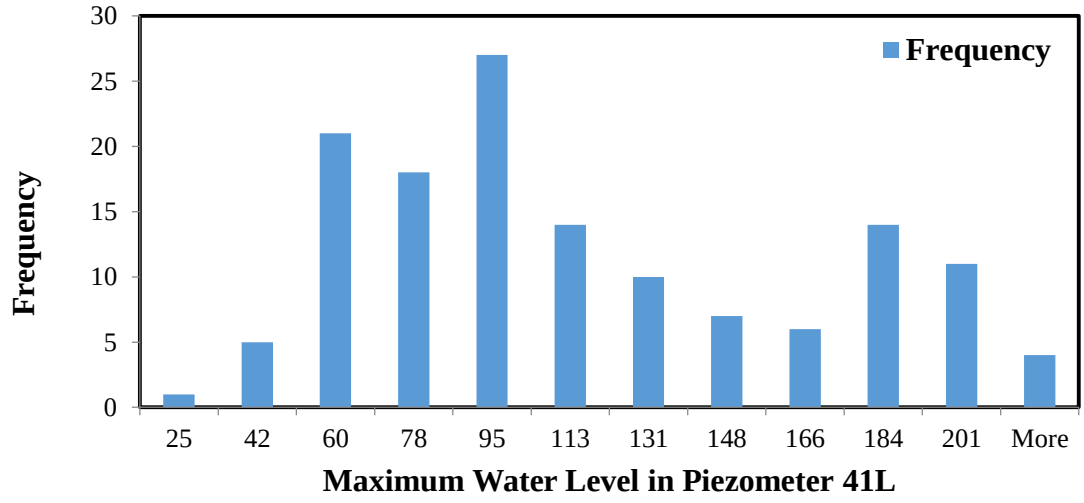
Frequency
30
25
20
15
10
5
0
25
42
60
78
95
113
131
148
166
184
201
More
Maximum Water Level in Piezometer 41L

(c)

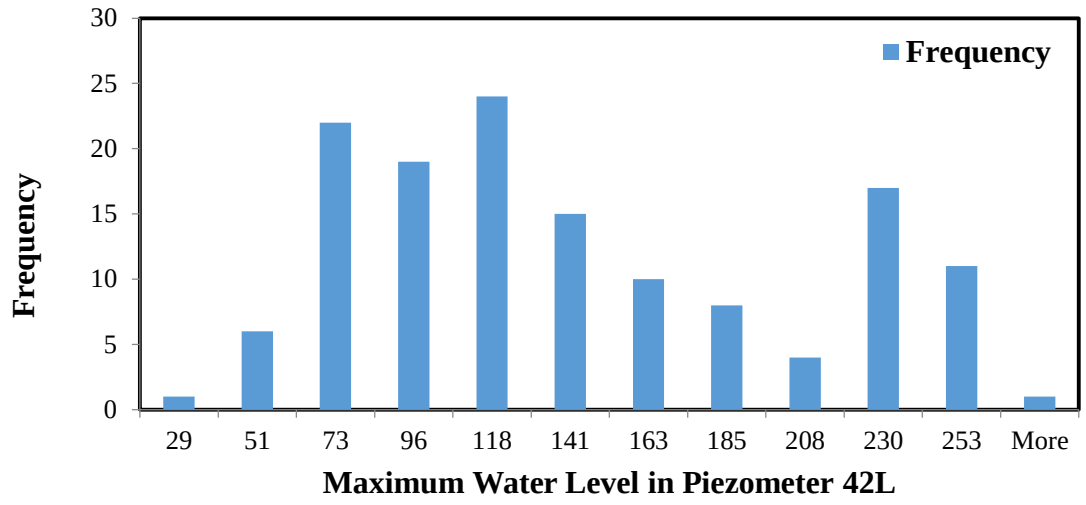

Figure 43. Histograms of the maximum water level used in the captured runoff model development of PICP 19G (a) Piezometer 40L (b) Piezometer 41L (c) Piezometer 42L

Table 21. Descriptive statistics of the variables used in the captured water model development of PICP 19H

Parameter	Cleaning Method	Duration	Rainfall Depth	Peak 5 min	Peak 15 min	Peak Duration	Cumulative Rainfall Depth from the installation
Mean	2.63	502	1.57	23.40	15.85	14.42	99.75
Standard Error	0.10	45	0.15	2.24	1.55	0.16	5.18
Median	3.00	380	0.94	12.19	9.14	15.00	102.01
Mode	4.00	605	0.25	6.10	4.06	15.00	107.14
Standard Deviation	1.17	532	1.74	26.20	18.18	1.92	60.61

Sample Variance	1.37	283178	3.02	686.37	330.34	3.70	3673.12
Kurtosis	-1.43	18	7.82	4.49	6.90	2.63	-0.89
Skewness	-0.22	3	2.34	2.11	2.50	-1.14	0.15
Range	3.00	4235	11.23	124.97	94.49	10.00	223.52
Minimum	1.00	10	0.13	3.05	2.03	10.00	0.05
Maximum	4.00	4245	11.35	128.01	96.52	20.00	223.57

Parameter	Cumulative Rainfall Depth from the last maintenance	ADP	Previous Rainfall Depth	Peak Water Level 1	Peak Water Level 2	Peak Water Level 3
Mean	26.41	4189	0.81	68.15	78.57	91.38
Standard Error	1.63	316	0.11	5.90	6.48	6.49
Median	23.32	2935	0.25	45.05	53.68	66.44
Mode	19.38	555	0.03	7.99	10.66	23.99
Standard Deviation	19.09	3702	1.26	69.03	75.84	75.94
Sample Variance	364.55	13704722	1.60	4764.47	5751.47	5766.25
Kurtosis	1.74	1	7.20	2.79	2.43	2.28
Skewness	1.25	1	2.48	1.74	1.65	1.61
Range	87.00	15880	7.09	316.78	337.63	340.55
Minimum	0.00	365	0.03	-0.28	0.78	5.55
Maximum	87.00	16245	7.11	316.50	338.40	346.10

(a)

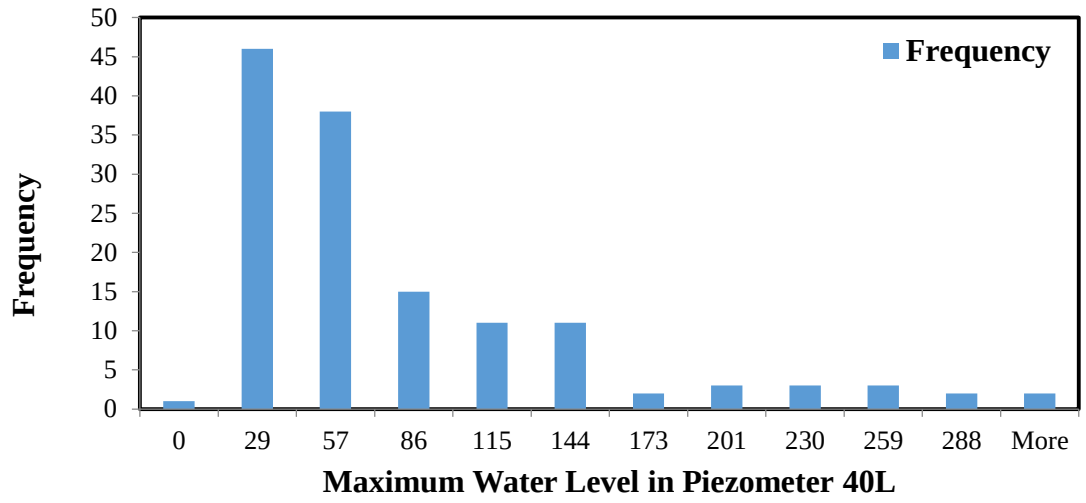
Frequency
50
45
40
35
30
25
20
15
10
5
0
0
29
57
86
115
144
173
201
230
259
288
More
Maximum Water Level in Piezometer 40L

(b)

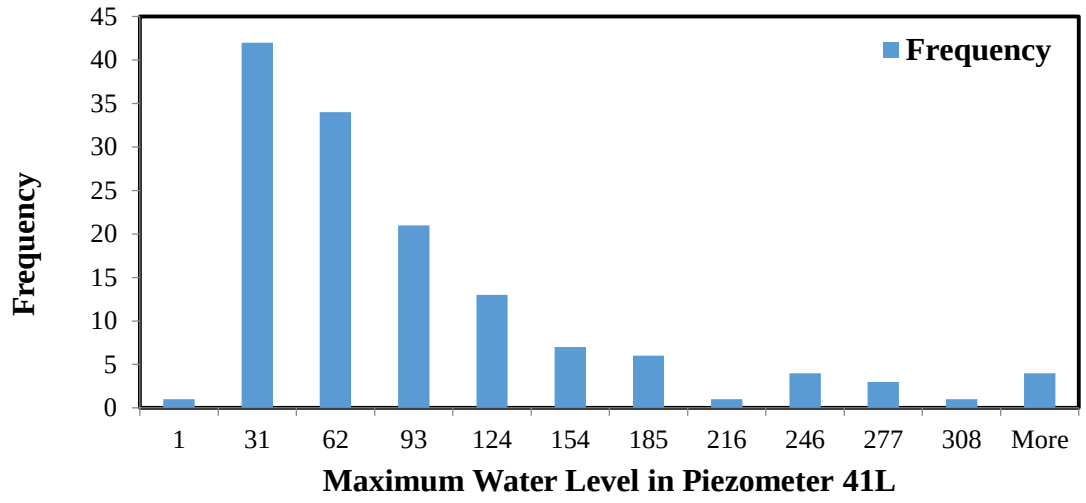
Frequency
45
40
35
30
25
20
15
10
5
0
1
31
62
93
124
154
185
216
246
277
308
More
Maximum Water Level in Piezometer 41L

(c)

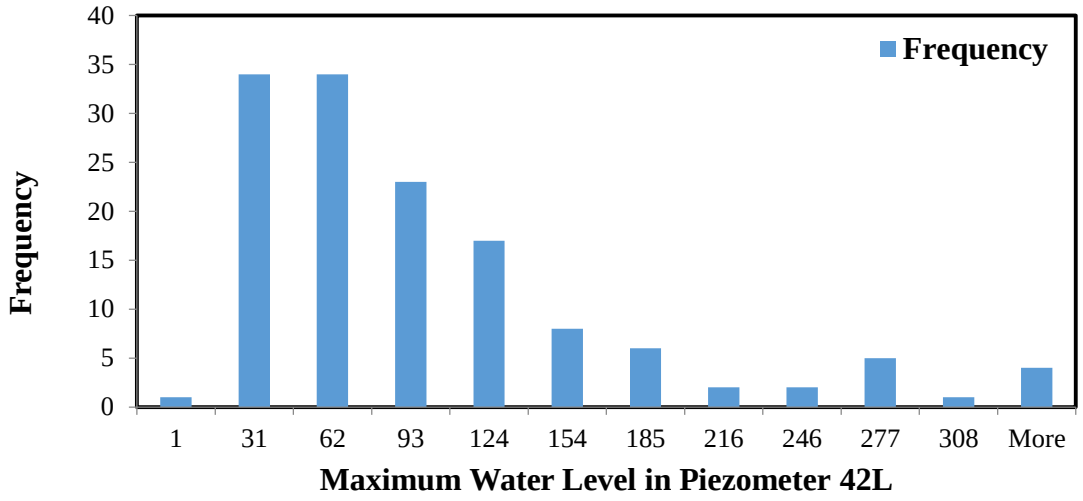

Figure 44. Histograms of the maximum water level used in the captured runoff model development of PICP 19H (a) Piezometer 40L (b) Piezometer 41L (c) Piezometer 42L

7.1.2. Peak VWC Model

Similar to the comprehensive statistical study on the captured runoff dataset, statistical indices were computed for the input and output parameters of the peak VWC dataset to determine the acceptable range for the developed models. The descriptive statistics of the peak VWC dataset for the PICP 19G is given in Table 22. Moreover, the frequency histograms of the input parameters for the developed model in PICP 19G are presented in Appendix K. The frequency histograms for the output parameters of the prediction model is obtained and presented in Figure 45.

Table 22. Descriptive statistics of the variables used in the peak VWC model development of PICP 19G

Parameter	Cleaning Method	Duration	Rainfall Depth	Peak 5 min	Peak 15 min	Peak Duration
Mean	3.66	498	1.55	23.19	15.78	14.38
Standard Error	0.14	46	0.15	2.22	1.53	0.17
Median	4.00	358	0.83	13.72	9.65	15.00
Mode	5.00	95	0.25	6.10	3.05	15.00
Standard Deviation	1.61	535	1.75	26.05	18.00	1.95
Sample Variance	2.58	285947	3.08	678.58	323.99	3.81
Kurtosis	-0.99	18	7.50	4.64	7.17	2.38
Skewness	-0.32	3	2.31	2.13	2.52	-1.12
Range	5.00	4235	11.23	124.97	94.49	10.00
Minimum	1.00	10	0.13	3.05	2.03	10.00
Maximum	6.00	4245	11.35	128.01	96.52	20.00

Parameter	Cumulative Rainfall Depth from the installation	Cumulative Rainfall Depth from the last maintenance	ADP	Previous Rainfall Depth
Mean	105.29	20.22	4305	0.81
Standard Error	5.43	1.07	326	0.11
Median	106.93	19.77	2993	0.24
Mode	#N/A	0.00	555	0.03
Standard Deviation	63.78	12.51	3828	1.28
Sample Variance	4068.15	156.53	14652903	1.63

Kurtosis	-1.04	-0.68	1	6.95
Skewness	0.12	0.28	1	2.47
Range	226.49	51.23	15880	7.09
Minimum	1.22	0.00	365	0.03
Maximum	227.71	51.23	16245	7.11

Parameter	Peak VWC 01	Peak VWC 05	Peak VWC 09	Peak VWC 13	Peak VWC 25
Mean	0.05	0.06	0.07	0.07	0.06
Standard Error	0.00	0.00	0.00	0.00	0.00
Median	0.05	0.06	0.06	0.07	0.05
Mode	0.04	0.05	0.06	0.06	0.05
Standard Deviation	0.02	0.02	0.03	0.03	0.03
Sample Variance	0.00	0.00	0.00	0.00	0.00
Kurtosis	2.70	22.18	10.44	17.84	8.81
Skewness	1.08	3.71	2.82	3.59	2.62
Range	0.11	0.18	0.21	0.23	0.18
Minimum	0.02	0.02	0.02	0.03	0.01
Maximum	0.13	0.19	0.23	0.27	0.20

(a)

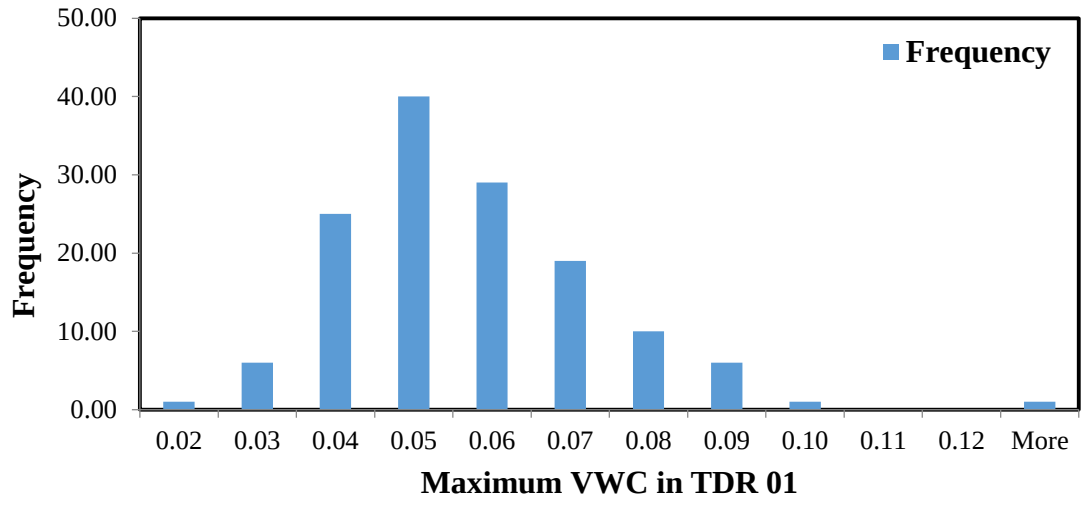
50.00
40.00
30.00
20.00
10.00
0.00
Frequency
Frequency
0.02
0.03
0.04
0.05
0.06
0.07
0.08
0.09
0.10
0.11
0.12
More
Maximum VWC in TDR 01

(b)

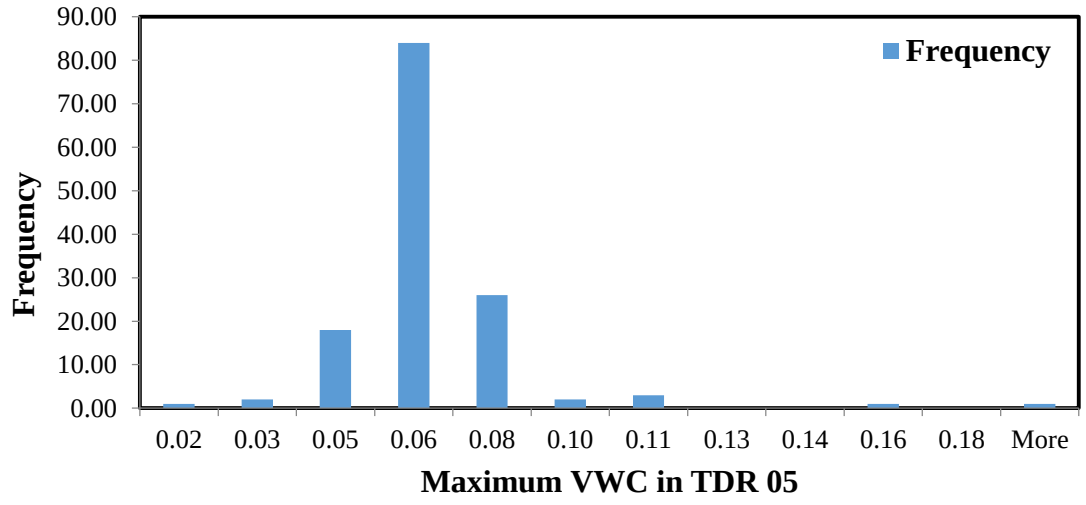
90.00
80.00
70.00
60.00
50.00
40.00
30.00
20.00
10.00
0.00
Frequency
Frequency
0.02
0.03
0.05
0.06
0.08
0.10
0.11
0.13
0.14
0.16
0.18
More
Maximum VWC in TDR 05

(c)

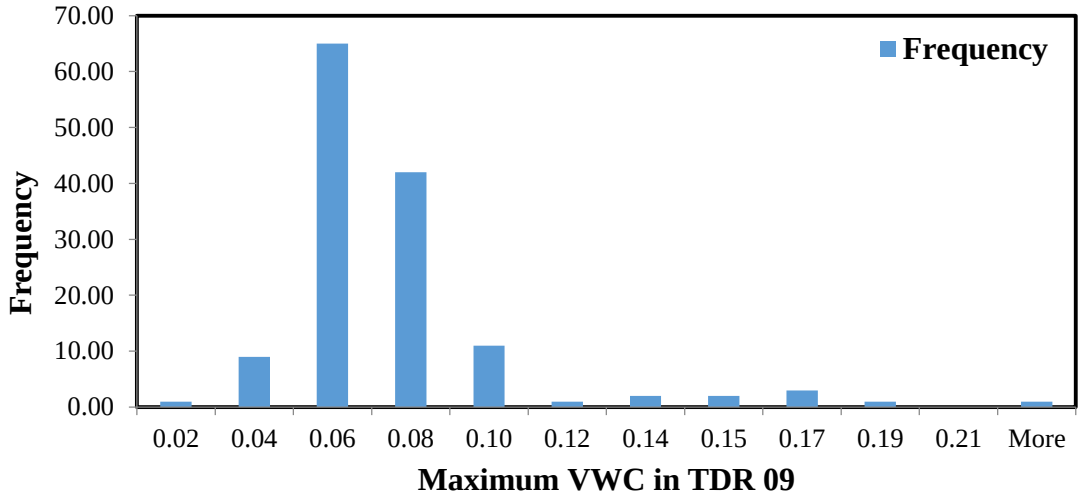
70.00
60.00
50.00
40.00
30.00
20.00
10.00
0.00
Frequency
Frequency
0.02
0.04
0.06
0.08
0.10
0.12
0.14
0.15
0.17
0.19
0.21
More
Maximum VWC in TDR 09

(d)

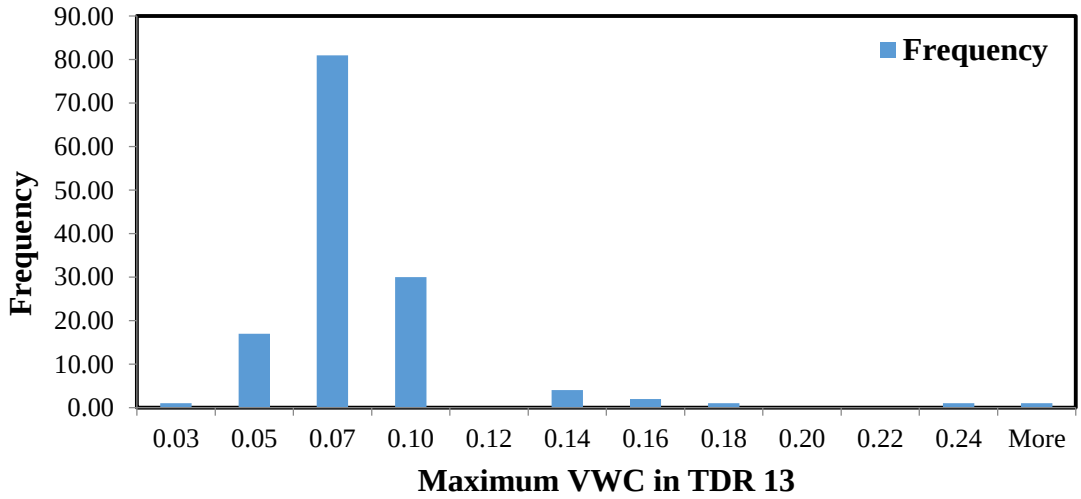
90.00
80.00
70.00
60.00
50.00
40.00
30.00
20.00
10.00
0.00
Frequency
Frequency
0.03
0.05
0.07
0.10
0.12
0.14
0.16
0.18
0.20
0.22
0.24
More
Maximum VWC in TDR 13

(e)

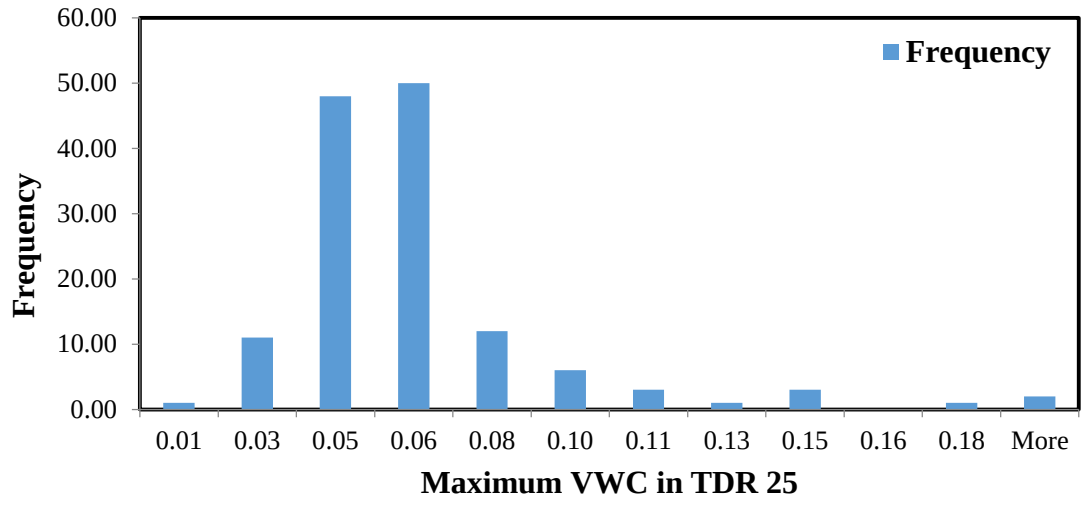

Figure 45. Histograms of the maximum VWC used in the peak VWC model development of PICP 19G (a) TDR 01 (b) TDR 05 (c) TDR 09 (d) TDR 13 (e) TDR 25

7.2. Typical Year Determination

An analysis was completed to determine a typical year of rainfall to predict the operational variables of the PICPs. The employed methodology for determining a typical rainfall year was based on the suggested methods by Sutherland and Jelen (2003). Rain events that occurred in the city of Louisville were identified and analyzed for the studied period. The historical rainfall data from 1948 up to 2015 was collected and assessed; thus more than 65 annual rainfall data studied to determine the average numbers for the main rain events variables. For each annual data, the studied rain events' characteristics included: number of events, total storm duration, total rainfall depth, maximum hourly precipitation, average rainfall intensity, and time since the last event. Therefore, the aforementioned rain events' characteristics values closest to the average numbers determine the typical annual rainfall.

OneRain, Inc. performed the study for Louisville MSD to cover the period from August 1948 through December 2002 (55-year period) (Charron, Charron et al. 2000). To update the analysis and cover more recent rainfall data, the analysis with the same approach is conducted from 2003 until 2015. In spring 2003, fifteen new telemetry-equipped rain gauges were installed throughout Jefferson County. The information from the rain gauge TR05, one of the newly installed rain bucket in the area, is used to monitor the detailed rain events characteristics near the pavement systems. Since TR05 was installed in the spring of 2003 and thus comprehensive annual rainfall data is not accessible for 2003, annual rainfall data from 2004 until 2014 was evaluated in order to determine the year of typical rainfall (Figure 46). The complete rainfall statistics data done by OneRain, Inc for 1980-2006 period are given in Appendix L.

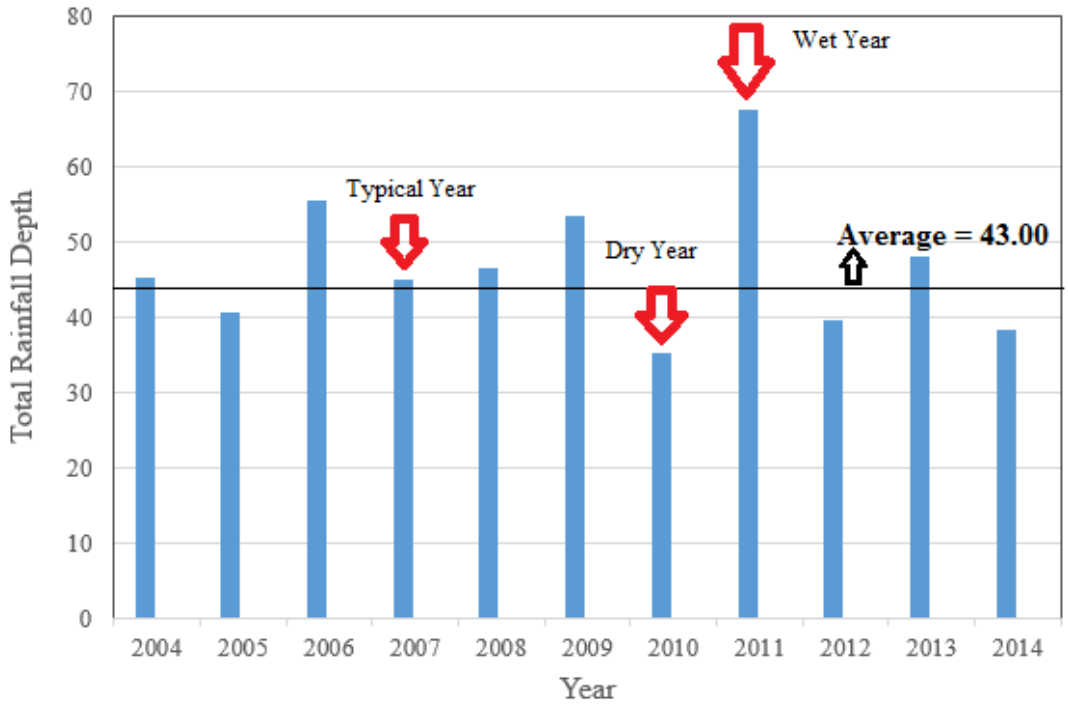

Figure 46. Total rainfall depth comparison with average for recent years

OneRain, Inc calculated the average annual rainfall depth for 55 years (1948-2002) in the City of Louisville equals 43.00 inches. Comparing the measured rainfall depth by TR05 with the average value, the typical rainfall year, dry year, and wet year was determined. As shown in Figure 46 and according to Table 23, the total rainfall depth in 2007 equals 45.1 inches which is the closest value to the average (43.00 inches). In addition, 2010 with 35.28 and 2011 with 67.7 total rainfall depth are the dry and wet year, respectively (Figure 46). Therefore, the PICP performances are evaluated for the typical year (2007) to compare their operation indices with the studied years.

Table 23. Measured Rainfall depth

Year	Total Rainfall Depth Measured by TR05
2004	45.26
2005	40.51
2006	55.44
2007	45.1
2008	46.61
2009	53.43
2010	35.28
2011	67.7
2012	39.51
2013	48.03
2014	38.3
Average	43.00
SD	6.97

7.3. Hydrologic Performance Prediction for Typical Year

In this study, the established prediction models are employed to determine the main characteristics of the PICP 19G. The application of the developed models tested for another precipitation data to investigate the hydrologic performance variables of the PICP. In order to grasp a more comprehensive knowledge of the predicted values, the predicted values by the models are compared with the recorded data by the installed instruments. As it was elaborated in chapter 4, the cleaning method along with the rainevents' variables are the studied parameters in the models. The rainevents' data computed and obtained from the recorded rainfall events for the typical rainfall year, while since the PICPs were not implemented in 2007 the conducted cleaning method is not accessible. Therefore, cleaning code 1 (which specifies the time from the PICP installation until the first maintenance) considered to complete the input data for the prediction models. The rainfall parameters' data for the first quarter of the typical annual rainfall (2007) are given in Appendix M.

7.3.1. Captured Runoff Prediction for 2007

The captured runoff model was used to predict the peak water level within the controls based on the precipitation data for the typical annual rainfall data (2007). At first, the rainfall variables' data of 2007 were assessed to determine if they are in the acceptable range for a reliable model. After assuring the reliability of the models and according to the inputs for the typical year (2007), the peak water levels were estimated at three different sections of the PICP 19G (Figure 47, Figure 48, and Figure 49).

It was concluded from the analysis that in comparison to the typical rainfall year (2007), 2012 and 2013 are more dry and wet, respectively (The measured rainfall depth

for 2007, 2012, and 2013 given in Table 23). Therefore, the peak water level for the first quarter of the typical year (2007) are slightly higher than the dry year (2012) and lower than the wet year (2013) at three piezometers' locations. In the following figures, the estimated and measured water levels plotted and compared with each other for 2007, 2012, and 2013. The predicted captured water level during rain events for a typical year demonstrate the applicability of the developed models and the obtained data can be used for efficient design.

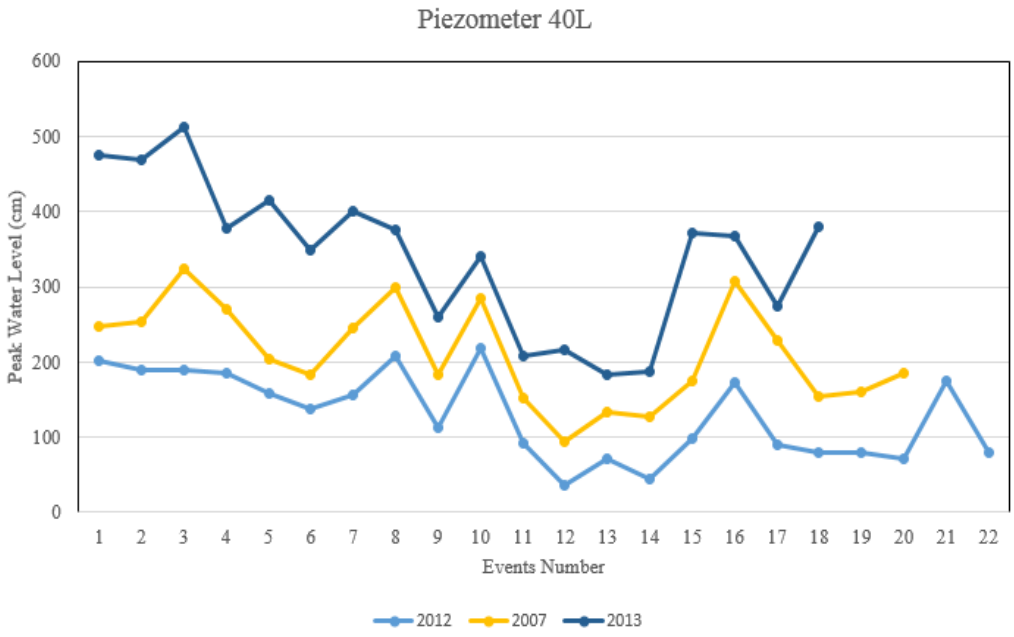

Figure 47. Comparison of the estimated and recorded peak water level at 40L of PICP 19G

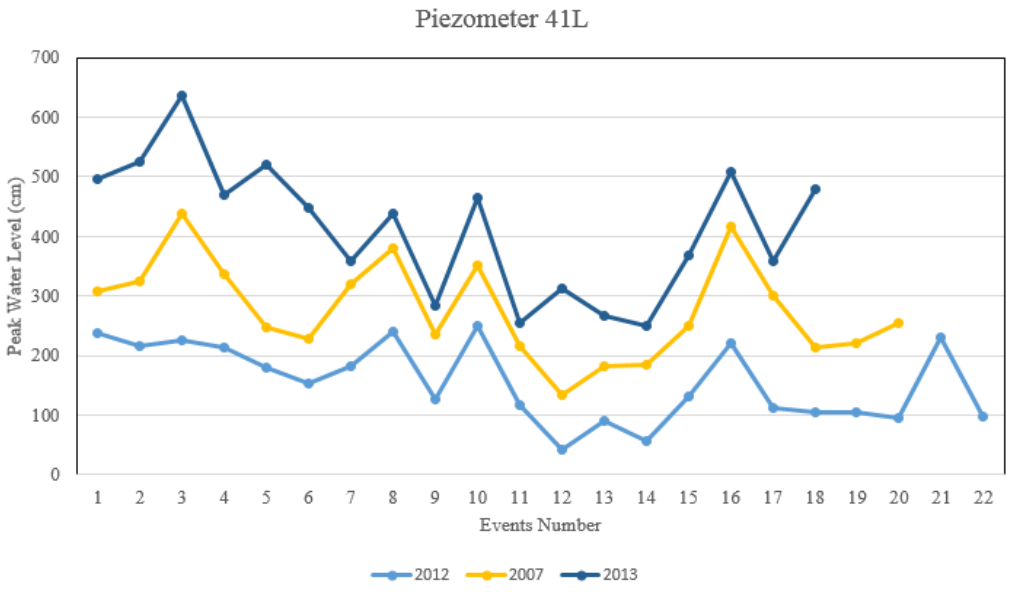

Figure 48. Comparison of the estimated and recorded peak water level at 41L of PICP 19G

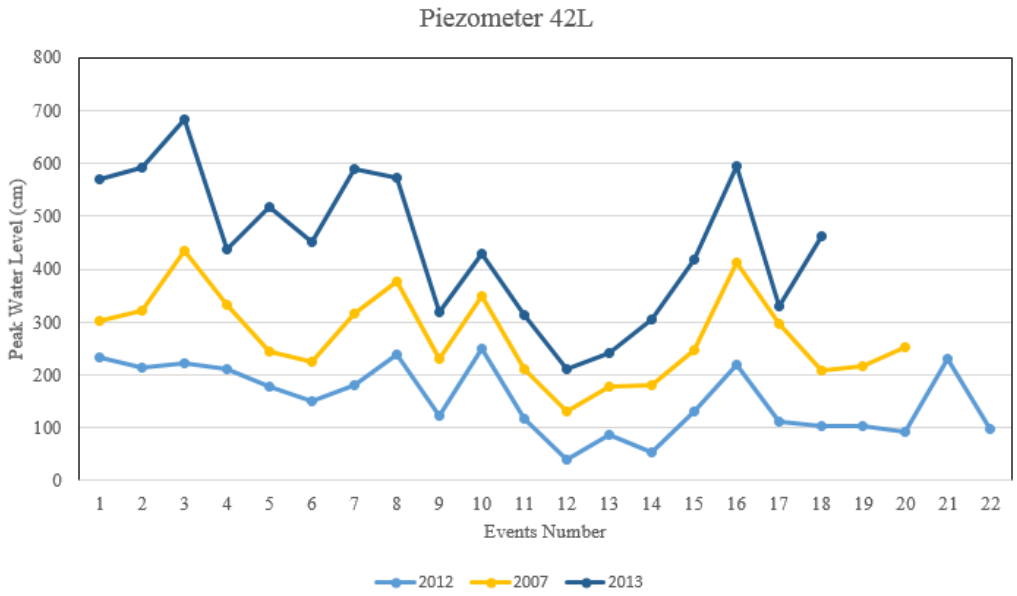

Figure 49. Comparison of the estimated and recorded peak water level at 42L of PICP 19G

7.3.2. Peak VWC Prediction for 2007

The peak VWC model was developed to predict the peak VWC based on the precipitation data for the typical annual rainfall data (2007). The similar approach that used to predict the water level, was employed to predict the peak VWC for the typical rainfall

year. Principally, after computing the required input data for the ANN models and assuring that they are in the acceptable range, the desired output parameter is estimated. In the following figures, the estimated and measured peak VWC values at five different sections of the PICP 19G were plotted and compared with each other for 2007, 2012, and 2013 (Figure 50, Figure 51, Figure 52, Figure 53, and Figure 54). The accurate VWC prediction during storm events of a typical year demonstrate the applicability of the prediction models and can be utilized to estimate the clogging progression length accordingly.

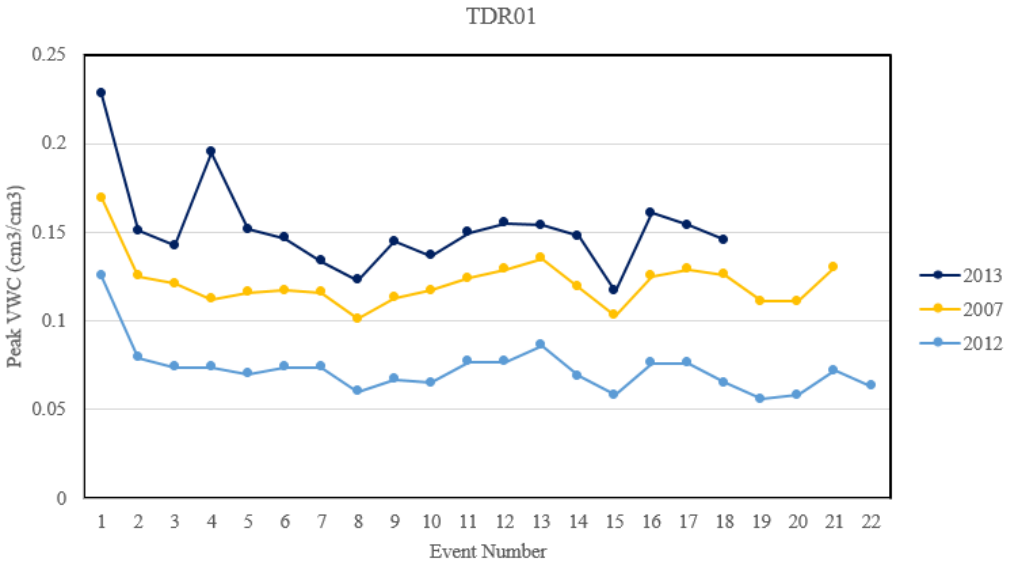

Figure 50. Comparison of the estimated and recorded peak VWC at TDR01 of PICP 19G

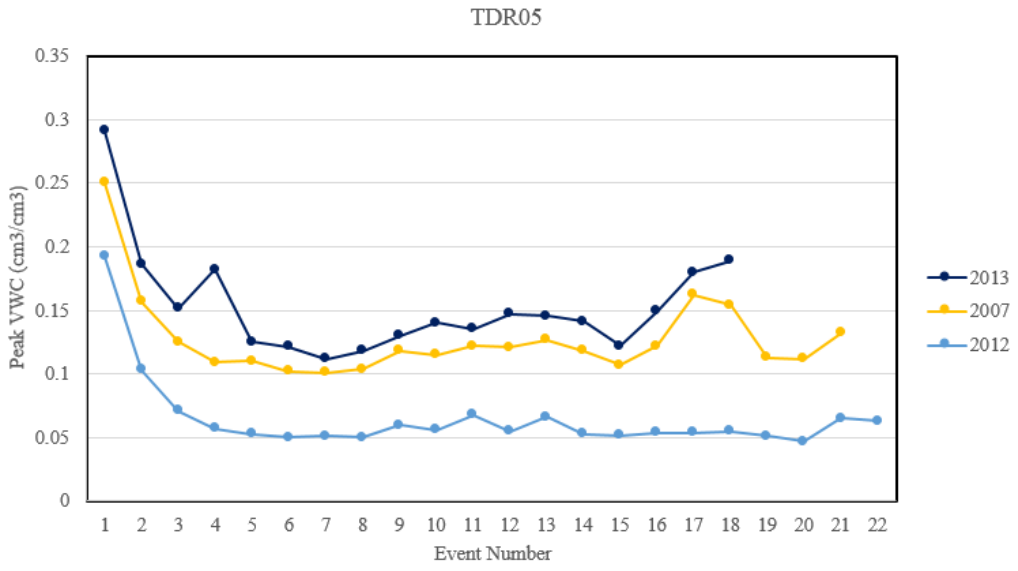

Figure 51. Comparison of the estimated and recorded peak VWC at TDR05 of PICP 19G

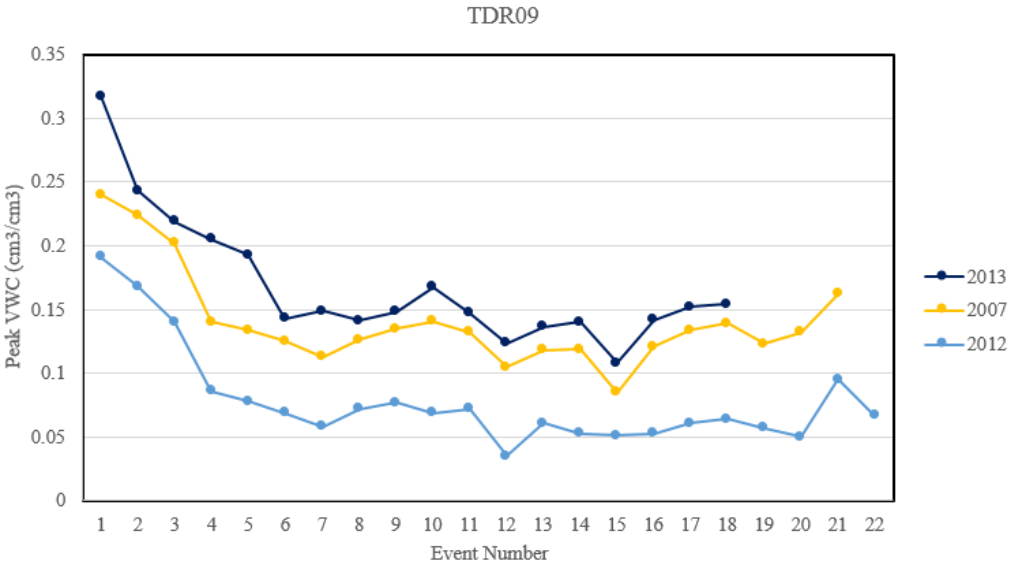

Figure 52. Comparison of the estimated and recorded peak VWC at TDR09 of PICP 19G

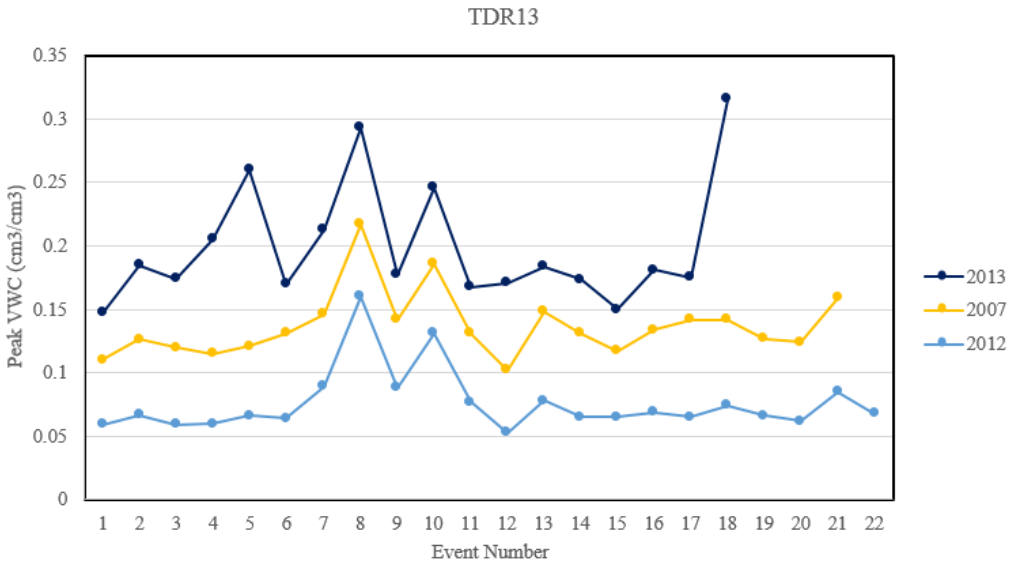

Figure 53. Comparison of the estimated and recorded peak VWC at TDR13 of PICP 19G

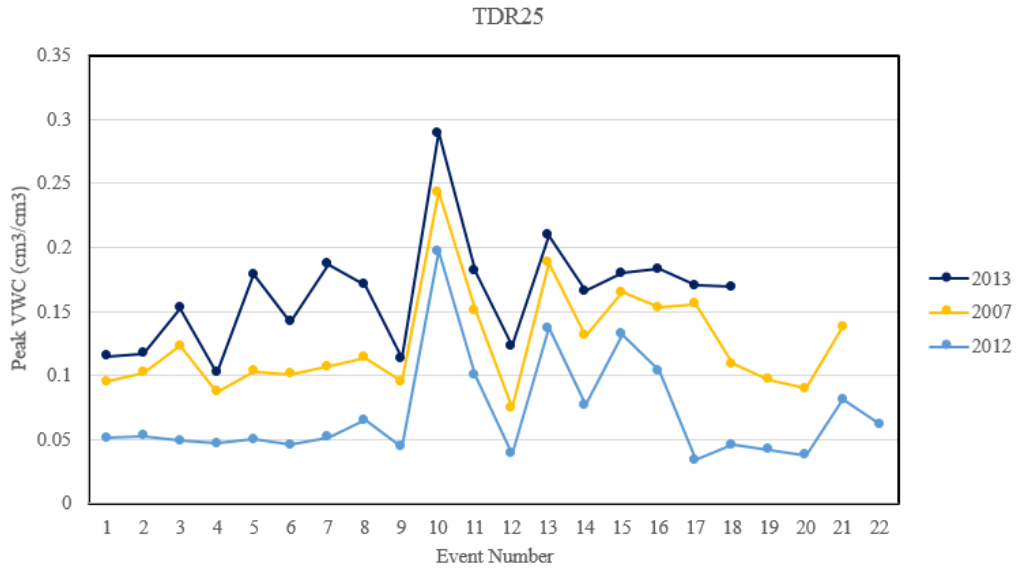

Figure 54. Comparison of the estimated and recorded peak VWC at TDR25 of PICP 19G

7.4. Maintenance Recommendation

The maintenance treatments are essential for the PICPs to restore their infiltration capacity. Conducting efficient cleaning method with the appropriate timetable play an

important role in recovering the PICPs' operation and prevent pavements deterioration over time. Proper cleaning method and effectual maintenance schedule vary based on permeable pavements' specification, site characteristics, and rain events' variables. Comprehensive permeable pavement design should study the watersheds' characteristics and pavements' specification; thus based on the aforementioned parameters, the efficient cleaning method along with the proper maintenance schedule can be planned and suggested prior to construction.

The results and conclusion learned from this research can be used as a platform to schedule the effective maintenances based on site characteristics. Assessing the predicted hydrologic performance variables for the typical year (2007) and comparing them with the recorded data of the dry and wet year (2012 and 2013), lead to proper maintenance schedule based on the annual rainfall pattern. The maintenance recommendations are concluded from the developed models and the recorded data. The author believes that there are many other effective factors exist or may form in the future that considerably alter the PICPs' performance over time. Hence, hereby and because of a lot of unforeseen circumstances he does not claim that the maintenance recommendations provide flawless PICPs' performance. However, he believes that the proposed models and the suggested maintenance schedule as the research study can be a great tool for future design and improve the maintenance schedule of the installed PICPs.

It is recommended that during wet year (with total rainfall depth over 46 inches; like 2013) conducting the hydro excavator method three times to remove the trapped sediment would be efficacious. While for the typical and dry year (with total rainfall depth less than 46 inches; like 2007 and 2012), it is advised to perform the hydro excavator

method two times in order to restore the designated infiltration capacity. Since the results demonstrated that air jet is not as effective as hydro excavator method, it is necessary to perform it with higher frequency to meet the designated operational variables. It is suggested to conduct the air jet method four times during wet year (2013) and three times during typical and dry year (2007 and 2012).

8. CONCLUSION

8.1. Introduction

As urbanization increases, impervious surfaces expands and results in significant changes to urban hydrology. These impervious surfaces result in stormwater runoff that carry pollutants along its path to nearby waterways. Implementation of LID techniques, and permeable pavement systems specifically, are commonly used to manage stormwater runoff and improve quality of water resources near urban areas. Hydrological performance of the permeable pavements, however, deteriorates over time mainly due to the sediment clogging on the surface. The effectiveness of permeable pavements and ultimately the captured runoff volume can be correlated to the extent of clogging on the surface. The clogging progression rates vary based on installation location, site characteristics, and rain events variables. Therefore, multiple ANN models were developed to predict the PICPs' performance characteristics based on the most effective parameters.

The installed PICPs in the Louisville, KY CSO 130 instrumented and monitored to investigate their detail performances over time. The study period started from December 2011, the installation time, until the end of December 2013 to deliver a wide variety of rain events' data. The obtained data from the monitoring equipment and the real occurred rain events provide a unique database to comprehend the operation of the PICPs in the watershed. Captured runoff prediction models that developed through utilizing the recorded water level by the pressure transducers are able to estimate the storage capacity

of the PICPs according to rain events' characteristics. This provides a unique tool to determine the possible overflow volume in the watershed by deducing the captured runoff by the PICPs from the total runoff volume. Also, peak VWC models to estimate the maximum VWC of the TDRs along the PICPs were built. The peak VWC indicates the clogging length on the PICPs and maintenance treatment schedule accordingly. The clogging length prediction models employed complete rain events' variables data and the recorded VWC by the TDRs in a two year study period. This prediction tool provides a unique means to schedule the required maintenance based on a wide range of rain data.

Twenty one laboratory models built and their performance assessed by applying theoretical rainfall over the PICPs. Multiple configurations of the PICPs and observing the monitoring equipment's results provide the opportunity to investigate the effects of different PICPs' specification. Clogging length and infiltration edge prediction models were developed to estimate the hydrologic performance variables according to the PICPs' specification. The recognized models developed through a complete set of experiments and the prepared database from the recorded value by the instruments. Hence, the most effective configuration of the PICPs that offers the best performance can be achieved to improve the future design.

The established prediction tools employed to estimate the main hydrologic performance variables of the PICPs for another precipitation data. The typical annual rainfall was found by studying the average precipitation data for the last 70 years in the city of Louisville, KY. After determining the typical rainfall year (2007), the measured rainfall parameters of that year were computed to utilize as an input in the models. By analyzing the models with the new rainfall data, captured water level and peak VWC

predicted. Therefore, the established robust tools accurately predict the performance variables of the PICPs based on the site characteristics. In the next four sections, the main conclusion derived from the conducted analyses and the developed models are elaborated and discussed.

8.2. Long Term Performance

In this research, MATLAB code was written to determine the infiltration and exfiltration rates of the GI controls. Since the developed model was based on the pressure transducers' data, the comprehensive observation can be obtained from the GI controls performances over time. Surface clogging that is occurred mostly in the gaps of the permeable pavements blocks lessen the surface infiltration rates of the permeable pavements and as a result the captured runoff volume by the control has been minimized. However, surface infiltration rates can be retrieved by conducting maintenance treatments after the accumulated debris was removed. The frequency of cleaning maintenances based on site characteristics and rain events properties was discovered to capture the maximum possible runoff volume. The second Air Jet maintenance was not very effective to retrieve surface infiltration rates because the maximum peak intensity values of occurred rain events for the time duration between the two maintenances are much greater than other time periods. The most effective conducted cleaning methods were hydro excavator truck and the third Air Jet maintenance based on the rain events data and observing the infiltration rates into the gallery. However, the hydro excavator truck removed more debris and retrieved most of the infiltration rates loss in comparison to all other cleaning methods.

Since the clogging concentrates in the upper edge of the permeable pavement, the infiltration rates decrement in the upgradient of the permeable pavement are higher in

comparison to the downgradient edge. More frequent cleaning method for specific locations based on the observed flow pattern can be useful to restore the loss of captured runoff volume. The infiltration rate index was introduced as a factor to determine the clogging progression and explore the location with sediment concentration. Linear increase on infiltration rates was observed between the two adjacent piezometers that demonstrate the clogging movement on the surface from the upper edge.

The filtration layers that ease the water movement in the storage gallery did not perform properly after several rain events since smaller debris can penetrate into the layers and reduce the porosity. By observing the water level fluctuation, about one fourth of infiltration rates loss cannot be retrieved because the smaller debris that penetrates into the storage gallery layers. The properties of sub layer soil that surrounds the GI controls is highly important on determining the runoff volume that exfiltrate from the gallery layers. The hydraulic conductivity of different soil layers are computed by the Matlab code from the observed water levels data. The soil layers at the bottom of the storage gallery is more saturated and as a result the hydraulic conductivity of the surrounding soil layers are lower in comparison to the permeability of upper soil layers. The hydraulic conductivity of soil layers, filtration layer characteristics and efficacy of cleaning methods can be used to have a better view for future design.

8.3. Captured Runoff

Permeable pavements performance deteriorate over time due to clogging and sediment accumulation on the surface and in the storage gallery layers. As a result, the permeable pavements performance degrades over time as runoff is unable to enter the PICP system. In this study, the captured runoff prediction models are developed at three different

locations for two installed PICPs, based on the comprehensive database from a two-year study. The developed neural network models, are able to predict accurately the water levels in the storage gallery of the monitored permeable pavements through the rain events characteristics and the last conducted maintenance treatment. Hence, by estimating the captured runoff for a theoretical storm event, the hydrologic performance of the PICPs in the watershed area can be foreseen during different storm events.

Sensitivity analyses were also completed to identify the factors with the highest influence on the surface runoff water captured by the permeable pavements. An understanding of the relative importance for each factor on the captured runoff is important for future design modifications. It is concluded that previous rainfall depth has the highest influence on the captured runoff volume and the duration and rainfall depth of the current rain events presented high relative importance values on the water levels of the piezometers. Thus, by scheduling more effective maintenance treatment and considering the effective factors in the design processes, greater runoff volume can be captured by PICPs.

8.4. Clogging Progression (VWC)

In this study, the ANN approach was employed to discover the complex interaction between the site characteristics and the clogging progression rates. Rain events variables and the last conducted maintenance are the studied site characteristics, while the VWC, an indication of clogging progression, is the predicted variable for the model. A large number of occurred rain events at the PICP site in a two year study period was considered and the associated peak VWC values during or after each event were computed. The rainfall

parameters, the peak VWC, and the last conducted maintenance for each event were scrutinized to develop the ANN-based models.

Results of the ANN analysis provided VWC prediction of the installed TDRs at different locations. Based on the ANN models, the clogging progression and the infiltration rates decline for various distances from the upgradient edge of the PICP can be predicted. Scheduling the maintenance treatment accordingly and locating the clogging concentration are some of the main benefits of the model. Sensitivity analysis on the influencing input parameters has shown the relative importance of the effective parameters. It was observed that the peak 5 minute intensity, the previous rainfall depth, and the cumulative rainfall depth from the installation have the highest efficacy on the clogging progression.

The ANN models have produced accurate results for predicting VWC based on the considered parameters. The prediction ability of the developed models makes scheduling the maintenance treatment possible and keep the PICP of preforming thoroughly. Although detecting clogging progression rates is challenging, the ANN models introduce explicit formulations to compute VWC and foresee the clogging development. Results of the parametric study are in accordance with the experimental results which indicate that the neural network models are robust and give accurate results.

8.5. Clogging/Infiltration Edge (Lab Model)

This study considers the neural network model to predict the hydrologic performance of PICPs. Slope, gap size, and filling joint material are the pavements specifications that investigated their effectiveness. Twenty one experiments are conducted with different combinations of pavements characteristics. Storm events are simulating by collecting the natural occurred rain events in the storage tank. Clogging

progression length and the infiltration edge are the two main factors that determine the PICPs performances.

The neural network models are able to predict accurately the rainfall depth in accordance with the main pavements characteristics and the recorded clogging length. The prediction model can be used as a useful tool on determining the clogging concentration and schedule the required maintenances. Planning efficient maintenance frequency is challenging and develop a model to predict the performance failure and therefore conducting maintenance accordingly is useful. Although detecting rainfall depth is challenging, the proposed model present explicit formulations to compute rainfall depth that result in failure in captured runoff. Moreover, the sensitivity analysis is completed to determine the efficacy of the studied pavements characteristics on clogging length. The results indicate that the slope and location from the upgradient edge are the most effective parameters on accumulating sediment.

It is shown that the infiltration edge is advanced along the permeable pavements over time. Determining the speed of infiltration edge progression in accordance with rainfall depth and the main pavements characteristics are helpful to predict the PICP performance. The proposed model is able to predict the rainfall depth amount that cause the specified infiltration edge advancement with 99% accuracy. The parametric study define the relative importance of the input parameters and their effectiveness on the amount of rainfall which is needed to shift the infiltration edge. As it is expected from the experimental results, slope and gap size are shown the highest influence on the cumulative rainfall depth. The proposed neural network models are robust and able to predict the pavements performance with high

accuracy. The most effective parameters on hydrologic operation of PICPs are determined and can be used for more efficient future design.

8.6. Future Reseach

The developed ANN models have been established as an effective methods to estimate the main hydrologic performance variables. In this study a complete set of rainevents' variables and the pavements' specifications have been assessed and considered to recommend prediction simulations. Although the proposed models are able to accurately predict the PICPs' performances, not all the aspects have been studied and their effects require further investigation. Each PICP has its own construction details and site characteristics which considering all these variables for comprehensive assessment is necessary.

Scrutinizing site characteristics such as drainage area and impervious area to the upgradient edge ratio of the PICPs can be the next step in developing a complete prediction model. Moreover, conducting sensitivity analysis on the potential factors to define the important site characteristics are much needed. Therefore, by determining the efficacies of the site characteristics and combining the most effective ones with the high importance rainevents' variables and pavements' specification, complete prediction tools can be developed.

Finally, there is still a lot to learn and investigate regarding the PICPs' performances, their operation and design. The proposed models are not able to estimate the operation variables for all the PICPs and understanding the variations of the PICPs specifications are required. The path for determining the most effective parameters is not fully known and thus flawless design need many experiments and studies to achieve. Using

the methods, results, and conclusion of this research as a platform along with the results from other studies can lead to developing a thorough design tool that considers all the effective factors.

REFERENCES

Al-Rubaei, A. M., et al. (2012). "Can vacuum cleaning recover the infiltration capacity of a clogged porous asphalt?" 7th international conference on water sensitive urban design: 49-54.

Alavi, A. H. and A. H. Gandomi (2011). "Prediction of principal ground-motion parameters using a hybrid method coupling artificial neural networks and simulated annealing." Computers & Structures **89**(23): 2176-2194.

Antunes, M. (2013). "Consulting with Industry Expert from EPHenry on Interlocking Concrete Pavers.".

Balades, J. D., et al. (1995). "Permeable Pavements: Pollution Management Tools." Wat. Sci. Tech. **32**(1): 49-56.

Basheer, I. and M. Hajmeer (2000). "Artificial neural networks: fundamentals, computing, design, and application." Journal of microbiological methods **43**(1): 3-31.

Baum, E. B. and F. Wilczek (1988). Supervised learning of probability distributions by neural networks. Neural information processing systems, New York: AIP.

Brattebo, B. O. and D. B. Booth (2003). "Long-term stormwater quantity and quality performance of permeable pavement systems." Water research **37**(18): 4369-4376.

Brown, R. A. and M. Borst (2013). "Assessment of Clogging Dynamics in Permeable Pavement Systems with Time Domain Reflectometers." Journal of Environmental Engineering **139**(10): 1255-1265.

Campbell Scientific, I. (2011). CS650 and CS655 Water

Content Reflectometers**:** 9-21.

Charron, A., et al. (2000). "Real Time Control Study to Reduce Combined Sewer Overflows in Louisville and Jefferson County." Proceedings of the Water Environment Federation **2000**(4): 91-103.

Cybenko, J. (1989). "Approximations by superpositions of a sigmoidal

function." Math. Control Signals Systems **2**: 303-314.

Damodaram, C., et al. (2010). Simulation of Combined Best Management Practices and Low Impact Development for Sustainable Stormwater Management1, Wiley Online Library.

Dunn, A. D. (2010). "SITING GREEN INFRASTRUCTURE: LEGAL AND POLICY SOLUTIONS TO ALLEVIATE URBAN POVERTY AND PROMOTE HEALTHY COMMUNITIES." Boston College Environmental Affairs Law Review **37**(1).

Ehsaei, A. (2013). Effect of Slope and Paver Characteristics on Performance of Permeable Pavement GI, University of Louisville.

Environmental Water Resources Institute (2007). ASCE GUIDELINE FOR MONITORING

STORMWATER GROSS SOLIDS.

Ferguson, B. K. (1998). Introduction to stormwater: concept, purpose, design, John Wiley & Sons.

Gillies, R. R., et al. (2003). "Effects of urbanization on the aquatic fauna of the Line Creek watershed, Atlanta—a satellite perspective." Remote Sensing of Environment **86**(3): 411-422.

Goh, A. (1995). "Back-propagation neural networks for modeling complex systems." Artificial Intelligence in Engineering **9**(3): 143-151.

Haktanir, T., et al. (2010). "Frequency analyses of annual extreme rainfall series from 5 min to 24 h." Hydrological processes **24**(24): 3574-3588.

Haselbach, L. M., et al. (2006). "Permeability predictions for sand-clogged Portland cement pervious concrete pavement systems." Journal of environmental management **81**(1): 42-49.

Heilig, G. K. (2012). "World urbanization prospects the 2011 revision." United Nations, Department of Economic and Social Affairs (DESA), Population Division, Population Estimates and Projections Section, New York.

Holman-Dodds, J. K. B. A. A. P. K. W. (2003). "EVALUATION OF HYDROLOGIC BENEFITS OF INFILTRATION BASED URBAN STORM WATER MANAGEMENT¹." JAWR JAWRA Journal of the American Water Resources Association **39**(1): 205-215.

Hossein Alavi, A., et al. (2010). "Modeling of maximum dry density and optimum moisture content of stabilized soil using artificial neural networks." Journal of Plant Nutrition and Soil Science **173**(3): 368-379.

James, W. and H. Von Langsdorff (2003). The use of permeable concrete block pavement in controlling environmental stressors in urban areas. 7th International Conference on Concrete Block Paving.

Kelly, V. R., et al. (2009). "Effect of climate change between 1984 and 2007 on precipitation chemistry at a site in northeastern USA." Environmental science & technology **43**(10): 3461-3466.

Kyoung, M. S., et al. (2011). "Dynamic characteristics of monthly rainfall in the Korean Peninsula under climate change." Stochastic Environmental Research and Risk Assessment **25**(4): 613-625.

Legret, M. and V. Colandini (1999). "Effects of a porous pavement with reservoir structure on runoff water: water quality and fate of heavy metals." Water Science and Technology **39**(2): 111-117.

Meehl, G. A., et al. (2009). "Relative increase of record high maximum temperatures compared to record low minimum temperatures in the US." Geophysical Research Letters **36**(23).

Mollahasani, A., et al. (2011). "Nonlinear neural-based modeling of soil cohesion intercept." KSCE Journal of Civil Engineering **15**(5): 831-840.

Newman, A. P., et al. (2001). "Oil retention and microbial ecology in porous pavement structures." European Forum of Environmental Research Laboratories **9**.

Ngongondo, C., et al. (2011). "Evaluation of spatial and temporal characteristics of rainfall in Malawi: a case of data scarce region." Theoretical and applied climatology **106**(1-2): 79-93.

Nirupama, N. and S. P. Simonovic (2007). "Increase of flood risk due to urbanisation: A canadian example." Natural Hazards **40**(1): 25-41.

Pitt, R. and A. Maestre (2005). Stormwater quality as described in the National Stormwater Quality Database (NSQD). Proceedings of the 10th International Conference on Urban Drainage, Copenhagen, Denmark.

Pooya Nejad, F., et al. (2009). "Prediction of pile settlement using artificial neural networks based on standard penetration test data." Computers and Geotechnics **36**(7): 1125-1133.

Pratt, C., et al. (1999). "Mineral oil bio-degradation within a permeable pavement: long term observations." Water Science and Technology **39**(2): 103-109.

Rafiq, M., et al. (2001). "Neural network design for engineering applications." Computers & Structures **79**(17): 1541-1552.

Schapp, M. G. and F. J. Leij (1998). "Using Neural Networks to predict soil water retention and soil hydraulic conductivity." Soil & Tillage Research.

Scholz, M. and P. Grabowiecki (2007). "Review of permeable pavement systems." Building and Environment **42**(11): 3830-3836.

Shahin, M. A., et al. (2008). "State of the art of artificial neural networks in geotechnical engineering." Electronic Journal of Geotechnical Engineering **8**: 1-26.

Shamseldin, A. Y. (1997). "Application of a neural network technique to rainfall-runoff modelling." Journal of Hydrology: 272-294.

Smith, D. R. (2006). Permeable Interlocking Concrete Pavements: Selection, Design, Construction, Maintenance, Interlocking Concrete Pavement Institute.

Tarefder, R. A., et al. (2005). "Neural Network Model for Asphalt Concrete Permeability." Journal of Materials in Civil Engineering **17**.

Trimble, S. W. (1997). "Contribution of stream channel erosion to sediment yield from an urbanizing watershed." Science **278**(5342): 1442-1444.

United States, E. P. A. (1994). "Combined Sewer Overflow (CSO) Control Policy : final policy." Federal register. **59**(75).

United States, G. A. O. (2005). "Clean Water Act improved resource planning would help EPA better respond to changing needs and fiscal constraints : report to congressional requesters." from http://purl.access.gpo.gov/GPO/LPS64272.

Villarini, G., et al. (2011). "On the frequency of heavy rainfall for the Midwest of the United States." Journal of Hydrology **400**(1): 103-120.

Walsh, C. J. (2000). "Urban impacts on the ecology of receiving waters: a framework for assessment, conservation and restoration." Hydrobiologia **431**(2): 107-114.

Waters, D., et al. (2003). "Adaptation of a storm drainage system to accommodate increased rainfall resulting from climate change." Journal of Environmental Planning and Management **46**(5): 755-770.

White, R. R. (2002). Building the ecological city, Elsevier.

Yang, T., et al. (2010). "Regional frequency analysis and spatio-temporal pattern characterization of rainfall extremes in the Pearl River Basin, China." Journal of Hydrology **380**(3): 386-405.

Zhang, G., et al. (1998). "Forecasting with artificial neural networks:: The state of the art." International journal of forecasting **14**(1): 35-62.

APPENDIX A

MATLAB Code

```
function result=Piezometer Data(x, y, step_hour, step_hum, Max_hum, flag, name)


if x(1,5)==0
   start_hour = x(1,4)+step_hour;
else
   %start from next hour+step_hour
   start_hour = x(1,4)+1+step_hour;
end


start_idx = mod(x(1,5),60) + step_hour*60;
resIdx=1;
result=0;
last_MAX=0;
last_period_hum=0;
last_period_time=0;
last_flag_left=false;
last_flag_right=false;
new_flag_right=false;
new_flag_left=false;
another_flag_right=false;
```

```
another_flag_left=false;
window_flag=true;
ctr=1;
last_ctr=1;
itr_counter=0;

for index=0:step_hour*2*60:length(x)
    itr_counter=itr_counter+1
    window_flag=true;
    while_window_ctr=0;
    while window_flag==true
        distance=0; right_hum=0; right_time=0; left_hum=0;
        left_time=0; period_hum=0; period_time=0; temp=0;
        minIdx=0; flag_small=false; window_flag=false;
        while_window_ctr=while_window_ctr+1;
        %find peak every step hour
        start_idx=index+step_hour*60;
        if start_idx+step_hour*60>length(x)
            period_hum=y(start_idx-step_hour*60+1:length(x),1);
            period_time=x(start_idx-step_hour*60+1:length(x),:);
        else
            period_hum=y(start_idx-step_hour*60+1:start_idx+step_hour*60,1);
            period_time=x(start_idx-step_hour*60+1:start_idx+step_hour*60,:);
```

```
        period_time(1,:);
        period_time(end,:);
    end

    MAX=max(period_hum);
    MIN=min(period_hum);

    if (MAX(1,1)-MIN(1,1)>= step_hum && MAX(1,1)>Max_hum) ||
new_flag_right==true || last_flag_right==true
        %There is a peak
        peak_hum=MAX;
        tempIdx=find(period_hum==peak_hum);
        peak_time=period_time(tempIdx(1,1),:);

        if flag==1
            start_idx=start_idx-step_hour*60+tempIdx;
            if start_idx+step_hour*60>length(x)
                period_hum=y(start_idx-step_hour*60+1:length(x),1);
                period_time=x(start_idx-step_hour*60+1:length(x),:);
            else
                period_hum=y(start_idx-step_hour*60+1:start_idx+step_hour*60,1);
                period_time=x(start_idx-step_hour*60+1:start_idx+step_hour*60,:);
            end
```

```
            tempIdx(1,1)=step_hour*60;
        end


        %if last period has a peak and we ignored it
        %beacuse right was empty, so we need to consider it now
        if ((last_MAX>MAX && last_flag_right==true )|| new_flag_right==true)&& ctr-
last_ctr==1
            %Merg current period and last period
            period_hum=cat(1,last_period_hum, period_hum);
            period_time=cat(1,last_period_time, period_time);
            if last_flag_right==true
                MAX=max(period_hum);
                peak_hum=MAX;
            end
            if new_flag_right==true
                peak_hum=last_MAX;
                if while_window_ctr<=1
                    window_flag=true;
                end
            end
            tempIdx=find(period_hum==peak_hum);
            peak_time=period_time(tempIdx(1,1),:);
```

```
end
last_flag_right=false;
new_flag_right=false;%
if tempIdx(1,1)~=1
   left_hum=period_hum(1:tempIdx(1,1)-1);
   left_time=period_time(1:tempIdx(1,1)-1,:);
   temp=find(left_hum==peak_hum-step_hum);
   if ~isempty(temp)
      %the point is valid
      point1_hum=left_hum(temp(1,1));
      point1_time=left_time(temp(1,1),:);
   else
      %find nearest point
      for i=1:length(left_hum)
         if left_hum(i)>peak_hum
            distance(i)=10000;
         else
            distance(i)=abs(peak_hum-step_hum - left_hum(i));
         end
      end
      MIN=min(distance);
      minIdx=find(distance==MIN);
      point1_hum=left_hum(minIdx(1,end));
```

```
        point1_time=left_time(minIdx(1,end),:);
        another_flag_left=true;
        if abs(point1_hum-peak_hum)<step_hum/2
            new_flag_left=true;
        end
    end
else
    %there is not left side
    point1_time=0;
    last_flag_left=true;
end
%if last period has a peak and we ignored it
%beacuse left was empty, so we need to consider it now
if ((last_MAX>MAX && last_flag_left==true )|| new_flag_left==true)
    %Merg current period and last period
    another_flag_left=false;
    period_hum=cat(1,last_period_hum, period_hum);
    period_time=cat(1,last_period_time, period_time);
    if last_flag_left==true
        MAX=max(period_hum);
        peak_hum=MAX;
    end
```

```
tempIdx=find(period_hum==peak_hum);
peak_time=period_time(tempIdx(1,1),:);

last_flag_left=false;
new_flag_left=false;%
if tempIdx(1,1)~=1
    left_hum=period_hum(1:tempIdx(1,1)-1);
    left_time=period_time(1:tempIdx(1,1)-1,:);

    temp=find(left_hum==peak_hum-step_hum);
    if ~isempty(temp)
        %the point is valid
        point1_hum=left_hum(temp(1,1));
        point1_time=left_time(temp(1,1),:);
    else
        %find nearest point
        for i=1:length(left_hum)
            if left_hum(i)>peak_hum
                distance(i)=10000;
            else
                distance(i)=abs(peak_hum-step_hum - left_hum(i));
            end
        end
```

```
            MIN=min(distance);
            minIdx=find(distance==MIN);
            point1_hum=left_hum(minIdx(1,end));
            point1_time=left_time(minIdx(1,end),:);
            another_flag_left=true;
        end
    else
        %there is not left side
        point1_time=0;
        last_flag_left=true;
    end
end

%Right hand
distance=0;
temp=0;
minIdx=0;
if tempIdx(1,1)<length(period_time)
    right_hum=period_hum(tempIdx(1,1)+1:end);
    right_time=period_time(tempIdx(1,1)+1:end,:);

    temp=find(right_hum==peak_hum-step_hum);
    if ~isempty(temp)
```

```
        %the point is valid
        point2_hum=right_hum(temp(1,1));
        point2_time=right_time(temp(1,1),:);
    else
        %find nearest point
        for i=1:length(right_hum)
            if right_hum(i)>peak_hum
                distance(i)=10000;
            else
                distance(i)=abs(peak_hum-step_hum - right_hum(i));
            end
        end
        MIN=min(distance);
        minIdx=find(distance==MIN);
        point2_hum=right_hum(minIdx(1,1));
        point2_time=right_time(minIdx(1,1),:);
        another_flag_right=true;
        if abs(point2_hum-peak_hum)<step_hum/2
            new_flag_right=true;
        end
    end
else
    %there is no right side
```

```
            point2_time=0;
            last_flag_right=true;
        end

        %Delta Time of rate_increase
        if length(point1_time)==1
            %there is no left side
            rate_inc=0;
        else
            if  peak_time(2) ~= point1_time(2) && peak_time(1) ~= point1_time(1)
                %Next month
                tmp=(30-point1_time(2))+peak_time(2)-1;
                delta=((24-point1_time(4)-1)*60 + 60 -point1_time(5)) + tmp*24*60 +
(peak_time(4)*60+peak_time(5));
            elseif point1_time(2)~= peak_time(2)
                %it means peak time is tomorrow
                tmp=peak_time(2)-point1_time(2)-1;
                delta=((24-point1_time(4)-1)*60 + 60 -point1_time(5)) + tmp*24*60 +
(peak_time(4)*60+peak_time(5));
            elseif point1_time(4) == peak_time(4)
                delta=peak_time(5)-point1_time(5);
            else
```

```
            delta=(peak_time(4)-point1_time(4)-1)*60+(60-
point1_time(5))+peak_time(5);
        end
        if  another_flag_left==true
            rate_inc=abs(point1_hum-peak_hum)/delta;
            another_flag_left=false;
        else
            rate_inc = step_hum/delta;
        end
    end

    %Delta Time of rate_decrease
    if length(point2_time)==1
        %there is no right side
        rate_dec=0;
    else
        if  peak_time(2) ~= point2_time(2) && peak_time(1) ~= point2_time(1)
            %Next month
            tmp=(30-peak_time(2))+point2_time(2)-1;
            delta=((24-peak_time(4)-1)*60 + 60 -peak_time(5)) + tmp*24*60 +
(point2_time(4)*60+point2_time(5));
        elseif peak_time(2) ~= point2_time(2)
            %it means peak time is tomorrow
```

```
            tmp=point2_time(2)-peak_time(2)-1;
            delta=((24-peak_time(4)-1)*60 + 60 -peak_time(5)) + tmp*24*60 +
(point2_time(4)*60+point2_time(5));
        elseif point2_time(4) == peak_time(4)
            delta=point2_time(5)-peak_time(5);
        else
            delta=(point2_time(4)-peak_time(4)-1)*60+(60-
peak_time(5))+point2_time(5);
        end
        if  another_flag_right==true
            rate_dec=abs(point2_hum-peak_hum)/delta;
            another_flag_right=false;
        else
            rate_dec = step_hum/delta;
        end

    end

    if rate_inc <= 0 || rate_dec <= 0
        %Do nothing
    elseif new_flag_right==true || new_flag_left==true
        %Do nothing
    elseif resIdx>1 &&...
```

```
        (result(resIdx-1,6)==peak_hum &&...
        sum(result(resIdx-1,1:5)==peak_time(1:5))==5)
    %Current and last peak are the same
    %Do nothing
elseif resIdx>1
    %current time of peak is befor last peak time
    if result(resIdx-1,3)>peak_time(3)
        flag_small=true;
    elseif result(resIdx-1,3)==peak_time(3)
        if result(resIdx-1,1)>peak_time(1)
            flag_small=true;
        elseif result(resIdx-1,1)==peak_time(1)
            if result(resIdx-1,2)>peak_time(2)
                flag_small=true;
            elseif result(resIdx-1,2)==peak_time(2)
                if result(resIdx-1,4)>peak_time(4)
                    flag_small=true;
                elseif result(resIdx-1,4)==peak_time(4)
                    if result(resIdx-1,5)>peak_time(5)
                        flag_small=true;
                    end
                end
            end
```

```
        end
    end
    if flag_small==true
        if peak_hum > result(resIdx-1,6)
            %it found better peak rather than last one
            result(resIdx-1,1:5)=peak_time(1:5);
            result(resIdx-1,6)=peak_hum;
            result(resIdx-1,7)=rate_inc;
            result(resIdx-1,8)=rate_dec;
        else
            %Do nothing
        end
        flag_small=false;
    else
        result(resIdx,1:5)=peak_time(1:5);
        result(resIdx,6)=peak_hum;
        result(resIdx,7)=rate_inc;
        result(resIdx,8)=rate_dec;
        resIdx=resIdx+1;
    end

else
    result(resIdx,1:5)=peak_time(1:5);
```

```
            result(resIdx,6)=peak_hum;
            result(resIdx,7)=rate_inc;
            result(resIdx,8)=rate_dec;
            resIdx=resIdx+1;
        end
        last_MAX=MAX;
        last_period_hum=period_hum;
        last_period_time=period_time;
        last_ctr=ctr;
    end%if
    ctr=ctr+1;
  end%while
end%for

% %check difference between results
% result2(1,:)=result(1,:);
% j=1;
% for i=2:length(result)
%     if result2(j,
%
% end
xlswrite(name,result)
end
```

Neural Network Code

Prediction Model Development Code

```
 %% FF Net Definition


% L=length(Train.P');
%
% Index=randperm(L);
% Train.P=Train.P(:,Index);
% Train.V=Train.V(:,Index);
for i = 4:8
   net=newff(minmax(Train.P),[i 1],{'logsig' 'logsig'},'trainlm');


   net.trainParam.epochs=1000;
%    net.trainParam.mu_max=10^100;
%    net.trainParam.mu=1e-4;
%    net.performFcn='mae';
%    net.trainParam.goal=.005;
%    net.trainParam.lr = 0.005;
%    net.trainParam.min_grad = 10^-30;
%    net.trainParam.max_grad = 10^15;


   % Trained_net=train(net,Train.P,Train.V,[],[],Validation,Test);
```

```
Trained_net = train(net,Train.P,Train.V,[],[],[],Test);



tr = sim(Trained_net,Train.P)';

trainset(:,i) = sim(Trained_net,Train.P)';


disp('mae trainig error =');

ma_train(i) = mae(Train.V-sim(Trained_net,Train.P));


disp('mse trainig error =');

ms_train(i) = mse(Train.V-sim(Trained_net,Train.P));


disp('coefficient of correlation trainig =')

r2_train(i) = corr2(Train.V,sim(Trained_net,Train.P));


%figure

%postreg(sim(Trained_net,Train.P),Train.V)


te = sim(Trained_net,Test.P)';

testset(:,i) = sim(Trained_net,Test.P)';


disp('mae test error =');

ma_test(i) = mae(Test.V-sim(Trained_net,Test.P));
```

```
disp('mse test error =');
ms_test(i) = mse(Test.V-sim(Trained_net,Test.P));

disp('coefficient of correlation trainig =')
r2_test(i) = corr2(Test.V,sim(Trained_net,Test.P));

%figure
%postreg(sim(Trained_net,Test.P),Test.V)

I_H_weight = net.iw{1}';
eval(['I_H_weight' int2str(i) '=' mat2str(I_H_weight)]);

H_O_weight = net.lw{2,1};
eval(['H_O_weight' int2str(i) '=' mat2str(H_O_weight)]);

I_H_bias = net.b{1,1}';
eval(['I_H_bias' int2str(i) '=' mat2str(I_H_bias)]);

H_O_bias = net.b{2,1};
eval(['H_O_bias' int2str(i) '=' mat2str(H_O_bias)]);

% %% Garson
```

```
%
% %nnmber of variable
   C = 4;


   RAS = zeros(i);
   for j = 1:i
      for k = 1:C
         RAS(j) = RAS(j) + abs(I_H_weight(k,j));
      end
   end


   for m = 1:i
      for n = 1:C
         Q(m,n) = (abs(I_H_weight(n,m)))/(RAS(m));
      end
   end


   for t = 1:C
      S = sum(Q);
      SS = (sum(S(t))/(sum(sum(Q))))*100;
      eval(['S' int2str(i) '(' int2str(t) ')=' num2str(SS)]);
   end
```

```
end

% net.iw{1}; % input weight

% net.lw{2,1};% 2 th layer

% net.lw{3,2};% 3 th layer
```

Error Calculation Code

```
%% Analysis

disp('MAE train error =');

MAE_Train = mae(Traina-Trainb)

disp('MSE train error =');

MSE_Train = mse(Traina-Trainb)

disp('RMSE train error =');

RMSE_Train = MSE_Train^.5

disp('coefficient of correlation training =');

R_Train = corr(Traina,Trainb)

R2_Train = R_Train^2
```

```
disp('MAE test error =');

MAE_Test = mae(Testa-Testb)


disp('MSE test error =');

MSE_Test = mse(Testa-Testb)


disp('RMSE test error =');

RMSE_Test = MSE_Test^.5


disp('coefficient of correlation testing =');

R_Test = corr(Testa,Testb)


R2_Test = R_Test^2
```

APPENDIX B

Peak Water Level Dataset of PICP 19G

Event	Cleaning Method	Duration (Min.)	Rainfall Depth (cm.)	Peak 5 min (mm/hr)	Peak 15 min (mm/hr)	Peak Duration (Min)	Cumulative Rainfall Depth from the installation (cm)	Cumulative Rainfall Depth from the last maintenance (cm)	ADP (Min)	Previous Rainfall Depth (cm)	Max Piezometer 1 (cm)	Max Piezometer 2 (cm)	Max Piezometer 3(cm)
1	1	480	1.68	21.34	16.26	15	1.22	1.22	7965	1.17	202.60	238.60	234.00
2	**1**	**605**	**1.55**	**6.10**	**4.06**	**15**	**2.90**	**2.90**	**1615**	**1.68**	**189.30**	**216.40**	**213.80**
3	1	820	2.11	9.14	8.13	15	4.50	4.50	1900	0.03	189.20	225.30	223.30
4	1	535	1.96	15.24	10.16	15	6.65	6.65	16245	0.05	185.50	214.00	212.10
5	1	140	0.38	3.05	3.05	15	8.61	8.61	370	1.96	158.70	179.60	177.70
6	1	135	0.20	3.05	2.03	15	8.99	8.99	805	0.38	137.00	152.40	150.50
7	**1**	**605**	**0.99**	**21.34**	**13.21**	**15**	**9.19**	**9.19**	**6545**	**0.20**	**157.20**	**182.10**	**180.20**
8	1	390	1.93	42.67	29.46	15	10.21	10.21	1815	0.03	208.50	240.80	238.60
9	**1**	**270**	**0.64**	**3.05**	**3.05**	**15**	**12.22**	**12.22**	**3000**	**0.08**	**113.20**	**125.60**	**123.90**
10	1	1520	4.37	36.58	19.30	15	12.85	12.85	470	0.64	219.10	251.00	250.20
11	**1**	**490**	**0.91**	**6.10**	**5.08**	**15**	**17.35**	**17.35**	**3650**	**0.03**	**91.00**	**117.70**	**115.90**
12	1	145	0.48	3.05	3.05	15	18.47	18.47	4920	0.05	35.87	43.03	41.18
13	1	645	0.84	9.14	9.14	10	18.95	18.95	2040	0.48	71.47	89.90	88.10
14	1	250	0.25	6.10	4.06	15	19.79	19.79	7050	0.84	43.37	56.00	54.10
15	**1**	**35**	**0.53**	**21.34**	**14.22**	**15**	**20.04**	**20.04**	**2210**	**0.25**	**97.80**	**132.20**	**130.40**
16	1	595	1.42	48.77	24.38	15	20.65	20.65	6520	0.08	172.80	220.20	218.40
17	1	635	0.25	3.05	3.05	15	22.07	22.07	2615	1.42	89.50	112.20	110.30

18	1	325	0.20	3.05	2.03	15	22.33	22.33	3140	0.25	79.12	105.60	103.70
19	1	60	0.13	3.05	3.05	10	22.53	22.53	900	0.20	78.68	105.20	103.30
20	1	200	0.66	6.10	4.06	15	22.66	22.66	820	0.13	72.24	94.90	93.00
21	**1**	**545**	**1.93**	**15.24**	**12.19**	**15**	**23.32**	**23.32**	**2650**	**0.66**	**173.80**	**231.00**	**229.40**
22	1	605	0.48	6.10	4.57	10	25.25	25.25	4925	1.93	79.62	98.70	96.90
23	2	1070	2.57	12.19	9.14	15	25.73	0.00	4130	0.48	169.40	225.80	224.10
24	**2**	**545**	**1.14**	**30.48**	**15.24**	**15**	**28.30**	**2.57**	**2355**	**2.57**	**139.00**	**178.90**	**177.10**
25	2	1340	4.14	33.53	26.42	15	29.44	3.71	6995	1.14	181.20	245.10	244.80
26	2	10	0.25	24.38	10.16	15	33.58	7.85	6710	4.14	65.61	88.50	86.50
27	2	110	0.46	6.10	5.08	15	33.83	8.10	3355	0.25	70.25	91.50	89.50
28	2	345	4.52	48.77	31.50	15	34.29	8.56	1825	0.46	170.30	245.60	244.00
29	2	565	0.61	18.29	15.24	10	38.89	13.16	555	0.08	92.70	112.90	111.00
30	**2**	**65**	**0.30**	**9.14**	**5.08**	**15**	**39.50**	**13.77**	**13390**	**0.61**	**40.71**	**43.27**	**41.22**
31	2	215	0.48	18.29	12.19	15	39.80	14.07	2700	0.30	46.74	53.00	50.97
32	2	560	0.58	12.19	7.11	15	40.28	14.55	6455	0.48	47.34	54.91	52.90
33	**2**	**710**	**2.46**	**9.14**	**8.13**	**15**	**41.20**	**15.47**	**2225**	**0.03**	**122.50**	**145.40**	**143.50**
34	2	540	3.58	18.29	16.26	15	43.76	18.03	440	0.10	146.20	194.70	192.90
35	3	4245	5.92	6.10	6.10	15	47.42	0.00	6955	0.08	183.00	236.80	233.90
36	3	415	5.74	30.48	22.35	15	53.72	6.30	12015	0.03	179.20	269.90	275.00
37	**3**	**770**	**3.35**	**21.34**	**16.26**	**15**	**59.46**	**12.04**	**3175**	**5.74**	**153.90**	**226.40**	**224.40**

38	3	470	0.51	3.05	2.03	15	62.84	15.42	2155	0.03	65.73	105.30	103.20
39	3	280	0.79	39.62	20.32	15	63.42	16.00	13865	0.05	50.72	59.13	56.99
40	3	380	0.36	15.24	7.11	15	64.21	16.79	9390	0.79	40.64	48.35	46.14
41	**3**	**310**	**2.67**	**82.30**	**49.78**	**15**	**64.57**	**17.15**	**8080**	**0.36**	**101.40**	**122.10**	**120.00**
42	3	235	1.19	51.82	33.53	15	67.23	19.81	5805	2.67	87.90	100.10	97.90
43	3	310	3.10	106.68	96.52	15	68.43	21.01	1070	1.19	190.80	250.10	248.30
44	3	45	0.23	9.14	7.11	15	71.53	24.10	7265	3.10	68.33	74.14	71.92
45	**3**	**120**	**0.53**	**36.58**	**20.32**	**15**	**71.76**	**24.33**	**2935**	**0.23**	**64.27**	**72.72**	**70.49**
46	3	70	1.63	45.72	34.54	15	72.31	24.89	495	0.03	123.80	151.00	149.00
47	3	510	0.43	9.14	6.10	10	73.96	26.54	8465	0.03	52.31	58.92	56.65
48	**3**	**330**	**0.15**	**9.14**	**7.62**	**10**	**74.45**	**27.03**	**1570**	**0.05**	**39.79**	**44.99**	**42.67**
49	3	105	0.30	3.05	3.05	15	74.63	27.20	10335	0.03	24.81	31.10	28.71
50	3	215	1.37	24.38	17.27	15	74.93	27.51	4770	0.30	61.64	73.08	70.77
51	3	20	0.28	18.29	15.24	10	76.30	28.88	6610	1.37	40.96	46.90	44.53
52	**3**	**305**	**1.24**	**36.58**	**25.40**	**15**	**76.58**	**29.16**	**15760**	**0.28**	**54.16**	**61.22**	**58.86**
53	3	900	2.06	36.58	19.30	15	77.83	30.40	820	1.24	72.30	85.80	83.40
54	3	25	0.13	6.10	6.10	10	79.88	32.46	950	2.06	70.93	81.90	79.57
55	3	75	2.97	115.82	75.18	15	80.01	32.59	2915	0.13	195.40	219.00	216.90
56	**3**	**495**	**2.41**	**24.38**	**15.24**	**15**	**82.98**	**35.56**	**3265**	**2.97**	**122.40**	**135.50**	**133.30**
57	3	780	2.16	24.38	13.21	15	85.60	38.18	4425	0.05	94.30	104.60	102.20

58	**4**	**145**	**0.64**	**6.10**	**5.08**	**15**	**87.88**	**0.13**	**4560**	**0.13**	**55.96**	**61.94**	**59.46**
59	4	785	1.83	9.14	7.11	15	88.62	0.86	8655	0.03	88.20	99.30	96.90
60	**4**	**425**	**0.38**	**6.10**	**4.06**	**15**	**90.47**	**2.72**	**5365**	**0.03**	**46.39**	**54.75**	**52.20**
61	4	605	1.14	6.10	4.06	15	91.01	3.25	6690	0.15	71.30	88.70	86.20
62	4	360	0.76	30.48	17.27	15	92.30	4.55	7695	0.15	70.20	90.30	88.30
63	**4**	**235**	**1.24**	**12.19**	**7.11**	**15**	**93.09**	**5.33**	**425**	**0.03**	**125.30**	**161.20**	**159.10**
64	4	1620	3.23	12.19	7.11	15	94.34	6.58	2730	1.24	141.80	184.00	181.90
65	**4**	**455**	**0.94**	**24.38**	**10.16**	**15**	**97.56**	**9.80**	**400**	**3.23**	**132.40**	**176.70**	**174.60**
66	4	1145	3.02	48.77	37.59	15	98.53	10.77	555	0.03	133.60	185.20	183.10
67	4	150	0.30	18.29	12.19	10	102.01	14.25	2985	0.46	61.88	94.60	92.70
68	4	280	0.15	3.05	3.05	10	104.34	16.59	4920	2.03	69.44	97.30	95.50
69	4	265	0.36	3.05	2.29	20	106.73	18.97	645	0.05	73.38	112.20	110.50
70	4	210	0.41	6.10	4.06	15	107.14	19.38	1500	0.03	44.85	68.58	66.86
71	4	415	1.63	27.43	17.27	15	107.54	19.79	675	0.41	64.73	109.10	107.30
72	4	1360	6.02	48.77	26.42	15	109.17	21.41	2140	1.63	134.70	212.40	210.40
73	4	195	0.46	3.05	2.29	20	115.29	27.53	1125	0.08	84.00	121.90	119.90
74	4	355	0.38	3.05	2.29	20	115.75	27.99	14670	0.46	44.48	67.74	65.99
75	**4**	**400**	**0.23**	**9.14**	**5.08**	**15**	**116.13**	**28.37**	**555**	**0.38**	**46.82**	**74.76**	**73.02**
76	4	280	2.49	97.54	48.77	15	116.38	28.63	1750	0.03	89.00	137.90	136.20
77	4	10	0.13	9.14	5.08	15	118.87	31.12	505	2.49	89.90	138.40	136.70

78	**4**	**95**	**0.25**	**6.10**	**4.06**	**15**	**119.10**	**31.34**	**3115**	**0.10**	**70.04**	**108.90**	**107.30**
79	4	180	0.25	3.05	2.03	15	119.35	31.60	4770	0.25	64.59	101.00	99.60
80	4	105	0.30	6.10	4.06	15	119.71	31.95	400	0.10	60.21	97.40	95.80
81	4	355	0.15	6.10	4.06	15	120.02	32.26	4135	0.30	57.42	90.30	88.70
82	4	465	0.69	6.10	3.05	15	120.17	32.41	7285	0.15	61.64	92.70	91.00
83	4	865	1.68	9.14	7.11	15	120.95	33.20	5500	0.03	83.20	128.10	126.40
84	**4**	**890**	**1.12**	**6.10**	**5.08**	**15**	**122.78**	**35.03**	**4565**	**0.13**	**77.60**	**117.40**	**115.60**
85	4	810	2.69	9.14	6.10	15	123.90	36.14	7420	1.12	135.20	195.20	193.50
86	4	2220	4.65	15.24	13.21	15	126.67	38.91	5630	0.05	138.20	189.00	187.40
87	**4**	**305**	**0.66**	**6.10**	**5.08**	**15**	**131.32**	**43.56**	**8160**	**4.65**	**75.40**	**107.50**	**105.80**
88	4	705	0.46	6.10	6.10	15	131.98	44.22	365	0.66	80.70	115.80	114.00
89	4	1165	3.12	60.96	23.37	15	132.64	44.88	15570	0.18	112.10	160.20	158.30
90	5	285	1.09	109.73	64.01	10	135.76	0.00	6960	3.12	86.00	129.60	127.80
91	5	475	2.44	30.48	22.35	15	136.91	1.14	1825	0.05	157.30	248.10	244.80
92	**5**	**390**	**1.73**	**12.19**	**11.18**	**15**	**139.34**	**3.58**	**7050**	**2.44**	**140.50**	**236.40**	**236.50**
93	5	170	0.13	3.05	2.03	15	141.07	5.31	4800	1.73	64.87	106.30	104.50
94	5	15	0.25	21.34	9.14	15	141.25	5.49	7790	0.05	49.72	84.60	82.80
95	5	2030	3.12	6.10	5.08	15	141.50	5.74	875	0.25	144.80	227.80	227.20
96	5	330	0.23	15.24	12.19	10	144.65	8.89	395	0.03	106.00	164.10	162.20
97	5	380	1.73	15.24	12.19	15	144.93	9.17	4750	0.05	139.70	226.00	224.40

98	5	95	0.53	15.24	9.14	15	146.66	10.90	440	1.73	127.40	201.50	199.80
99	**5**	**30**	**0.15**	**6.10**	**4.06**	**15**	**147.19**	**11.43**	**1125**	**0.53**	**103.20**	**155.80**	**153.90**
100	5	95	0.53	36.58	20.32	15	147.35	11.58	6610	0.15	80.80	132.70	130.80
101	**5**	**95**	**0.58**	**45.72**	**22.35**	**15**	**147.93**	**12.17**	**1945**	**0.05**	**75.72**	**127.70**	**125.70**
102	5	395	0.20	3.05	3.05	10	148.62	12.85	7010	0.03	34.85	59.44	57.32
103	**5**	**655**	**0.58**	**24.38**	**13.72**	**10**	**148.82**	**13.06**	**665**	**0.20**	**49.21**	**83.20**	**81.20**
104	**5**	**345**	**0.81**	**12.19**	**11.18**	**15**	**149.48**	**13.72**	**500**	**0.03**	**57.69**	**91.00**	**89.10**
105	5	60	1.68	64.01	54.86	15	150.34	14.58	465	0.05	66.32	106.80	104.90
106	**5**	**670**	**3.48**	**106.68**	**96.52**	**15**	**152.02**	**16.26**	**1360**	**1.68**	**137.20**	**216.50**	**213.70**
107	5	75	1.50	54.86	30.48	15	155.52	19.76	2435	0.03	73.74	109.90	107.90
108	5	225	2.18	57.91	36.58	15	157.18	21.41	2500	0.15	87.80	136.70	134.60
109	5	310	7.11	128.01	72.14	15	159.36	23.60	550	2.18	148.10	230.20	228.30
110	**5**	**70**	**0.33**	**6.10**	**6.10**	**15**	**166.47**	**30.71**	**7045**	**7.11**	**71.17**	**113.60**	**111.50**
111	5	30	0.36	24.38	19.81	10	166.80	31.04	1025	0.33	71.45	114.60	112.60
112	**5**	**80**	**0.15**	**6.10**	**6.10**	**10**	**167.16**	**31.39**	**1665**	**0.36**	**62.99**	**96.60**	**94.70**
113	5	930	1.37	9.14	5.08	15	167.31	31.55	530	0.15	101.80	153.50	151.50
114	5	80	1.30	54.86	45.72	15	172.42	36.65	5945	1.68	55.58	98.00	95.90
115	5	1100	5.89	109.73	82.30	15	173.74	37.97	4500	0.03	120.40	213.10	211.10
116	5	305	0.28	9.14	7.62	10	179.63	43.87	6680	5.89	47.50	74.92	72.90
117	5	385	0.33	6.10	4.57	10	179.91	44.15	4735	0.28	36.18	63.34	61.26

118	5	940	1.75	27.43	21.34	15	180.39	44.63	375	0.03	46.53	80.70	78.59
119	5	75	0.71	18.29	16.26	15	182.17	46.41	4365	0.03	38.68	67.72	65.62
120	5	560	4.11	48.77	39.62	15	182.88	47.12	15855	0.71	100.50	153.30	151.10
121	5	20	0.33	12.19	11.18	15	186.99	51.23	1965	4.11	73.42	114.80	112.70
122	6	10	0.36	15.24	14.22	15	187.55	0.00	9925	0.10	35.94	61.98	58.46
123	**6**	**820**	**4.34**	**21.34**	**14.22**	**15**	**187.91**	**0.36**	**1725**	**0.36**	**147.90**	**220.00**	**218.40**
124	6	2125	11.35	42.67	35.56	15	192.43	4.88	965	0.08	167.30	251.90	248.70
125	6	245	0.48	3.05	3.05	15	203.91	16.36	2700	0.08	32.20	61.41	59.33
126	6	730	2.62	21.34	15.24	15	204.42	16.87	11255	0.03	127.00	220.40	219.50
127	**6**	**855**	**1.55**	**21.34**	**12.19**	**15**	**207.04**	**19.48**	**1425**	**2.62**	**117.10**	**182.10**	**180.30**
128	6	695	0.66	3.05	3.05	15	208.58	21.03	8025	1.55	41.61	77.45	75.25
129	6	260	0.15	3.05	3.05	10	209.27	21.72	6525	0.03	39.03	56.24	54.03
130	6	200	0.25	6.10	4.06	15	209.42	21.87	5210	0.15	31.36	60.87	58.49
131	**6**	**980**	**6.93**	**45.72**	**26.42**	**15**	**209.68**	**22.12**	**1770**	**0.25**	**128.00**	**234.60**	**236.50**
132	6	145	0.13	3.05	3.05	10	216.64	29.08	2385	0.03	33.01	61.91	59.86
133	**6**	**880**	**1.63**	**18.29**	**14.22**	**15**	**216.87**	**29.31**	**12375**	**0.05**	**81.20**	**135.70**	**133.40**
134	6	170	0.25	3.05	3.05	15	218.49	30.94	395	1.63	86.60	140.00	137.60
135	6	1570	2.06	9.14	6.10	15	218.85	31.29	2855	0.08	82.40	144.00	141.80
136	6	630	2.51	21.34	12.19	15	221.06	33.50	890	0.15	93.20	171.00	168.70
137	**6**	**535**	**4.09**	**45.72**	**35.56**	**15**	**223.57**	**36.02**	**525**	**2.51**	**111.50**	**211.90**	**211.40**

138	6	840	1.30	3.05	3.05	15	227.71	40.16	8490	0.05	67.34	131.30	129.10

APPENDIX C

Peak Water Level Dataset of PICP 19H

Event	Cleaning Method	Duration (Min.)	Rainfall Depth (cm.)	Peak 5 min (mm/hr)	Peak 15 min (mm/hr)	Peak Duration (Min)	Cumulative Rainfall Depth from the installation (cm)	Cumulative Rainfall Depth from the last maintenance (cm)	ADP (Min)	Previous Rainfall Depth (cm)	Max Piezometer 1 (cm)	Max Piezometer 2 (cm)	Max Piezometer 3(cm)
1	1	395	1.17	18.29	11.18	15	0.05	0.05	1470	0.05	64.20	88.30	101.30
2	1	480	1.68	21.34	16.26	15	1.22	1.22	7965	1.17	192.50	248.90	261.90
3	1	605	1.55	6.10	4.06	15	2.90	2.90	1615	1.68	141.50	179.70	192.80
4	**1**	**820**	**2.11**	**9.14**	**8.13**	**15**	**4.50**	**4.50**	**1900**	**0.03**	**116.70**	**153.20**	**166.30**
5	1	535	1.96	15.24	10.16	15	6.65	6.65	16245	0.05	186.10	224.20	237.80
6	1	140	0.38	3.05	3.05	15	8.61	8.61	370	1.96	128.30	154.60	168.10
7	**1**	**135**	**0.20**	**3.05**	**2.03**	**15**	**8.99**	**8.99**	**805**	**0.38**	**79.10**	**98.60**	**112.10**
8	1	605	0.99	21.34	13.21	15	9.19	9.19	6545	0.20	78.27	108.10	121.70
9	1	390	1.93	42.67	29.46	15	10.21	10.21	1815	0.03	252.70	291.40	305.00
10	**1**	**270**	**0.64**	**3.05**	**3.05**	**15**	**12.22**	**12.22**	**3000**	**0.08**	**62.54**	**74.38**	**87.90**
11	1	1520	4.37	36.58	19.30	15	12.85	12.85	470	0.64	283.80	313.90	327.50
12	1	490	0.91	6.10	5.08	15	17.35	17.35	3650	0.03	51.80	75.99	89.60
13	1	145	0.48	3.05	3.05	15	18.47	18.47	4920	0.05	12.07	19.24	32.01

14	**1**	**645**	**0.84**	**9.14**	**9.14**	**10**	**18.95**	**18.95**	**2040**	**0.48**	**42.05**	**58.01**	**70.89**
15	1	250	0.25	6.10	4.06	15	19.79	19.79	7050	0.84	0.01	15.98	28.92
16	1	35	0.53	21.34	14.22	15	20.04	20.04	2210	0.25	28.27	39.09	52.12
17	**1**	**595**	**1.42**	**48.77**	**24.38**	**15**	**20.65**	**20.65**	**6520**	**0.08**	**53.54**	**73.00**	**86.20**
18	1	635	0.25	3.05	3.05	15	22.07	22.07	2615	1.42	10.00	26.75	40.02
19	1	325	0.20	3.05	2.03	15	22.33	22.33	3140	0.25	52.79	77.23	90.60
20	1	60	0.13	3.05	3.05	10	22.53	22.53	900	0.20	48.90	66.24	79.60
21	**1**	**200**	**0.66**	**6.10**	**4.06**	**15**	**22.66**	**22.66**	**820**	**0.13**	**36.54**	**48.39**	**61.74**
22	1	545	1.93	15.24	12.19	15	23.32	23.32	2650	0.66	62.01	85.40	98.70
23	1	605	0.48	6.10	4.57	10	25.25	25.25	4925	1.93	14.28	32.42	45.76
24	1	1070	2.57	12.19	9.14	15	25.73	25.73	4130	0.48	56.66	80.80	94.10
25	**1**	**545**	**1.14**	**30.48**	**15.24**	**15**	**28.30**	**28.30**	**2355**	**2.57**	**59.51**	**78.23**	**91.60**
26	1	1340	4.14	33.53	26.42	15	29.44	29.44	6995	1.14	133.70	159.70	173.10
27	1	10	0.25	24.38	10.16	15	33.58	33.58	6710	4.14	0.25	12.28	25.57
28	1	110	0.46	6.10	5.08	15	33.83	33.83	3355	0.25	9.69	18.71	32.03
29	1	345	4.52	48.77	31.50	15	34.29	34.29	1825	0.46	210.40	241.30	254.80
30	1	565	0.61	18.29	15.24	10	38.89	38.89	555	0.08	34.14	49.50	62.80
31	**1**	**65**	**0.30**	**9.14**	**5.08**	**15**	**39.50**	**39.50**	**13390**	**0.61**	**9.65**	**18.64**	**30.98**
32	1	215	0.48	18.29	12.19	15	39.80	39.80	2700	0.30	10.32	23.44	35.95
33	1	560	0.58	12.19	7.11	15	40.28	40.28	6455	0.48	7.41	14.08	26.80

34	**1**	**710**	**2.46**	**9.14**	**8.13**	**15**	**41.20**	**41.20**	**2225**	**0.03**	**51.20**	**59.44**	**71.86**
35	1	540	3.58	18.29	16.26	15	43.76	43.76	440	0.10	124.00	142.60	155.40
36	2	4245	5.92	6.10	6.10	15	47.42	0.00	6955	0.08	312.20	337.70	344.80
37	2	415	5.74	30.48	22.35	15	53.72	6.30	12015	0.03	316.50	338.40	346.10
38	**2**	**770**	**3.35**	**21.34**	**16.26**	**15**	**59.46**	**12.04**	**3175**	**5.74**	**217.10**	**236.60**	**249.00**
39	2	470	0.51	3.05	2.03	15	62.84	15.42	2155	0.03	39.17	50.06	62.65
40	2	280	0.79	39.62	20.32	15	63.42	16.00	13865	0.05	31.83	40.85	53.24
41	2	380	0.36	15.24	7.11	15	64.21	16.79	9390	0.79	4.04	12.19	24.44
42	2	310	2.67	82.30	49.78	15	64.57	17.15	8080	0.36	86.30	96.90	110.00
43	**2**	**235**	**1.19**	**51.82**	**33.53**	**15**	**67.23**	**19.81**	**5805**	**2.67**	**54.07**	**65.04**	**77.98**
44	2	310	3.10	106.68	96.52	15	68.43	21.01	1070	1.19	272.50	308.90	321.60
45	2	45	0.23	9.14	7.11	15	71.53	24.10	7265	3.10	9.73	26.83	40.31
46	**2**	**120**	**0.53**	**36.58**	**20.32**	**15**	**71.76**	**24.33**	**2935**	**0.23**	**11.89**	**26.71**	**40.20**
47	2	70	1.63	45.72	34.54	15	72.31	24.89	495	0.03	115.90	130.10	143.60
48	2	510	0.43	9.14	6.10	10	73.96	26.54	8465	0.03	-0.26	15.40	28.11
49	2	330	0.15	9.14	7.62	10	74.45	27.03	1570	0.05	-0.25	0.96	15.71
50	**2**	**105**	**0.30**	**3.05**	**3.05**	**15**	**74.63**	**27.20**	**10335**	**0.03**	**-0.27**	**7.63**	**18.21**
51	2	215	1.37	24.38	17.27	15	74.93	27.51	4770	0.30	71.31	81.40	94.30
52	2	20	0.28	18.29	15.24	10	76.30	28.88	6610	1.37	-0.28	14.65	27.77
53	**2**	**305**	**1.24**	**36.58**	**25.40**	**15**	**76.58**	**29.16**	**15760**	**0.28**	**60.21**	**69.26**	**82.20**

54	2	900	2.06	36.58	19.30	15	77.83	30.40	820	1.24	87.10	95.60	108.40
55	2	25	0.13	6.10	6.10	10	79.88	32.46	950	2.06	70.03	76.91	89.70
56	2	75	2.97	115.82	75.18	15	80.01	32.59	2915	0.13	223.50	244.30	256.90
57	2	495	2.41	24.38	15.24	15	82.98	35.56	3265	2.97	90.20	98.80	111.50
58	**2**	**780**	**2.16**	**24.38**	**13.21**	**15**	**85.60**	**38.18**	**4425**	**0.05**	**128.40**	**157.90**	**171.40**
59	3	145	0.64	6.10	5.08	15	87.88	0.13	4560	0.13	44.33	56.30	69.70
60	3	785	1.83	9.14	7.11	15	88.62	0.86	8655	0.03	96.20	110.20	123.80
61	3	425	0.38	6.10	4.06	15	90.47	2.72	5365	0.03	6.00	21.23	34.37
62	**3**	**605**	**1.14**	**6.10**	**4.06**	**15**	**91.01**	**3.25**	**6690**	**0.15**	**68.80**	**78.48**	**91.80**
63	3	360	0.76	30.48	17.27	15	92.30	4.55	7695	0.15	54.54	61.09	74.43
64	3	235	1.24	12.19	7.11	15	93.09	5.33	425	0.03	76.86	89.60	103.00
65	3	1620	3.23	12.19	7.11	15	94.34	6.58	2730	1.24	99.30	109.20	122.70
66	**3**	**455**	**0.94**	**24.38**	**10.16**	**15**	**97.56**	**9.80**	**400**	**3.23**	**95.80**	**105.30**	**118.80**
67	3	1145	3.02	48.77	37.59	15	98.53	10.77	555	0.03	120.00	130.80	144.40
68	3	150	0.46	9.14	6.10	15	101.55	13.79	7615	3.02	13.52	29.40	42.80
69	3	150	0.30	18.29	12.19	10	102.01	14.25	2985	0.46	11.96	21.77	35.16
70	**3**	**670**	**2.03**	**15.24**	**11.18**	**15**	**102.31**	**14.55**	**3690**	**0.30**	**51.93**	**66.72**	**80.30**
71	3	280	0.15	3.05	3.05	10	104.34	16.59	4920	2.03	12.65	21.57	35.06
72	3	745	2.08	12.19	7.11	15	104.50	16.74	2375	0.15	73.23	88.20	101.80
73	3	265	0.36	3.05	2.29	20	106.73	18.97	645	0.05	33.95	40.71	54.20

74	3	210	0.41	6.10	4.06	15	107.14	19.38	1500	0.03	7.99	10.66	23.99
75	3	415	1.63	27.43	17.27	15	107.54	19.79	675	0.41	36.73	51.56	64.88
76	**3**	**1360**	**6.02**	**48.77**	**26.42**	**15**	**109.17**	**21.41**	**2140**	**1.63**	**113.00**	**129.60**	**143.10**
77	**3**	**195**	**0.46**	**3.05**	**2.29**	**20**	**115.29**	**27.53**	**1125**	**0.08**	**40.05**	**43.45**	**56.82**
78	3	355	0.38	3.05	2.29	20	115.75	27.99	14670	0.46	20.55	21.75	35.25
79	3	400	0.23	9.14	5.08	15	116.13	28.37	555	0.38	18.74	19.34	32.79
80	3	280	2.49	97.54	48.77	15	116.38	28.63	1750	0.03	30.91	39.04	52.47
81	**3**	**10**	**0.13**	**9.14**	**5.08**	**15**	**118.87**	**31.12**	**505**	**2.49**	**28.67**	**37.83**	**51.25**
82	**3**	**95**	**0.25**	**6.10**	**4.06**	**15**	**119.10**	**31.34**	**3115**	**0.10**	**13.85**	**10.21**	**23.34**
83	3	180	0.25	3.05	2.03	15	119.35	31.60	4770	0.25	20.29	19.16	32.23
84	3	105	0.30	6.10	4.06	15	119.71	31.95	400	0.10	21.73	16.70	29.80
85	3	355	0.15	6.10	4.06	15	120.02	32.26	4135	0.30	20.85	10.14	23.09
86	3	465	0.69	6.10	3.05	15	120.17	32.41	7285	0.15	22.10	29.70	43.31
87	**3**	**865**	**1.68**	**9.14**	**7.11**	**15**	**120.95**	**33.20**	**5500**	**0.03**	**38.75**	**49.09**	**62.25**
88	3	890	1.12	6.10	5.08	15	122.78	35.03	4565	0.13	35.16	45.26	58.47
89	3	810	2.69	9.14	6.10	15	123.90	36.14	7420	1.12	49.89	53.68	66.44
90	3	2220	4.65	15.24	13.21	15	126.67	38.91	5630	0.05	78.06	82.20	94.70
91	3	305	0.66	6.10	5.08	15	131.32	43.56	8160	4.65	24.97	35.06	47.51
92	3	705	0.46	6.10	6.10	15	131.98	44.22	365	0.66	32.52	38.62	51.08
93	**3**	**1165**	**3.12**	**60.96**	**23.37**	**15**	**132.64**	**44.88**	**15570**	**0.18**	**52.84**	**57.15**	**70.93**

94	**4**	**285**	**1.09**	**109.73**	**64.01**	**10**	**135.76**	**0.00**	**6960**	**3.12**	**28.42**	**26.84**	**39.93**
95	4	475	2.44	30.48	22.35	15	136.91	1.14	1825	0.05	44.26	50.56	63.66
96	4	390	1.73	12.19	11.18	15	139.34	3.58	7050	2.44	38.79	43.36	56.37
97	4	170	0.13	3.05	2.03	15	141.07	5.31	4800	1.73	22.70	6.32	14.98
98	4	15	0.25	21.34	9.14	15	141.25	5.49	7790	0.05	19.53	7.24	16.03
99	4	2030	3.12	6.10	5.08	15	141.50	5.74	875	0.25	90.70	96.80	110.00
100	4	330	0.23	15.24	12.19	10	144.65	8.89	395	0.03	48.28	51.55	64.92
101	**4**	**380**	**1.73**	**15.24**	**12.19**	**15**	**144.93**	**9.17**	**4750**	**0.05**	**50.46**	**56.53**	**69.48**
102	**4**	**95**	**0.53**	**36.58**	**20.32**	**15**	**147.35**	**11.58**	**6610**	**0.15**	**27.67**	**8.20**	**21.60**
103	4	95	0.58	45.72	22.35	15	147.93	12.17	1945	0.05	24.86	10.77	23.73
104	4	395	0.20	3.05	3.05	10	148.62	12.85	7010	0.03	13.44	0.78	5.93
105	4	655	0.58	24.38	13.72	10	148.82	13.06	665	0.20	26.91	16.99	30.21
106	4	345	0.81	12.19	11.18	15	149.48	13.72	500	0.03	27.19	31.75	45.13
107	**4**	**60**	**1.68**	**64.01**	**54.86**	**15**	**150.34**	**14.58**	**465**	**0.05**	**45.05**	**49.66**	**63.22**
108	4	670	3.48	106.68	96.52	15	152.02	16.26	1360	1.68	118.10	123.00	136.60
109	4	75	1.50	54.86	30.48	15	155.52	19.76	2435	0.03	37.03	42.90	56.07
110	4	65	0.15	6.10	4.06	15	157.02	21.26	1160	1.50	24.54	27.01	40.20
111	**4**	**225**	**2.18**	**57.91**	**36.58**	**15**	**157.18**	**21.41**	**2500**	**0.15**	**50.67**	**57.30**	**70.57**
112	**4**	**310**	**7.11**	**128.01**	**72.14**	**15**	**159.36**	**23.60**	**550**	**2.18**	**237.80**	**247.60**	**261.10**
113	4	70	0.33	6.10	6.10	15	166.47	30.71	7045	7.11	44.15	48.73	62.49

114	4	30	0.36	24.38	19.81	10	166.80	31.04	1025	0.33	48.51	55.17	68.94
115	4	80	0.15	6.10	6.10	10	167.16	31.39	1665	0.36	21.97	19.81	33.54
116	**4**	**930**	**1.37**	**9.14**	**5.08**	**15**	**167.31**	**31.55**	**530**	**0.15**	**80.60**	**87.40**	**101.20**
117	**4**	**635**	**1.96**	**12.19**	**9.14**	**15**	**168.68**	**32.92**	**1660**	**1.37**	**196.00**	**204.40**	**218.10**
118	4	140	1.68	64.01	51.82	15	170.74	34.98	1755	0.10	133.80	140.40	154.40
119	4	80	1.30	54.86	45.72	15	172.42	36.65	5945	1.68	36.24	41.82	54.25
120	4	1100	5.89	109.73	82.30	15	173.74	37.97	4500	0.03	113.60	119.20	132.60
121	4	305	0.28	9.14	7.62	10	179.63	43.87	6680	5.89	25.83	8.76	17.34
122	4	385	0.33	6.10	4.57	10	179.91	44.15	4735	0.28	26.81	9.66	13.03
123	4	10	0.36	15.24	14.22	15	187.55	51.56	9925	0.10	10.54	6.34	15.40
124	**4**	**820**	**4.34**	**21.34**	**14.22**	**15**	**187.91**	**51.92**	**1725**	**0.36**	**161.90**	**170.10**	**183.30**
125	4	2125	11.35	42.67	35.56	15	192.43	56.26	965	0.08	249.90	255.30	269.10
126	4	730	2.62	21.34	15.24	15	204.42	68.10	11255	0.03	131.70	141.10	154.50
127	4	855	1.55	21.34	12.19	15	207.04	70.71	1425	2.62	93.10	98.40	111.50
128	4	695	0.66	3.05	3.05	15	208.58	72.26	8025	1.55	24.94	31.46	44.71
129	4	260	0.15	3.05	3.05	10	209.27	72.92	6525	0.03	-0.16	0.98	5.55
130	**4**	**980**	**6.93**	**45.72**	**26.42**	**15**	**209.68**	**73.33**	**1770**	**0.25**	**163.00**	**172.60**	**186.00**
131	**4**	**880**	**1.63**	**18.29**	**14.22**	**15**	**216.87**	**80.39**	**12375**	**0.05**	**42.53**	**50.73**	**64.12**
132	4	170	0.25	3.05	3.05	15	218.49	82.02	395	1.63	42.53	49.25	62.65
133	4	1570	2.06	9.14	6.10	15	218.85	82.27	2855	0.08	92.20	107.20	120.70

134	4	630	2.51	21.34	12.19	15	221.06	84.48	890	0.15	54.20	65.33	78.59
135	4	535	4.09	45.72	35.56	15	223.57	87.00	525	2.51	77.57	87.70	101.10

APPENDIX D

Peak VWC Dataset of PICP 19G

Event	Cleaning Method	Duration (Min.)	Rainfall Depth (cm.)	Peak 5 min (mm/hr)	Peak 15 min (mm/hr)	Peak Duration (Min)	Cumulative Rainfall Depth from the installation (cm)	Cumulative Rainfall Depth from the last maintenance (cm)	ADP (Min)	Previous Rainfall Depth (cm)
1	**1**	**480**	**1.68**	**21.34**	**16.26**	**15**	**1.22**	**1.22**	**7965**	**1.17**
2	1	605	1.55	6.10	4.06	15	2.90	2.90	1615	1.68
3	1	820	2.11	9.14	8.13	15	4.50	4.50	1900	0.03
4	1	535	1.96	15.24	10.16	15	6.65	6.65	16245	0.05
5	1	140	0.38	3.05	3.05	15	8.61	8.61	370	1.96
6	1	135	0.20	3.05	2.03	15	8.99	8.99	805	0.38
7	**1**	**605**	**0.99**	**21.34**	**13.21**	**15**	**9.19**	**9.19**	**6545**	**0.20**
8	1	390	1.93	42.67	29.46	15	10.21	10.21	1815	0.03
9	1	270	0.64	3.05	3.05	15	12.22	12.22	3000	0.08
10	**1**	**1520**	**4.37**	**36.58**	**19.30**	**15**	**12.85**	**12.85**	**470**	**0.64**
11	1	490	0.91	6.10	5.08	15	17.35	17.35	3650	0.03
12	1	145	0.48	3.05	3.05	15	18.47	18.47	4920	0.05
13	1	645	0.84	9.14	9.14	10	18.95	18.95	2040	0.48
14	**1**	**250**	**0.25**	**6.10**	**4.06**	**15**	**19.79**	**19.79**	**7050**	**0.84**

15	1	35	0.53	21.34	14.22	15	20.04	20.04	2210	0.25
16	1	595	1.42	48.77	24.38	15	20.65	20.65	6520	0.08
17	1	635	0.25	3.05	3.05	15	22.07	22.07	2615	1.42
18	**1**	**325**	**0.20**	**3.05**	**2.03**	**15**	**22.33**	**22.33**	**3140**	**0.25**
19	1	60	0.13	3.05	3.05	10	22.53	22.53	900	0.20
20	1	200	0.66	6.10	4.06	15	22.66	22.66	820	0.13
21	1	545	1.93	15.24	12.19	15	23.32	23.32	2650	0.66
22	**1**	**605**	**0.48**	**6.10**	**4.57**	**10**	**25.25**	**25.25**	**4925**	**1.93**
23	2	1070	2.57	12.19	9.14	15	25.73	0.00	4130	0.48
24	**2**	**545**	**1.14**	**30.48**	**15.24**	**15**	**28.30**	**2.57**	**2355**	**2.57**
25	2	1340	4.14	33.53	26.42	15	29.44	3.71	6995	1.14
26	2	10	0.25	24.38	10.16	15	33.58	7.85	6710	4.14
27	**2**	**110**	**0.46**	**6.10**	**5.08**	**15**	**33.83**	**8.10**	**3355**	**0.25**
28	2	345	4.52	48.77	31.50	15	34.29	8.56	1825	0.46
29	2	565	0.61	18.29	15.24	10	38.89	13.16	555	0.08
30	2	65	0.30	9.14	5.08	15	39.50	13.77	13390	0.61
31	2	215	0.48	18.29	12.19	15	39.80	14.07	2700	0.30
32	**2**	**560**	**0.58**	**12.19**	**7.11**	**15**	**40.28**	**14.55**	**6455**	**0.48**
33	2	710	2.46	9.14	8.13	15	41.20	15.47	2225	0.03
34	2	540	3.58	18.29	16.26	15	43.76	18.03	440	0.10

35	3	4245	5.92	6.10	6.10	15	47.42	0.00	6955	0.08
36	**3**	**415**	**5.74**	**30.48**	**22.35**	**15**	**53.72**	**6.30**	**12015**	**0.03**
37	3	770	3.35	21.34	16.26	15	59.46	12.04	3175	5.74
38	3	470	0.51	3.05	2.03	15	62.84	15.42	2155	0.03
39	3	280	0.79	39.62	20.32	15	63.42	16.00	13865	0.05
40	3	380	0.36	15.24	7.11	15	64.21	16.79	9390	0.79
41	**3**	**310**	**2.67**	**82.30**	**49.78**	**15**	**64.57**	**17.15**	**8080**	**0.36**
42	3	235	1.19	51.82	33.53	15	67.23	19.81	5805	2.67
43	3	310	3.10	106.68	96.52	15	68.43	21.01	1070	1.19
44	3	45	0.23	9.14	7.11	15	71.53	24.10	7265	3.10
45	3	120	0.53	36.58	20.32	15	71.76	24.33	2935	0.23
46	3	70	1.63	45.72	34.54	15	72.31	24.89	495	0.03
47	**3**	**510**	**0.43**	**9.14**	**6.10**	**10**	**73.96**	**26.54**	**8465**	**0.03**
48	3	330	0.15	9.14	7.62	10	74.45	27.03	1570	0.05
49	3	105	0.30	3.05	3.05	15	74.63	27.20	10335	0.03
50	**3**	**215**	**1.37**	**24.38**	**17.27**	**15**	**74.93**	**27.51**	**4770**	**0.30**
51	3	20	0.28	18.29	15.24	10	76.30	28.88	6610	1.37
52	3	305	1.24	36.58	25.40	15	76.58	29.16	15760	0.28
53	3	900	2.06	36.58	19.30	15	77.83	30.40	820	1.24
54	**3**	**25**	**0.13**	**6.10**	**6.10**	**10**	**79.88**	**32.46**	**950**	**2.06**

55	3	75	2.97	115.82	75.18	15	80.01	32.59	2915	0.13
56	**3**	**495**	**2.41**	**24.38**	**15.24**	**15**	**82.98**	**35.56**	**3265**	**2.97**
57	3	780	2.16	24.38	13.21	15	85.60	38.18	4425	0.05
58	4	145	0.64	6.10	5.08	15	87.88	0.13	4560	0.13
59	4	785	1.83	9.14	7.11	15	88.62	0.86	8655	0.03
60	4	425	0.38	6.10	4.06	15	90.47	2.72	5365	0.03
61	4	605	1.14	6.10	4.06	15	91.01	3.25	6690	0.15
62	4	360	0.76	30.48	17.27	15	92.30	4.55	7695	0.15
63	4	235	1.24	12.19	7.11	15	93.09	5.33	425	0.03
64	4	1620	3.23	12.19	7.11	15	94.34	6.58	2730	1.24
65	4	455	0.94	24.38	10.16	15	97.56	9.80	400	3.23
66	4	1145	3.02	48.77	37.59	15	98.53	10.77	555	0.03
67	4	150	0.30	18.29	12.19	10	102.01	14.25	2985	0.46
68	4	280	0.15	3.05	3.05	10	104.34	16.59	4920	2.03
69	4	265	0.36	3.05	2.29	20	106.73	18.97	645	0.05
70	**4**	**210**	**0.41**	**6.10**	**4.06**	**15**	**107.14**	**19.38**	**1500**	**0.03**
71	**4**	**415**	**1.63**	**27.43**	**17.27**	**15**	**107.54**	**19.79**	**675**	**0.41**
72	4	1360	6.02	48.77	26.42	15	109.17	21.41	2140	1.63
73	4	195	0.46	3.05	2.29	20	115.29	27.53	1125	0.08
74	4	355	0.38	3.05	2.29	20	115.75	27.99	14670	0.46

75	4	400	0.23	9.14	5.08	15	116.13	28.37	555	0.38
76	4	280	2.49	97.54	48.77	15	116.38	28.63	1750	0.03
77	4	10	0.13	9.14	5.08	15	118.87	31.12	505	2.49
78	4	95	0.25	6.10	4.06	15	119.10	31.34	3115	0.10
79	4	180	0.25	3.05	2.03	15	119.35	31.60	4770	0.25
80	**4**	**105**	**0.30**	**6.10**	**4.06**	**15**	**119.71**	**31.95**	**400**	**0.10**
81	**4**	**355**	**0.15**	**6.10**	**4.06**	**15**	**120.02**	**32.26**	**4135**	**0.30**
82	4	465	0.69	6.10	3.05	15	120.17	32.41	7285	0.15
83	**4**	**865**	**1.68**	**9.14**	**7.11**	**15**	**120.95**	**33.20**	**5500**	**0.03**
84	4	890	1.12	6.10	5.08	15	122.78	35.03	4565	0.13
85	**4**	**810**	**2.69**	**9.14**	**6.10**	**15**	**123.90**	**36.14**	**7420**	**1.12**
86	4	2220	4.65	15.24	13.21	15	126.67	38.91	5630	0.05
87	**4**	**305**	**0.66**	**6.10**	**5.08**	**15**	**131.32**	**43.56**	**8160**	**4.65**
88	4	705	0.46	6.10	6.10	15	131.98	44.22	365	0.66
89	**4**	**1165**	**3.12**	**60.96**	**23.37**	**15**	**132.64**	**44.88**	**15570**	**0.18**
90	5	285	1.09	109.73	64.01	10	135.76	0.00	6960	3.12
91	5	475	2.44	30.48	22.35	15	136.91	1.14	1825	0.05
92	5	390	1.73	12.19	11.18	15	139.34	3.58	7050	2.44
93	5	170	0.13	3.05	2.03	15	141.07	5.31	4800	1.73
94	5	15	0.25	21.34	9.14	15	141.25	5.49	7790	0.05

95	**5**	**2030**	**3.12**	**6.10**	**5.08**	**15**	**141.50**	**5.74**	**875**	**0.25**
96	5	330	0.23	15.24	12.19	10	144.65	8.89	395	0.03
97	5	380	1.73	15.24	12.19	15	144.93	9.17	4750	0.05
98	5	95	0.53	15.24	9.14	15	146.66	10.90	440	1.73
99	**5**	**30**	**0.15**	**6.10**	**4.06**	**15**	**147.19**	**11.43**	**1125**	**0.53**
100	5	95	0.53	36.58	20.32	15	147.35	11.58	6610	0.15
101	5	95	0.58	45.72	22.35	15	147.93	12.17	1945	0.05
102	5	395	0.20	3.05	3.05	10	148.62	12.85	7010	0.03
103	**5**	**655**	**0.58**	**24.38**	**13.72**	**10**	**148.82**	**13.06**	**665**	**0.20**
104	5	345	0.81	12.19	11.18	15	149.48	13.72	500	0.03
105	**5**	**60**	**1.68**	**64.01**	**54.86**	**15**	**150.34**	**14.58**	**465**	**0.05**
106	5	670	3.48	106.68	96.52	15	152.02	16.26	1360	1.68
107	5	75	1.50	54.86	30.48	15	155.52	19.76	2435	0.03
108	**5**	**225**	**2.18**	**57.91**	**36.58**	**15**	**157.18**	**21.41**	**2500**	**0.15**
109	5	310	7.11	128.01	72.14	15	159.36	23.60	550	2.18
110	5	70	0.33	6.10	6.10	15	166.47	30.71	7045	7.11
111	**5**	**30**	**0.36**	**24.38**	**19.81**	**10**	**166.80**	**31.04**	**1025**	**0.33**
112	5	80	0.15	6.10	6.10	10	167.16	31.39	1665	0.36
113	5	930	1.37	9.14	5.08	15	167.31	31.55	530	0.15
114	5	80	1.30	54.86	45.72	15	172.42	36.65	5945	1.68

115	5	1100	5.89	109.73	82.30	15	173.74	37.97	4500	0.03
116	5	305	0.28	9.14	7.62	10	179.63	43.87	6680	5.89
117	5	385	0.33	6.10	4.57	10	179.91	44.15	4735	0.28
118	**5**	**940**	**1.75**	**27.43**	**21.34**	**15**	**180.39**	**44.63**	**375**	**0.03**
119	5	75	0.71	18.29	16.26	15	182.17	46.41	4365	0.03
120	**5**	**560**	**4.11**	**48.77**	**39.62**	**15**	**182.88**	**47.12**	**15855**	**0.71**
121	5	20	0.33	12.19	11.18	15	186.99	51.23	1965	4.11
122	6	10	0.36	15.24	14.22	15	187.55	0.00	9925	0.10
123	**6**	**820**	**4.34**	**21.34**	**14.22**	**15**	**187.91**	**0.36**	**1725**	**0.36**
124	6	2125	11.35	42.67	35.56	15	192.43	4.88	965	0.08
125	6	245	0.48	3.05	3.05	15	203.91	16.36	2700	0.08
126	6	730	2.62	21.34	15.24	15	204.42	16.87	11255	0.03
127	6	855	1.55	21.34	12.19	15	207.04	19.48	1425	2.62
128	6	695	0.66	3.05	3.05	15	208.58	21.03	8025	1.55
129	6	260	0.15	3.05	3.05	10	209.27	21.72	6525	0.03
130	**6**	**200**	**0.25**	**6.10**	**4.06**	**15**	**209.42**	**21.87**	**5210**	**0.15**
131	6	980	6.93	45.72	26.42	15	209.68	22.12	1770	0.25
132	**6**	**145**	**0.13**	**3.05**	**3.05**	**10**	**216.64**	**29.08**	**2385**	**0.03**
133	6	880	1.63	18.29	14.22	15	216.87	29.31	12375	0.05
134	6	170	0.25	3.05	3.05	15	218.49	30.94	395	1.63

135	6	1570	2.06	9.14	6.10	15	218.85	31.29	2855	0.08
136	**6**	**630**	**2.51**	**21.34**	**12.19**	**15**	**221.06**	**33.50**	**890**	**0.15**
137	6	535	4.09	45.72	35.56	15	223.57	36.02	525	2.51
138	**6**	**840**	**1.30**	**3.05**	**3.05**	**15**	**227.71**	**40.16**	**8490**	**0.05**

Event	Max TDR 01 (cm^3/ cm^3)	Max TDR 05 (cm^3/ cm^3)	Max TDR 09 (cm^3/ cm^3)	Max TDR 13 (cm^3/ cm^3)	Max TDR 25 (cm^3/ cm^3)
1	**0.125**	**0.192**	**0.191**	**0.059**	**0.051**
2	0.079	0.103	0.168	0.067	0.053
3	0.074	0.071	0.14	0.059	0.049
4	0.074	0.057	0.086	0.06	0.047
5	0.07	0.053	0.078	0.066	0.05
6	0.074	0.05	0.069	0.064	0.046
7	**0.074**	**0.051**	**0.058**	**0.089**	**0.052**
8	0.06	0.05	0.072	0.16	0.065
9	0.067	0.06	0.077	0.088	0.044
10	**0.065**	**0.056**	**0.069**	**0.131**	**0.197**
11	0.077	0.068	0.072	0.077	0.1
12	0.077	0.055	0.035	0.053	0.039
13	0.086	0.066	0.061	0.078	0.137
14	**0.069**	**0.053**	**0.053**	**0.065**	**0.077**
15	0.058	0.052	0.051	0.065	0.132
16	0.076	0.054	0.053	0.069	0.104
17	0.076	0.054	0.061	0.065	0.034
18	**0.065**	**0.055**	**0.064**	**0.074**	**0.046**

19	0.056	0.051	0.057	0.066	0.042
20	0.058	0.047	0.05	0.062	0.038
21	0.072	0.065	0.095	0.085	0.081
22	**0.063**	**0.063**	**0.067**	**0.068**	**0.062**
23	0.082	0.055	0.055	0.071	0.053
24	**0.058**	**0.056**	**0.058**	**0.072**	**0.049**
25	0.074	0.073	0.069	0.145	0.081
26	0.047	0.058	0.048	0.058	0.046
27	**0.062**	**0.068**	**0.057**	**0.075**	**0.065**
28	0.088	0.072	0.069	0.076	0.055
29	0.061	0.063	0.059	0.065	0.054
30	0.043	0.051	0.042	0.057	0.049
31	0.052	0.054	0.053	0.058	0.046
32	**0.067**	**0.065**	**0.058**	**0.066**	**0.057**
33	0.027	0.042	0.035	0.046	0.027
34	0.064	0.06	0.053	0.094	0.051
35	0.084	0.156	0.231	0.07	0.05
36	**0.047**	**0.064**	**0.08**	**0.139**	**0.193**
37	0.05	0.062	0.079	0.093	0.078
38	0.055	0.066	0.061	0.074	0.036

39	0.024	0.045	0.045	0.051	0.039
40	0.021	0.049	0.049	0.054	0.04
41	**0.028**	**0.051**	**0.049**	**0.056**	**0.04**
42	0.032	0.052	0.053	0.063	0.044
43	0.035	0.051	0.049	0.058	0.043
44	0.031	0.045	0.047	0.058	0.042
45	0.036	0.049	0.053	0.056	0.04
46	0.038	0.053	0.051	0.058	0.05
47	**0.041**	**0.051**	**0.06**	**0.055**	**0.059**
48	0.031	0.042	0.023	0.036	0.014
49	0.028	0.038	0.056	0.055	0.016
50	**0.034**	**0.043**	**0.054**	**0.056**	**0.052**
51	0.033	0.044	0.048	0.048	0.038
52	0.03	0.04	0.052	0.055	0.048
53	0.034	0.034	0.05	0.052	0.04
54	**0.026**	**0.03**	**0.033**	**0.041**	**0.025**
55	0.031	0.049	0.047	0.056	0.047
56	**0.033**	**0.044**	**0.045**	**0.061**	**0.049**
57	0.037	0.051	0.053	0.06	0.048
58	0.04	0.058	0.049	0.052	0.036

59	0.052	0.062	0.123	0.058	0.035
60	0.033	0.035	0.02	0.043	0.027
61	0.038	0.057	0.082	0.057	0.034
62	0.035	0.043	0.043	0.067	0.087
63	0.035	0.046	0.049	0.066	0.081
64	0.039	0.049	0.055	0.066	0.049
65	0.042	0.055	0.057	0.061	0.048
66	0.039	0.056	0.056	0.058	0.049
67	0.047	0.057	0.058	0.061	0.045
68	0.043	0.057	0.049	0.056	0.031
69	0.045	0.053	0.057	0.064	0.052
70	**0.044**	**0.058**	**0.049**	**0.051**	**0.044**
71	**0.046**	**0.054**	**0.056**	**0.059**	**0.049**
72	0.047	0.054	0.062	0.061	0.074
73	0.038	0.052	0.054	0.055	0.04
74	0.046	0.057	0.056	0.055	0.053
75	0.043	0.052	0.056	0.067	0.055
76	0.042	0.05	0.055	0.057	0.055
77	0.041	0.054	0.054	0.057	0.049
78	0.046	0.058	0.058	0.054	0.051

79	0.052	0.059	0.072	0.055	0.046
80	**0.047**	**0.054**	**0.06**	**0.054**	**0.051**
81	**0.052**	**0.066**	**0.07**	**0.049**	**0.036**
82	0.049	0.061	0.057	0.07	0.051
83	**0.05**	**0.065**	**0.066**	**0.066**	**0.054**
84	0.049	0.068	0.068	0.065	0.049
85	**0.053**	**0.108**	**0.073**	**0.077**	**0.122**
86	0.061	0.099	0.075	0.068	0.063
87	**0.055**	**0.062**	**0.066**	**0.061**	**0.055**
88	0.053	0.065	0.082	0.062	0.052
89	**0.058**	**0.067**	**0.067**	**0.074**	**0.057**
90	0.036	0.061	0.055	0.067	0.044
91	0.042	0.094	0.17	0.224	0.074
92	0.042	0.073	0.078	0.08	0.145
93	0.044	0.051	0.035	0.038	0.017
94	0.043	0.058	0.052	0.078	0.045
95	**0.055**	**0.083**	**0.09**	**0.086**	**0.092**
96	0.048	0.05	0.068	0.062	0.057
97	0.061	0.073	0.074	0.082	0.082
98	0.056	0.067	0.075	0.077	0.067

99	**0.053**	**0.063**	**0.056**	**0.049**	**0.03**
100	0.04	0.06	0.064	0.078	0.049
101	0.048	0.058	0.049	0.071	0.046
102	0.048	0.059	0.023	0.038	0.021
103	**0.055**	**0.079**	**0.06**	**0.072**	**0.066**
104	0.057	0.059	0.137	0.072	0.051
105	**0.035**	**0.056**	**0.058**	**0.06**	**0.047**
106	0.057	0.068	0.1	0.138	0.06
107	0.043	0.057	0.061	0.072	0.051
108	**0.057**	**0.07**	**0.07**	**0.074**	**0.055**
109	0.061	0.065	0.084	0.085	0.049
110	0.055	0.066	0.073	0.133	0.046
111	**0.046**	**0.056**	**0.05**	**0.072**	**0.043**
112	0.047	0.051	0.057	0.042	0.02
113	0.061	0.076	0.122	0.132	0.05
114	0.039	0.055	0.051	0.064	0.042
115	0.044	0.057	0.071	0.089	0.044
116	0.034	0.059	0.054	0.064	0.037
117	0.038	0.067	0.073	0.087	0.031
118	**0.042**	**0.047**	**0.054**	**0.075**	**0.041**

119	0.033	0.055	0.048	0.064	0.037
120	**0.046**	**0.05**	**0.061**	**0.079**	**0.039**
121	0.04	0.045	0.052	0.06	0.032
122	0.039	0.043	0.036	0.052	0.032
123	**0.056**	**0.072**	**0.155**	**0.072**	**0.055**
124	0.058	0.062	0.096	0.266	0.179
125	0.047	0.069	0.07	0.091	0.043
126	0.042	0.057	0.061	0.085	0.105
127	0.042	0.056	0.063	0.091	0.064
128	0.046	0.057	0.073	0.093	0.033
129	0.019	0.017	0.022	0.032	0.016
130	**0.036**	**0.037**	**0.041**	**0.076**	**0.029**
131	0.042	0.056	0.067	0.084	0.078
132	**0.029**	**0.026**	**0.026**	**0.036**	**0.017**
133	0.041	0.051	0.054	0.074	0.062
134	0.053	0.057	0.057	0.069	0.038
135	0.065	0.061	0.06	0.069	0.058
136	**0.052**	**0.054**	**0.056**	**0.075**	**0.065**
137	0.056	0.051	0.057	0.09	0.061
138	**0.051**	**0.06**	**0.059**	**0.075**	**0.064**

Event	Max TDR 03 (cm^3/ cm^3)	Max TDR 07 (cm^3/ cm^3)	Max TDR 11 (cm^3/ cm^3)	Max TDR 15 (cm^3/ cm^3)	Max TDR 27 (cm^3/ cm^3)	Max TDR 12 (cm^3/ cm^3)	Max TDR 16 (cm^3/ cm^3)
1	0.043	0.074	0.021	0.046	0.052	0.066	0.051
2	0.043	0.078	0.05	0.055	0.06	0.07	0.063
3	0.041	0.08	0.051	0.049	0.057	0.067	0.058
4	0.036	0.073	0.051	0.046	0.058	0.065	0.053
5	0.038	0.073	0.051	0.049	0.063	0.066	0.055
6	0.037	0.068	0.045	0.047	0.063	0.061	0.056
7	0.039	0.072	0.047	0.042	0.059	0.071	0.051
8	0.151	0.297	0.153	0.039	0.057	0.072	0.051
9	0.022	0.044	0.034	0.032	0.056	0.06	0.053
10	0.128	0.212	0.059	0.058	0.07	0.078	0.064
11	0.014	0.052	0.036	0.03	0.054	0.057	0.045
12	0.011	0.052	0.029	0.027	0.051	0.063	0.045
13	0.02	0.069	0.05	0.044	0.066	0.07	0.058
14	0.021	0.051	0.03	0.025	0.053	0.044	0.041
15	0.034	0.102	0.045	0.036	0.058	0.06	0.051
16	0.07	0.151	0.053	0.138	0.056	0.065	0.056

17	0.025	0.053	0.04	0.026	0.058	0.055	0.049
18	0.027	0.061	0.042	0.042	0.058	0.066	0.06
19	0.026	0.06	0.043	0.043	0.057	0.061	0.059
20	0.026	0.056	0.044	0.04	0.056	0.058	0.055
21	0.042	0.085	0.057	0.042	0.062	0.071	0.07
22	0.024	0.062	0.036	0.034	0.059	0.062	0.051
23	0.037	0.078	0.056	0.042	0.061	0.067	0.059
24	0.046	0.083	0.057	0.061	0.063	0.068	0.064
25	0.068	0.101	0.063	0.117	0.065	0.077	0.075
26	0.015	0.039	0.023	0.023	0.044	0.045	0.038
27	0.02	0.05	0.029	0.033	0.048	0.052	0.044
28	0.063	0.089	0.1	0.103	0.08	0.077	0.07
29	0.03	0.057	0.032	0.041	0.052	0.063	0.053
30	0.009	0.03	0.029	0.023	0.039	0.023	0.032
31	0.01	0.035	0.039	0.037	0.049	0.042	0.041
32	0.009	0.031	0.03	0.037	0.045	0.043	0.036
33	0.021	0.059	0.038	0.036	0.05	0.055	0.046
34	0.093	0.087	0.083	0.074	0.054	0.075	0.068
35	0.082	0.186	0.057	0.057	0.058	0.076	0.068
36	0.09	0.124	0.139	0.11	0.064	0.075	0.076

37	0.041	0.084	0.061	0.062	0.058	0.07	0.063
38	0.016	0.053	0.035	0.042	0.047	0.047	0.046
39	0.021	0.049	0.037	0.036	0.04	0.035	0.046
40	0.017	0.049	0.036	0.03	0.038	0.03	0.042
41	0.04	0.12	0.044	0.077	0.055	0.051	0.06
42	0.031	0.079	0.05	0.057	0.05	0.049	0.049
43	0.137	0.09	0.107	0.075	0.064	0.07	0.064
44	0.02	0.058	0.017	0.038	0.027	0.041	0.039
45	0.02	0.065	0.037	0.04	0.046	0.039	0.041
46	0.052	0.086	0.073	0.061	0.058	0.061	0.06
47	0.007	0.058	0.041	0.033	0.042	0.037	0.04
48	0.008	0.032	0.018	0.023	0.031	0.027	0.028
49	0.008	0.028	0.029	0.027	0.037	0.029	0.034
50	0.032	0.075	0.061	0.05	0.052	0.052	0.056
51	0.008	0.028	0.022	0.023	0.035	0.021	0.03
52	0.032	0.083	0.084	0.056	0.056	0.051	0.05
53	0.037	0.078	0.062	0.054	0.06	0.058	0.055
54	0.028	0.062	0.05	0.048	0.053	0.05	0.047
55	0.052	0.076	0.061	0.059	0.071	0.069	0.057
56	0.032	0.076	0.022	0.056	0.056	0.06	0.054

57	0.027	0.069	0.056	0.049	0.05	0.078	0.057
58	0.017	0.058	0.039	0.036	0.041	0.042	0.042
59	0.014	0.054	0.043	0.046	0.047	0.051	0.049
60	0.008	0.032	0.023	0.031	0.038	0.033	0.041
61	0.02	0.06	0.046	0.024	0.046	0.049	0.051
62	0.025	0.072	0.03	0.051	0.046	0.071	0.045
63	0.035	0.064	0.042	0.037	0.053	0.075	0.06
64	0.042	0.075	0.044	0.048	0.048	0.069	0.063
65	0.04	0.076	0.074	0.05	0.049	0.066	0.062
66	0.037	0.074	0.075	0.054	0.055	0.07	0.071
67	0.027	0.057	0.031	0.052	0.041	0.066	0.059
68	0.025	0.052	0.025	0.035	0.038	0.052	0.04
69	0.024	0.068	0.032	0.046	0.043	0.063	0.054
70	0.015	0.048	0.03	0.029	0.035	0.05	0.045
71	0.033	0.079	0.069	0.046	0.049	0.063	0.072
72	0.039	0.08	0.069	0.052	0.058	0.073	0.073
73	0.031	0.068	0.045	0.042	0.045	0.057	0.05
74	0.017	0.039	0.015	0.04	0.044	0.038	0.038
75	0.025	0.037	0.017	0.043	0.05	0.062	0.058
76	0.039	0.068	0.06	0.05	0.078	0.068	0.113

77	0.04	0.065	0.056	0.046	0.052	0.062	0.065
78	0.035	0.047	0.023	0.029	0.026	0.066	0.059
79	0.026	0.053	0.026	0.038	0.043	0.06	0.053
80	0.031	0.057	0.02	0.042	0.037	0.067	0.058
81	0.026	0.053	0.022	0.033	0.039	0.046	0.044
82	0.027	0.065	0.052	0.023	0.051	0.067	0.058
83	0.035	0.059	0.064	0.041	0.054	0.073	0.07
84	0.036	0.067	0.063	0.045	0.045	0.072	0.067
85	0.048	0.078	0.067	0.044	0.056	0.072	0.07
86	0.045	0.078	0.071	0.056	0.057	0.074	0.07
87	0.022	0.07	0.05	0.039	0.052	0.069	0.065
88	0.03	0.072	0.057	0.044	0.053	0.068	0.066
89	0.045	0.077	0.066	0.053	0.057	0.084	0.076
90	0.031	0.067	0.043	0.043	0.05	0.062	0.058
91	0.042	0.164	0.065	0.053	0.037	0.072	0.068
92	0.04	0.101	0.051	0.039	0.056	0.061	0.058
93	0.013	0.035	0.02	0.025	0.036	0.03	0.031
94	0.015	0.03	0.017	0.027	0.03	0.025	0.035
95	0.049	0.075	0.05	0.055	0.059	0.068	0.064
96	0.027	0.094	0.051	0.042	0.05	0.056	0.05

97	0.042	0.11	0.123	0.043	0.05	0.074	0.051
98	0.044	0.081	0.073	0.046	0.055	0.066	0.058
99	0.026	0.054	0.043	0.038	0.049	0.05	0.047
100	0.048	0.078	0.066	0.06	0.044	0.06	0.043
101	0.043	0.073	0.06	0.052	0.046	0.055	0.042
102	0.009	0.026	0.017	0.02	0.029	0.034	0.028
103	0.026	0.067	0.017	0.04	0.045	0.07	0.05
104	0.022	0.066	0.054	0.024	0.049	0.049	0.049
105	0.032	0.074	0.057	0.048	0.048	0.064	0.057
106	0.04	0.079	0.062	0.058	0.068	0.067	0.07
107	0.032	0.072	0.047	0.053	0.048	0.061	0.057
108	0.043	0.085	0.062	0.063	0.055	0.097	0.07
109	0.047	0.086	0.079	0.069	0.071	0.125	0.09
110	0.024	0.039	0.052	0.049	0.035	0.06	0.061
111	0.034	0.073	0.056	0.054	0.047	0.069	0.065
112	0.02	0.041	0.027	0.035	0.039	0.039	0.043
113	0.038	0.073	0.055	0.05	0.054	0.074	0.07
114	0.029	0.07	0.047	0.054	0.05	0.068	0.062
115	0.049	0.094	0.057	0.075	0.069	0.112	0.086
116	0.013	0.027	0.019	0.043	0.037	0.039	0.041

117	0.022	0.042	0.039	0.04	0.043	0.043	0.046
118	0.038	0.074	0.051	0.057	0.053	0.091	0.069
119	0.024	0.061	0.046	0.04	0.047	0.065	0.056
120	0.04	0.073	0.052	0.067	0.057	0.069	0.069
121	0.033	0.057	0.043	0.055	0.047	0.061	0.05
122	0.028	0.046	0.028	0.044	0.046	0.038	0.03
123	0.074	0.115	0.054	0.072	0.06	0.078	0.066
124	0.11	0.16	0.074	0.112	0.062	0.088	0.076
125	0.01	0.023	0.015	0.04	0.047	0.048	0.052
126	0.06	0.084	0.104	0.067	0.056	0.074	0.07
127	0.037	0.074	0.075	0.065	0.057	0.083	0.072
128	0.017	0.026	0.017	0.049	0.05	0.057	0.057
129	0.01	0.027	0.017	0.022	0.031	0.023	0.03
130	0.012	0.028	0.027	0.037	0.04	0.029	0.045
131	0.067	0.097	0.118	0.155	0.097	0.099	0.078
132	0.014	0.028	0.019	0.026	0.033	0.033	0.033
133	0.049	0.086	0.077	0.059	0.044	0.075	0.064
134	0.05	0.052	0.04	0.065	0.05	0.068	0.064
135	0.048	0.082	0.051	0.072	0.057	0.079	0.072
136	0.051	0.083	0.057	0.07	0.057	0.083	0.075

137	0.051	0.079	0.068	0.079	0.078	0.094	0.09
138	0.032	0.029	0.036	0.065	0.049	0.069	0.065

APPENDIX E

Peak VWC Dataset of PICP 19H

Event	Cleaning Method	Duration (Min.)	Rainfall Depth (cm.)	Peak 5 min (mm/hr)	Peak 15 min (mm/hr)	Peak Duration (Min)	Cumulative Rainfall Depth from the installation (cm)	Cumulative Rainfall Depth from the last maintenance (cm)	ADP (Min)	Previous Rainfall Depth (cm)
1	1	395.00	1.17	18.29	11.18	15.00	0.05	0.05	1470.00	0.05
2	1	480.00	1.68	21.34	16.26	15.00	1.22	1.22	7965.00	1.17
3	1	605.00	1.55	6.10	4.06	15.00	2.90	2.90	1615.00	1.68
4	1	820.00	2.11	9.14	8.13	15.00	4.50	4.50	1900.00	0.03
5	1	535.00	1.96	15.24	10.16	15.00	6.65	6.65	16245.00	0.05
6	1	140.00	0.38	3.05	3.05	15.00	8.61	8.61	370.00	1.96
7	1	135.00	0.20	3.05	2.03	15.00	8.99	8.99	805.00	0.38
8	1	605.00	0.99	21.34	13.21	15.00	9.19	9.19	6545.00	0.20
9	1	390.00	1.93	42.67	29.46	15.00	10.21	10.21	1815.00	0.03
10	1	270.00	0.64	3.05	3.05	15.00	12.22	12.22	3000.00	0.08
11	1	1520.0	4.37	36.58	19.30	15.00	12.85	12.85	470.00	0.64
12	1	490.00	0.91	6.10	5.08	15.00	17.35	17.35	3650.00	0.03
13	1	145.00	0.48	3.05	3.05	15.00	18.47	18.47	4920.00	0.05
14	1	645.00	0.84	9.14	9.14	10.00	18.95	18.95	2040.00	0.48

15	1	250.00	0.25	6.10	4.06	15.00	19.79	19.79	7050.00	0.84
16	1	35.00	0.53	21.34	14.22	15.00	20.04	20.04	2210.00	0.25
17	1	595.00	1.42	48.77	24.38	15.00	20.65	20.65	6520.00	0.08
18	1	635.00	0.25	3.05	3.05	15.00	22.07	22.07	2615.00	1.42
19	1	325.00	0.20	3.05	2.03	15.00	22.33	22.33	3140.00	0.25
20	1	60.00	0.13	3.05	3.05	10.00	22.53	22.53	900.00	0.20
21	1	200.00	0.66	6.10	4.06	15.00	22.66	22.66	820.00	0.13
22	1	545.00	1.93	15.24	12.19	15.00	23.32	23.32	2650.00	0.66
23	1	605.00	0.48	6.10	4.57	10.00	25.25	25.25	4925.00	1.93
24	1	1070.0	2.57	12.19	9.14	15.00	25.73	25.73	4130.00	0.48
25	1	545.00	1.14	30.48	15.24	15.00	28.30	28.30	2355.00	2.57
26	1	1340.0	4.14	33.53	26.42	15.00	29.44	29.44	6995.00	1.14
27	1	10.00	0.25	24.38	10.16	15.00	33.58	33.58	6710.00	4.14
28	1	110.00	0.46	6.10	5.08	15.00	33.83	33.83	3355.00	0.25
29	1	345.00	4.52	48.77	31.50	15.00	34.29	34.29	1825.00	0.46
30	1	565.00	0.61	18.29	15.24	10.00	38.89	38.89	555.00	0.08
31	1	65.00	0.30	9.14	5.08	15.00	39.50	39.50	13390.00	0.61
32	1	215.00	0.48	18.29	12.19	15.00	39.80	39.80	2700.00	0.30
33	1	560.00	0.58	12.19	7.11	15.00	40.28	40.28	6455.00	0.48
34	1	710.00	2.46	9.14	8.13	15.00	41.20	41.20	2225.00	0.03

35	1	540.00	3.58	18.29	16.26	15.00	43.76	43.76	440.00	0.10
36	2	770.00	3.35	21.34	16.26	15.00	59.46	12.04	3175.00	5.74
37	2	470.00	0.51	3.05	2.03	15.00	62.84	15.42	2155.00	0.03
38	2	280.00	0.79	39.62	20.32	15.00	63.42	16.00	13865.00	0.05
39	2	380.00	0.36	15.24	7.11	15.00	64.21	16.79	9390.00	0.79
40	2	310.00	2.67	82.30	49.78	15.00	64.57	17.15	8080.00	0.36
41	2	235.00	1.19	51.82	33.53	15.00	67.23	19.81	5805.00	2.67
42	2	310.00	3.10	106.68	96.52	15.00	68.43	21.01	1070.00	1.19
43	2	45.00	0.23	9.14	7.11	15.00	71.53	24.10	7265.00	3.10
44	2	120.00	0.53	36.58	20.32	15.00	71.76	24.33	2935.00	0.23
45	2	70.00	1.63	45.72	34.54	15.00	72.31	24.89	495.00	0.03
46	2	510.00	0.43	9.14	6.10	10.00	73.96	26.54	8465.00	0.03
47	2	330.00	0.15	9.14	7.62	10.00	74.45	27.03	1570.00	0.05
48	2	105.00	0.30	3.05	3.05	15.00	74.63	27.20	10335.00	0.03
49	2	215.00	1.37	24.38	17.27	15.00	74.93	27.51	4770.00	0.30
50	2	20.00	0.28	18.29	15.24	10.00	76.30	28.88	6610.00	1.37
51	2	305.00	1.24	36.58	25.40	15.00	76.58	29.16	15760.00	0.28
52	2	900.00	2.06	36.58	19.30	15.00	77.83	30.40	820.00	1.24
53	2	25.00	0.13	6.10	6.10	10.00	79.88	32.46	950.00	2.06
54	2	75.00	2.97	115.82	75.18	15.00	80.01	32.59	2915.00	0.13

55	2	495.00	2.41	24.38	15.24	15.00	82.98	35.56	3265.00	2.97
56	2	780.00	2.16	24.38	13.21	15.00	85.60	38.18	4425.00	0.05
57	3	145.00	0.64	6.10	5.08	15.00	87.88	0.13	4560.00	0.13
58	3	785.00	1.83	9.14	7.11	15.00	88.62	0.86	8655.00	0.03
59	3	425.00	0.38	6.10	4.06	15.00	90.47	2.72	5365.00	0.03
60	3	605.00	1.14	6.10	4.06	15.00	91.01	3.25	6690.00	0.15
61	3	360.00	0.76	30.48	17.27	15.00	92.30	4.55	7695.00	0.15
62	3	235.00	1.24	12.19	7.11	15.00	93.09	5.33	425.00	0.03
63	3	1620.0	3.23	12.19	7.11	15.00	94.34	6.58	2730.00	1.24
64	3	455.00	0.94	24.38	10.16	15.00	97.56	9.80	400.00	3.23
65	3	1145.0	3.02	48.77	37.59	15.00	98.53	10.77	555.00	0.03
66	3	150.00	0.46	9.14	6.10	15.00	101.55	13.79	7615.00	3.02
67	3	150.00	0.30	18.29	12.19	10.00	102.01	14.25	2985.00	0.46
68	3	670.00	2.03	15.24	11.18	15.00	102.31	14.55	3690.00	0.30
69	3	280.00	0.15	3.05	3.05	10.00	104.34	16.59	4920.00	2.03
70	3	745.00	2.08	12.19	7.11	15.00	104.50	16.74	2375.00	0.15
71	3	265.00	0.36	3.05	2.29	20.00	106.73	18.97	645.00	0.05
72	3	210.00	0.41	6.10	4.06	15.00	107.14	19.38	1500.00	0.03
73	3	415.00	1.63	27.43	17.27	15.00	107.54	19.79	675.00	0.41
74	3	1360.0	6.02	48.77	26.42	15.00	109.17	21.41	2140.00	1.63

75	3	195.00	0.46	3.05	2.29	20.00	115.29	27.53	1125.00	0.08
76	3	355.00	0.38	3.05	2.29	20.00	115.75	27.99	14670.00	0.46
77	3	400.00	0.23	9.14	5.08	15.00	116.13	28.37	555.00	0.38
78	3	280.00	2.49	97.54	48.77	15.00	116.38	28.63	1750.00	0.03
79	3	10.00	0.13	9.14	5.08	15.00	118.87	31.12	505.00	2.49
80	3	180.00	0.25	3.05	2.03	15.00	119.35	31.60	4770.00	0.25
81	3	105.00	0.30	6.10	4.06	15.00	119.71	31.95	400.00	0.10
82	3	355.00	0.15	6.10	4.06	15.00	120.02	32.26	4135.00	0.30
83	3	465.00	0.69	6.10	3.05	15.00	120.17	32.41	7285.00	0.15
84	3	865.00	1.68	9.14	7.11	15.00	120.95	33.20	5500.00	0.03
85	3	890.00	1.12	6.10	5.08	15.00	122.78	35.03	4565.00	0.13
86	3	810.00	2.69	9.14	6.10	15.00	123.90	36.14	7420.00	1.12
87	3	2220.0	4.65	15.24	13.21	15.00	126.67	38.91	5630.00	0.05
88	3	305.00	0.66	6.10	5.08	15.00	131.32	43.56	8160.00	4.65
89	3	705.00	0.46	6.10	6.10	15.00	131.98	44.22	365.00	0.66
90	3	1165.0	3.12	60.96	23.37	15.00	132.64	44.88	15570.00	0.18
91	4	285.00	1.09	109.73	64.01	10.00	135.76	0.00	6960.00	3.12
92	4	475.00	2.44	30.48	22.35	15.00	136.91	1.14	1825.00	0.05
93	4	390.00	1.73	12.19	11.18	15.00	139.34	3.58	7050.00	2.44
94	4	170.00	0.13	3.05	2.03	15.00	141.07	5.31	4800.00	1.73

95	4	15.00	0.25	21.34	9.14	15.00	141.25	5.49	7790.00	0.05
96	4	2030.0	3.12	6.10	5.08	15.00	141.50	5.74	875.00	0.25
97	4	330.00	0.23	15.24	12.19	10.00	144.65	8.89	395.00	0.03
98	4	380.00	1.73	15.24	12.19	15.00	144.93	9.17	4750.00	0.05
99	4	95.00	0.53	36.58	20.32	15.00	147.35	11.58	6610.00	0.15
100	4	95.00	0.58	45.72	22.35	15.00	147.93	12.17	1945.00	0.05
101	4	395.00	0.20	3.05	3.05	10.00	148.62	12.85	7010.00	0.03
102	4	655.00	0.58	24.38	13.72	10.00	148.82	13.06	665.00	0.20
103	4	345.00	0.81	12.19	11.18	15.00	149.48	13.72	500.00	0.03
104	4	60.00	1.68	64.01	54.86	15.00	150.34	14.58	465.00	0.05
105	4	670.00	3.48	106.68	96.52	15.00	152.02	16.26	1360.00	1.68
106	4	75.00	1.50	54.86	30.48	15.00	155.52	19.76	2435.00	0.03
107	4	65.00	0.15	6.10	4.06	15.00	157.02	21.26	1160.00	1.50
108	4	225.00	2.18	57.91	36.58	15.00	157.18	21.41	2500.00	0.15
109	4	310.00	7.11	128.01	72.14	15.00	159.36	23.60	550.00	2.18
110	4	70.00	0.33	6.10	6.10	15.00	166.47	30.71	7045.00	7.11
111	4	30.00	0.36	24.38	19.81	10.00	166.80	31.04	1025.00	0.33
112	4	80.00	0.15	6.10	6.10	10.00	167.16	31.39	1665.00	0.36
113	4	930.00	1.37	9.14	5.08	15.00	167.31	31.55	530.00	0.15
114	4	635.00	1.96	12.19	9.14	15.00	168.68	32.92	1660.00	1.37

115	4	140.00	1.68	64.01	51.82	15.00	170.74	34.98	1755.00	0.10
116	4	80.00	1.30	54.86	45.72	15.00	172.42	36.65	5945.00	1.68
117	4	1100.0	5.89	109.73	82.30	15.00	173.74	37.97	4500.00	0.03
118	4	305.00	0.28	9.14	7.62	10.00	179.63	43.87	6680.00	5.89
119	4	385.00	0.33	6.10	4.57	10.00	179.91	44.15	4735.00	0.28
120	4	10.00	0.36	15.24	14.22	15.00	187.55	51.56	9925.00	0.10
121	4	820.00	4.34	21.34	14.22	15.00	187.91	51.92	1725.00	0.36
122	4	2125.0	11.35	42.67	35.56	15.00	192.43	56.26	965.00	0.08
123	4	730.00	2.62	21.34	15.24	15.00	204.42	68.10	11255.00	0.03
124	4	855.00	1.55	21.34	12.19	15.00	207.04	70.71	1425.00	2.62
125	4	695.00	0.66	3.05	3.05	15.00	208.58	72.26	8025.00	1.55
126	4	260.00	0.15	3.05	3.05	10.00	209.27	72.92	6525.00	0.03
127	4	980.00	6.93	45.72	26.42	15.00	209.68	73.33	1770.00	0.25
128	4	880.00	1.63	18.29	14.22	15.00	216.87	80.39	12375.00	0.05
129	4	170.00	0.25	3.05	3.05	15.00	218.49	82.02	395.00	1.63
130	4	630.00	2.51	21.34	12.19	15.00	221.06	84.48	890.00	0.15
131	4	535.00	4.09	45.72	35.56	15.00	223.57	87.00	525.00	2.51

Event	Max TDR 01 (cm^3/ cm^3)	Max TDR 03 (cm^3/ cm^3)	Max TDR 05 (cm^3/ cm^3)	Max TDR 07 (cm^3/ cm^3)	Max TDR 09 (cm^3/ cm^3)
1	0.054	0.056	0.046	0.045	0.063
2	0.19	0.053	0.189	0.043	0.241
3	0.119	0.054	0.082	0.051	0.199
4	0.118	0.029	0.077	0.027	0.201
5	0.097	0.023	0.068	0.019	0.163
6	0.089	0.023	0.065	0.019	0.113
7	0.075	0.025	0.062	0.02	0.141
8	0.079	0.026	0.064	0.021	0.118
9	0.077	0.11	0.062	0.156	0.106
10	0.089	0.047	0.06	0.032	0.092
11	0.114	0.067	0.066	0.054	0.111
12	0.083	0.046	0.064	0.038	0.109
13	0.088	0.036	0.065	0.028	0.102
14	0.085	0.054	0.065	0.055	0.095
15	0.071	0.029	0.045	0.028	0.082
16	0.071	0.042	0.052	0.036	0.086

17	0.086	0.055	0.049	0.066	0.082
18	0.082	0.036	0.059	0.041	0.087
19	0.088	0.034	0.064	0.04	0.084
20	0.078	0.031	0.058	0.046	0.076
21	0.07	0.03	0.056	0.047	0.072
22	0.086	0.053	0.063	0.053	0.093
23	0.098	0.045	0.06	0.044	0.092
24	0.08	0.054	0.055	0.05	0.087
25	0.076	0.053	0.057	0.051	0.086
26	0.079	0.063	0.054	0.064	0.085
27	0.057	0.032	0.042	0.03	0.074
28	0.068	0.043	0.048	0.034	0.082
29	0.078	0.125	0.05	0.103	0.078
30	0.088	0.041	0.063	0.032	0.089
31	0.074	0.024	0.043	0.021	0.069
32	0.081	0.042	0.048	0.03	0.081
33	0.076	0.046	0.047	0.036	0.087
34	0.05	0.036	0.038	0.036	0.052
35	0.088	0.081	0.057	0.059	0.088
36	0.083	0.064	0.066	0.06	0.092

37	0.102	0.042	0.066	0.037	0.081
38	0.056	0.055	0.038	0.042	0.066
39	0.054	0.023	0.04	0.032	0.067
40	0.06	0.072	0.042	0.074	0.075
41	0.06	0.07	0.041	0.096	0.077
42	0.058	0.114	0.04	0.123	0.074
43	0.055	0.043	0.038	0.021	0.068
44	0.059	0.027	0.041	0.021	0.072
45	0.063	0.068	0.045	0.068	0.075
46	0.062	0.047	0.039	0.037	0.072
47	0.052	0.028	0.038	0.022	0.062
48	0.054	0.04	0.034	0.019	0.067
49	0.053	0.059	0.047	0.047	0.069
50	0.044	0.025	0.029	0.02	0.061
51	0.065	0.105	0.039	0.087	0.07
52	0.063	0.086	0.041	0.062	0.07
53	0.057	0.061	0.034	0.052	0.063
54	0.064	0.062	0.04	0.059	0.074
55	0.062	0.06	0.042	0.056	0.074
56	0.197	0.071	0.047	0.061	0.133

57	0.095	0.049	0.066	0.041	0.044
58	0.122	0.056	0.063	0.047	0.092
59	0.07	0.028	0.045	0.022	0.129
60	0.073	0.05	0.047	0.02	0.163
61	0.051	0.053	0.031	0.069	0.101
62	0.058	0.051	0.037	0.045	0.093
63	0.064	0.057	0.039	0.057	0.086
64	0.066	0.088	0.04	0.064	0.078
65	0.073	0.064	0.045	0.055	0.08
66	0.05	0.044	0.032	0.034	0.067
67	0.065	0.052	0.031	0.048	0.068
68	0.067	0.059	0.04	0.051	0.097
69	0.064	0.029	0.036	0.031	0.088
70	0.072	0.062	0.047	0.046	0.093
71	0.069	0.045	0.041	0.044	0.086
72	0.068	0.023	0.033	0.02	0.078
73	0.071	0.059	0.042	0.05	0.082
74	0.11	0.062	0.046	0.058	0.1
75	0.052	0.049	0.038	0.044	0.071
76	0.075	0.041	0.041	0.035	0.095

77	0.076	0.056	0.045	0.049	0.085
78	0.071	0.057	0.045	0.057	0.103
79	0.071	0.062	0.046	0.058	0.087
80	0.073	0.038	0.046	0.037	0.113
81	0.071	0.041	0.051	0.041	0.087
82	0.073	0.051	0.05	0.032	0.083
83	0.073	0.025	0.046	0.021	0.085
84	0.076	0.058	0.051	0.053	0.099
85	0.08	0.048	0.063	0.048	0.09
86	0.071	0.057	0.053	0.053	0.101
87	0.078	0.062	0.053	0.056	0.11
88	0.067	0.054	0.051	0.047	0.101
89	0.073	0.054	0.053	0.049	0.1
90	0.079	0.063	0.054	0.052	0.139
91	0.065	0.057	0.038	0.041	0.08
92	0.075	0.065	0.055	0.052	0.119
93	0.071	0.061	0.058	0.053	0.088
94	0.072	0.03	0.032	0.029	0.042
95	0.065	0.035	0.043	0.044	0.075
96	0.089	0.065	0.061	0.065	0.109

97	0.065	0.052	0.047	0.05	0.073
98	0.106	0.061	0.057	0.054	0.088
99	0.059	0.054	0.043	0.049	0.064
100	0.076	0.055	0.038	0.052	0.095
101	0.113	0.027	0.032	0.024	0.054
102	0.083	0.054	0.055	0.038	0.094
103	0.076	0.057	0.05	0.047	0.087
104	0.055	0.06	0.048	0.051	0.109
105	0.1	0.065	0.055	0.052	0.1
106	0.07	0.057	0.05	0.045	0.14
107	0.138	0.04	0.048	0.038	0.092
108	0.145	0.063	0.055	0.05	0.08
109	0.191	0.069	0.062	0.062	0.089
110	0.107	0.029	0.061	0.046	0.103
111	0.082	0.051	0.053	0.065	0.072
112	0.073	0.039	0.073	0.034	0.076
113	0.088	0.064	0.071	0.055	0.12
114	0.089	0.065	0.067	0.055	0.235
115	0.076	0.062	0.056	0.061	0.084
116	0.055	0.059	0.047	0.049	0.081

117	0.093	0.072	0.058	0.068	0.132
118	0.079	0.029	0.054	0.023	0.086
119	0.087	0.047	0.055	0.042	0.06
120	0.066	0.029	0.036	0.026	0.079
121	0.092	0.068	0.056	0.067	0.108
122	0.097	0.075	0.06	0.078	0.189
123	0.141	0.027	0.097	0.065	0.17
124	0.099	0.057	0.083	0.059	0.108
125	0.09	0.052	0.049	0.038	0.101
126	0.025	0.024	0.02	0.023	0.036
127	0.103	0.061	0.059	0.068	0.095
128	0.109	0.05	0.061	0.063	0.102
129	0.099	0.045	0.06	0.045	0.075
130	0.104	0.058	0.07	0.059	0.104
131	0.105	0.061	0.07	0.138	0.097

Event	Max TDR 11 (cm^3/ cm^3)	Max TDR 12 (cm^3/ cm^3)	Max TDR 13 (cm^3/ cm^3)	Max TDR 15 (cm^3/ cm^3)	Max TDR 16 (cm^3/ cm^3)
1	0.069	0.05	0.056	0.049	0.063
2	0.075	0.052	0.066	0.049	0.066
3	0.074	0.06	0.064	0.052	0.065
4	0.074	0.058	0.058	0.042	0.068
5	0.063	0.059	0.057	0.05	0.062
6	0.069	0.054	0.058	0.05	0.061
7	0.064	0.049	0.054	0.049	0.059
8	0.053	0.058	0.054	0.045	0.061
9	0.07	0.055	0.096	0.05	0.067
10	0.053	0.055	0.067	0.053	0.058
11	0.079	0.069	0.072	0.06	0.074
12	0.066	0.055	0.065	0.037	0.051
13	0.033	0.055	0.042	0.026	0.051
14	0.033	0.06	0.066	0.025	0.064
15	0.037	0.036	0.059	0.025	0.047
16	0.046	0.053	0.057	0.026	0.055
17	0.072	0.052	0.055	0.076	0.064
18	0.049	0.044	0.063	0.033	0.052

19	0.068	0.051	0.071	0.038	0.057
20	0.064	0.055	0.059	0.04	0.056
21	0.06	0.052	0.055	0.04	0.053
22	0.068	0.055	0.064	0.056	0.061
23	0.059	0.045	0.06	0.039	0.055
24	0.06	0.056	0.064	0.039	0.064
25	0.071	0.058	0.06	0.056	0.063
26	0.079	0.083	0.069	0.097	0.089
27	0.033	0.035	0.046	0.029	0.033
28	0.052	0.046	0.053	0.038	0.042
29	0.13	0.085	0.057	0.106	0.096
30	0.055	0.058	0.055	0.043	0.059
31	0.045	0.025	0.042	0.019	0.03
32	0.051	0.037	0.048	0.019	0.044
33	0.051	0.039	0.038	0.019	0.034
34	0.044	0.037	0.039	0.032	0.041
35	0.1	0.068	0.063	0.059	0.089
36	0.081	0.062	0.068	0.061	0.075
37	0.051	0.041	0.058	0.04	0.04
38	0.039	0.037	0.049	0.035	0.043

39	0.053	0.029	0.048	0.034	0.032
40	0.055	0.051	0.053	0.074	0.069
41	0.045	0.043	0.053	0.078	0.077
42	0.226	0.08	0.05	0.081	0.111
43	0.056	0.038	0.049	0.021	0.041
44	0.056	0.04	0.046	0.038	0.048
45	0.087	0.066	0.055	0.065	0.081
46	0.054	0.042	0.055	0.027	0.043
47	0.031	0.029	0.027	0.02	0.021
48	0.043	0.032	0.05	0.029	0.028
49	0.074	0.054	0.055	0.056	0.062
50	0.037	0.028	0.039	0.024	0.02
51	0.11	0.071	0.046	0.059	0.068
52	0.08	0.059	0.047	0.052	0.069
53	0.066	0.056	0.041	0.048	0.06
54	0.08	0.067	0.047	0.055	0.073
55	0.076	0.062	0.049	0.057	0.08
56	0.08	0.058	0.053	0.05	0.064
57	0.029	0.044	0.045	0.019	0.045
58	0.074	0.052	0.052	0.048	0.055

59	0.026	0.034	0.037	0.029	0.037
60	0.028	0.05	0.049	0.032	0.052
61	0.049	0.048	0.053	0.068	0.049
62	0.07	0.059	0.056	0.046	0.052
63	0.09	0.059	0.053	0.046	0.054
64	0.086	0.057	0.062	0.064	0.054
65	0.076	0.059	0.059	0.079	0.051
66	0.029	0.051	0.045	0.019	0.043
67	0.055	0.048	0.047	0.041	0.045
68	0.074	0.061	0.058	0.051	0.054
69	0.037	0.042	0.031	0.022	0.042
70	0.077	0.057	0.059	0.059	0.062
71	0.07	0.059	0.054	0.02	0.056
72	0.046	0.049	0.052	0.029	0.038
73	0.075	0.075	0.054	0.059	0.05
74	0.08	0.088	0.063	0.057	0.057
75	0.038	0.052	0.045	0.034	0.047
76	0.043	0.051	0.049	0.016	0.033
77	0.061	0.065	0.052	0.033	0.047
78	0.071	0.089	0.061	0.045	0.052

79	0.071	0.069	0.053	0.041	0.051
80	0.038	0.061	0.056	0.025	0.048
81	0.043	0.055	0.057	0.02	0.045
82	0.042	0.048	0.042	0.023	0.046
83	0.073	0.053	0.053	0.049	0.051
84	0.071	0.064	0.065	0.046	0.055
85	0.075	0.063	0.06	0.051	0.054
86	0.075	0.061	0.058	0.052	0.057
87	0.074	0.061	0.062	0.049	0.056
88	0.06	0.056	0.053	0.033	0.052
89	0.066	0.059	0.055	0.036	0.054
90	0.076	0.059	0.057	0.048	0.056
91	0.063	0.049	0.048	0.046	0.045
92	0.071	0.057	0.055	0.048	0.054
93	0.079	0.049	0.056	0.047	0.051
94	0.039	0.045	0.025	0.023	0.039
95	0.037	0.039	0.039	0.026	0.035
96	0.08	0.062	0.056	0.067	0.055
97	0.069	0.058	0.048	0.038	0.052
98	0.071	0.065	0.059	0.059	0.059

99	0.041	0.045	0.038	0.035	0.046
100	0.062	0.048	0.042	0.038	0.047
101	0.031	0.04	0.019	0.02	0.038
102	0.058	0.057	0.05	0.046	0.052
103	0.074	0.049	0.046	0.047	0.052
104	0.045	0.05	0.04	0.044	0.065
105	0.084	0.064	0.057	0.057	0.076
106	0.073	0.059	0.092	0.048	0.07
107	0.062	0.053	0.086	0.031	0.035
108	0.081	0.064	0.089	0.053	0.082
109	0.084	0.07	0.069	0.055	0.147
110	0.064	0.058	0.054	0.033	0.061
111	0.075	0.058	0.062	0.051	0.068
112	0.058	0.051	0.034	0.03	0.03
113	0.078	0.066	0.064	0.047	0.071
114	0.086	0.069	0.084	0.049	0.077
115	0.07	0.055	0.066	0.042	0.07
116	0.07	0.049	0.051	0.047	0.066
117	0.103	0.072	0.079	0.059	0.1
118	0.05	0.053	0.027	0.022	0.048

119	0.058	0.058	0.035	0.027	0.043
120	0.042	0.036	0.028	0.029	0.045
121	0.083	0.066	0.058	0.052	0.077
122	0.088	0.064	0.062	0.057	0.089
123	0.086	0.062	0.062	0.074	0.076
124	0.082	0.062	0.061	0.064	0.072
125	0.033	0.054	0.037	0.034	0.062
126	0.031	0.032	0.016	0.02	0.02
127	0.083	0.061	0.062	0.086	0.072
128	0.079	0.052	0.058	0.058	0.062
129	0.075	0.057	0.056	0.051	0.057
130	0.081	0.06	0.063	0.052	0.062
131	0.082	0.06	0.062	0.052	0.068

APPENDIX F

Clogging Length Dataset of the Laboratory Model

Clogging Proggression	Slope	Gap siza	Material	Clogging	Rainfall
Experiment #1	1	6	1	28.58	3.471333
	1	6	1	57.15	14.224
	1	6	1	85.73	20.48933
	1	**6**	**1**	**142.88**	**38.94667**
	1	6	1	171.45	51.13867
Experiment #2	1	6	1	28.58	5.672667
	1	6	1	57.15	8.805333
	1	**6**	**1**	**85.73**	**17.69533**
	1	6	1	114.3	34.544
	1	6	1	142.88	50.37667
	1	6	1	171.45	50.96933
Experiment #3	1	6	1	28.58	5.503333
	1	**6**	**1**	**57.15**	**12.86933**

	1	6	1	85.73	38.354
	1	6	1	114.3	42.33333
	1	**6**	**1**	**142.88**	**46.736**
	1	6	1	171.45	49.10667
Experiment #4	1	6	2	28.58	2.794
	1	6	2	85.73	4.233333
	1	**6**	**2**	**114.3**	**20.828**
	1	6	2	142.88	47.83667
	1	6	2	171.45	47.92133
Experiment #5	1	9	1	28.58	3.302
	1	9	1	57.15	10.668
	1	**9**	**1**	**85.73**	**13.208**
	1	9	1	114.3	28.194
	1	9	1	142.88	48.34467
	1	9	1	171.45	50.12267
	1	9	1	200.03	50.88467
Experiment #6	1	9	2	28.58	2.455333
	1	9	2	57.15	7.789333

	1	9	2	114.3	13.97
	1	**9**	**2**	**85.73**	**21.75933**
	1	9	2	142.88	25.4
	1	9	2	200.03	48.42933
Experiment #7	**1**	**12**	**1**	**28.58**	**6.180667**
	1	12	1	57.15	15.66333
	1	12	1	85.73	32.258
	1	12	1	114.3	49.10667
Experiment #8	**1**	**12**	**2**	**28.58**	**5.334**
	1	12	2	57.15	23.53733
	1	12	2	85.73	27.432
	1	**12**	**2**	**114.3**	**51.13867**
Experiment #9	3	12	2	28.58	1.947333
	3	12	2	57.15	8.720667
	3	**12**	**2**	**85.73**	**11.59933**
	3	12	2	142.88	15.07067
	3	12	2	171.45	35.47533
	3	12	2	200.03	39.03133

Experiment #10	**3**	**12**	**1**	**28.58**	**4.064**
	3	12	1	57.15	12.78467
	3	12	1	85.73	19.05
	3	**12**	**1**	**114.3**	**31.58067**
	3	12	1	142.88	50.546
Experiment #11	3	9	1	28.58	3.640667
	3	**9**	**1**	**57.15**	**12.27667**
	3	9	1	85.73	19.21933
	3	9	1	114.3	28.87133
	3	9	1	142.88	40.97867
	3	**9**	**1**	**171.45**	**50.88467**
Experiment #12	3	9	2	28.58	3.132667
	3	9	2	57.15	5.334
	3	**9**	**2**	**114.3**	**8.043333**
	3	9	2	142.88	11.938
	3	9	2	171.45	15.66333
	3	**9**	**2**	**200.03**	**25.146**
Experiment #13	3	6	1	28.58	4.826

	3	6	1	57.15	12.192
	3	**6**	**1**	**85.73**	**18.45733**
	3	6	1	114.3	31.07267
	3	6	1	171.45	49.784
	3	6	1	200.03	50.96933
Experiment #14	3	6	2	28.58	3.302
	3	6	2	57.15	3.556
	3	**6**	**2**	**114.3**	**8.466667**
	3	6	2	142.88	18.796
	3	6	2	200.03	35.052
Experiment #15	**5**	**12**	**1**	**28.58**	**2.878667**
	5	12	1	57.15	10.16
	5	12	1	85.73	25.73867
	5	12	1	114.3	41.06333
	5	12	1	142.88	50.8
Experiment #16	5	12	2	28.58	1.185333
	5	12	2	57.15	5.249333
	5	12	2	85.73	7.789333

	5	**12**	**2**	**114.3**	**13.03867**
	5	12	2	142.88	17.94933
	5	12	2	171.45	28.87133
	5	12	2	200.03	43.434
Experiment #17	5	9	1	28.58	2.54
	5	**9**	**1**	**57.15**	**9.144**
	5	9	1	85.73	16.84867
	5	9	1	114.3	22.26733
	5	**9**	**1**	**142.88**	**35.56**
	5	9	1	171.45	48.42933
	5	**9**	**1**	**200.03**	**50.71533**
Experiment #18	5	9	2	28.58	0.508
	5	**9**	**2**	**57.15**	**4.487333**
	5	9	2	85.73	6.180667
	5	**9**	**2**	**114.3**	**8.636**
	5	9	2	142.88	17.61067
	5	9	2	171.45	22.94467
	5	**9**	**2**	**200.03**	**37.76133**

Experiment #19	**5**	**6**	**1**	**28.58**	**2.709333**
	5	6	1	57.15	11.00667
	5	6	1	85.73	15.748
	5	**6**	**1**	**114.3**	**22.94467**
	5	6	1	142.88	33.44333
	5	6	1	171.45	38.862
	5	6	1	200.03	48.93733
Experiment #20	5	6	2	28.58	0.592667
	5	6	2	85.73	4.148667
	5	6	2	57.15	4.487333
	5	6	2	114.3	7.366
	5	6	2	142.88	16.51
	5	6	2	200.03	20.066
Experiment #21	1	6	1	28.58	18.20333
	1	**6**	**1**	**57.15**	**47.92133**

APPENDIX G

Infiltration Edge Dataset of the Laboratory Model

Infiltration edge Progression	Slope	Gap siza	Material	Infiltration Edge	Rainfall
Experiment #1	**1**	**6**	**1**	**28.58**	**0**
	1	6	1	57.15	1.439333
	1	6	1	85.73	8.89
	1	**6**	**1**	**114.3**	**16.17133**
	1	6	1	142.88	16.84867
	1	6	1	171.45	19.304
Experiment #2	1	6	1	28.58	0.169333
	1	**6**	**1**	**57.15**	**1.185333**
	1	6	1	85.73	8.382
	1	6	1	114.3	14.56267
	1	6	1	142.88	24.55333
	1	6	1	171.45	32.08867
Experiment #3	1	6	1	28.58	0.254

	1	6	1	57.15	4.148667
	1	6	1	85.73	11.00667
	1	6	1	114.3	16.002
	1	6	1	142.88	21.336
	1	6	1	171.45	39.79333
Experiment #4	1	6	2	28.58	0.084667
	1	**6**	**2**	**57.15**	**0.423333**
	1	6	2	85.73	0.762
	1	6	2	114.3	5.757333
	1	6	2	142.88	7.704667
	1	6	2	171.45	20.574
	1	6	2	200.03	21.75933
Experiment #5	1	9	1	28.58	0
	1	**9**	**1**	**57.15**	**3.048**
	1	9	1	85.73	8.212667
	1	9	1	114.3	13.12333
	1	9	1	142.88	18.88067
	1	9	1	171.45	26.75467

	1	9	1	200.03	36.576
Experiment #6	1	9	2	28.58	0.084667
	1	9	2	57.15	0.169333
	1	9	2	85.73	3.471333
	1	**9**	**2**	**114.3**	**8.466667**
	1	9	2	142.88	10.16
	1	9	2	171.45	11.00667
	1	9	2	200.03	37.76133
Experiment #7	1	12	1	28.58	0
	1	**12**	**1**	**57.15**	**7.112**
	1	12	1	85.73	22.098
	1	**12**	**1**	**114.3**	**33.86667**
Experiment #8	1	12	2	28.58	0.254
	1	12	2	57.15	5.08
	1	**12**	**2**	**85.73**	**11.176**
	1	12	2	114.3	13.97
	1	12	2	142.88	46.99
Experiment #9	3	12	2	28.58	0.084667

	3	**12**	**2**	**57.15**	**0.762**
	3	12	2	85.73	4.064
	3	12	2	114.3	8.382
	3	**12**	**2**	**142.88**	**14.224**
	3	12	2	171.45	23.70667
	3	12	2	200.03	27.85533
Experiment #10	3	12	1	28.58	0
	3	12	1	57.15	3.217333
	3	**12**	**1**	**85.73**	**13.88533**
	3	12	1	114.3	21.67467
	3	**12**	**1**	**142.88**	**38.354**
Experiment #11	3	9	1	28.58	0.423333
	3	**9**	**1**	**57.15**	**3.471333**
	3	9	1	85.73	11.09133
	3	**9**	**1**	**114.3**	**20.23533**
	3	**9**	**1**	**142.88**	**29.972**
	3	9	1	171.45	41.06333
Experiment #12	**3**	**9**	**2**	**28.58**	**0.254**

	3	9	2	57.15	0.338667
	3	9	2	85.73	1.016
	3	**9**	**2**	**114.3**	**5.926667**
	3	9	2	142.88	7.535333
	3	9	2	171.45	10.49867
	3	9	2	200.03	14.56267
Experiment #13	3	6	1	28.58	0.169333
	3	6	1	57.15	0.254
	3	**6**	**1**	**85.73**	**6.011333**
	3	6	1	114.3	13.462
	3	6	1	142.88	18.88067
	3	**6**	**1**	**171.45**	**34.96733**
	3	**6**	**1**	**200.03**	**48.34467**
Experiment #14	**3**	**6**	**2**	**28.58**	**0.338667**
	3	6	2	57.15	0.423333
	3	6	2	85.73	0.846667
	3	6	2	114.3	1.354667
	3	6	2	142.88	5.926667

	3	**6**	**2**	**171.45**	**8.551333**
	3	6	2	200.03	11.00667
Experiment #15	**5**	**12**	**1**	**28.58**	**0.169333**
	5	**12**	**1**	**57.15**	**2.794**
	5	12	1	85.73	13.29267
	5	12	1	114.3	26.162
	5	12	1	142.88	42.672
Experiment #16	5	12	2	28.58	0
	5	12	2	57.15	0.423333
	5	12	2	85.73	3.471333
	5	12	2	114.3	5.926667
	5	12	2	142.88	10.414
	5	**12**	**2**	**171.45**	**16.002**
	5	12	2	200.03	20.15067
Experiment #17	5	9	1	28.58	0
	5	9	1	57.15	1.354667
	5	**9**	**1**	**85.73**	**7.196667**
	5	9	1	114.3	10.668

	5	9	1	142.88	24.46867
	5	9	1	171.45	36.23733
	5	9	1	200.03	45.55067
Experiment #18	5	9	2	28.58	0
	5	**9**	**2**	**57.15**	**0.084667**
	5	9	2	85.73	0.592667
	5	9	2	114.3	1.354667
	5	**9**	**2**	**142.88**	**8.212667**
	5	9	2	171.45	9.652
	5	9	2	200.03	14.81667
Experiment #19	**5**	**6**	**1**	**28.58**	**0.084667**
	5	6	1	57.15	0.677333
	5	6	1	85.73	3.386667
	5	**6**	**1**	**114.3**	**11.43**
	5	6	1	142.88	18.37267
	5	6	1	171.45	29.972
	5	6	1	200.03	39.96267
Experiment #20	5	6	2	28.58	0.169333

	5	6	2	57.15	0.254
	5	6	2	85.73	0.338667
	5	6	2	114.3	1.016
	5	6	2	142.88	5.757333
	5	6	2	171.45	6.096
	5	**6**	**2**	**200.03**	**8.89**
Experiment #21	**1**	**6**	**1**	**28.58**	**0.084667**
	1	6	1	57.15	3.386667

APPENDIX H

Peak VWC Prediction Results in PICP 19G

TDR01

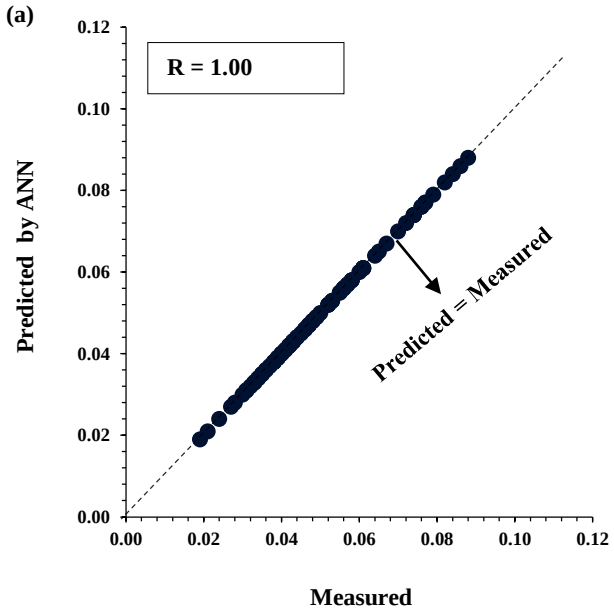

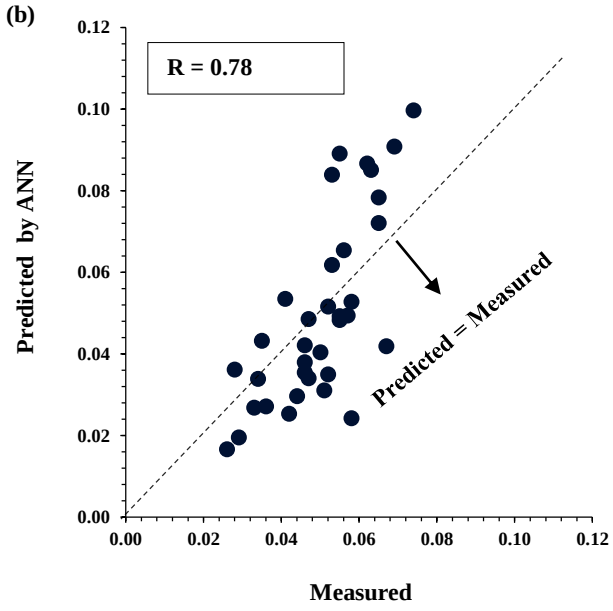

Correlation of Coefficient (Training Data)	1.00
Correlation of Coefficient (Testing Data)	0.78
Number of Neurons in the Hidden Layer	13

Input Parameters	Relative Importance (%)
Cleaning Method	10.68
Duration (Min.)	11.08
Rainfall Depth (cm.)	8.11
Peak 5 min (mm/hr)	10.78
Peak 15 min (mm/hr)	9.02
Peak Duration (Min)	11.27
Cumulative Rainfall Depth before the event from the installation (cm)	10.34
Cumulative Rainfall Depth before the event from the last maintenance (cm)	8.58
ADP (Min)	8.48
Previous Rainfall Depth (cm)	11.66

TDR03

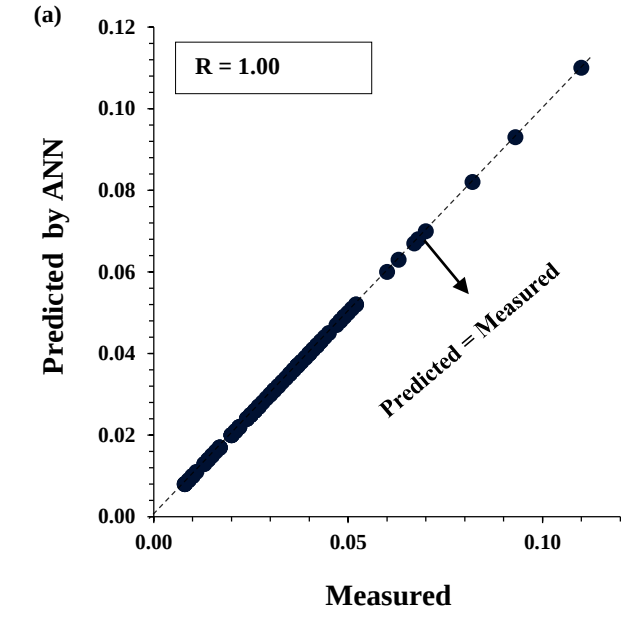
(a)
R = 1.00
Predicted by ANN
Measured
Predicted = Measured
0.00
0.02
0.04
0.06
0.08
0.10
0.12
0.00
0.05
0.10

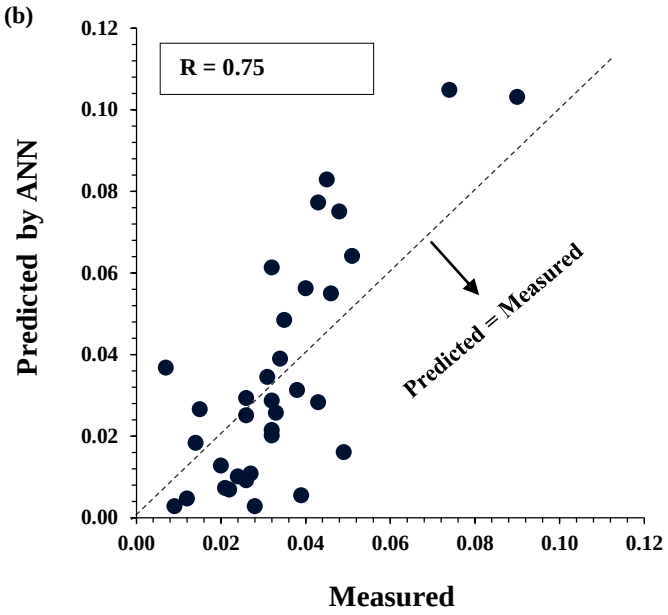
(b)
R = 0.75
Predicted by ANN
Measured
Predicted = Measured
0.00
0.02
0.04
0.06
0.08
0.10
0.12

Correlation of Coefficient (Training Data)	1.00
Correlation of Coefficient (Testing Data)	0.75
Number of Neurons in the Hidden Layer	12

Input Parameters	Relative Importance (%)
Cleaning Method	9.74
Duration (Min.)	10.06
Rainfall Depth (cm.)	10.14
Peak 5 min (mm/hr)	8.64
Peak 15 min (mm/hr)	8.33
Peak Duration (Min)	10.30
Cumulative Rainfall Depth before the event from the installation (cm)	12.37
Cumulative Rainfall Depth before the event from the last maintenance (cm)	10.30
ADP (Min)	10.06
Previous Rainfall Depth (cm)	10.05

TDR05

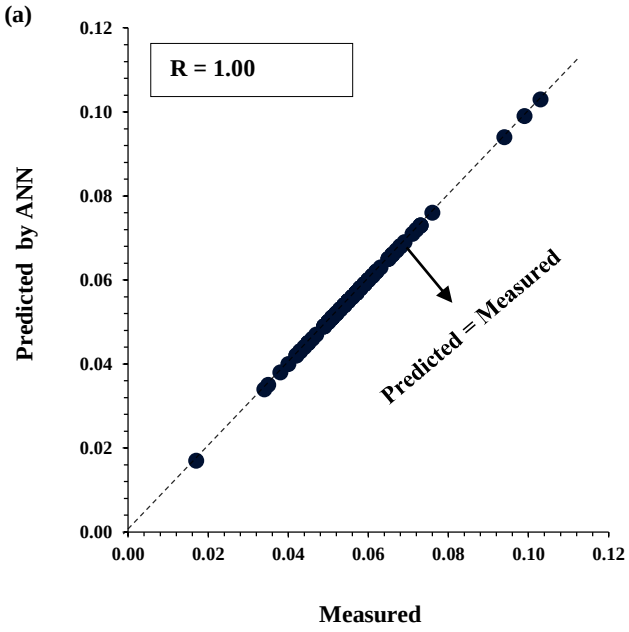
(a)
R = 1.00
Predicted = Measured
Predicted by ANN
Measured
0.00
0.02
0.04
0.06
0.08
0.10
0.12

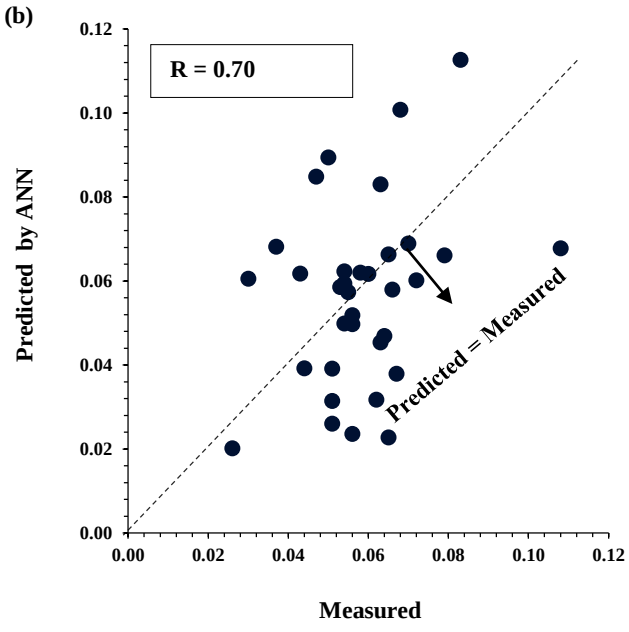
(b)
R = 0.70
Predicted = Measured
Predicted by ANN
Measured
0.00
0.02
0.04
0.06
0.08
0.10
0.12

Correlation of Coefficient (Training Data)	1.00
Correlation of Coefficient (Testing Data)	0.70
Number of Neurons in the Hidden Layer	10

Input Parameters	Relative Importance (%)
Cleaning Method	8.40
Duration (Min.)	10.31
Rainfall Depth (cm.)	7.88
Peak 5 min (mm/hr)	11.88
Peak 15 min (mm/hr)	11.17
Peak Duration (Min)	6.67
Cumulative Rainfall Depth before the event from the installation (cm)	11.28
Cumulative Rainfall Depth before the event from the last maintenance (cm)	9.60
ADP (Min)	11.38
Previous Rainfall Depth (cm)	11.44

TDR07

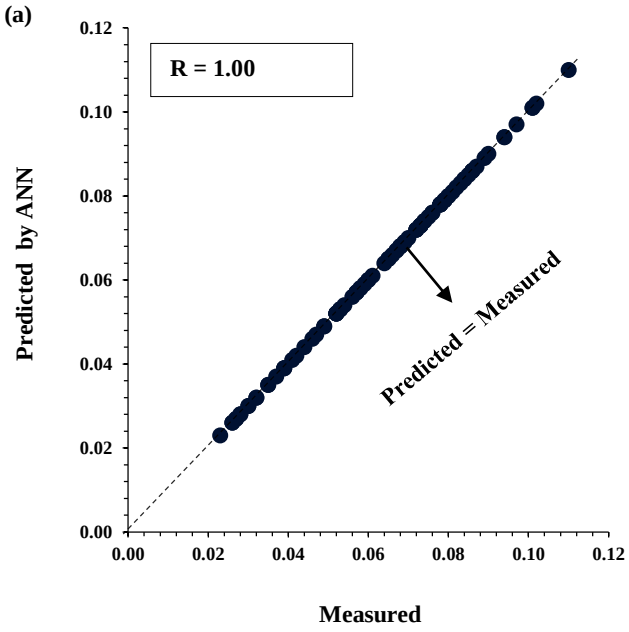
(a)
R = 1.00
Predicted = Measured
Predicted by ANN
Measured
0.00
0.02
0.04
0.06
0.08
0.10
0.12

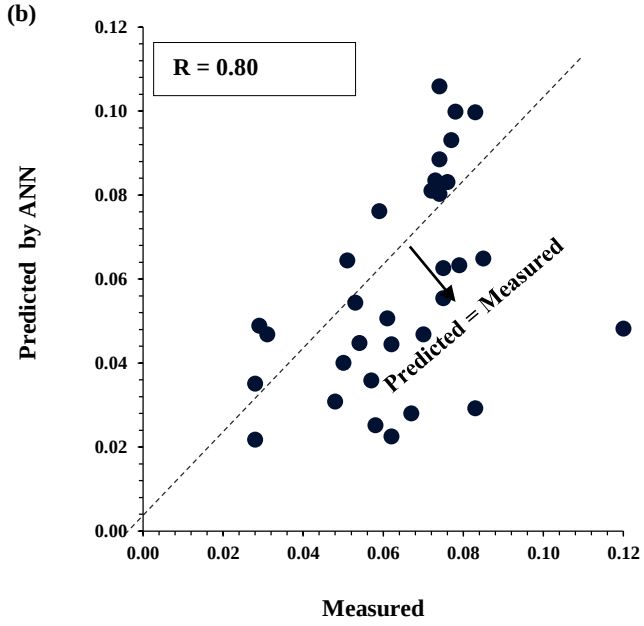
(b)
R = 0.80
Predicted = Measured
Predicted by ANN
Measured
0.00
0.02
0.04
0.06
0.08
0.10
0.12

Correlation of Coefficient (Training Data)	1.00
Correlation of Coefficient (Testing Data)	0.80
Number of Neurons in the Hidden Layer	11

Input Parameters	Relative Importance (%)
Cleaning Method	10.65
Duration (Min.)	9.77
Rainfall Depth (cm.)	12.86
Peak 5 min (mm/hr)	13.55
Peak 15 min (mm/hr)	8.61
Peak Duration (Min)	7.04
Cumulative Rainfall Depth before the event from the installation (cm)	10.31
Cumulative Rainfall Depth before the event from the last maintenance (cm)	9.62
ADP (Min)	9.95
Previous Rainfall Depth (cm)	7.65

TDR09

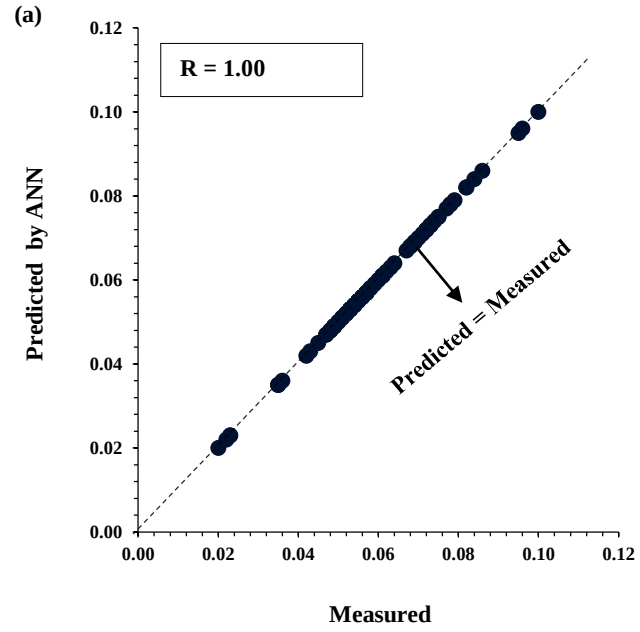
(a)
R = 1.00
Predicted = Measured
Predicted by ANN
Measured
0.00
0.02
0.04
0.06
0.08
0.10
0.12

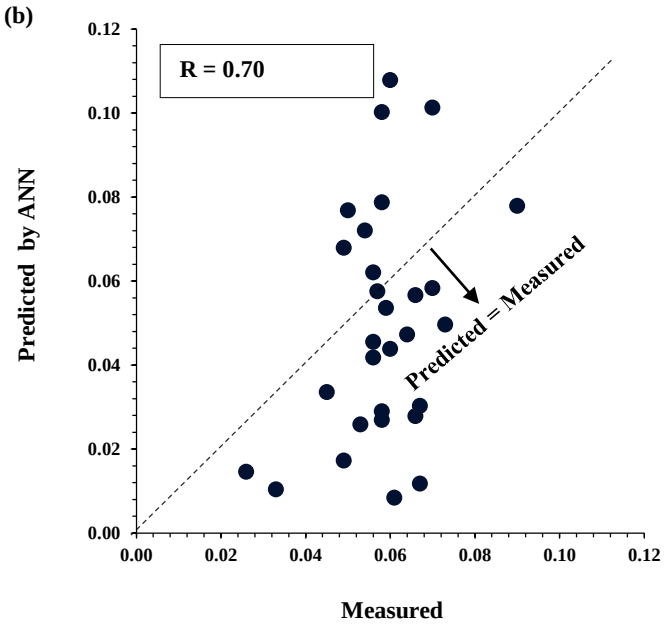
(b)
R = 0.70
Predicted = Measured
Predicted by ANN
Measured
0.00
0.02
0.04
0.06
0.08
0.10
0.12

Correlation of Coefficient (Training Data)	1.00
Correlation of Coefficient (Testing Data)	0.70
Number of Neurons in the Hidden Layer	17

Input Parameters	Relative Importance (%)
Cleaning Method	9.41
Duration (Min.)	9.58
Rainfall Depth (cm.)	7.79
Peak 5 min (mm/hr)	11.10
Peak 15 min (mm/hr)	10.72
Peak Duration (Min)	10.58
Cumulative Rainfall Depth before the event from the installation (cm)	11.82
Cumulative Rainfall Depth before the event from the last maintenance (cm)	10.69
ADP (Min)	6.13
Previous Rainfall Depth (cm)	12.19

TDR 11

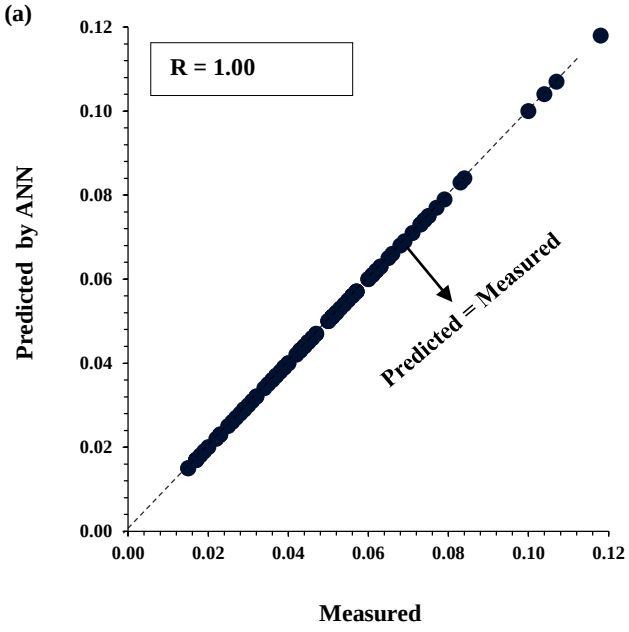
(a)
R = 1.00
Predicted = Measured
Predicted by ANN
Measured
0.00
0.02
0.04
0.06
0.08
0.10
0.12

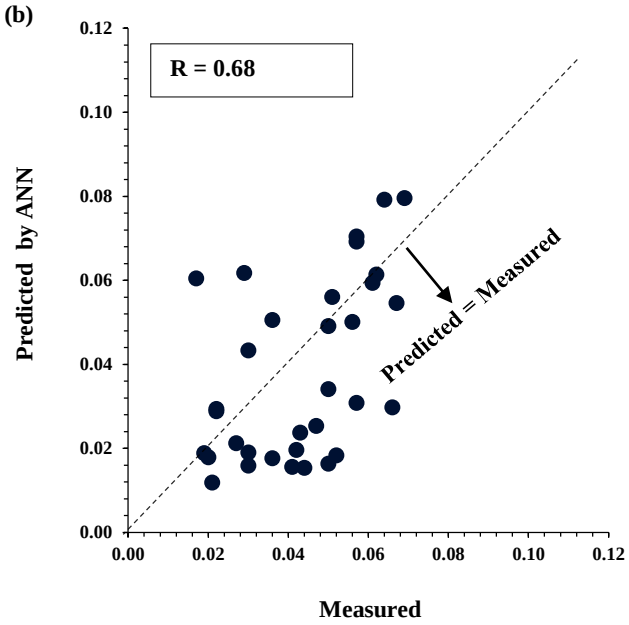

Correlation of Coefficient (Training Data)	1.00
Correlation of Coefficient (Testing Data)	0.68
Number of Neurons in the Hidden Layer	15

Input Parameters	Relative Importance (%)
Cleaning Method	6.72
Duration (Min.)	8.99
Rainfall Depth (cm.)	11.72
Peak 5 min (mm/hr)	12.87
Peak 15 min (mm/hr)	9.87
Peak Duration (Min)	11.15
Cumulative Rainfall Depth before the event from the installation (cm)	9.87
Cumulative Rainfall Depth before the event from the last maintenance (cm)	9.75
ADP (Min)	9.55
Previous Rainfall Depth (cm)	9.50

TDR12

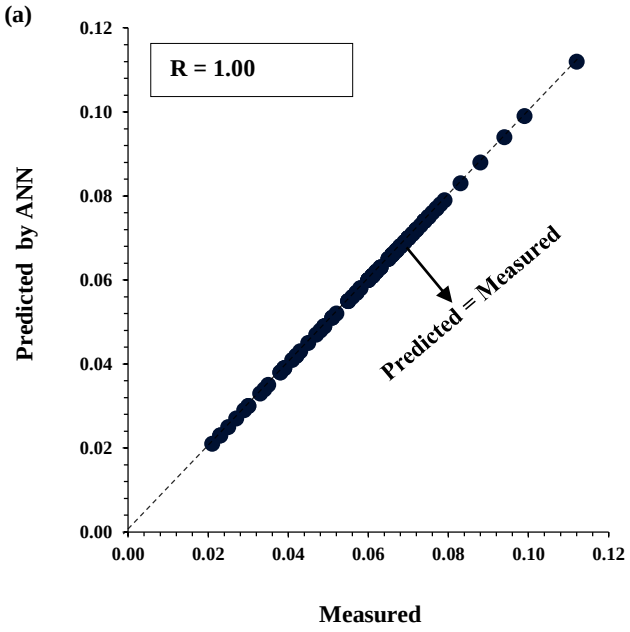
(a)
R = 1.00
Predicted = Measured
Predicted by ANN
Measured
0.00
0.02
0.04
0.06
0.08
0.10
0.12

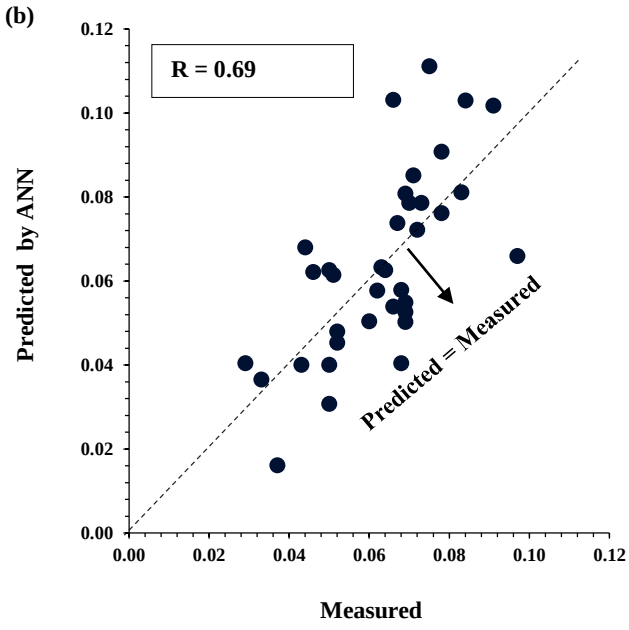
(b)
R = 0.69
Predicted = Measured
Predicted by ANN
Measured
0.00
0.02
0.04
0.06
0.08
0.10
0.12

Correlation of Coefficient (Training Data)	1.00
Correlation of Coefficient (Testing Data)	0.69
Number of Neurons in the Hidden Layer	14

Input Parameters	Relative Importance (%)
Cleaning Method	11.84
Duration (Min.)	10.55
Rainfall Depth (cm.)	8.71
Peak 5 min (mm/hr)	9.65
Peak 15 min (mm/hr)	11.02
Peak Duration (Min)	11.70
Cumulative Rainfall Depth before the event from the installation (cm)	11.47
Cumulative Rainfall Depth before the event from the last maintenance (cm)	8.59
ADP (Min)	7.05
Previous Rainfall Depth (cm)	9.40

TDR13

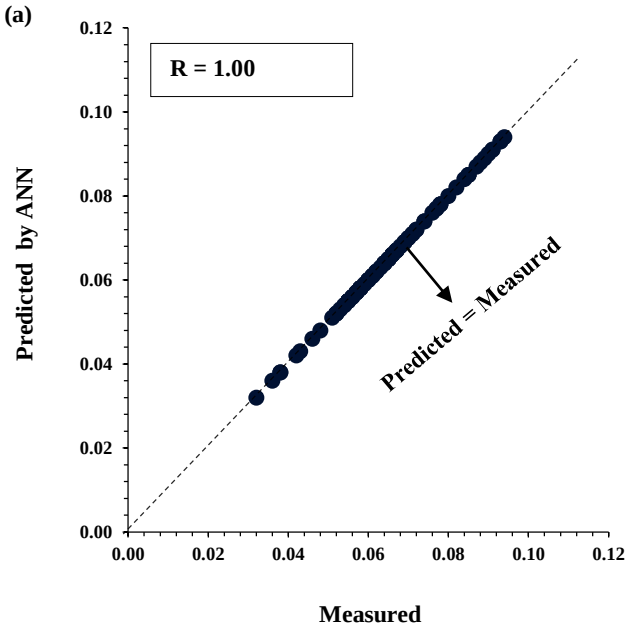
(a)
R = 1.00
Predicted = Measured
Predicted by ANN
Measured
0.00
0.02
0.04
0.06
0.08
0.10
0.12

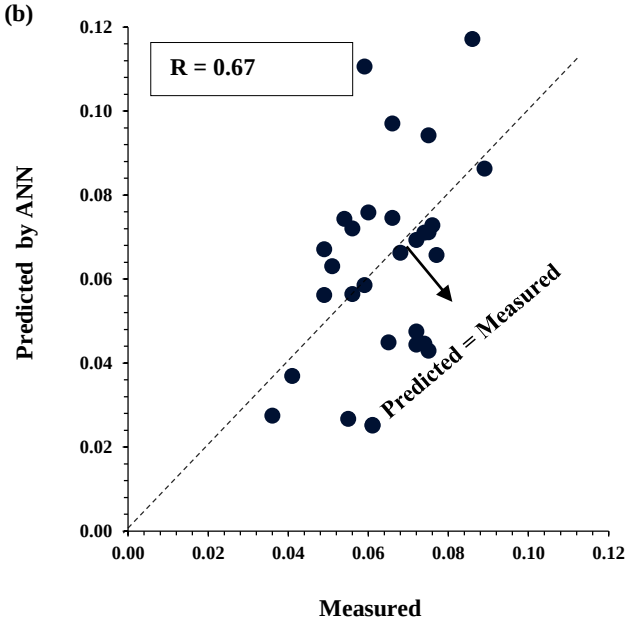
(b)
R = 0.67
Predicted = Measured
Predicted by ANN
Measured
0.00
0.02
0.04
0.06
0.08
0.10
0.12

Correlation of Coefficient (Training Data)	1.00
Correlation of Coefficient (Testing Data)	0.67
Number of Neurons in the Hidden Layer	16

Input Parameters	Relative Importance (%)
Cleaning Method	11.30
Duration (Min.)	7.60
Rainfall Depth (cm.)	10.88
Peak 5 min (mm/hr)	9.68
Peak 15 min (mm/hr)	11.53
Peak Duration (Min)	10.37
Cumulative Rainfall Depth before the event from the installation (cm)	10.65
Cumulative Rainfall Depth before the event from the last maintenance (cm)	9.52
ADP (Min)	9.81
Previous Rainfall Depth (cm)	8.66

TDR15

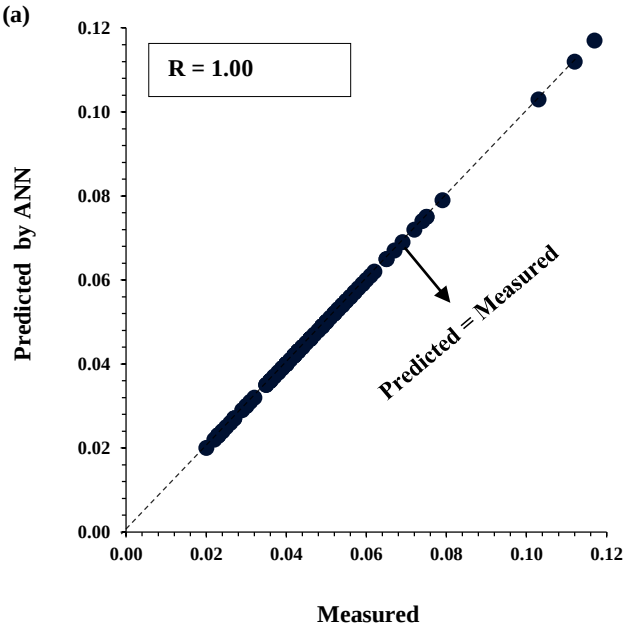
(a)
R = 1.00
Predicted = Measured
Predicted by ANN
Measured
0.00
0.02
0.04
0.06
0.08
0.10
0.12

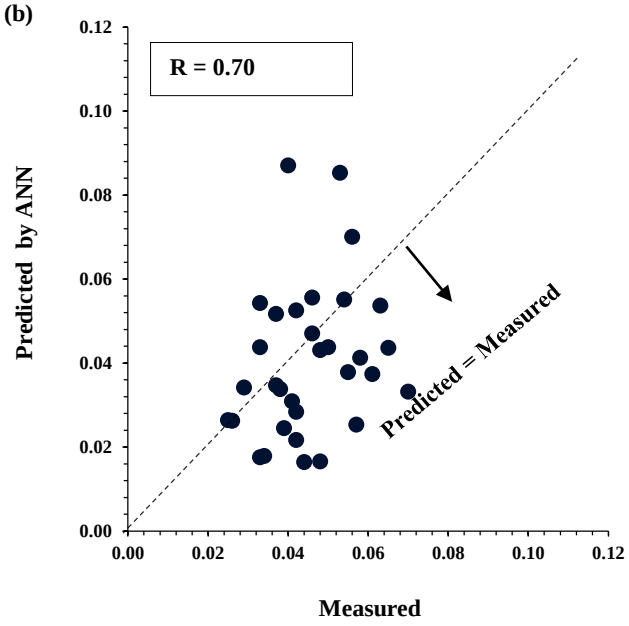
(b)
R = 0.70
Predicted = Measured
Predicted by ANN
Measured
0.00
0.02
0.04
0.06
0.08
0.10
0.12

Correlation of Coefficient (Training Data)	1.00
Correlation of Coefficient (Testing Data)	0.70
Number of Neurons in the Hidden Layer	16

Input Parameters	Relative Importance (%)
Cleaning Method	10.61
Duration (Min.)	11.42
Rainfall Depth (cm.)	11.03
Peak 5 min (mm/hr)	7.65
Peak 15 min (mm/hr)	10.79
Peak Duration (Min)	10.77
Cumulative Rainfall Depth before the event from the installation (cm)	8.56
Cumulative Rainfall Depth before the event from the last maintenance (cm)	6.66
ADP (Min)	11.29
Previous Rainfall Depth (cm)	11.21

TDR16

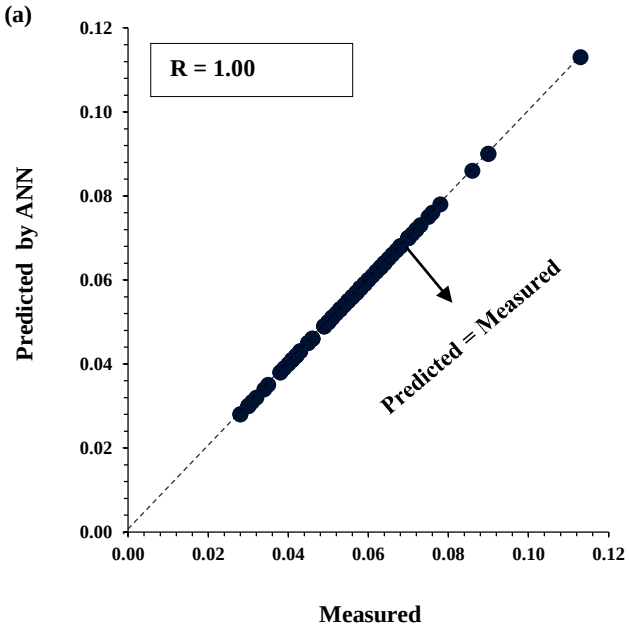
(a)
R = 1.00
Predicted = Measured
Predicted by ANN
Measured
0.00
0.02
0.04
0.06
0.08
0.10
0.12

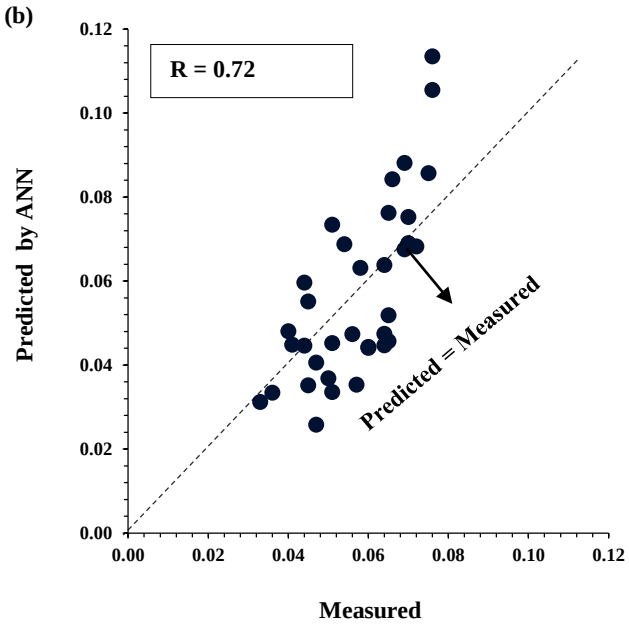
(b)
R = 0.72
Predicted = Measured
Predicted by ANN
Measured
0.00
0.02
0.04
0.06
0.08
0.10
0.12

Correlation of Coefficient (Training Data)	1.00
Correlation of Coefficient (Testing Data)	0.72
Number of Neurons in the Hidden Layer	15

Input Parameters	Relative Importance (%)
Cleaning Method	12.09
Duration (Min.)	12.23
Rainfall Depth (cm.)	8.12
Peak 5 min (mm/hr)	9.87
Peak 15 min (mm/hr)	8.57
Peak Duration (Min)	9.05
Cumulative Rainfall Depth before the event from the installation (cm)	9.74
Cumulative Rainfall Depth before the event from the last maintenance (cm)	11.74
ADP (Min)	8.74
Previous Rainfall Depth (cm)	9.84

TDR25

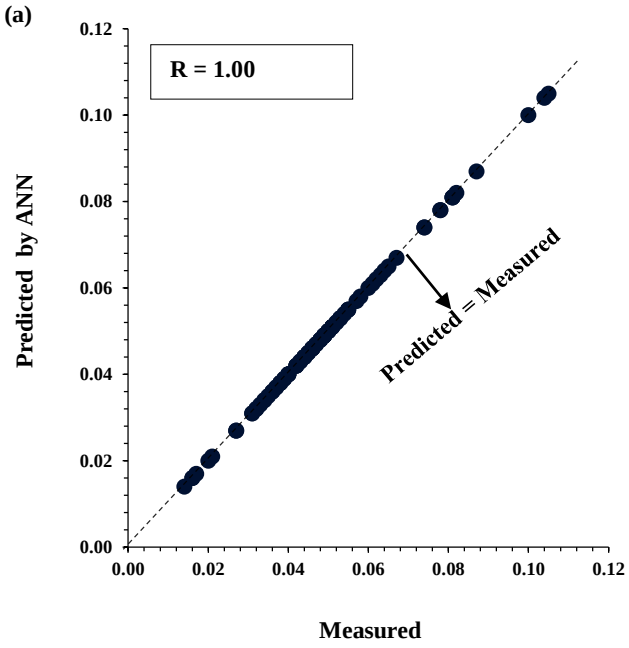
(a)
R = 1.00
Predicted = Measured
Predicted by ANN
Measured
0.00
0.02
0.04
0.06
0.08
0.10
0.12

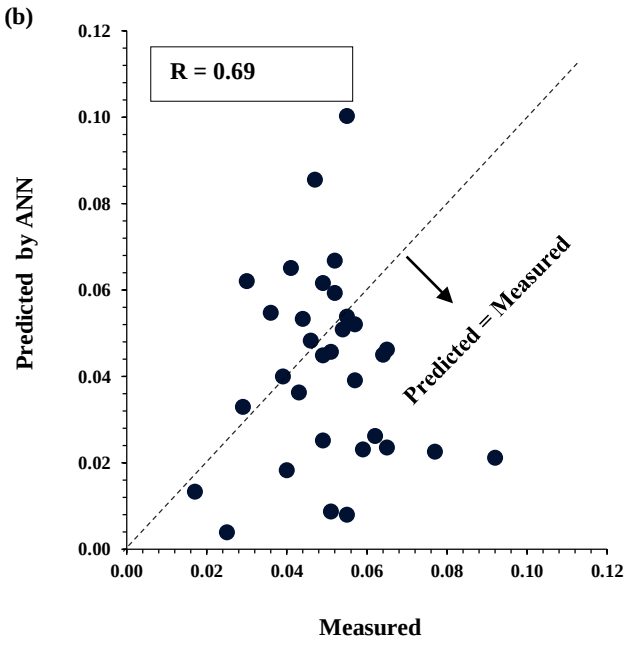
(b)
R = 0.69
Predicted = Measured
Predicted by ANN
Measured
0.00
0.02
0.04
0.06
0.08
0.10
0.12

Correlation of Coefficient (Training Data)	1.00
Correlation of Coefficient (Testing Data)	0.69
Number of Neurons in the Hidden Layer	14

Input Parameters	Relative Importance (%)
Cleaning Method	13.04
Duration (Min.)	7.39
Rainfall Depth (cm.)	10.98
Peak 5 min (mm/hr)	12.08
Peak 15 min (mm/hr)	10.47
Peak Duration (Min)	9.33
Cumulative Rainfall Depth before the event from the installation (cm)	9.35
Cumulative Rainfall Depth before the event from the last maintenance (cm)	9.25
ADP (Min)	8.40
Previous Rainfall Depth (cm)	9.69

TDR27

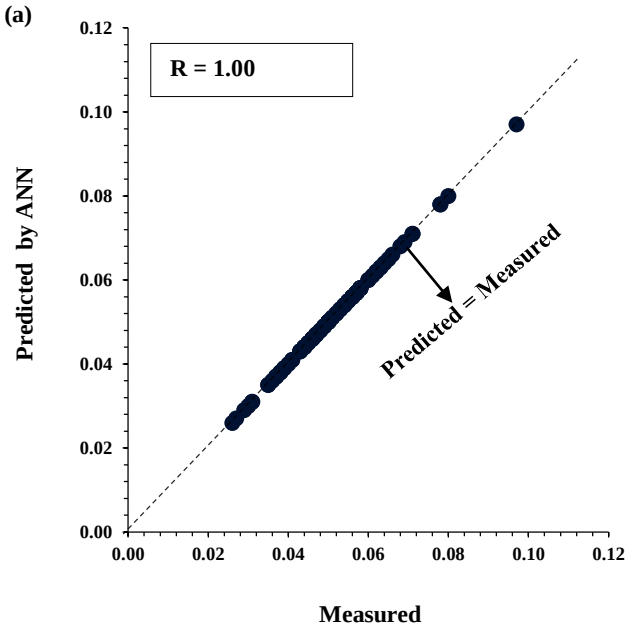
(a)
R = 1.00
Predicted = Measured
Predicted by ANN
Measured
0.00
0.02
0.04
0.06
0.08
0.10
0.12

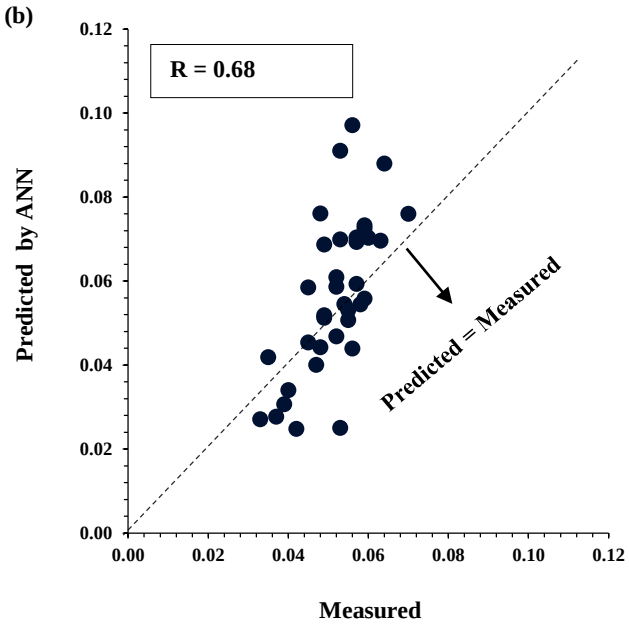
(b)
R = 0.68
Predicted = Measured
Predicted by ANN
Measured
0.00
0.02
0.04
0.06
0.08
0.10
0.12

Correlation of Coefficient (Training Data)	1.00
Correlation of Coefficient (Testing Data)	0.68
Number of Neurons in the Hidden Layer	11

Input Parameters	Relative Importance (%)
Cleaning Method	10.07
Duration (Min.)	9.16
Rainfall Depth (cm.)	8.89
Peak 5 min (mm/hr)	7.86
Peak 15 min (mm/hr)	12.57
Peak Duration (Min)	11.70
Cumulative Rainfall Depth before the event from the installation (cm)	12.13
Cumulative Rainfall Depth before the event from the last maintenance (cm)	9.52
ADP (Min)	8.11
Previous Rainfall Depth (cm)	9.98

APPENDIX I

Histograms of the Input Variables in the Captured Runoff Model of PICP

19G

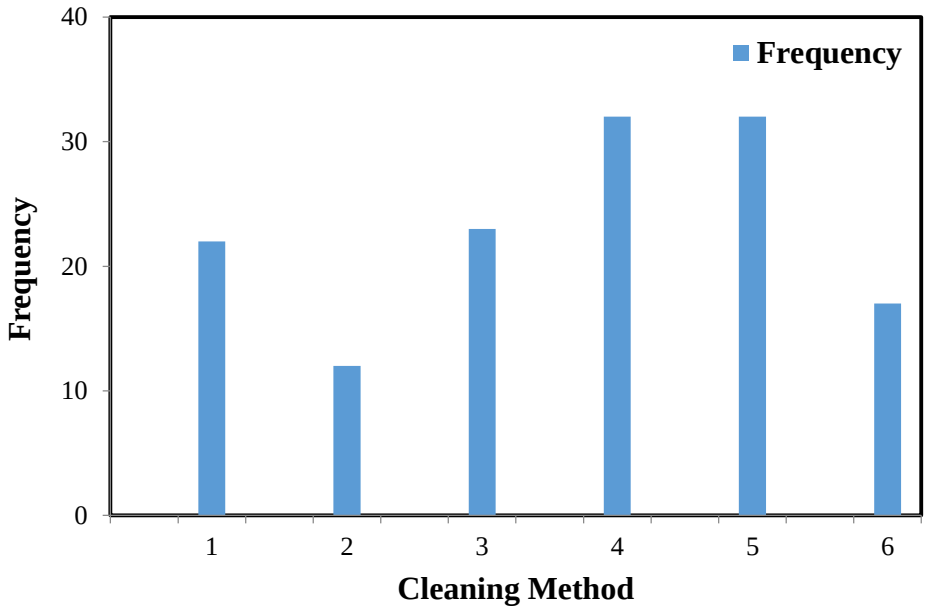

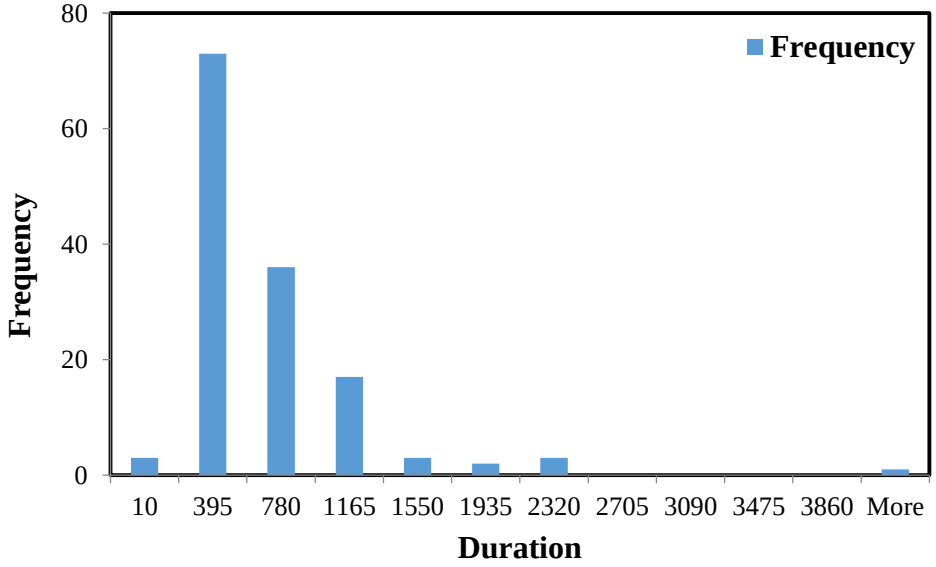

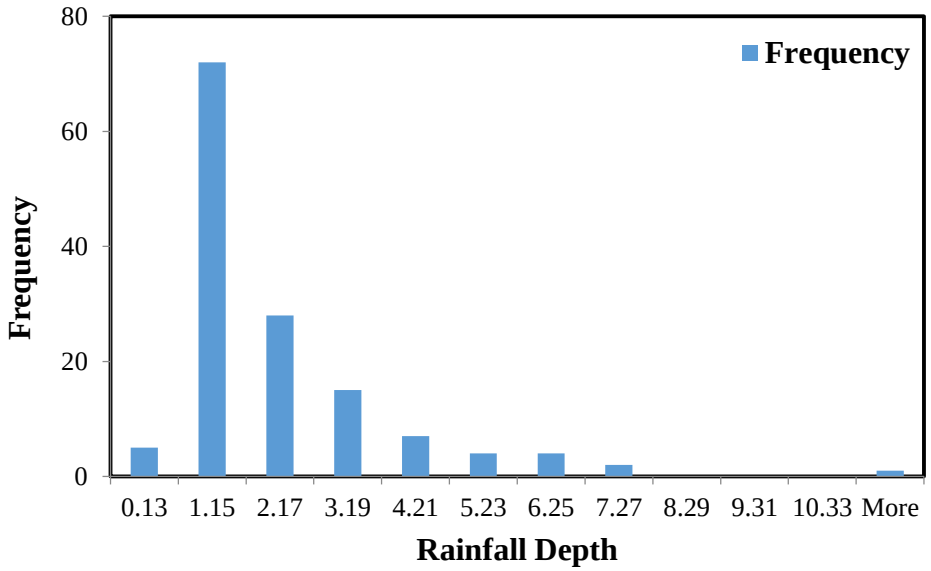
80
60
40
20
0
Frequency
Frequency
0.13
1.15
2.17
3.19
4.21
5.23
6.25
7.27
8.29
9.31
10.33
More
Rainfall Depth

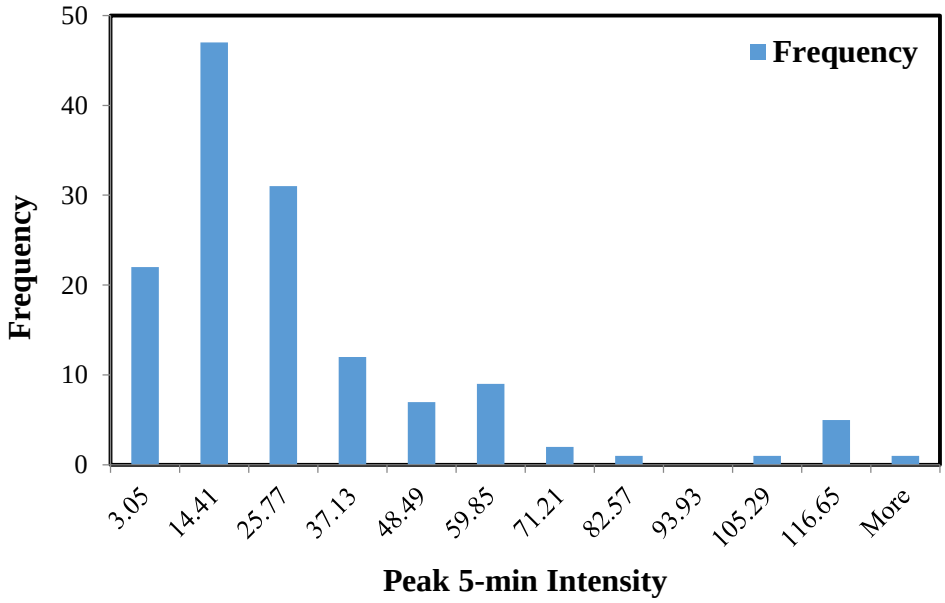
50
40
30
20
10
0
Frequency
Frequency
3.05
14.41
25.77
37.13
48.49
59.85
71.21
82.57
93.93
105.29
116.65
More
Peak 5-min Intensity

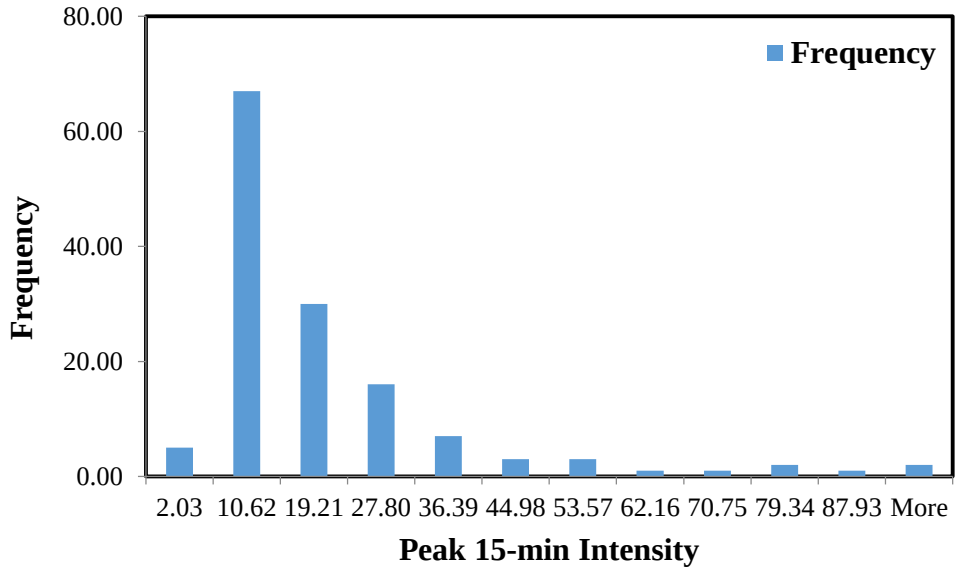
80.00
60.00
40.00
20.00
0.00
Frequency
Frequency
2.03
10.62
19.21
27.80
36.39
44.98
53.57
62.16
70.75
79.34
87.93
More
Peak 15-min Intensity

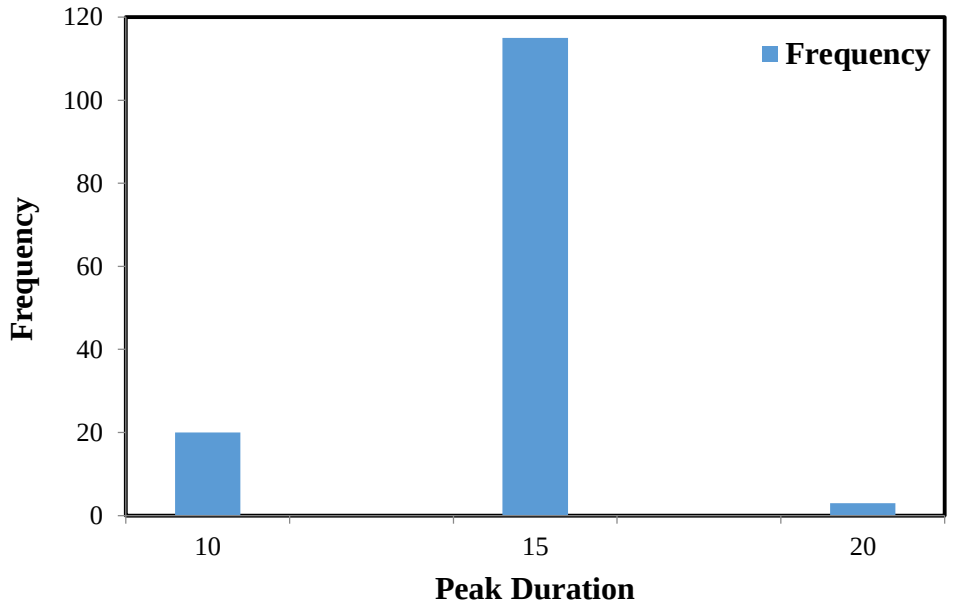
120
100
80
60
40
20
0
Frequency
Frequency
10
15
20
Peak Duration

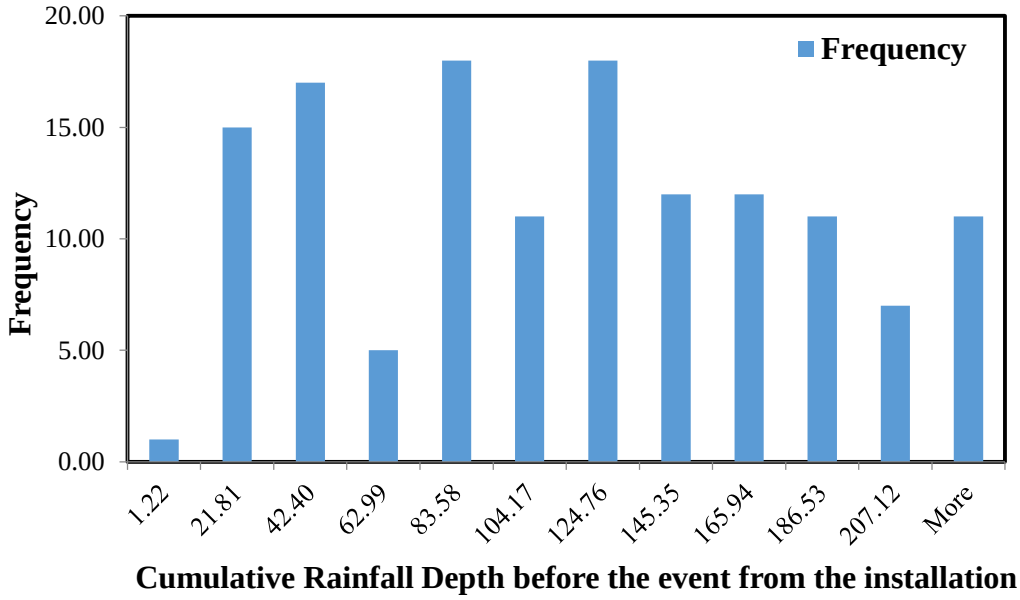
20.00
15.00
10.00
5.00
0.00
Frequency
Frequency
1.22
21.81
42.40
62.99
83.58
104.17
124.76
145.35
165.94
186.53
207.12
More
Cumulative Rainfall Depth before the event from the installation

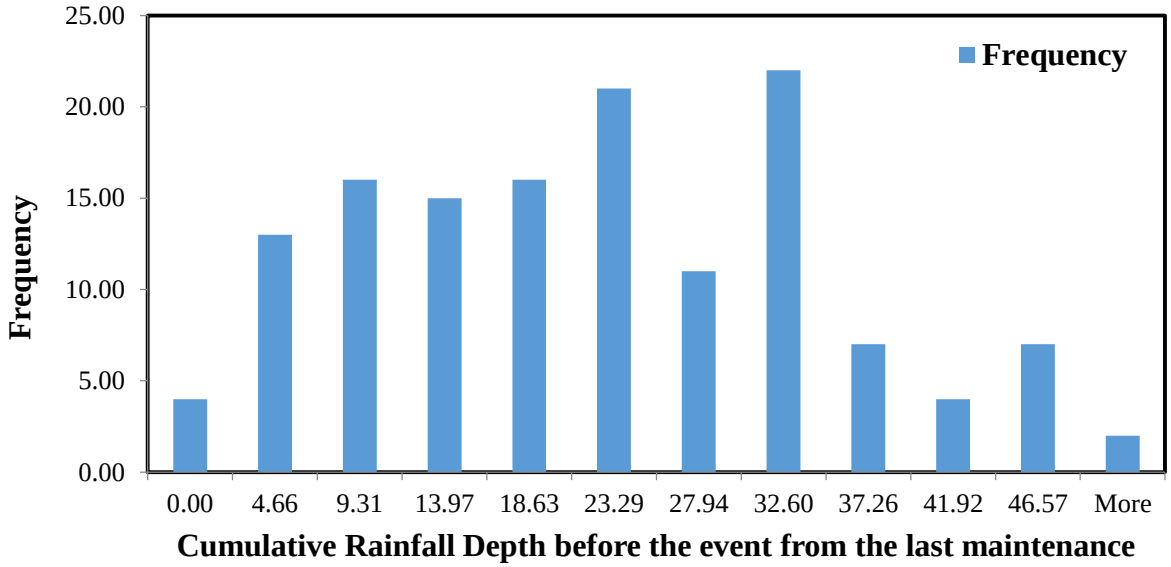
25.00
20.00
15.00
10.00
5.00
0.00
Frequency
Frequency
0.00
4.66
9.31
13.97
18.63
23.29
27.94
32.60
37.26
41.92
46.57
More
Cumulative Rainfall Depth before the event from the last maintenance

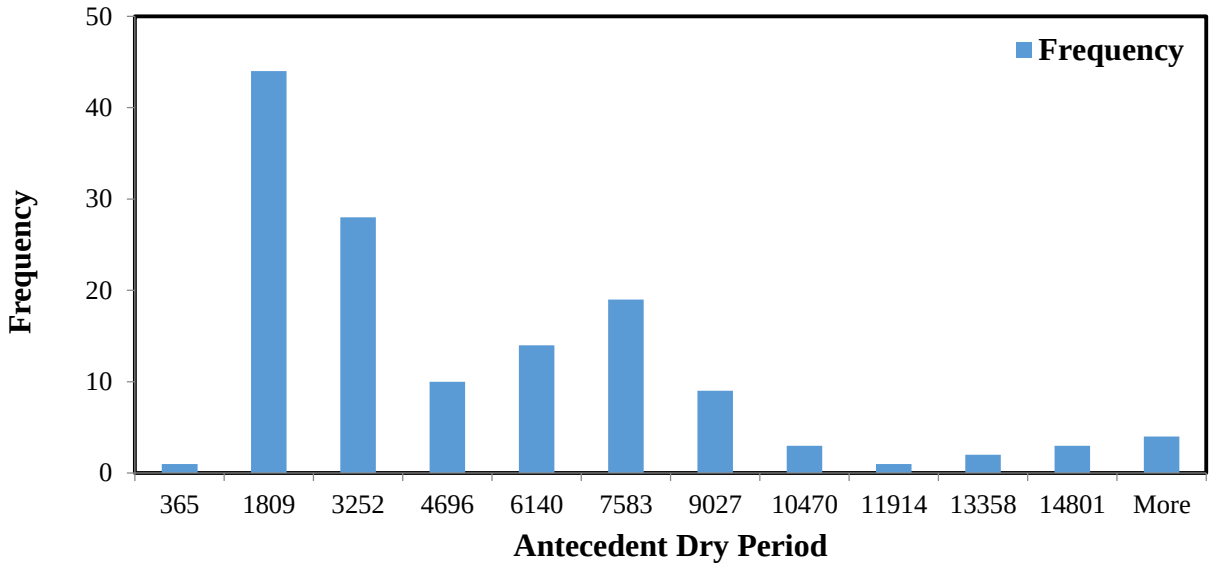
Frequency
50
40
30
20
10
0
Frequency
365
1809
3252
4696
6140
7583
9027
10470
11914
13358
14801
More
Antecedent Dry Period

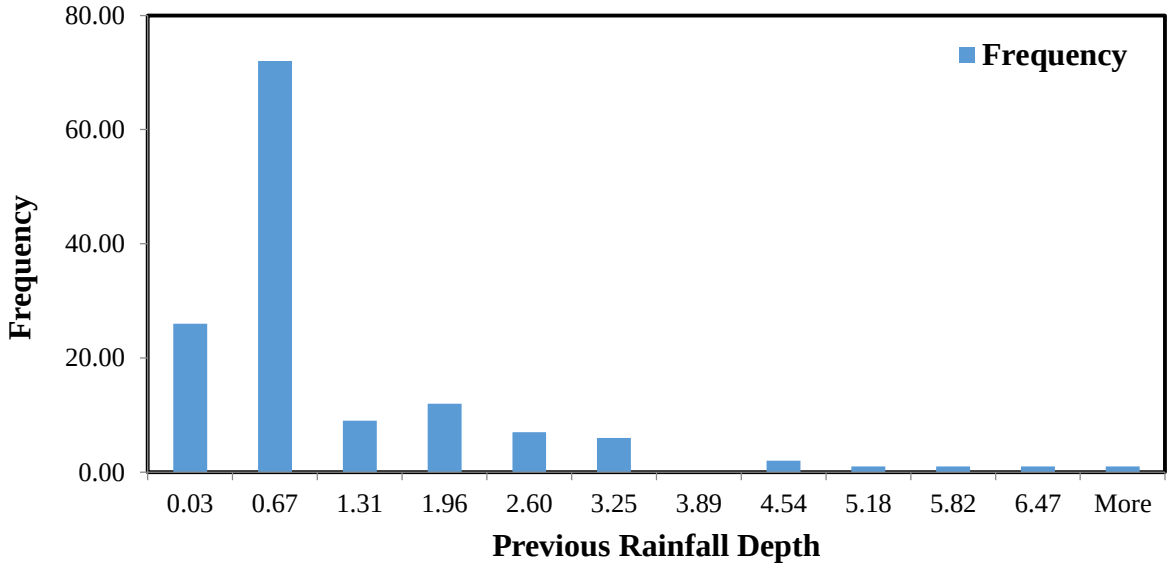
Frequency
80.00
60.00
40.00
20.00
0.00
Frequency
0.03
0.67
1.31
1.96
2.60
3.25
3.89
4.54
5.18
5.82
6.47
More
Previous Rainfall Depth

APPENDIX J

Histograms of the Input Variables in the Captured Runoff Model of PICP

19H

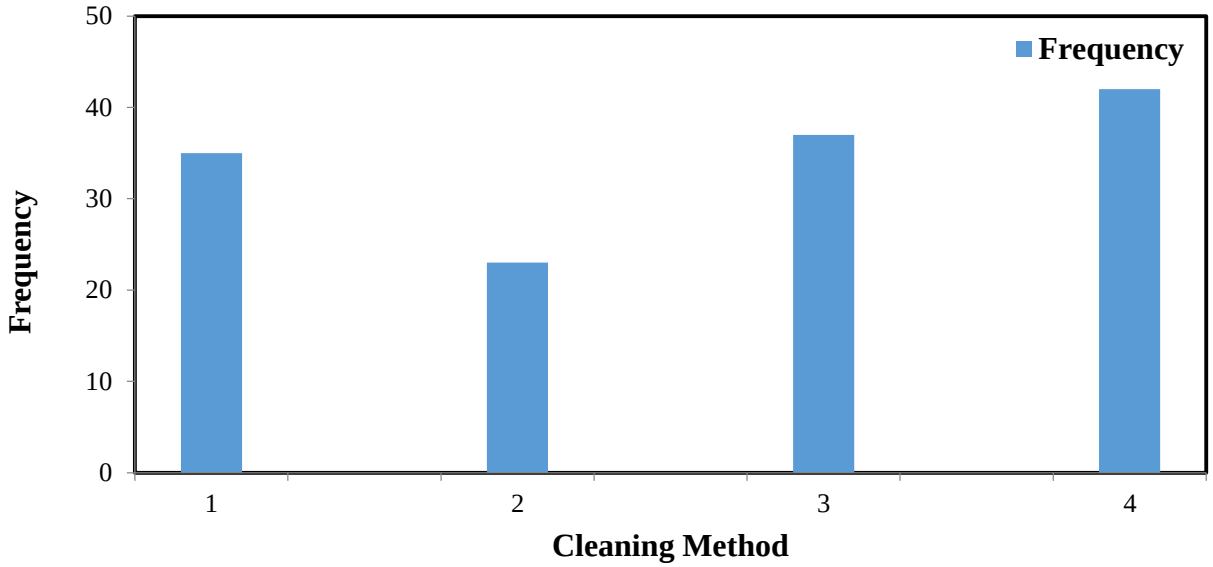

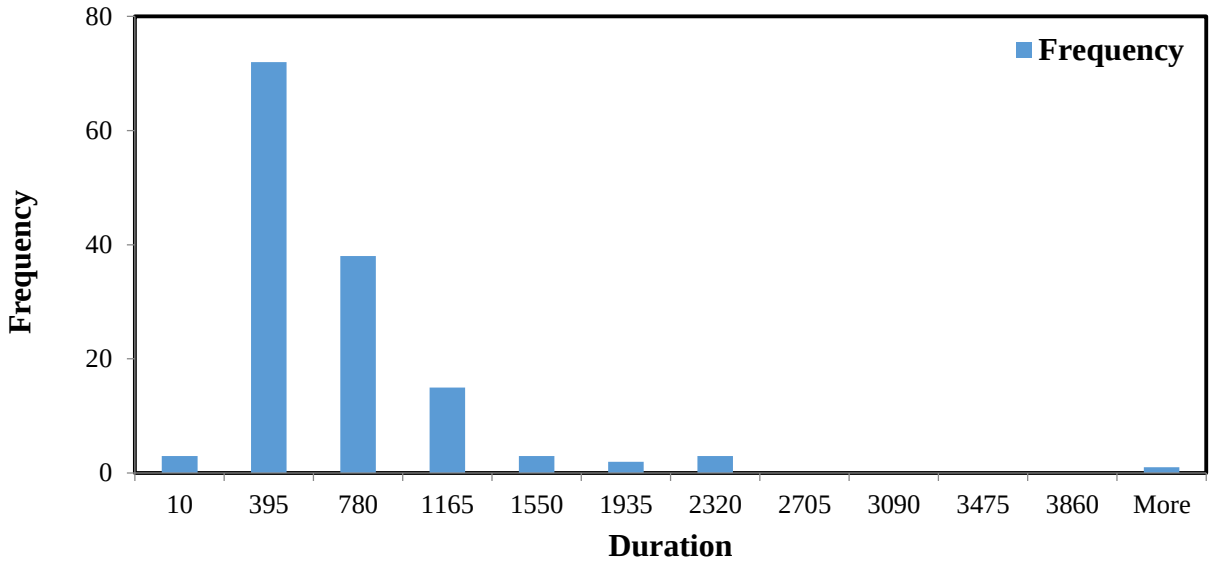
Frequency
80
60
40
20
0
Frequency
10
395
780
1165
1550
1935
2320
2705
3090
3475
3860
More
Duration

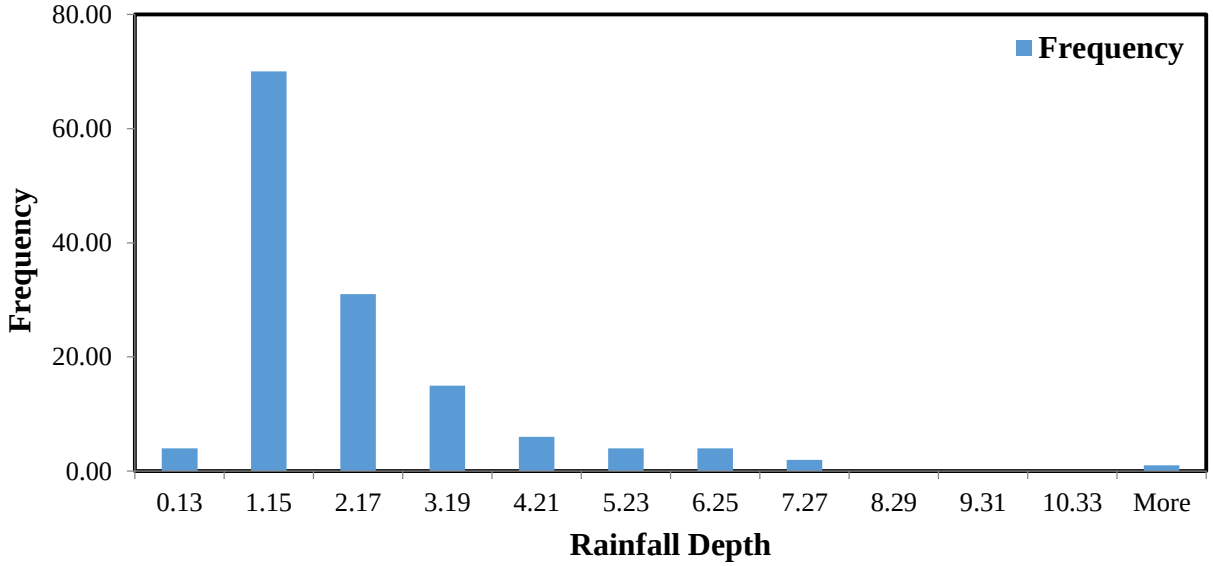
Frequency
80.00
60.00
40.00
20.00
0.00
Frequency
0.13
1.15
2.17
3.19
4.21
5.23
6.25
7.27
8.29
9.31
10.33
More
Rainfall Depth

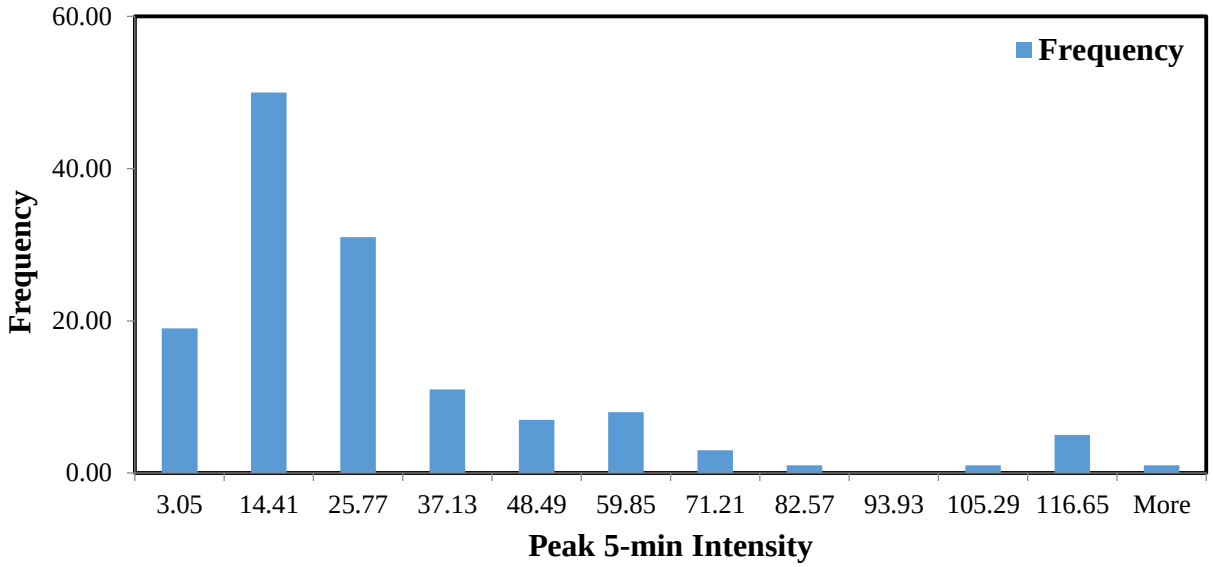
60.00
40.00
20.00
0.00
Frequency
Frequency
3.05
14.41
25.77
37.13
48.49
59.85
71.21
82.57
93.93
105.29
116.65
More
Peak 5-min Intensity

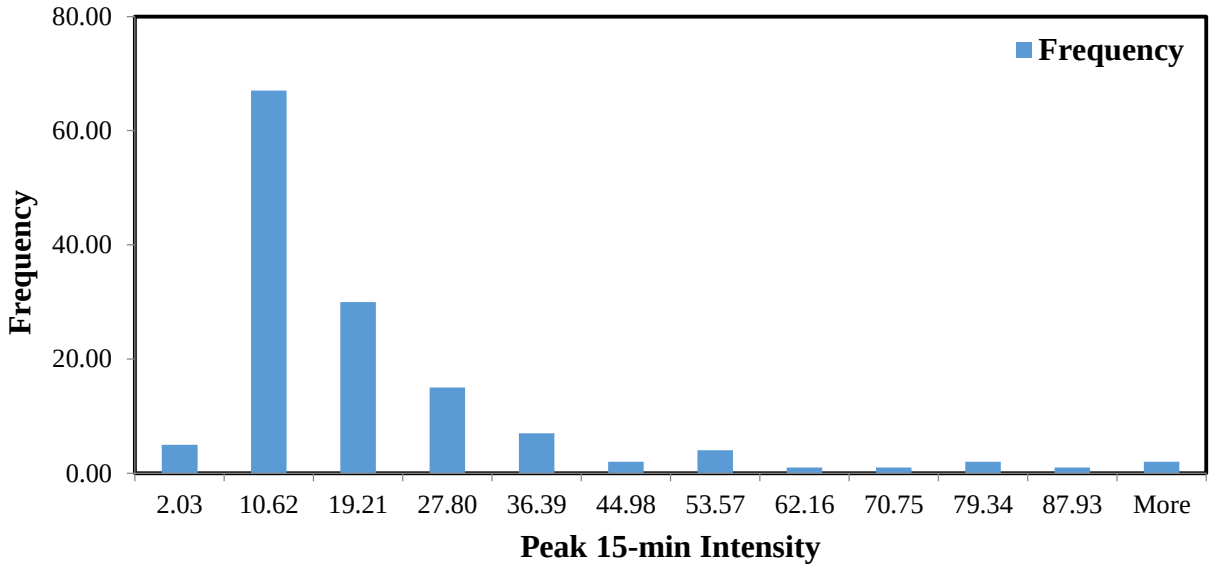
80.00
60.00
40.00
20.00
0.00
Frequency
Frequency
2.03
10.62
19.21
27.80
36.39
44.98
53.57
62.16
70.75
79.34
87.93
More
Peak 15-min Intensity

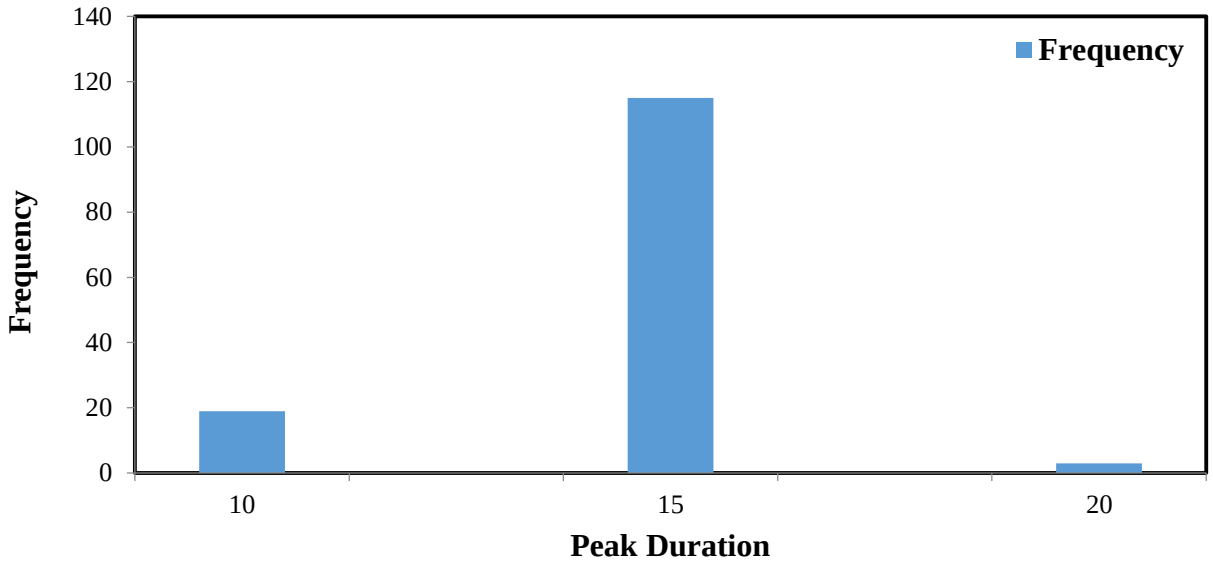
Frequency
140
120
100
80
60
40
20
0
Frequency
10
15
20
Peak Duration

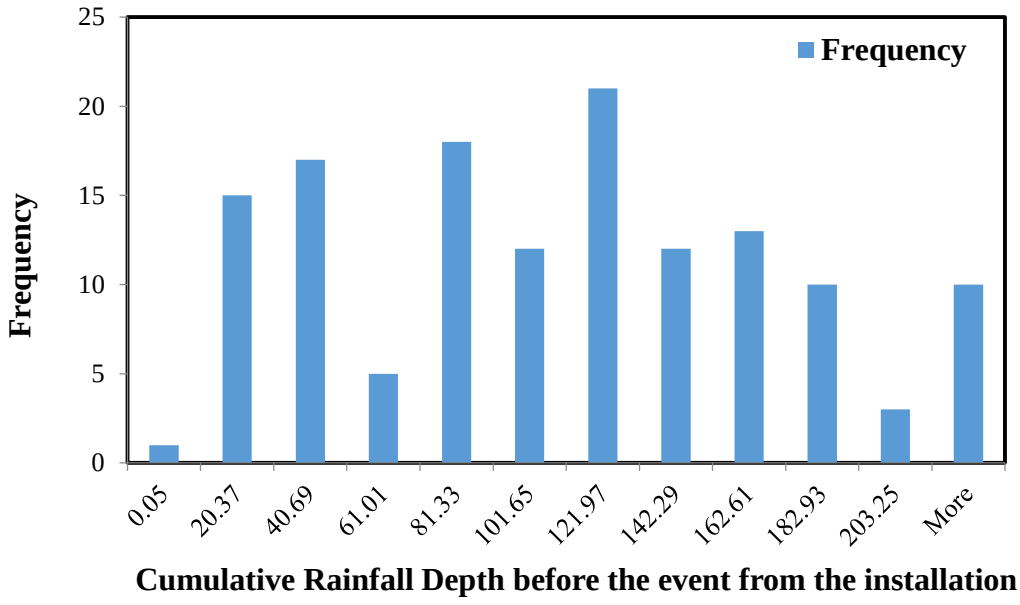
Frequency
25
20
15
10
5
0
Frequency
0.05
20.37
40.69
61.01
81.33
101.65
121.97
142.29
162.61
182.93
203.25
More
Cumulative Rainfall Depth before the event from the installation

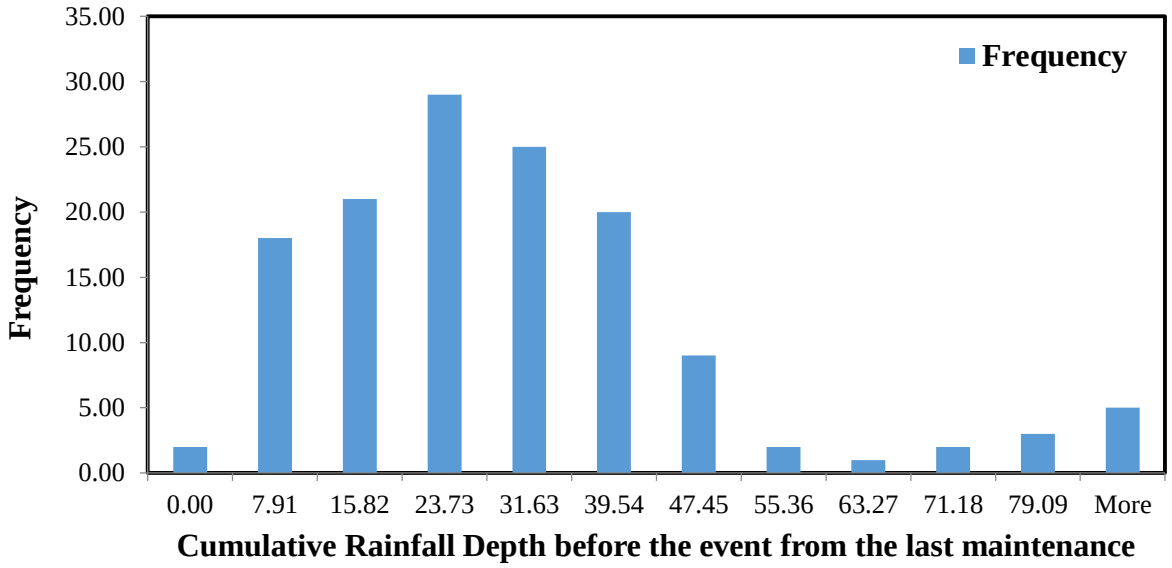
35.00
30.00
25.00
20.00
15.00
10.00
5.00
0.00
Frequency
Frequency
0.00
7.91
15.82
23.73
31.63
39.54
47.45
55.36
63.27
71.18
79.09
More
Cumulative Rainfall Depth before the event from the last maintenance

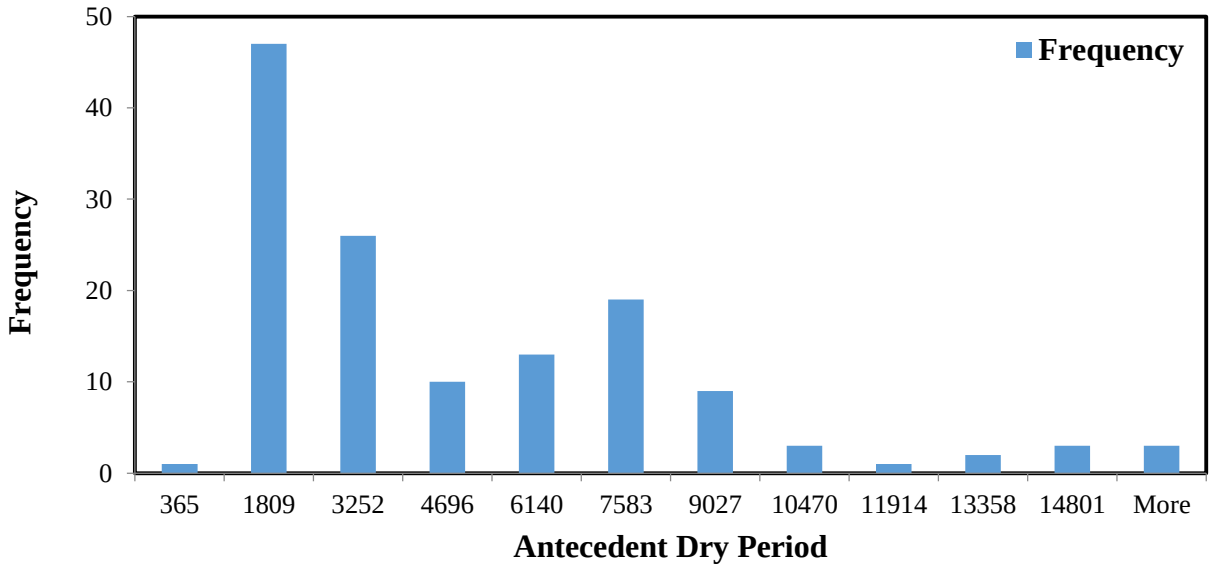
50
40
30
20
10
0
Frequency
Frequency
365
1809
3252
4696
6140
7583
9027
10470
11914
13358
14801
More
Antecedent Dry Period

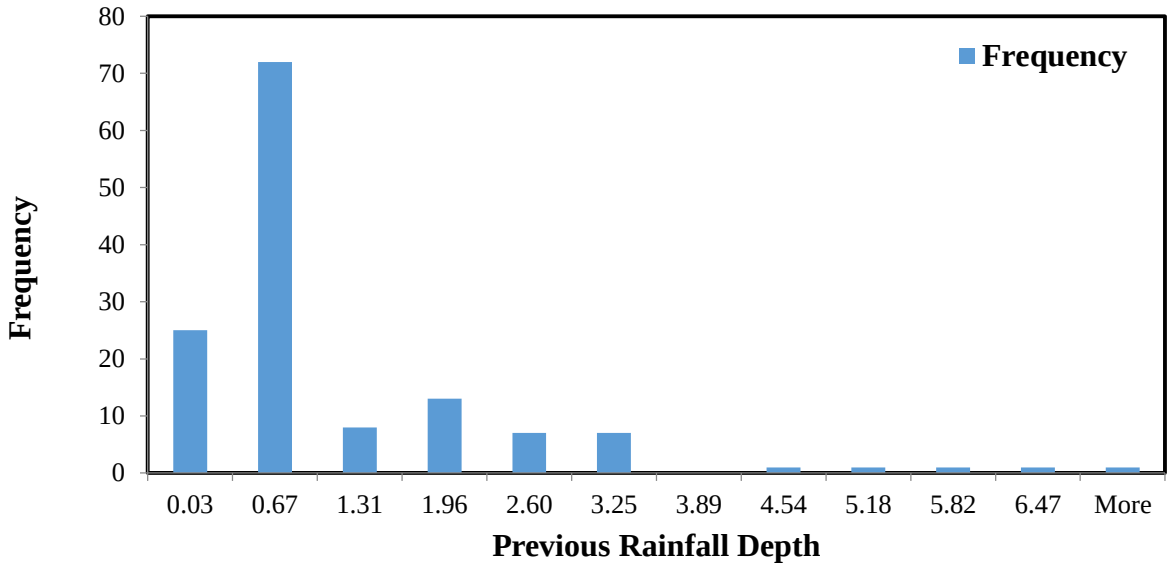
Frequency
80
70
60
50
40
30
20
10
0
Frequency
0.03
0.67
1.31
1.96
2.60
3.25
3.89
4.54
5.18
5.82
6.47
More
Previous Rainfall Depth

APPENDIX K

Histograms of the Input Variables in the Peak VWC Model of PICP 19G

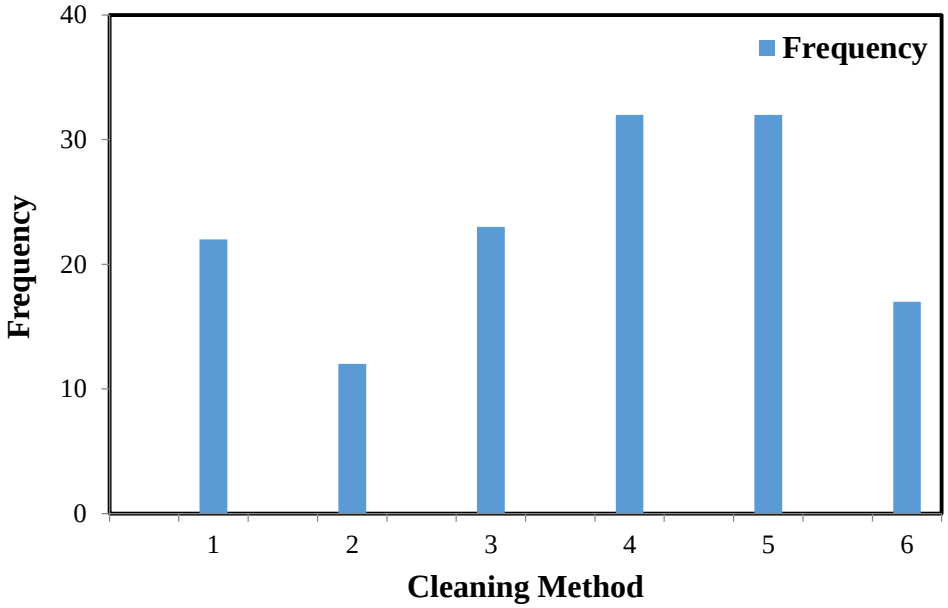

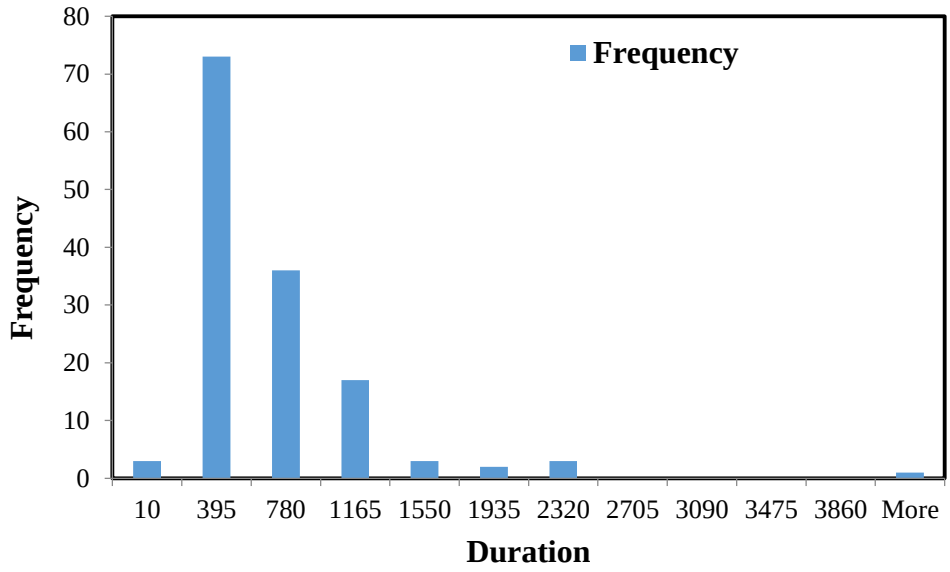
Frequency
80
70
60
50
40
30
20
10
0
Frequency
10
395
780
1165
1550
1935
2320
2705
3090
3475
3860
More
Duration

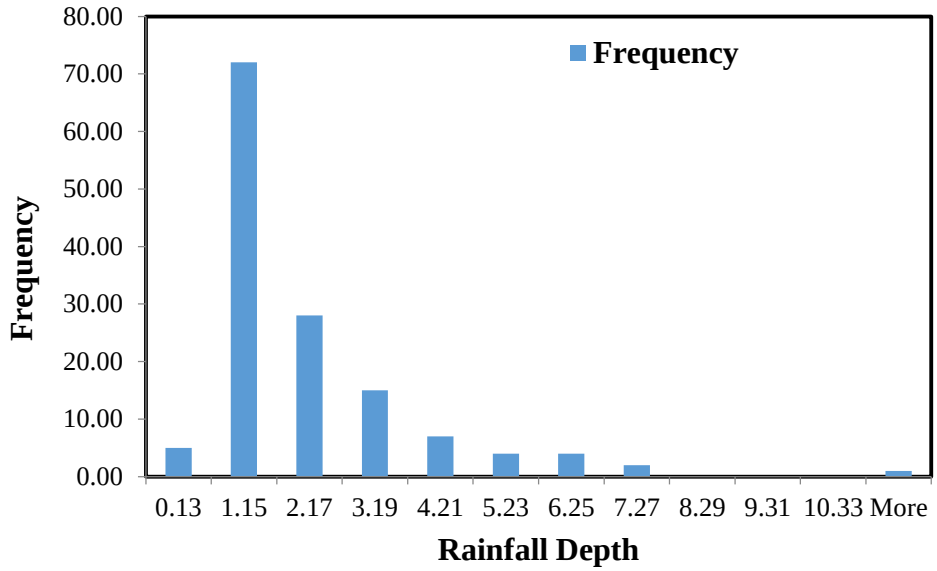
Frequency
80.00
70.00
60.00
50.00
40.00
30.00
20.00
10.00
0.00
Frequency
0.13
1.15
2.17
3.19
4.21
5.23
6.25
7.27
8.29
9.31
10.33
More
Rainfall Depth

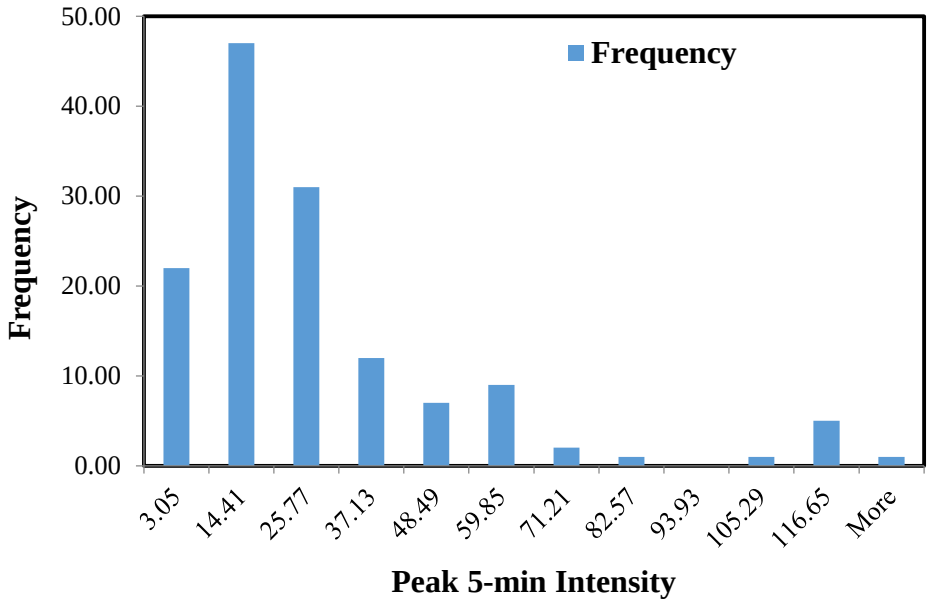
50.00
40.00
30.00
20.00
10.00
0.00
Frequency
Frequency
3.05
14.41
25.77
37.13
48.49
59.85
71.21
82.57
93.93
105.29
116.65
More
Peak 5-min Intensity

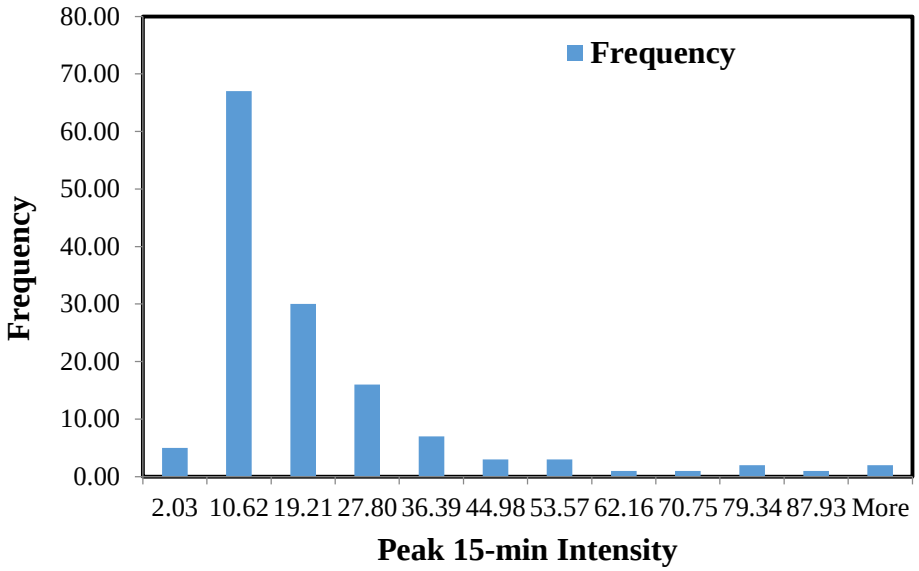
80.00
70.00
60.00
50.00
40.00
30.00
20.00
10.00
0.00
Frequency
Frequency
2.03
10.62
19.21
27.80
36.39
44.98
53.57
62.16
70.75
79.34
87.93
More
Peak 15-min Intensity

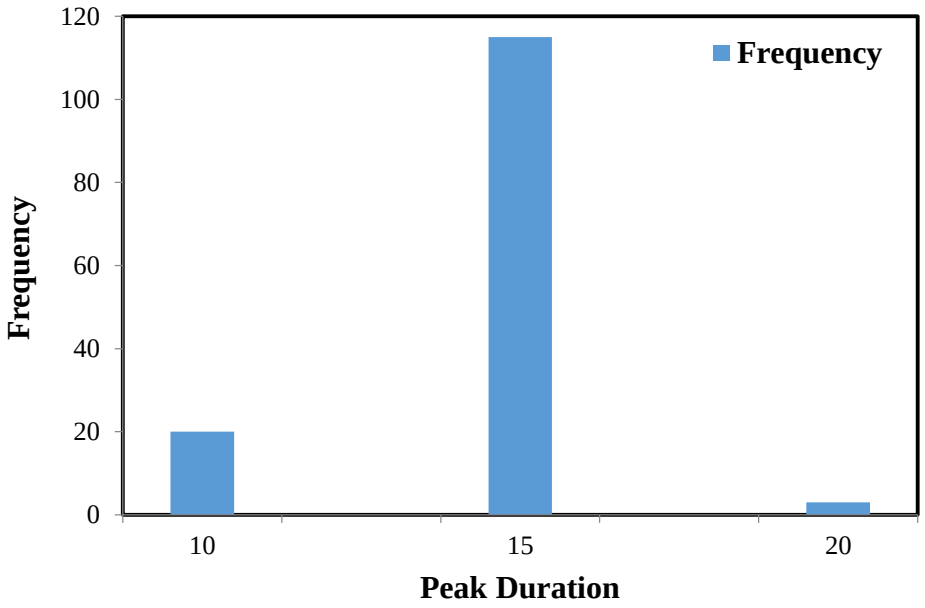
120
100
80
60
40
20
0
Frequency
Frequency
10
15
20
Peak Duration

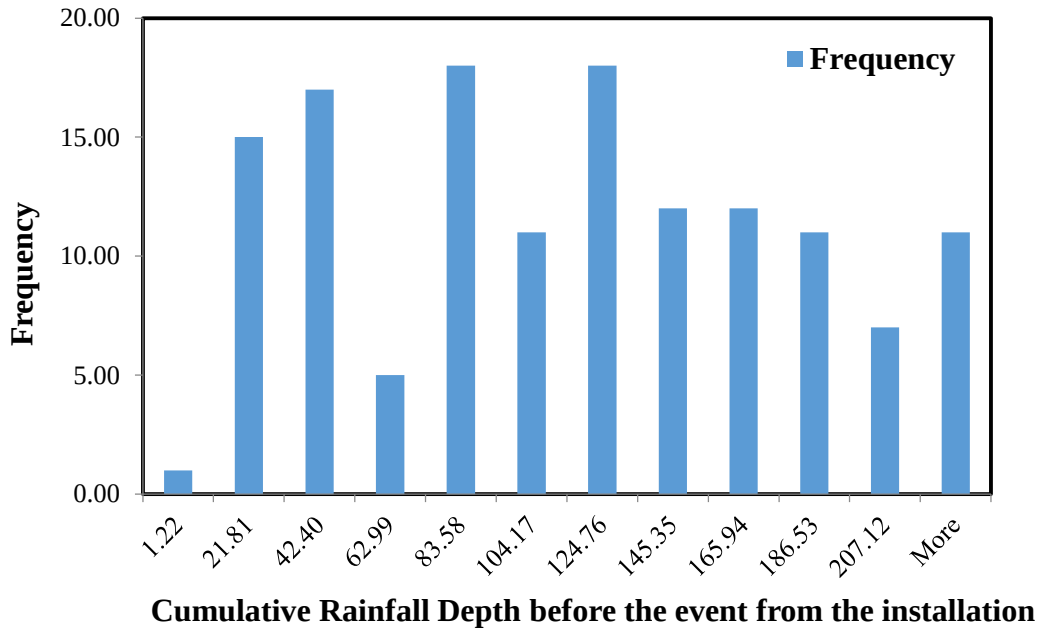
20.00
15.00
10.00
5.00
0.00
Frequency
Frequency
1.22
21.81
42.40
62.99
83.58
104.17
124.76
145.35
165.94
186.53
207.12
More
Cumulative Rainfall Depth before the event from the installation

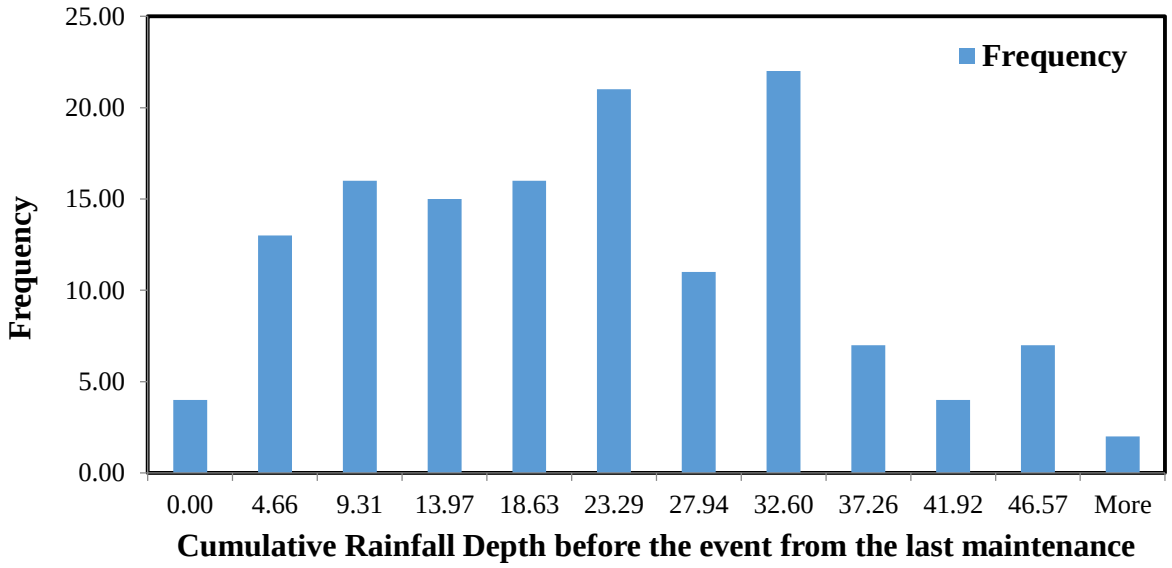
25.00
20.00
15.00
10.00
5.00
0.00
Frequency
Frequency
0.00
4.66
9.31
13.97
18.63
23.29
27.94
32.60
37.26
41.92
46.57
More
Cumulative Rainfall Depth before the event from the last maintenance

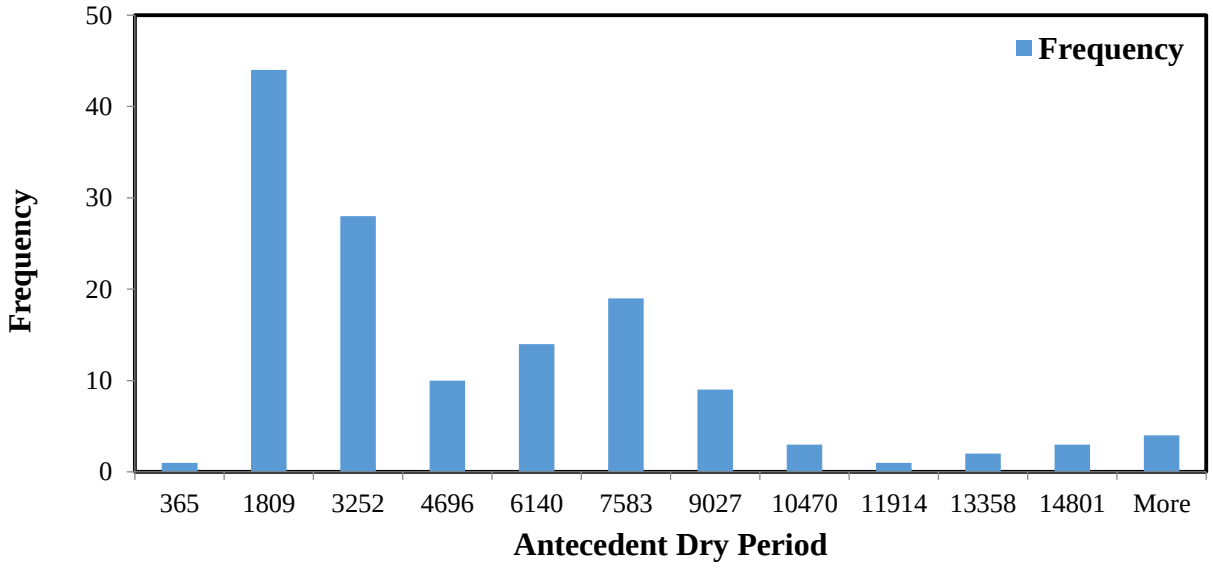
50
40
30
20
10
0
Frequency
Frequency
365
1809
3252
4696
6140
7583
9027
10470
11914
13358
14801
More
Antecedent Dry Period

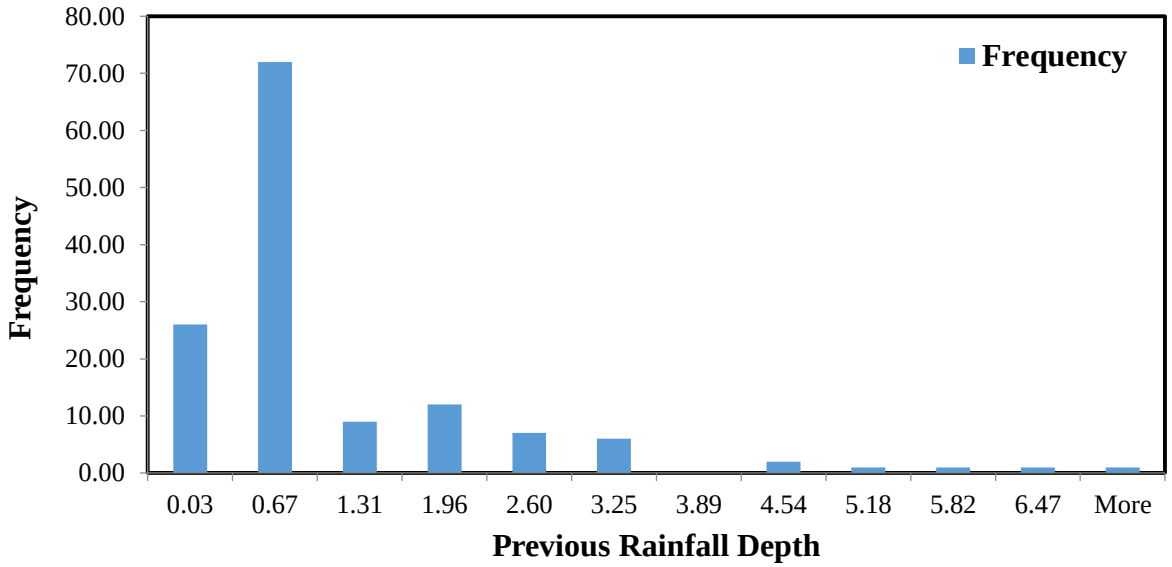
80.00
70.00
60.00
50.00
40.00
30.00
20.00
10.00
0.00
Frequency
Frequency
0.03
0.67
1.31
1.96
2.60
3.25
3.89
4.54
5.18
5.82
6.47
More
Previous Rainfall Depth

APPENDIX L

Rainfall Statistics Data by OneRain

Rainfall Variables	1980	1981	1982	1983	1984	1985	1986	1987	1988	1989	1990	1991	1992	1993	1994
Duration (hrs)	671	645	741	851	897	786	746	638	659	860	856	857	782	967	794
Average Intensity	0.07	0.04	0.06	0.05	0.05	0.04	0.05	0.04	0.06	0.06	0.06	0.04	0.05	0.05	0.05
Total Depth	37.8	33.7	45.3	47.3	49.3	37.7	37.5	32.4	37.4	50.9	57.4	37.2	40.7	47.3	35.7
Number of Events	105	111	126	113	131	116	116	110	89	119	117	113	131	117	102
Maximum Intensity	1.42	1.13	0.89	1.04	1.45	0.93	1.26	1.1	0.95	1.26	2.57	1.3	1.52	1.31	1.15
Time Interval	76.8	72.4	63.1	67.5	60.3	66.3	65.8	74.2	90.6	66.2	67.8	67.8	61.2	65.9	79.4

Rainfall Variables	1995	1996	1997	1998	1999	2000	2001	2002	2003	2004	2005	2006	Average	SD
Duration (hrs)	588	721	785	762	689	761	683	771	914	812	776	820	771.56	91.384
Average Intensity	0.05	0.08	0.05	0.06	0.05	0.06	0.07	0.06	0.06	0.05	0.05	0.06	0.059	0.01
Total Depth	33.9	45.6	40.9	42.3	35.7	44.1	43.9	49.8	48.1	52.1	39.1	56.5	43.00	6.97
Number of Events	89	107	103	121	92	109	109	108	124	114	107	122	111.8	11.01
Maximum Intensity	0.98	1.14	0.79	1.21	1.34	1.23	0.83	0.91	1.09	1.36	1.3	1.98	1.24	0.365
Time Interval	92.6	74.1	76.9	65.9	87.3	73.6	74.1	73.9	62.8	70.8	74.3	65.2	71.8	8.380

APPENDIX M

Typical Annual Rainfall Data (2007)

Event	Cleaning Method	Duration (Min.)	Rainfall Depth (cm.)	Peak 5 min (mm/hr)	Peak 15 min (mm/hr)	Peak Duration (Min)	Cumulative Rainfall Depth from the installation (cm)	Cumulative Rainfall Depth from the last maintenance (cm)	ADP (Min)	Previous Rainfall Depth (cm)
1	1	730	0.4826	3.048	3.048	15	0.4826	0.4826	4955	1.6764
2	1	40	0.2032	6.096	5.08	15	0.6858	0.6858	795	0.4826
3	**1**	**225**	**1.0668**	**9.144**	**9.144**	**15**	**1.7526**	**1.7526**	**2225**	**0.2032**
4	1	500	0.2032	3.048	3.048	10	1.9558	1.9558	6565	1.0668
5	1	1680	3.9116	15.24	12.192	15	5.8674	5.8674	485	0.2032
6	**1**	**675**	**1.778**	**6.096**	**5.08**	**15**	**7.6454**	**7.6454**	**1000**	**3.9116**
7	1	1650	4.1656	6.096	5.08	15	11.811	11.811	13190	1.778
8	1	610	2.7432	1.2192	8.128	15	14.5542	14.5542	3585	4.1656
9	**1**	**200**	**0.4064**	**12.192**	**7.112**	**15**	**14.9606**	**14.9606**	**4980**	**2.7432**
10	1	230	2.1082	2.4384	16.256	15	17.0688	17.0688	395	0.4064
11	1	375	1.143	15.24	11.176	15	18.2118	18.2118	5150	2.1082
12	1	215	2.2098	33.528	25.4	15	20.4216	20.4216	480	1.143

13	1	265	0.5842	9.144	6.096	15	21.0058	21.0058	710	2.2098
14	1	660	1.397	18.288	13.208	15	22.4028	22.4028	5190	0.5842
15	1	65	0.1778	9.144	3.048	20	22.5806	22.5806	3595	1.397
16	**1**	**615**	**1.1176**	**9.144**	**6.096**	**15**	**23.6982**	**23.6982**	**7940**	**0.1778**
17	1	10	0.1524	12.192	9.144	10	23.8506	23.8506	3645	1.1176
18	**1**	**210**	**2.9718**	**60.96**	**40.64**	**15**	**26.8224**	**26.8224**	**3465**	**0.1524**

CURRICULUM VITAE

Ata Radfar, EIT

Center for Infrastructure Research, Department of Civil and Environmental Engineering

University of Louisville, Louisville, KY 40292

Phone: (502) 608-3401, E-mail: ata.radfar@louisville.edu

Education

- **Doctor of Philosophy in Civil Engineering**

  Aug. 2011-May 2015

  University of Louisville (UL), Louisville, Kentucky

- **Master of Science in Geotechnical Engineering**

  Sep. 2008-Mar. 2011

  Ferdowsi University of Mashhad (FUM), Mashhad, Iran

- **Bachelor of Science in Civil Engineering**

  Sep. 2002-Oct. 2007

  Iran University of Science & Technology (IUST), Tehran, Iran

Selected Publications

- **Peer-reviewed Journal Papers**

  - **Radfar A.,** Gandomi A.H., Tabatabaie S.M., Moradian M.H., and Alavi A.H., "A New Prediction Model for Load Capacity of Castellated Steel Beams," *Journal of Constructional Steel Research, Elsevier,* 67(7): 1096-1105, 2011

  - **Radfar A.**, Rockaway T., "Neural Network Model for Volumetric Water Content Prediction of Permeable Pavement," *Journal of Irrigation and Drainage Engineering,* (Manuscript number #IRENG-7080)

- **Radfar A.**, Rockaway T., "Captured Runoff Prediction Model by Permeable Pavements using Artificial Neural Networks," *ASCE Journal of Infrastructure systems* (Manuscript number #ISENG-768)
- **Radfar A.**, Rockaway T., Ehsaei A., "Artificial Neural Network Models for Clogging Prediction of Permeable Pavement Laboratory Models," *ASCE Journal of Hydrologic Engineering* (Manuscript number #HEENG-2806)
- **Radfar A.**, Rockaway T., "Long-term Performance of GI Stormwater Control Systems," Proceedings of the 46th American Geophysical Union Conference, San Francisco, CA, Dec. 2013

- **Presentations**
  - **Radfar A.,** Rockaway T., Fagan R., "Normalization of Pervious Paver Infiltration Testing Parameters," Environmental & Water Resources Congress, Cincinnati, OH, May 2013
  - **Radfar A.**, Bolouri-Bazaz J., "Seismic Analysis of Anchored Wall with FLAC3D," 6th International Conference on Seismology and Earthquake Engineering, Tehran, Iran, May 16-18, 2011
- **Conference Papers**
  - **Radfar A.,** Rockaway T., "Neural Networks Models for Captured Runoff Prediction of Permeable Interlocking Concrete Pavements," Environmental & Water Resources Congress, Austin, TX, May 2015
  - **Radfar A.,** Rockaway T., Ehsaei A., "Clogging Progression Prediction of Permeable Pavement Laboratory Model Using Artificial Neural Networks ," Watershed Management Symposium, Washington, D.C., Aug. 2015

- **Radfar A.**, Rockaway T., "Long-term Performance of GI Stormwater Control Systems," Proceedings of the 46th American Geophysical Union Conference, San Francisco, CA, Dec. 2013
- **Radfar A.**, Amini B. "Analysis on Influence of Surcharge on Excavation with FLAC3D," Proceeding of the 4th International Conference on Geotechnical Engineering and Soil Mechanics, Tehran, Iran, Nov. 2-3, 2010

Professional Development

- Member of Interlocking Concrete Pavement Institute (ICPI)

  Aug. 2014-Present
- Member of American Society of Civil Engineers (ASCE)

  Oct. 2011-Present
- Member of Environmental Water Resources Institute (EWRI)

  Oct. 2011-Present